Bulletin

of

The Geological Society of America

VOLUME 54 SEPTEMBER 1, 1943 NUMBER 9

CONTENTS

PAGES

History of the development of geologic maps. By H. A. Ireland.. 1227–1280

Pre-Cretaceous of Colombia. By D. Trumpy..... 1281–1304

Packing in ionic minerals. By H. W. Fairbairn..... 1305–1374

Reverse faulting north of Harrisburg, Pennsylvania. By Ernst Cloos and Carl H. Broedel..... 1375–1398

Recrystallization and flowage in Appalachian quartzite. By Robert E. Fellows 1399–1432

Subscription, $10 per year.

Publication Office: Florida Avenue and Eckington Place, Washington 2, D. C.

Communications for publication should be addressed to The Geological Society of America, Dr. H. R. Aldrich, Secretary, 419 West 117th Street, New York, N. Y.

NOTICE.—In accordance with the rules established by the Council, claims for non-receipt of the preceding number of the Bulletin must be sent to the Secretary of the Society within three months of the date of the receipt of this number in order to be filled gratis.

Entered as second-class matter in the Post-Office at Washington, D. C. under the Act of Congress of July 16, 1894.

Accepted for mailing at special rate of postage provided for in Section 1103, Act of October 3, 1917, authorized on July 8, 1918.

PRESS OF JUDD & DETWEILER, INC., WASHINGTON, D. C.

PAPERS IN PRESS FOR FORTHCOMING ISSUES

Perennially Frozen Ground in Alaska; Its Origin and History. By Stephen Taber

Late Pleistocene Coast Range Orogenesis in Southern California. By Thomas L. Bailey

Fossiliferous Tills and Intertill Beds of Cape Cod, Massachusetts. By Robert W. Sayles and Arthur S. Knox

Geology of the Santiago Peak Quadrangle, Texas. By Gus K. Eifler, Jr.

Stratigraphy and Structure of West-Central Vermont. By Wallace M. Cady

Stratigraphy of the Genesee Group of New York. By William L. Grossman

Correlation of the Cenozoic Formations of the Atlantic and Gulf Coastal Plain and the Caribbean Region. By C. Wythe Cooke, Julia Gardner, and W. P. Woodring

Plagioclase Twinning. By J. D. H. Donnay

Lower Mississippi Valley Loess. By Richard Joel Russell

Transportation and Deposition of Heavy Minerals. By Gordon Rittenhouse

Lower and Middle Cambrian Stratigraphy in the Great Basin Area. By Harry E. Wheeler

BULLETIN OF THE GEOLOGICAL SOCIETY OF AMERICA
VOL. 54, PP. 1227-1280 SEPTEMBER 1, 1943

HISTORY OF THE DEVELOPMENT OF GEOLOGIC MAPS

BY H. ANDREW IRELAND

CONTENTS

	Page
Abstract	1227
Introduction	1228
Acknowledgments	1230
Source of material	1231
Development of geologic maps in Europe	1231
General statement	1231
France and Belgium	1233
Great Britain	1235
Germany	1240
Switzerland	1243
Southeastern Europe	1244
Russia	1245
Scandinavia	1246
Miscellaneous European maps	1247
Continental Europe	1248
Maps of Asia	1249
Maps of Australia and New Zealand	1251
Maps of Africa	1252
Maps of British America	1252
Maps of Middle America	1253
Maps of South America	1254
World maps	1256
Development of geologic maps in the United States	1257
First period, 1809–1842	1257
Second period, 1842–1867	1261
Third period, 1867–present	1265
List of maps of the United States	1270
List of outstanding and some of the most interesting geologic maps	1270
References cited	1272
Bibliography of source books and catalogues of geologic maps	1279

ABSTRACT

Features on the early geologic maps were illustrated by symbols, ruling, stippling, letters, and numerals. From 1775 to 1851 hand-colored maps on printed bases were the chief medium of illustration. Chromolithography began to supersede hand coloring about 1851, and the present multicolored maps are results of the development of color printing. Hand-colored maps are still made but not published.

About 300 of the 375 maps mentioned were personally examined, but they represent only a small part of the thousands in existence.

Maps that are outstanding because of early date, cartographic technique, important contribution to geology, advances in methodology, or some other special interest are described. Maps for all parts of the world are included in the descriptions, but most of the discussion and description is of maps of Europe and North America.

INTRODUCTION

The oldest known map is dated at about 2500 B. C. It was found on a clay tablet in Babylonian ruins at Ga Sur, about 200 miles north of Babylon, and is now preserved in the Semitic Museum of Harvard University. Other Babylonian tablets have been found that demonstrate the antiquity of cartography. The Babylonians originated the method of dividing the earth into 360° according to sun time.

The ancient Greek civilization made outstanding contributions to cartography. Anaximander is credited with making the first map of the world in 611 B. C., showing it as a disk because he considered the earth a section of an imaginary cylinder in the celestial sphere. Democritus developed the concept of latitude and longitude about 400 B. C., and Eratosthenes used the principle on a map of the world about 225 B. C. showing seven parallels and seven meridians. Eratosthenes also computed the circumference and diameter of the earth by measuring an arc in Egypt from Syene to Alexandria.

Claudius Ptolemy made a map of the world in 150 A. D. using latitude and longitude. This was one of the most important maps because it was copied, revised, modified, and the basic idea and material utilized for centuries. Errors in the degrees of longitude for the Mediterranean Sea gave the features of the map a distorted appearance, which was partly corrected by Kepler in 1630, but not corrected to the true length of 41° until 1700 by Guillaume Delisle. Ptolemy's map was lost for several centuries but was redrawn when his book *Geographia* was translated into Latin in 1410. It was reproduced in quantity in 1475 from an engraved copper plate. In 1425 Clavus, a Dane, extended Ptolemy's map to include Greenland, and it is one of the earliest maps of the Arctic region. The influence of Ptolemy did not decline until 1822 when Magellan's expedition proved America to be a continent and the world to be round.

An early map by Gerardus Mercator made in 1538 showed some of the influence of Ptolemy, but this influence was not present in 1569 when Mercator's famous map of the world appeared. This map was engraved on copper and overcame the long-standing errors of Ptolemy's map. Mercator's cylindrical projection map is still used extensively.

The Renaissance brought new advances in cartography. Reproduction of maps in quantity was not effected until about 1570, even though maps had been printed for nearly a century. The first printed maps were those taken from Ptolemy's *Geographia* in 1475. A map of Germany made in

Hanover in 1490 was an early printing from a wood cut. Engraved copper plates were found to be much better than wood cuts, and the use of copper plates continued for over 3 centuries.

Maps of the Renaissance were brilliant with flourishing scroll and decorative work, red-roofed castles and houses, colored trees, and multicolored fruits. Borders or unused portions of the maps were filled with monsters, serpents, ships, castles, or scenic features. Maps were handcolored on the printed base until chromolithography was developed about the middle of the nineteenth century.

Primitive crude maps on bark have been made by Eskimos and Indians in North America. Indians have carved directions to water holes on the cliffs in the arid part of the United States. Montezuma presented a cloth map of his empire to Cortes. The first maps in relief were made by the Incas about 1191 A. D. Natives of the Marshall Islands make maps of their area using shells for islands and palm leaf ribs for a framework and representation of fringing reefs.

The use of hachures and contour lines to show altitudes of the land was one of the greatest advances in cartography of importance to geologic mapping. This was suggested by the lines of equal sounding below sea level which were placed on maps by early Dutch surveyors. The first topographic map was a small one made by David Vivier in 1674 entitled *Environs de Paris*. He used hachures instead of the scenographic portrayal of topography (Encyclopedia Britannica, 1929). The first topographic map using contour lines was made by Nicholas Cruquius in 1728 of a small area along the Merwede River in The Netherlands (Encyclopedia Britannica, 1929). Philip Buache used the contour-line method for a map of the English Channel area in 1737.

The first official topographic map of France, printed about 1750, was based on triangulation by César Cassini, Compte de Thury, and his son in 1744 (Thiele, 1938). Cassini and his son were commissioned by Louis XV in 1747 to make a map of France which was completed in 1793, but all sheets were not printed until 1815. The set contained 160 sheets and 24 quarter sheets on a scale of 1:86,400. The type of hachures on the sheets is transitional between the early pictorial representation and later systematic hachuring. The method of contour-line mapping was officially adopted in France in 1816, but by 1833 only four sheets had appeared.

Nicolas Desmarest had a special topographic map drawn of the volcanic area of the Auvergne in order to do his geologic mapping. In 1771 he placed on this map the location of the various types of lava flows, using engraved designs to represent the four types of lava which he described.

The first contour map made in England was one of Perthshire in 1778.

The English triangulation system was started in 1783, stimulated by the work of Cassini, and the Ordnance Survey was organized in 1791. The first map appeared in 1801, but topographic mapping was not officially adopted by Great Britain until 1843 (Fordham, 1927).

Beginning with the early nineteenth century, the development and use of contour maps progressed rapidly, and by the end of the nineteenth century all of Europe, except Russia, was covered by topographic maps of various degrees of accuracy, most of which have been revised, some several times. Most of the topographic maps for Europe and other foreign areas are produced by the General Staffs of the armies. In contrast most of those of the United States are produced by the U. S. Geological Survey in the Department of the Interior. A few other government agencies make topographic maps of special areas. The location and survey of the vast and relatively unknown natural resources of the United States was necessary for and a part of the rapid expansion after the War between the States, and the Geological Survey when organized lacked essential topographic base maps. Major Powell and his successors found it necessary to procure funds for and make the basic maps for the use of the field geologists. Contour mapping of the United States is not complete, but it has been greatly advanced with the use of aerial photography. In the twentieth century, the use of topographic maps for geologic, military, engineering and other purposes is very common and essential.[1]

The International Map on a scale of 1:1,000,000, often called the "Millionth Map", was suggested in 1891 by Albrecht Penck. It was proposed to a committee of the International Geographic Congress in 1908 and was adopted in 1913. The map will have 2084 sheets, of which 974 will be mostly continental areas. Many of the sheets have been completed and are being used as base maps for geologic information. The entire continent of South America is complete on the millionth scale.

ACKNOWLEDGMENTS

I appreciate the facilities given for the study and examination of maps, old geologic journals, and publications from Europe and America at the University of Chicago, The Ohio State University, U. S. Geological Survey, and the Library of Congress. I am especially indebted to Col. Lawrence Martin of the Division of Maps in the Library of Congress for suggestions and criticisms of the paper and for the assistance of his staff in going through the files of geologic maps. G. W. Stose and C. H. Birdseye of the U. S. Geological Survey were very helpful in examining the

[1] Raisz (1938, p. 203-213) gives an excellent list and sources of topographic maps available throughout the world.

manuscript and giving valuable suggestions, particularly on the sections relating to American maps. I am further indebted to C. W. Thornthwaite, Lois Olson, and Helen Eddy of the Soil Conservation Service for suggestions and criticism of the manuscript.

SOURCE OF MATERIAL

Map files, old geologic journals, and publications printed in Europe and America furnished most of the information. These were examined at the University of Chicago, The Ohio State University, Library of Congress, and the Library of the U. S. Geological Survey. The Map Division of the Library of Congress has an excellent file of unattached early and recent geologic maps, especially those for United States and western Europe. I was fortunate in being able to examine the large number of old geologic publications in the James Hall Collection at the University of Chicago. About 300 of the 375 or more maps mentioned were examined. At the end of references cited are the chief works giving lists or descriptions of geologic maps.

The geologic maps referred to in this discussion are by no means a complete list of all the early maps or later ones which might be mentioned. Only those which are significant because of the early date, cartographic technique, important contribution to geologic knowledge, advances in methodology, or some other particular interest are mentioned. The discussion includes maps from all continents, but most of the description is for maps of Europe and America. Because of the many political and boundary changes during the last 150 years, many of the maps are of nations whose boundaries or political status have been modified.

DEVELOPMENT OF GEOLOGIC MAPS IN EUROPE

GENERAL STATEMENT

The geologic features on maps prior to 1775 were depicted by symbols, line rulings, stippling, letters, and numerals printed in black. The earliest geologic map known was made by Abbé Coulon in Paris in 1664 and appeared in a small volume entitled *Les rivieres des France* (Marcou, 1884). Christopher Packe made the first geologic map of English origin in 1742 of about 30 square miles near Canterbury in Kent (Zittel, 1908, p. 35). The map is entitled *New philosophy and chronographic chart of East Kent.* Guettard (1746) made a map of northern France and England and (1752) the first geologic map of North America. The first geologic map from Germany was issued by Füchsel (1762).

Between 1700 and 1750 Johann Scheuchzer, a Swiss professor in Zürich, drew some geologic cross sections of the vicinity of Lucerne which

were reproduced in his works. These are the earliest attempts in the literature at showing folded strata and mountain structure (Zittel, 1908, p. 31).

The first geologic map in color was made in Germany in 1775 by Gottlieb Gläser. Later, color was combined with symbols and rulings, first by Von Charpentier, but color alone grew to be preferred. Water coloring was the chief method used. Contrasting colors were chosen in order to give maximum differentiation and distinction of the units mapped. Until 1841 all coloring was done by hand, which greatly increased the cost of publications and restricted the number of copies printed. Often boundary lines were overlapped, colors were too dense or of poor quality or poorly applied and many of the maps were imperfect, depending on the skill and care of the colorist.

The English developed the best skill at hand coloring by setting a minimum standard and rejecting imperfect work. The maps of Sir Roderick Murchison show the effect of these strict standards exceptionally well. A large number of unusually fine hand-colored geologic maps, illustrating the excellent technique of the English colorists, were published in the Transactions of the Geological Society of London in 1821; some of these are described later.

The increased demand for many copies of publications made it necessary to have large quantities of hand-colored maps. The process of hand coloring was too slow and too expensive and new developments resulted.

Between 1840 and 1870 a great change occurred in the methods of coloring maps. Methods were devised in France in 1841 to print colors using patterns cut from tin foil, but the results were unsatisfactory. The tin foil was cut to the shape of the area to be printed in a color and then an impression taken. Other patterns were cut for different colors. A geologic map by Victor Raulin was the first to be so printed, but the colors were dull, and the borders overlapped or failed to meet. A map of the Jurassic by Jules Marcou (1848) was similarly printed, but it had the same defects, and the method was abandoned. Cardboard pieces were used in a similar way by Sonrel, the Swiss lithographic technician working for Louis Agassiz. The colors when printed were better, but the gaps and overlaps along the boundary lines were not eliminated.

The process of chromolithography was not satisfactory when first tried in Germany in 1842, because the color had an oil base.

The technique of chromolithography was developed rapidly between 1851 and 1854. Each color was printed from a separate lithographic stone cut with the patterns of each color to be used. The stones could be adjusted accurately to eliminate gaps and overlaps. This method became the dominant process for the reproduction of maps in color, but

hand coloring of multiple copies was not entirely abandoned until 1877.

The geologic map by E. Beyrich (1851) published by the Zeitschrift der Deutschen Geologische Gesellschaft, was probably the first geologic map successfully and satisfactorily printed using chromolithography. In 1854 the Imperial Press of France printed an excellent colored map of France, which had been made by Élie de Beaumont and P. A. Dufrenoy in 1841, using separate lithographic stones for each color. Marcou's (1855) map of the United States and Logan's (1855) map of Canada were two of the earliest maps chromolithographed in France and are very excellent prints. In England, the earliest chromolithograph was probably *A geological map of the northermost part of America* by A. K. Isbister (1855, p. 497). This map is poorly executed and much inferior to the excellent hand-colored maps typical of the English publications of that date. In contrast, the map of the Turkish-Persian frontier by W. K. Loftus (1855, p. 247), which occurs in the same volume, is well done. The geologic map of Belgium published by Andrés Dumont in 1855 was chromolithographed in 42 colors and shades, a real masterpiece, which required great skill. It was a remarkable production considering that chromolithography was still in its infancy.

FRANCE AND BELGIUM

Jean Guettard deserves the credit for making the first important contribution to geologic mapping, though he did not make the first true geologic map. In 1746 he noticed that the bands of formations in Brittany terminated abruptly at the English Channel, and he believed that they extended beneath the sea and were continuous into England; he drew his map accordingly (Guettard, 1746). Symbols were used for the location of mines, quarries, mineral deposits, coal, fossils, springs, and rock outcrops. Shading was employed to aid in the differentiation of the mapped features, as color was not used on geologic maps until 1775.

Guettard (1752) made the first geologic map of North America, though he had never visited the New World. The map is chiefly mineralogic with locations of 39 types of reported minerals, rocks, and fossils, and the rock formations from Southern Canada to the Rio Grande east of the Rocky Mountains.

The influence of Guettard is important because he stressed geologic mapping and his work started other geologists looking for additional information which they placed on maps. He may well be called the "Father of Geologic Maps" as well as the "Father of Vulcanism". He first recognized the Auvergne area in France as being of volanic origin and was followed by Nicolas Desmarest and others in work on that area. Guettard expressed ideas regarding stratigraphic geology which were

greatly emphasized later by Hutton and Playfair and marked the change to what have become the present ideas on stratigraphy.

Guettard enlarged his area of activitiy and made a geologic map of western Europe and then started upon his ambition to publish an atlas of France, of which he completed only 29 sheets. Monnett continued his work and published an additional 31 sheets in 1780 (Zittel, 1908, p. 39).

In 1810 the celebrated *Description géognostique des environs Paris* by Cuvier and Brongniart (1810) was published with an accompanying hand-colored map. This map is important not only as a notable advance in the science of geology, but also because it shows a distinct change from the Wernerian classification of rock formations.

About 1813 Jean d'Omalius d'Halloy made a colored map of France which was revised later and included in the first edition of his book *Éléments de géologie* in 1822. The second edition (1835) contains a splendid hand-colored map of Belgium and France which includes part of England, northern Italy, and east to central Germany. This is one of the best maps of the early nineteenth century.

A hand-colored map of the mouth of the Seine River was published in England by H. T. de la Bache (1824).

The best and most accurate map of France was made in six sheets for the French government by Élie de Beaumont and P. A. Dufrenoy, and it remained the best map for many decades. It was started in 1825 but was not issued until 1841 (Dewalque, 1884). The map is much larger than the one by D'Halloy and shows details more accurately. A later edition was chromolithographed in 1854 by the Imperial Press of France and is one of the first maps to be printed by that new method. The map was reduced later from six sheets to one sheet in order to appear in the book *La stratigraphie* by De Beaumont and Dufrenoy (1869). This issue was reproduced beautifully by color printing and is one of the finest examples of all cartography.

An interesting small hand-colored map entitled *Carte du terrain erratique de la Vallée de St. Amarin* by Edouard Collomb (1846) is probably one of the first maps of glacial deposits. It is on a heavily hachured base with colors showing the positions of moraines, glaciers, and erratics.

Another interesting map is a lithographic color print of the vicinity around Montpellier published by Paul Rouville (1868). Various lines, symbols, and stippling were overprinted in red for differentiation of the patterns. The same volume contains an attractive print of the French subdivision of Constantine in Algeria by M. L. Hardouin (1868) with the geology shown by 10 colors.

The French publication Annales des Mines has quite a number of small maps in early issues. They are not of great importance but some of them are listed because they represent early types.

Carte géologique des districts métallifères de Najac, de Villefranc, d'Asprieres, de la Vallée du Tarn, by Ad. Boisse (1852).

Carte géologique du Lac Superieur. État de Michigan, by J. W. Foster and J. D. Whitney (Rivot, 1855, Pl. 6).

Cartes de l'Ile Royale de la Pointe de Keweenaw et de l'Ontonacon, by J. W. Foster and J. D. Whitney (Rivot, 1855, Pl. 7).

Carte géologique du Pay Messin, E. Jacquot (1857).

The maps by Foster and Whitney cover the north and south shores of Lake Superior and are of interest because they were color-printed in an early French publication from the original hand-colored copies published in America in 1851.

A map of France in 36 sheets by C. Vasseur and L. Carez appeared in 1885 (U. C.).[2] It is a color print, but the base map is so heavily covered with railroad, stream, and hachure lines that the appearance is poor and usefulness of the map is lessened. Probably the most recent map of France is the third edition in 1933 of the map compiled in 1905 under the direction of Michel-Levy for the Ministry of Public Works. The scale is 1:1,000,000, and the dimensions of the map 46 by 48 inches (L. C.).

A complete map of Belgium was published in 9 sheets employing 42 colors and designs by Andrés Dumont in 1855, with a second edition in 1878 (L. C.). Each of the 9 sheets is 19 by 22 inches on a scale of 1:160,000. Dumont also made a geologic map of Europe in 1857 (Dewalque, 1884). This is in 4 sheets on a scale of 1:4,000,000. Dewalque made a geologic map of Belgium in 1875 which was revised in 1903 (L. C.). A more detailed map of Belgium in several sheets by E. Dupont and M. Maurlon appeared from Bruxelles in 1882 (Dewalque, 1884). In 1920 the Belgian government had geologic maps made in sheets on a scale of 1:160,000 (L. C.). In 1932 these were reduced to a scale of 1:1,000,000 on sheets 9½ by 10 inches by the Institute Cartographique Militaire and are the most recent maps.

GREAT BRITAIN

In England the first geologic map was made by Christopher Packe in 1743 (Zittel, 1908, p. 35). The most important map of early geology was that made by William Smith, the "Father of Stratigraphy" and the "Father of English Geology". This was one of the most remarkable con-

[2] Sources of unattached maps examined in files have been abbreviated throughout the text as follows: L.C.—Library of Congress, Division of Maps; U.C.—Library of the University of Chicago; O.S.U.—Library of The Ohio State University.

tributions of the nineteenth century and was the inauguration of a new era in mapping. From 1794 until 1801 Smith (1815) made a series of small county maps and then incorporated them into a large map of England. After much delay this map appeared in 1815 in 15 sheets, which covered not only England, but Wales and part of Scotland. Four hundred copies were printed, numbered, and most of them autographed by Smith. The map was colored by hand with 20 colors and showed the location of quarries, mines, and other features by symbols, and all the major formations as delineated by fossils and lithology. Each color was graded from dark to light tints so that the contrast accentuated the contact of adjacent beds. A cross section of the strata accompanied the map. The engraving was done by the famous John Cary. From 1819 to 1824, William Smith issued 21 other county maps of England which were included in his *New geological atlas of England and Wales.*

Early issues of the Transactions of the Geological Society of London have a number of small though noteworthy maps. Holland (1811) made a small hand-colored map of the Salt series in Cheshire near Liverpool. The map is interesting because of its appearance in the first volume of the publication of the Geological Society of London. Thomas Webster (1814) published two hand-colored maps on the *Strata overlying the chalk;* one of the vicinity of the Isle of Wight and the other of the London Basin. He relates both of them to the study of Cuvier and Brongniart on the Paris Basin. A small colored map of the Isle of Man by J. F. Berger (1814) appears in the same volume. J. S. Henslow (1821) made another map of the Isle of Man in discussion of Berger's work. Berger (1816) also made two of the earliest geologic maps of Ireland. One is an excellent hand-colored map of northeastern Ireland which includes part of western Scotland. A good example of early English hand coloring is a map of Durham and Northumberland in eight light-tinted colors made by N. J. Winch in 1814 (1817).

The 1821 volume of the Transactions of the Geological Society of London has an unusual number of excellent hand-colored maps which illustrate the early technique of English hand coloring. W. T. H. F. Strangeways (1821) published a map of the Karelian Isthmus of Russia in eight colors which he had made in 1818, and one on a larger scale of the St. Petersburg area to the south. Both these maps and a third one by the same author will be discussed later. The map of the island of Antigua was made in four colors in 1819 by Nicholas Nugent (1821) and is of interest as one of the earliest geologic maps of the West Indies.

A handsome map of the coal basin of Bristol was made by W. D. Conybeare and William Buckland (1824). The map is 14 by 20 inches and illustrates especially how 11 colors may be used to give a larger

number of patterns by stippling one color with small dots of another color. Though different and darker than the usual light tints of most English maps before 1855, the map has a very pleasing appearance.

Richard Griffith made the first sheet of a geologic map of Ireland in 1815, and other sheets were completed by 1821, but were not printed. A new scale was ordered by the Trigonometric Survey in order to be consistent with other maps, and the sheets were not issued officially until 1839 though they were exhibited publicly in 1835. However, Griffith published the entire map unofficially in his report *Outline of the geology of Ireland* made to the Railway Commission in 1838 (Judd, 1898).

Conybeare (1816) published a map of northeastern Ireland similar to the one by Berger, but on a much larger scale, using Berger's notes. Thomas Weaver (1821) who made a large number of excellent maps, published a large map of *East Ireland* (24 by 16 inches, 10 miles per inch). Nine colors were used, each of light tint, giving a very beautiful and pleasing map.

Author's names do not appear on the maps of early issues of Transactions of the Geological Society of London but may be identified by the articles which they illustrate.

An excellently color-printed geologic map of Ireland was issued in 1878 by the Geological Survey of Ireland under the direction of Edward Hull (L. C.), and a later edition appeared in 1891 (L. C.). The map is 28 by 36 inches on a scale of 1:500,000 and was derived from earlier work of Richard Griffith and J. B. Jukes. A later map by the Geological Survey of Ireland with Grenville A. J. Cole as Director was published in 1921 (L. C.). The map is in 16 sheets on a base map of the Ordnance Survey with a scale of 41 miles to the inch. A reduced map of Ireland by A. M. Davis with printed patterns instead of color appeared as the frontispiece of a book by Cole (1924). The latest map of Ireland is apparently the one made in 1928 by T. Hallissy on the Ordnance Survey base of 1:1,000,000 (L. C.).

John MacCulloch (1816) published a map entitled *Sky* which he had completed in 1813. It has nine colors on a double page (15 by 9½ inches, 3 miles per inch) and was made on a base map by McKenzie. A new map of the same area with the same scale, but with 12 colors, was made in 1817 on a better base by Arrowsmith and shows considerable improvement in map technique and many changes in geology. In 1826 MacCulloch was appointed the first geologist for the Trigonometric Survey and instructed to make the first geologic map of all Scotland. It was completed in 1832 but was not published until 1835. For a long time this was called the Arrowsmith map as the label with MacCulloch's name on it was not attached until later (Judd, 1898).

Adam Sedgwick and Sir Roderick Murchison (1835) made a small hand-colored map of the part of Scotland north of Edinburgh which was presented before the Geological Society in 1828 but not published until 1835. James Nicol made a new map of Scotland in 1846 revising, augmenting, and improving the map of MacCulloch (Judd, 1898). The excellent map of Scotland made by Sir Andrew Ramsey in 1854 was one of his great contributions to geologic cartography in Great Britain. He later served as Director of the Geological Survey of Great Britain.

The famous map of England and Wales by George Greenough was published in six sheets on a scale of 5 miles to the inch, by the Geological Society of London in 1819 (Judd, 1898; U. C.). The map was completed in 1812 and engraved by Thomas Webster, who was the best geologic engraver of that time. Using the work of Conybeare, de la Beche, Buckland, and others, as well as some of his own work, Greenough compiled a splendid map which was used for decades. At first he used a great deal of the private material of William Smith, as it was thought that Smith was not going to complete his long-delayed map. Greenough made a much better map than Smith because it was a compilation and composite of all known information, while Smith's map was entirely from his own material. This does not depreciate Smith's map, however, as it was excellent. The Greenough map was revised and reduced in scale in 1826 (15 miles per inch), reached a third edition in 1865, and is still printed for use. Greenough was very capable at compilation and made an excellent map of India in nine sheets in 1855 using the records of the India Geological Survey (U. C.). He founded the Geological Society of London in 1807 of which the first publication was issued in 1811. The originals of the three famous early maps of England, Ireland, and Scotland by Smith, Griffith, and MacCulloch, respectively, are now preserved by the Geological Society of London in the Science Division of the South Kensington Museum.

A small hand-colored map of England and Wales, according to the Wernerian classification, appeared in a book by Robert Bakewell (1829). Though Bakewell generally followed the Wernerian system, he was for the most part neutral on controversial questions. He recognized and appreciated the work of James Hutton, but continued to cling to his Wernerian ideas and omitted recognition of the work of William Smith, even as late as 1838.

In Sir Charles Lyell's third edition of *Principles of Geology* (1834), volume I contains probably the first published hand-colored map of Europe and one of the earliest paleogeographic maps, showing the distribution of the Eocene in Europe. In volume IV there is a small map of southeastern England showing the Wealden area. In the American

edition of Lyell's book (1841) there is a small hand-colored map of Sicily as well as many other hand-colored ones.

In 1829 Adam Sedgwick and Sir Roderick Murchison (1835) made a hand-colored map with cross sections entitled *Sketch of the structure of the Eastern Alps* which was not published until in 1835. This was a study chiefly of the Triassic beds and was a starting point for the research of others. The sections and the conceptions of tectonics for the Alpine area were correct and fundamental even at that early date. Its influence was no less important than their later work in Wales and western England where the lower Paleozoic stratigraphy was first studied.

The great classic work of Sir Roderick Murchison, *The Silurian system*, appeared in 1838. It contains nine hand-colored plates with 121 cross sections and a splendid geologic map in colors. An additional small map shows the Carboniferous paleogeography for England. This book was part of the basis for the controversy between Murchison and Sedgwick over the lower Paleozoic stratigraphy. De la Beche made a map of Devonshire and Cornwall in 1832 and was therefore a few years ahead of Murchison's publication on that area (Geikie, 1897).

A later volume by Murchison (1853) entitled *Siluria* contains a beautiful and minutely hand-colored map with cross sections of England and Wales. The map is truly a fitting work of art for the important volume and represents the highest development of hand coloring. Two years later chromolithography superseded hand coloring. The exactness of detail, the uniform coloring, and the lack of overlap along boundary lines was a result of the very careful rejection of all imperfect coloring on maps of earlier date, so that by 1853 the colorists were truly skillful, or they could not be employed. The same beauty of technique is on the map of Murchison's work in the province of Perm in the Ural Mountains of Russia, as discussed later (Murchison, 1845). *Siluria* was reprinted in 1867 by chromolithography, but the colors are dark and of poor quality. The third edition appeared in 1872.

The first chromolithographic map of the British Isles was printed in John Phillips' *Manual of geology* (1855) and reprinted in the second edition of 1885. He was a nephew of William Smith and succeeded William Buckland as the second professor of geology at Oxford University. Sir Roderick Murchison and James Nichols jointly made a map of Europe in 1856 in four sheets which was published in Edinburgh as one of the early British chromolithographs (Marcou, 1884). Nichols also made a new map of Scotland in 1846 revising the map of MacCulloch (Judd, 1898). A map of the world, still used extensively, appeared in the textbook by Joseph Prestwich (1888), who succeeded John Phillips at Oxford in 1874.

The Geological Survey of Great Britain was organized in 1835 with H. T. de la Beche as the head. He was succeeded by Sir Roderick Murchison. Sir Andrew Ramsey followed Murchison and made an excellent map of England in 1859 which went through five editions by 1881. Due to the early efforts of these men and the later work of Sir Charles Lyell, Sir Archibald Geikie, J. J. H. Teall, and Sir John Flett, the Geological Survey of Great Britain has issued the most excellent series of maps up to the present. There are over 400 maps of England and Wales, chiefly revisions of earlier surveys, but many of them new. Some of the maps have been through 15 editions. Originally the maps were based on the Trigonometric Survey, later on the Ordnance Survey. Over 100 sheets of the new geological map of Scotland on the Ordnance Survey base were published by 1933. The first sheet was printed in 1871, revised, and reprinted in 1922; other sheets have been revised from time to time.

A book published by Reed (1921) has a series of page-size black and white maps of the British Empire: the Maltese Islands, Egypt, Pretoria, South Africa, Canada, Burma, India, Australia, New Zealand, Jamaica, and Cyprus.

GERMANY

In Germany the first geologic map was made by Füchsel (1762) to accompany his article on the Triassic of Thuringia. He depicted the geology by symbols, letters, and numerals. This work laid the foundation for later stratigraphic geology in Germany and is therefore important. J. G. Lehmann is equally prominent for his work in Thuringia. In 1756 he published several geologic diagrams and cross sections though no true geologic map (Zittel, 1908, p. 35).

The first colored geologic map was made in Leipzig in 1775 by Gottlieb Gläser. Three years later Wilhelm von Charpentier made a large geologic map of an area in Saxony and added to colors additional symbols for veins, dikes, and other features (Zittel, 1908, p. 38). This map was important because it showed the Quader sandstone and was used as reference by many later geologists.

Abraham Gottlieb Werner did much to develop the art of coloring maps. He established the custom of marking the contact boundaries with a deeper hue of the corresponding color in order to accentuate the divisions. This custom is still used and many maps of today are color-printed with the deeper-colored boundary lines.

Von Buch was one of the great geologists of the early nineteenth century and a wide traveler. About 1797 he made a colored map to accompany his geognostic description of Silesia (Zittel, 1908, p. 85) where he had spent his first year after student days. While working on the Triassic of South Tyrol he made a map of that area which was published

in 1822. The first colored geologic map of all Germany was compiled by Von Buch and published in Berlin in 1826 (Zittel, 1908, p. 464). Von Buch edited another map of all Germany in 1832 which was one of the best ever issued and went into five editions by 1843 (Zittel, 1908, p. 63).

A colored map of Thuringia in northern Germany by Johann Freiesleben in 1807 was a very carefully executed map and shows quite an advance in detailed geologic mapping (U. C.; 1807). Ami Boué, who later made the first geologic map of the world, published a series of colored sketch maps in a paper called *Geognostische Skizze von Deutschland,* dated 1829 (Zittel, 1908).

The first edition of *Geognostische Uebersichtskarte von Deutschland, Frankreich, England, und der angrenzenden Laendern* appeared in 1839. It was a compilation of geologic maps made by Leopold von Buch, Élie de Beaumont, P. A. Dufrenoy, and George Greenough. The first edition was hand-colored, but the second edition in 1869 by Heinrich von Dechen was a chromolithograph (L. C.). The 1869 map is in two sheets (each 24 by 34 inches) and includes southern England, France, northern Italy, and western Poland on a scale of 17 miles per inch. This map was important because after its revision in 1880 it continued to be one of the best geologic maps of Germany and is still used considerably. The work of Von Dechen is of note because his influence secured a systematic geologic survey of Germany (Elles, 1931).

Another early map covering all Germany was published in Esslingen by Daniel Volter in 1842. This was a large hand-colored map 52 by 55 inches entitled *Geognostische Wandkarte von Deutschland und den angrenzenden Lænderne* (L. C.). It included the area from Paris to Warsaw and from Copenhagen to northern Italy on a scale approximately 1:1,000,000. The earlier map of 1839 was probably used to some extent by Volter.

The first map published in the Zeitschrift der Deutschen Geologischen Gesellschaft is a beautifully hand-colored map made in 1849. The author's name does not appear on it, but it must be by E. Beyrich, as it illustrates his article (1849). In the same volume Beyrich published another excellent hand-colored map called *Geognostische Karte der Umgegend von Regensburg* (Pl. 5). Both of Beyrich's maps are part of his excellent work on the Cretaceous. Volume 2 has a well-executed hand-colored map entitled *Geognostische Karte des nördlichen Venezuela* by Hermann Karsten (1850).

Probably the first geologic map to be printed in color in Europe is *Geognostische Karte des nördlichen Harzrandes* by E. Beyrich (1851). It was printed by Zeitschrift der Deutschen Geologischen Gesellschaft,

and has 10 colors giving 23 patterns by the use of ruled lines and stippling.

Another early color print is *Uebersichtskarte des östlichen Thüringer Waldes* by Von Richter (1851, Pl. 20). This map is unique because of its association with two other illustrations which together represent the three phases in the advance of geologic map publication. The map immediately preceding, by Ernst Boll (1851, Pl. 19), is black and white, with rules and symbols, of an area in Mecklenburg. The print following (Pl. 21), though not strictly a map, is a hand-colored cross section. These illustrations show respectively, the old, new, and intermediate methods of reproduction in quantity.

Several other maps in early volumes of the Zeitschrift der Deutschen Geologischen Gesellschaft deserve mention. A chromolithographic map and cross sections of part of Turkey by Von Schlehan (1852) appeared in volume 4 under the name *Plan der nordküsten Anatoliens.* Volume 5 for 1853 has two small color-printed maps, one on the Kupferberg area in Silesia by Von Websky (1853, Pl. 9) and *Uebersichtskarte des Herzogthums Coburg* by Von Schauroth (1853, Pl. 15). Ferdinand Roemer published a color-printed map on the Cretaceous in Westphalia entitled *Geognostische Uebersichtskarte der Kreidebildungen Westphalens* (1854, Pl. I). He later made a large map of Prussia and Silesia in 12 sheets and one of upper Silesia in 1867.

C. W. von Gümbel, who was an authority on the Mesozoic deposits of South Tyrol and Bavaria, issued in 1861 a map of Bavaria in five sheets dealing with the Alpine Triassic (Zittel, 1908, p. 480). In the paper accompanying the map he enlarges upon his idea of the Vindelic Chain of the Ancestral Alps. Von Gümbel was prominent in Germany as Director of the Bavarian Geological Survey and as a paleontologist.

Melchior Neumayr (1890) published a very interesting colored map of the Alps in his book *Erdgeschichte.* A series of paintings made by W. H. Holmes of scenes in western United States are reproduced in color in the same volume. These had first appeared in publications of the U. S. Geological Survey (Dutton, 1882) and were reprinted in Germany. They are very excellent, being somewhat more distinct than those printed in America, but otherwise very similar.

A geological map of Germany in 27 sheets by Richard Lepsius appeared in 1894 (L. C.). The sheets measure 19 by 17 inches and are on a scale of 1:500,000. Since 1921 maps of Germany in sheets on a scale of 1:200,000 have been issued by the Preussischen Geologischen Landesanstalt (L. C.). The sheets of the geologic map of Europe compiled by W. Schriel from 1931 to 1937 also serve as an excellent map of Germany, and the Justus Perthes map of Europe has a similar value (L. C.).

Geologic cartography in Germany became well developed since the many problems of the Alpine regions, the complexities of the Mesozoic strata, and the mineral deposits gave a great opportunity and stimulus for study and required maps to show the geology. Many of the same men exerted their efforts in Russia, Austria, and the Balkan States.

SWITZERLAND

The Swiss have been prominent in the development of maps on Alpine geology. De Saussure, the "Father of Alpine Geology," made a map of his travels in the Alps, using symbols for dip and strike, but it was not a true geologic map. He is best known for his writing of *Voyages dans les Alps* (1779). He was the first person to use of the term geology in publications, but the term geognosy continued for several decades.

Ebels (1808) published a paper on the structure of the Alpine mountain system and accompanied it with a map of the Alps and numerous cross sections. The article is important, not only for its early date and great value to structural geology, but also because the author did not follow the orthodox Wernerian classification of rock formations. His observations did not permit structural interpretation according to the Wernerian ideas, and he courageously did not follow the existing concepts.

A geologic map of Switzerland was published by Bernhard von Studer and Arnold Escher von der Linth in 1853 (L. C.). The map is 40 by 30 inches on a scale of 1:380,000. It is unusually well executed in light colors and is an excellent example of the early efforts with chromolithography. Without close examination it is difficult to distinguish whether the map is a color print or an excellent example of hand coloring. The map was reduced one half and reprinted in 1855.

Maps by J. M. Zeigler and Isadore Bachmann appeared in 1864 and 1867 (Royal Geog. Soc., 1882). In Zürich in 1878 Albert Heim published two maps, lithographed by himself, of a complicated structural area. This famous work is entitled *Untersuchungen über des Mechanismus der Gebirgsbildung* (Zittel, 1908, p. 312).

Geognostische Karte des Sanct Gotthard by Karl von Fritsch in 1873 illustrates the early combination of contour lines, color printing, and ruled and stippled patterns (L. C.). Another map of the St. Gotthard area is a set of 10 sheets by F. M. Stapff made in 1885 on a scale of 1:25,000 showing the geology along the route through the St. Gotthard area. A colored profile accompanying the map adds to its interest (L. C.). *Carte des anciens glaciers de la Suisse,* printed in color in 1883, shows the lines of flow and the distribution of the extinct glaciers in Switzerland

(L. C.). There are four sheets on a scale of 1:250,000, each sheet being 28 by 20 inches on the inside border.

A geological map of all Switzerland was made by A. Franke in 1904 (U. C.). The most recent map of Switzerland appeared in 1932 as *Einführung zur geologische Wandkarte der Schweiz* by Walter Staub (L. C.). The map is about 60 by 80 inches on a scale of 1:200,000 and has bright heavily printed contrasting colors, much like the maps printed by Justus Perthes.

SOUTHEASTERN EUROPE

Wilhelm Ritter von Hardinger established the Imperial Geological Survey of Austria-Hungary in 1849 (Woodward, 1911). A systematic survey was introduced, and by 1871 a geologic map of the empire of Austria-Hungary was completed under the direction of Franz Ritter von Hauer, who succeeded Von Hardinger. The map is entitled *Geologische Übersichtskarte der Österreichische-Ungarischen Monarchie* and was printed in Vienna in 12 sheets on a scale of 1:576,000 (L. C.). The printing was in color with colored ruled lines overprinted to give additional differentiation of formations. Part of Italy and a large area of the Balkan States then under Austrian rule are included. Work for the map was done from 1850 to 1865 with contributions by Franz Foetterle, Ferdinand von Hochstetter, Edmund von Mojsisovics, Melchoir Newmayr, and Ferdinand von Richthofen, all of whom published other maps individually, some of which are listed elsewhere. Through the efforts of Von Hauer, the Austrian Survey was responsible for a great extension and development of paleontology and Alpine geology. The extent of the empire of Austria-Hungary of that date accounts for the lack of early geologic maps of the Balkan countries.

The Mountaineering Club of Tyrol and Vorarlberg published a geognostic map of Tyrol in 1849 (Zittel, 1908, p. 469). Though not of great importance, the map is interesting because of its early date and because it was published outside the usual geologic channels.

In 1879 the Austrian Survey published a colored map of six sheets by Edmond von Mojsisovics on the dolomite reefs of South Tyrol (Zittel, 1908, p. 250). A special geologic map for military use was printed in Vienna in 1898 by the Austrian Survey, under the direction of Guido Stache (L.C.) The entire map contains 460 sheets and includes the greater part of southeastern Europe under Austrian rule.

An early geologic map of Turkey in Europe and part of Greece (about 17 miles to the inch) was made by G. Palma in 1814. A map of part of southeastern Bulgaria by G. Bontcheff was printed in 1903. The Ministry of Business and Agriculture published in Sofia a colored map by

Lazar Vankov of the Principality of Bulgaria in 1905 (L.C.). A colored geologic map of Albania on a scale of 1:200,000 by Ernst Nowack and Franz Nopcsa was issued by the Albanian government from 1922 to 1924 (L.C.). In 1931 a colored map of Czechoslovakia (30 by 13 inches, scale 1:1,250,000) was issued in *Atlas de la République Tchécoslovague* (L.C.).

RUSSIA

W. T. H. F. Strangeways (1821) published the first map on Russia. This was entitled *Map of the River Voxa and Lake Souvando,* and it covered the Karelian area in southeastern Finland. The map is page size (9½ by 7½ inches) with eight colors in light tints. In the same volume he published a large-scale map of St. Petersburg and vicinity in four colors (1821a). Both maps are excellent examples of hand coloring. The first map of all of European Russia was completed by Strangeways in 1821, but not published until later (1824). The map is 25 by 18 inches and includes the southern parts of Norway, Sweden, and Finland up to Lat. N. 65°. No scale is given, but it is about 100 miles per inch. Twenty-one color combinations are used, but there are broad areas on the map without color which are labelled boulders and gravel that today would probably be mapped as glacial material. Areas mapped as sand hills also appear without color. Strangeways did not present the map as a completed work because he called it a sketch to serve as a basis for a geological map of Russia.

The famous work of Murchison, De Verneuil, and Von Keyserling in Russia appeared in 1845. Murchison went to Russia in 1841 and with the others worked out the stratigraphy of the Permian system in the Ural Mountains. The report was published in England and contains the finest hand-colored geologic map examined and is probably one of the finest of all time (Murchison *et al,* 1845). Minute patches of gold represent deposits of gold, and one has to examine the map very closely in order to determine whether the map is hand-colored or chromolithographed. Not only is the map excellent, but the geology is shown in much detail, and the map is reported as still dependable in most of its details. Another map of Russia was made by Murchison, Von Gelmerson, and Muller on a scale of 1:7,350,000. The date is not given, but as it is a chromolithograph it probably appeared about 1855-1860 (L.C.).

An excellent hand-colored map of the mining districts of Russia was issued in 1849 (L.C.). The map also includes Finland, Norway, Sweden, and part of the Balkan area. A map of the Caucasus was published by K. Koch in Berlin in 1850 and one of the Crimea by T. B. Jervis appeared in 1855 (Royal Geog. Soc., 1882). Valerian de Moller published a chromolithographic map of the portion of Russia west of the Ural Moun-

tains in 1869 (L.C.). The map measures 18 by 47 inches with a scale of 1:840,000. An excellent color-printed map of Russia compiled from several sources appeared in 1892.

In 1897 the Seventh International Geological Congress met in St. Petersburg, and the Committee issued a handsome colored map of European Russia to accompany the guidebook. The book also contains several maps of smaller areas printed in black and white.

A colored map of Russia in 139 sheets was printed between 1884 and 1904 by the geologic committee of the International Congress (L.C.). D. V. Nalivkin compiled a map of European Russia on a scale of 1:7,000,000, which was printed in St. Petersburg about 1903 (L.C.). In 1922 the Comité Géologique issued a map of Asiatic Russia which included most of European Russia. The map measures 34 by 26 inches and has a scale of 1:10,500,000 (L.C.). The most recent maps on Russia are in a folio by the U. S. S. R. for the Seventeenth International Geological Congress, which met in Moscow in 1937.

SCANDINAVIA

The map of West Gothland made by W. Hisinger in 1797 is thought to be the earliest geologic map of any part of Sweden and is also one of the earliest of all geologic maps. East Gothland and other areas were mapped by Gustaf Hermelin from 1797 to 1807 (Zittel, 1908, p. 117).

The Geological Survey of Sweden was organized in 1858, and that of Finland in 1865. These organizations initiated a systematic co-ordinated geologic survey, and the maps were issued continuously until the entire area was completed. The first sheet of the Sveriges Geologiska Undersökning was a chromolithograph issued in 1861. By 1933 over 170 sheets of the geologic map of Sweden had been issued, many of them being revisions. Much of the mapping was done by A. Erdman, Albert Blomberg, and Gerard de Geer.

Among the geologic maps of special interest is one of eastern Sweden, 15 by 9 inches, on a scale of 1:200,000. It was printed in 1870 on a very heavy paper or light cardboard with a red overprint and symbols for the differentiation of formations (L.C.).

A map of the geology in southeastern Sweden was printed in 1884 on a scale of 1:1,000,000 in two sheets, each 23 by 30 inches (L.C.). A map showing the glacial moraines over all Sweden was published in 1898 with a scale of 1:2,000,000 (L.C.). A map for all Sweden was issued by the Sveriges Geologiska Undersökning in 1901 (L.C.). It was printed in two sheets, each 24 by 23 inches, with heavy bright colors. The scale is 1:1,500,000.

Early maps of the geology of Finland may be seen on the Russian maps issued before Finland became independent. A recent map of Fennoscandia (9 by 10 inches) was published by J. J. Sederhölm (1932).

A map entitled *Geologisk Karte over det Sondenjeldske Norge* for southeastern Norway was made between 1858 and 1865 by B. M. Keilhau for the Norwegian Department of Interior (L.C.). It is in 10 sheets, each 17 by 18 inches, and is printed on a light cardboard base in dull colors.

The Norge Geologiske Undersogelse published its first colored sheet in 1869. All sheets for the country were completed or nearly so by 1899. In 1877 the Norwegian survey issued a map entitled *Geologisk Oversigtskart over det Sydlige Norge* (L.C.). This was printed in Christiania on a scale of 1:1,000,000 and has light-tinted colors with a very fine stippled appearance as if the ink had flocculated, but such does not lessen the attractiveness of the map. The same map was revised in 1915 and reprinted with a more uniform register of color (L.C.).

A geologic map of southern Norway was compiled by Charles Lapworth from the works of Th. Kjerulf, W. C. Brögger, and H. Reusch (L.C.). It is published in color in 1890 by the Edinburgh Geographical Institute for use on a geological excursion to Norway. The map measures 13 by 8 inches on a scale of 32 miles to the inch. It is an excellent example of color printing.

A colored map of Denmark entitled *Carte géologique de Danemarc* was made by G. Forchhammer in 1865 (L.C.). The geology is shown on a base map 35 by 44 (scale 1:480,000) made by Olsen in 1857. The copy seen was hand-colored and had the legend written in longhand. One of the most recent maps of Denmark was made by J. P. J. Ravin in 1922 on a scale of 1:5,000,000 (L.C.)

MISCELLANEOUS EUROPEAN MAPS

Information on maps of other countries in Europe is difficult to find. The empire of Austria-Hungary in southeastern Europe explains the lack of maps of countries which later became independent.

W. C. H. Staring published a geologic map of Netherlands in 1858 (L.C.) and a later one in 1867 (Royal Geog. Soc., 1882). Italy was not unified until the latter part of the nineteenth century. The maps of central Europe by Heinrich von Dechen in 1839 and 1869 and by Daniel Volter in 1842, as mentioned previously, show Italy north of Florence. An early map of Italy and adjacent areas (24 miles per inch) was published in Paris by H. de Collegno in 1846 (Royal Geog. Soc., 1882). In 1863, L. Torelli published in Florence a large-scale map of the western part of Tuscany (Royal Geog. Soc., 1882). The Italian Geographical

Survey issued a map of Italy (scale 1:1,000,000) by several authors in 1881 and a more recent one in 1931 (L. C.).

One of the earliest maps known was one of the Pyrenees Mountains made by Abbé Palassou in 1782 (Zittel, 1908, p. 102). The map is in eight sheets with the information, chiefly mineralogical, shown with symbols. In 1849 E. P. de Verneuil and E. Collomb made a map of Spain and Portugal. A colored map of Spain and Portugal in 16 sheets by Manuel Fernandes de Costro was published by the Ministry of Works in 1889. Each sheet is 21 by 30 inches on a scale of 1:400,000 (L.C.). The 16 sheets were reduced to a scale of 1:1,500,000 on a single sheet 25 by 34 inches and reprinted with a much better color register in 1893 (L.C.). A small colored geologic map of Spain and Portugal is in the Enciclopedia Universal Illustrada (1924, vol. 21). The best recent map of Spain and Portugal was made in 1932 by Luis de la Peña y Braña, and printed in Madrid by Instituto Geologico y Minero de España (L.C.). The map is on a scale of 1:1,000,000 in four sheets each 30 by 22 inches. The same map was reissued on a scale of 1:1,500,000 in 1934 but it has poor color, poor engraving, and is in every way inferior.

CONTINENTAL EUROPE

The hand-colored map of Europe in Lyell's (1834) *Principles of geology* was probably the first published. Another early one by Sir Roderick Murchison and James Nichols appeared in 1856 (Marcou, 1884). It represents the first map of Europe printed by chromolithography. A geological map of Europe (about 200 miles per inch) by H. Habenicht was printed in Gotha in 1876 (Royal Geog. Soc., 1882). Another one by William Topley and J. G. Goodchild, under the direction of Joseph Prestwich, was printed in London in 1888 by the Oxford University Press (L.C.). The map measures 22½ by 17½ inches and is on a scale of 150 miles to the inch. The colors are dark and some colors are overprinted with stippling or ruled lines. A smaller map in solid color on a scale of 250 miles to the inch, printed by Stanford of London, was probably derived from the map of Prestwich (L.C.).

Most of the nations of Europe had geologic maps completed by 1850 but all with different scales and color schemes. Revisions and new ones were combined at the end of the century into *Carte géologique internationale d'Europe* (1:1,500,000) on which a standard color scheme was used.

An excellent color-printed map of Europe with a transparent overprint showing structural lines was made by F. Beyschlag and W. Schriel in 1925 (U.C.). The detail is excellent, and it is a very convenient map, because of the size; about 18 by 24 inches. The large geologic wall map

of Europe (79 by 64 inches, scale 1:3,000,000), compiled by Richard Rein and printed by Justus Perthes, is a very excellent map with heavy contrasting colors characteristic of that printer (L.C.). The new large-scale map of Europe being compiled by W. Schriel for the International Geological Congress is incomplete. The map is in sheets 20 by 19 inches on a scale of 1:1,500,000 and until the start of the war in 1939 was being color-printed in Berlin by the Preussischen Geologischen Landesanstalt. The sheets printed to date were issued from 1931 to 1937 (L.C.). This is a revision of an earlier map by Beyschlag completed in 1913. A small map of Europe 8½ by 13 inches, exclusive of the northern half of Scandinavia and Russia, was printed in Bartholomew's (1936) atlas on a scale of 1:15,000,000. An excellent small map of central Europe with 26 colors on a scale of 1:3,500,000 was compiled by Von Köcher from the international map of Europe and published in Andrees' atlas (1930).

MAPS OF ASIA

A small uncolored sketch map of Japan was published by Godfrey (1878) with his paper *Notes of the geology of Japan.* A year later under the leadership of E. Nauman, the Imperial Geological Survey of Japan was organized with T. Wada as the director (Zittell, 1908). Probably the first map issued by the new geologic survey was one made by B. S. Lyman, Chief Geologist, and others in 1882 (L.C.). The map measures 42 by 68 inches on a scale of 1:60,000 and shows mineral and oil locations without the use of color. The Survey issued a complete map of Japan in colors in 1899, which was reprinted in 1926 (O.S.U.). A map of the Japanese Empire on the international scale of 1:1,000,000 in 15 sheets was printed in 1902 (L.C.). Under the directorship of Inouye, the Survey published in 1911 a colored map of the Japanese Empire made by Kinosuhe (L.C.). The legend and title are in English and Japanese, as are many other Japanese maps. The five sheets are each 24 by 22 inches with a scale of 1:2,000,000 and were printed in Tokyo. The map is of interest as an example of Japanese lithographic work. The second edition was issued in 1922. Also from 1911 to 1916 a set of geologic maps on a scale of 1:400,000 was printed for parts of Japan. From 1921 to 1931 still larger-scale maps were printed in color on scales from 1:15,000 to 1:30,000 (L.C.). These are on contoured base maps and show in more detail some of the oil land of Japan

Pumpelly made a *Hypothetical map of China* which was published in 1866. He had traveled extensively in China and probably knew more about the geology of China than any other man of his time. He indicated the lack of information by entitling the map a hypothetical one.

Willis (1907) presented several colored geologic maps, colored isostatic adjustment maps, and paleogeographic maps in his book on research in China.

The National Geological Survey of China was initiated in 1917 shortly after the arrival of Amadeus Grabau, and maps and information on China began to appear in quantity. A number of new maps have appeared since 1920, all by Chinese geologists, and many of them on the "Millionth" international scale. Many of the provinces are covered with contour maps made in the last 10 years by the direction of the General Staff of the Chinese Army, and with these geologic mapping can advance rapidly.

A colored geologic map of Asiatic Russia and most of Russia in Europe was issued in 1922 by the Thirteenth International Geological Congress held in Brussels. The map is 26 by 34 inches on a scale of 1:10,500,000 (L.C.). The Congress also issued in 1922 a tectonic map of Eurasia made by Émile Argand which was reprinted in 1928 but was reduced to 1:25,000,000 from 1:8,000,000 of the original (L.C.). An excellent colored map of Russia in Asia by a dozen or more authors was published in 6 sheets in 1925. This map *Carte géologique de la partie asiatique de l'Ursas* was issued with French and Russian legends and titles (O.S.U.). A similar map for Turkestan was published by the Comité Géologique of the International Geological Congress in Leningrad in 1928 (O.S.U.). It was compiled by V. N. Weber and D. Nalivkin in 1925 from maps by several authors, and has a scale of 1:6,800,000 on a sheet 40 by 30 inches. Twenty colors supplemented by overprints give 32 divisions. The colors are dark and contrasting but give a very good general appearance.

Several colored maps of Mongolia by C. P. Berkey and F. K. Morris (1932) appeared in volume II of the Central Asiatic Expedition under Roy Chapman Andrews.

A geological map of parts of Bundelcund and Boghelcund in India was published in England by Capt. James Franklin of the Bengal Cavalry (1835). The Indian Branch of the Trigonometric Survey was established in 1811, and the Geological Survey of India was organized in 1848 with John McClelland as the first director. He was succeeded in 1850 by Thomas Oldham formerly of the Irish Branch of the Trigonometric Survey. A large hand-colored map of the entire Peninsula of India was compiled from maps of the Indian Survey, records, and other sources by George Greenough in 1855 (U.C.). This was an important contribution, as it was the first map of all India. A geologic map of the western part of Nagpur Territory in central India was published by S. Hislop and R. Hunter (1855). This was one of the early chromolithographs printed in England and it poorly registered with dark and imperfect colors. An early map of western India and southeastern Arabia was

published by H. Carter in Bombay in 1857 (U.C.). In 1877 a colored map of all India in four sheets on a scale of 64 miles to an inch was issued by the Geological Survey of India. The map is of interest since it was engraved and printed in Calcutta (L.C.). The textbook by Dosabhai Wadia (1939) contains several black and white geological and structural maps of various parts of India which were taken from maps made by several men and from the records of the Geological Survey of India. A large wall map of India and adjacent areas, 84 by 76 inches, was printed in 8 sheets with a scale of 32 miles to the inch in 1931 by the Geological Survey of India. This was the fifth edition and is probably the most recent map of India (L.C.).

One of the early color prints was a map of part of Turkey entitled *Plan der nordküsten Anatoliens* by Von Schlehan (1852). A geologic map of the Turkish-Persian frontier by W. K. Loftus (1855), as mentioned before, was published in London. P. A. Tchihatchef published in Gotha a geologic map made in 1866 of parts of Asia Minor (Royal Geog. Soc., 1882).

Over 72 sheets of geologic maps of Java have been issued by the Netherlands government within the last ten years. The sheets are 14½ by 14½ inches measured on the border lines and have a scale of 1:100,000. Similar maps for Sumatra on a scale of 1:200,000 have also been made (L.C.).

MAPS OF AUSTRALIA AND NEW ZEALAND

Many maps of Australian geology were issued by the geological surveys of the Australian states. The first ones are grouped from 1872 to 1875. A map of Western Australia by H. Y. Brown was published in Perth in 1872 and a map of Victoria (15 miles per inch) by R. B. Smythe appeared in 1873 (Royal Geog. Soc., 1882). R. B. Smythe also made a map of Australia and Tasmania (94 miles per inch) which was published in Melbourne in 1875. Another map of Victoria was made by H. Y. Brown in 1888 and was followed with one by R. A. F. Ramsey and James Stribig in 1902 (U.C.). A map of New South Wales was published in London in 1873 by Jules Joubert (Royal Geog. Soc., 1882). In 1931 Sir Edgeworth David published a complete map of all Australia, Tasmania, and New Guinea from a compilation of all preceding maps and his own work (U.C.).

A year before the Geological Survey of New Zealand was established, Von Hochstetter (1864) published an altas of geologic and topographic maps of New Zealand. James Hectar published a map of New Zealand in Wellington in 1873 (Royal Geog. Soc., 1882). Many more recent maps have been issued by the Geological Survey of New Zealand.

MAPS OF AFRICA

Early maps of parts of Africa include two of Nubia by G. Russegger printed in Stuttgart, and one of Angola made by J. B. d'Andrade in 1858 (Royal Geog. Soc., 1882). The one of northern Nubia is dated 1843 and southern Nubia 1846.

Andrew G. Bain (1852) published what is believed to be the first geologic map concerning South Africa. This was chiefly of the southern tip of Cape Colony. Another early map is an excellent color print of Natal made by Greisbach (1871). Much geologic work had been done by private companies before 1852, and since then there have been many maps of small areas by private companies dealing with diamond, gold, or other economic deposits.

Before the union of the British South African colonies, the Geological Survey of Cape Colony issued from Capetown many excellent color-printed geologic maps. Sheet 1 appeared in 1907, and sheet 52 in 1908, most of the work being done by A. M. Rogers, Alexander du Toit, and L. Swartz (O. S. U.).

A small map of South Africa appeared in the book by Hatch and Corstorphine (1905). Alexander du Toit (1926) published a splendid small colored map of South Africa to accompany his book on the geology of South Africa. It was reduced to a scale of 1:5,000,000 from the International Map of South Africa and shows the area from the Zambesi River to the border of Angola. The book contains many other small geologic maps in black and white. Du Toit published the second edition in 1937.

Over 150 sheets of geologic mapping on the International scale of 1:1,000,000 had been issued up to 1937 from Pretoria by the Geological Survey of South Africa. These were mapped chiefly by or under the direction of Alexander du Toit and S. H. Houghton (O. S. U.).

A colored geologic map of Africa in several sheets was printed in 1932 for the International Geological Congress. The map was compiled by W. Schriel and printed by the Preussischen Geologischen Landesanstalt (L. C.).

Other published maps of Africa include the Belgian Congo by F. Kelhaye and M. Sluys in 1923, Angola by F. Morita and H. O'Donnel in 1933, and several color sheets made by the Survey Department of Egypt in 1910 (O. S. U.).

MAPS OF BRITISH AMERICA

One of the earliest maps of British America was made of the north shore of Lake Huron in 1820 by J. J. Bigsby (1821) and published in the American Journal of Science. The map is very small, hand-colored

in green and brown, and crowded on a half page with other illustrations at the rear of the volume. Bigsby (1824) made a larger and more detailed map of the same area which was published as a fold-in sheet by the Geological Society of London.

Another early hand-colored map was for a part of Nova Scotia by C. T. Jackson and Francis Alger (1828). This was followed by one of the same general region by A. Gesner (1836) and others by J. W. Dawson in 1845, 1847, and 1855. Gesner's name appears as author on the light-tinted hand-colored map published by Dawson (1845) on which Dawson has inserted some additional mapping done in New Brunswick.

McCormick (1824) published a map of Newfoundland with geologic symbols in black. Later ones on Newfoundland were made by J. B. Jukes in 1842 and 1843, and others by Alexander Murray appeared from 1861 to 1881 (Marcou, 1884). Many other more recent maps of the Maritime Provinces have been made, but the chief interest in this discussion is in the older maps.

Bigsby (1851) made a very early glacial map of North America showing the trails of erratics from Canada into the United States. He also published an early map of the Lake of the Woods area (1852), and of the province of Quebec (1853). *A geological map of the northernmost part of America* by A. K. Isbister (1855) was one of the first geologic maps produced by color lithography to appear in an English publication. It was very poorly executed with overlaps and gaps in color and far inferior to the excellent hand-colored maps which were typical of English publications up to this date. In contrast, the same publication has a very commendable color print of *Sketch map of the Turkish-Persian frontier* by W. K. Loftus (1855).

The first outstanding map of Canada as a whole was published by W. E. Logan in 1855. It was made to accompany the Canadian exhibit at the World's Fair in 1855 in Paris. The map includes about half of northern United States (Logan, 1855). Logan (1852) had published an earlier map, but it covered only the eastern portion of Canada. Under the leadership of Logan and Dawson the greater part of Canada was covered by numerous geologic maps before 1880, and since that time many large-scale maps have been issued and old ones revised. (*See* Geographical Board under bibliography of source books and catalogues.)

MAPS OF MIDDLE AMERICA

The following is a list of some of the early geologic maps of Middle America:

1821 A map of the island of Antigua made in 1819 by Nicholas Nugent (1821)
1821 Map of Barbadoes by J. D. Maycock (1821)

1829 Map of the eastern part of Jamaica by H. T. de la Beche (1829)
1838 Map of the vicinity of Zinopan in Mexico by H. G. Galeotti (1838)
1846 Map of the copper region of Cuba by R. C. Taylor (1846)
1850 A very interesting colored map of Panama was made by an unknown author for the benefit of the goldseekers going to California, possibly in the hope of detaining a few for gold prospecting in Panama (Marcou, 1884)
1855 Map of Nicaragua by F. Ferrer. (*See* Library of Congress, 1904, under bibliography of source books and catalogues.)
1865 First geologic map of Guatemala and Salvador by August Dolfuss and Eugene Montserrat (Marcou, 1884)

The geology of Mexico and Central America may be observed on the colored map of North America prepared by Bailey Willis for the International Geological Congress held in Mexico City in 1906. The map is approximately 60 by 80 inches on a scale of 1:5,000,000 and is printed in French (L.C.). The U. S. Geological Survey map of North America compiled in 1911 by Stose and Willis is a revision of the same map (L.C.).

MAPS OF SOUTH AMERICA

Maps of South America are well listed by Marcou (1884) and Sullivan (1922). Some of the early and outstanding maps are discussed.

Probably the first map on South America was a small map by M. de Rivero on the Pasco mine area in Peru. It was made in 1827 in five colors and reprinted in the American Journal of Science (Rivero, 1830). Another early one was made in 1839 on the southern part of Antioquia Province, Colombia, by Carl Degenhardt (1839).

Early geologic mapping in Chile is well represented. Ignace Domeyko published in 1840 an uncolored map, 7 by 4 inches, of a small area near Coquimbo. The map is on a scale of 10 miles to an inch, and patterns of line rulings differentiate the areas. A larger more important map of most of Chile was made by Ignace Domeyko (1846) entitled *Carte Géologique et minéralogique du Chili*. The map is 7 by 18 inches on a scale of 1:8,000,000 and is not colored but has ruled patterns. Two years later he made another interesting page-size map of the vicinity of Coquimbo showing the ancient shore line of the Pacific Ocean during the Tertiary (Domeyko, 1848). This is one of the earliest paleogeographic maps of South America. Associated with it are a number of sketches and cross sections.

The geologic maps and the extensive report of D'Orbigny (1843) on his travels in South America are a classic publication. It contains the first maps of this portion of the Andes which are important because of the structures shown and the difficulties encountered in exploring and mapping the mountainous area. D'Orbigny's explorations were carried on from

1826 to 1833, but the maps were made from 1835 to 1838. Map I shows Uruguay, most of Argentina to the Andes, and part of Patagonia from about Lat. 31° to 43° S. This map was made in 1838 and is 18 by 19 inches. The light-tinted hand coloring deserves special note. Color has been applied so uniformly over large areas that brush strokes are not observable. Colored cross sections are the second part of the illustrations. Map III is 20 by 27 inches and shows the geology of Argentina from Lat. 27° to 31° S. on a scale of about 14 miles per inch. It was made in 1835 and shows the same excellent hand coloring as the other maps. D'Orbigny also made a map of Bolivia on a scale of 1:1,600,000. Map X made in 1842 is a geologic map of all South America about 12 by 19 inches. The lower right-hand corner has four small maps showing paleogeography which are the first known of that type for South America.

The colored map of Bolivia, part of Chile, and southern Peru made by David Forbes (1861) includes about half of Chile when it was part of Bolivia. Forbes' work corrects some parts of the maps by D'Orbigny. It was printed page size (4 by 7 inches) on a scale of 1:7,000,000. Pissis (1873) published a fold-in map 7 by 17 inches of northern Chile. The map is on a scale of 1:5,000,000 from Lat. 12° to 23° S. and is hand-colored with 11 attractive light tints. A large colored map of Chile in 13 sections was made in 1873 for the Chilean government by Pissis (Marcou, 1884).

Geologic maps of Brazil have been made by several men (Branner, 1919). Claussen (1841) made some hand-colored diagrams and cross sections of the now famous gold area in Minas Geraes Province which were published in Belgium. Pissis (1848) made a map of the Minas Geraes area and a larger map of southeastern Brazil in the same year. One of the best early maps showing Brazil (scale 1:15,000,000) is a map of South America made by Franz Foetterle in 1854 and published in Vienna under the direction of Wilhelm Haidinger (Branner, 1919). The same map on a scale of 1:25,000,000 was published in Gotha (Foetterle, 1856). O. A. Derbey made a map of Brazil on a scale of 1:90,000,000 for Wappaeus' *Geographia physica do Brasil* (1884). A map of all South America by G. Steinmann published by Justus Perthes shows the geology of Brazil on a small scale (Berghaus, 1892). A large map, 73 by 23½ inches, on a scale of 1:12,000,000 was published in 1908 by the Sociedade Nacionale de Agricultura de Brazil (L.C.). One of the best maps of Brazil was published in six divisions in Bolivia by Theodoro Sampaio (1911).

The best map of Brazil was published by Branner (1919). The scale is 1:5,000,000 on a sheet 36 by 39 inches with 13 colors excellently printed

with good register. All of Brazil is shown except for a large uncolored area in the west-central part south of the Amazon River.

One of the earliest maps of Venezuela is a hand-colored one of the northeastern part made by Hermann Karsten (1850). S. P. Wall (1860) published a small map (8 by 11 inches) of Venezuela and Trinidad in the Quarterly Journal of the Geological Society of London. One of British Guiana by J. G. Sawkins (1871) appeared in the same journal. A geologic map of Ecuador appeared in the *Nouvelle géographie universelle* of Élisée Reclus (1893).

Several maps of the entire continent of South America have been published. The earliest one by D'Orbigny in 1843 and the two by Foetterle in 1854 and its revision in 1856 have been mentioned. Martin de Moussy (1873) published a map of South America in Paris (15½ by 19½ inches on a scale of 1:17,000,000). A map of the southern part of South America made by Du Toit (1927) includes the area between Lat. 14° to 39° S. and Long. 38° to 72° W. on a scale of 1:5,000,000. This area includes Uruguay, Paraguay, and portions of Brazil, Argentina, Chile, and Bolivia.

WORLD MAPS

The first geologic map of the world was made in 1843 by Ami Boué and entitled *Carte géologique du globe terrestre* (Marcou, 1884). It is very generalized due to the lack of information. The English edition of Boué's map appeared in Johnston's (1855) *Physical atlas of natural phenomena.* A geologic map of the coal strata of the world was made by Taylor (1848).

As far as is known, Edward Hitchcock (1853) was the first in the United States and the second person in the world to make a geologic map of the world. Hitchcock combined Boué's map, the map of the United States made by Marcou in 1853, and Lyell's 1845 map of Europe and published the compilation in his book *Outline of the geology of the globe.* A map of the United States and Canada, probably derived from Marcou's map, also appears in the same book. The maps were reprinted in the second and third editions.

A geologic map of the world in eight sheets made by Marcou in 1860 was the best map for many years. It was reproduced to accompany the book *La terre* by Reclus (1868). The first edition was not seen, but the second edition (1871) had eight sheets each 18 by 25 inches on a scale of 1:23,000,000 based on the Mercator projection. The map is colored, and the titles are in French and English (L.C.). From 1876 to 1878 Marcou's map was reprinted in English, French, German, Russian, Italian, and Hungarian editions of the book by Reclus.

H. B. Milner's map printed by Stanford in London in 1921 is one of the most recent maps of the world (L.C.). It appears unfinished as there is no printing on it except the legend. Place names, boundaries, and all matter that generally appears on a base map are absent.

The large wall map *Geologische Karte der Erde* printed by Justus Perthes is one of the best known geologic maps of the world (L.C.) and was prepared by Richard Rein for *Physikalische Wandatlas* by Hermann Haack. The map is in eight sheets, each 32 by 20 inches with a scale of 1:20,000,000. The colors are heavy and printed with the contrast characteristic of Justus Perthes' maps.

The Prussian Geological Survey published in 1935 in Berlin a geologic map of the world made by Franz Beyschlag in 1929-1932. This is in 12 sheets each on a scale of 1:15,000,000 (L.C.).

A small map of the world appears in Bartholomew's *Oxford advanced atlas* (1936). The map is only 18½ by 8½ inches and on such a scale that the colors indicate only geologic periods.

In 1932 the International Geological Congress sponsored a new geologic map of the world on a scale of 1:5,000,000. W. Schriel was assigned to the compilation of it, and the printing was assigned to the Prussian Geological Survey. Only a few sheets—chiefly for Africa—of the 80 sheets were completed by 1939. The appearance of future sheets will depend on the conditions after the current war.

DEVELOPMENT OF GEOLOGIC MAPS IN THE UNITED STATES

FIRST PERIOD, 1809–1842

The first geologic map of any portion of North America was published in Paris by Jean Guettard (1752). His map includes the area east of the Rocky Mountains from the mouth of the Rio Grande to slightly above the Arctic Circle. The map is 10½ inches long by 12½ inches wide, and though no scale is given it is about 310 miles per inch. An insert in the lower right-hand corner shows the St. Lawrence River area on a larger scale. Map symbols locate 39 types of deposits such as iron, silver, pyrite, copper, clay, talc, schist, granite, lead, quicksand, oil, and fossils.

An almost exact copy of Guettard's map was printed in English in 1757 in volume I of the *Literary Magazine* (L.C.). The title of the reprinted map is *A map of North America showing the places where metals, numerous fossils, and medicinal waters are to be found.* Labrador is named New Britain, Rivière de Hays is called Nelson, and many other place names are changed or omitted. The insert on Guettard's map is absent. A reproduction of this map was published in London by Fuller (1760) to illustrate a book of travel.

An anonymous map made about 1750 portrays two interesting geologic features, though the map itself is not geologic (L.C.). "Sea Coal" is indicated near "Quemahonning" east of the present Pittsburgh and near "French Margaret" east of the present Coshocton, Ohio. The name "Mouskinoome" is interesting as the origin of the present name for the Muskingum River. "Sea Coal" was a term used in Europe for Welsh coal transported from Bristol by sea, and the term was used similarly for coal found in America.

Although not geologic maps, some of the early maps of the colonies are interesting because of the geologic information on them (Bloom, 1937-1938). The map of Connecticut made by Bernard Romans in 1777 shows some hills with "mines" above them, north of Simsbury, near the Massachusetts line, a few miles west of the Connecticut River. The mines are reported to have been used as prisons during the Revolutionary War. An early map of Kentucky made by John Filson in 1784 has "a fine Lead Mine" noted at the base of the sheet on a spot between the Green and Cumberland rivers. Many salt licks and springs are also indicated on the map. On the northern part of a map made by Bernard Ratger in 1769 and revised in 1778, which includes New Jersey, is printed the name "Sterling Iron Works." This was the source of the iron for the great chain placed across the Hudson River during the Revolutionary War. A map of the United States in 1783 by Abel Buell has the term "Extensive Beach ridge" in the central part of what is now Ohio. Today this is recognized as a glacial moraine. The same map has "Coal" indicated south of the Ohio River at the mouth of the Muskingum River. A map of Virginia and adjacent areas compiled by Thomas Jefferson in 1787 has "coal" and "freestone" located near the present Hocking River (then the Hochhocking) in southern Ohio.

The history of geology in America is considered to have begun with the map of eastern United States by William Maclure (1809; L.C.). The geologic information was overprinted on a base map of the United States by Samuel G. Lewis and then hand-colored. The rock formations were classified according to the Wernerian system, because Maclure had been a student of Werner. The map measures 21½ by 17 inches and includes the area east of the Mississippi River from Florida to the Great Lakes. The same map was reprinted in France by De la Métherie (1811; L.C.). Because of his place in early American geology, Maclure has been called the "William Smith of America."

A revised edition of Maclure's map, on a new base by John Melish, was issued in 1818 (L.C.). The geologic subdivisions are hand-colored and placed on a much better base closely resembling modern engraved

maps. The State boundaries and mountains are more distinct, and more detail is shown by the location of towns and Indian areas. This map is smaller than the original, being 17 by 13 inches with about 1 inch representing 93 miles.

Parker Cleaveland reproduced Maclure's map with his own modifications in the first geologic textbook to appear in America (1817; 1822).

Reproductions of Maclure's original map may be seen in a reduced form in Merrill's (1906; 1927) books on the history of American geology.

Edwin James, the geologist for the Long Expedition, published a map in 1822 which showed the area west of the Mississippi River to the Rocky Mountains. This map continued to be the most reliable map for that area during the succeeding 2 or 3 decades (Merrill, 1927).

A number of small hand-colored maps appeared in the early volumes of the American Journal of Science organized in 1818 by Benjamin Silliman at Yale University. These maps are of interest because of their early date and their appearance in an American journal. Two maps by Edward Hitchcock (1818) appear in volume I: one of western Massachusetts along the Connecticut River and another of northwestern Massachusetts. A map of J. F. and S. L. Dana on the vicinity of Boston is reported to be in the same volume but was not found (Merrill, 1906). Volume 3, issued in 1821, has a small half-page map of the northwestern shore of Lake Huron by J. J. Bigsby. Zachariah Cist (1822) published a map showing the range of anthracite coal formations by means of dashed rulings.

Hitchcock made an important contribution to the advance of American geology when he published his paper on the Triassic formations of the Connecticut River valley (1823). The map accompanying it will be described later in discussion of Hitchcock's work on maps. The 1824 volume of the American Journal of Science has another map by Hitchcock (1824) of Martha's Vineyard.

John Finch (1824) published a small map of the area around Easton, Pennsylvania, in 1824. In the same volume Chester Dewey (1824) of Williams College published a map of western Massachusetts adjacent to the area mapped by Hitchcock.

The map of the gold area in south-central North Carolina by Elisha Mitchell (1829) is one of the few maps having the old Wernerian classification, which was being abandoned about that date. A later map, still continuing the use of the Wernerian classification, and therefore of interest, is *On watercourses, and the alluvial and rock formations of the Connecticut River valley* made by Alfred Smith (1832). The same volume contains a map by Edward Hitchcock which is the first geologic map of an entire State.

The map of the Pasco mine area in Peru made by M. de Rivero in 1827 was reprinted in the 1830 volume of the American Journal of Science (Rivero, 1830).

A geological map of the United States, known as the Hinton map, was printed in London in 1832 (L.C.). The base map (15 by 10 inches, no scale) includes all the United States, but the colors representing the geology did not extend far beyond the Rocky Mountains and stopped at the Red River boundary of Mexico. The map is important in extending geologic mapping beyond the Mississippi River, but it is chiefly after Maclure's maps and continues the obsolete Wernerian classification of rock formations.

Featherstonehaugh in 1834 made a colored geologic cross section from New Jersey to Texas and included with it a map of the traverse. Though not strictly a geologic map, the cross section was an important contribution and was one of the first in America to have the Murchison system of nomenclature for rock formations. Featherstonehaugh's work (1835) was the first to be done by the direction of the United States Government.

The first geologic survey by a State was inaugurated in North Carolina by Denison Olmstead in 1824. A year later, South Carolina followed with Lardner Vanuxem as State Geologist. These surveys did not continue long and should not be considered as true functioning surveys. Massachusetts was the third State to organize a survey and the first to make important contributions to the advance of geologic knowledge. Edward Hitchcock initiated this survey in 1830 and published the first State map of Massachusetts two years later (1832). Next, Tennessee established a State survey, and Gerald Troost, the State Geologist, issued a map of the State in 1839.

Fifteen State geological surveys were organized before 1840. These organizations produced a large number of maps during the following years, although some of the surveys were discontinued. Other states organized new surveys, and several of the old ones were revived after 1840 (Merrill, 1920). The colored map of South Carolina by Oscar Lieber was issued in 1855 during the third reorganization; until the 1932 map of the United States, it was considered the best map for most of the State, although many other maps of smaller areas in South Carolina had appeared. Elisha Mitchell published the first geologic map of North Carolina in 1842 as part of his textbook for students (Merrill, 1906).

Edward Hitchcock was a pioneer in American geologic cartography and one of the best early geologists. His first contribution was a hand-colored map and cross section of western Massachusetts along the Connecticut River (1818). Another one on northwestern Massachusetts was published in the same year. A geologic map completed by Hitchcock

in 1822, in connection with the first work in America on the Triassic beds of the Connecticut Basin, is one of the most important maps of early American geology (Hitchcock, 1823). This map is 7 by 21 inches on a scale of 7 miles per inch, is hand-colored with 15 patterns, and has other marks such as stippling and rulings for differentiation of the beds. Another small, but interesting contribution is Hitchcock's (1824) map of Martha's Vineyard.

Hitchcock made a geologic map of the entire State of Massachusetts during 1830 and 1831. This map is of outstanding interest because it was the first map to accompany the first publication by an active State geological survey and, according to Hitchcock (1832) it was the first map covering an entire State. The map has five colors, 18 patterns, and nine colored symbols for ore localities. Pleasing light tints are used, and markings or stippling on each of the colors provide additional patterns. The scale is 7 miles to 1 inch on a sheet 18 by 28 inches. A revision was made in 1833 and a final one in 1841 (Hitchcock, 1841).

The work of Hitchcock extended into the second period of development in the United States which started about 1842. One of his contributions during the later period was a geologic map of the United States and Canada. This was published in 1853 and accompanied a map of the world in his book outlining the geology of the globe (1853). His later contributions of a dozen or more maps were chiefly of small areas or revisions of earlier maps.

The mantle of Edward Hitchcock fell on his son, and from 1861 to 1878 C. H. Hitchcock published more than 15 maps of parts of New England, chiefly Maine and New Hampshire. The map of the United States made with W. P. Blake in 1872 was one of his most outstanding contributions (L.C.).

SECOND PERIOD, 1842–1867

About 1842 American geology had advanced into a youthful stage during which many of the major foundations of geology in America were established. The old Wernerian classification of rocks was abandoned, the concepts of Murchison and Lyell were developed, and the geologic maps were based on these concepts. Most of the maps made during this period display the results of geologic work fundamental to our modern geology. Many of the maps were so accurate that only minor changes in boundaries and names of formations have been necessary. During the second period many maps were made in all parts of the country, chiefly of small areas, States, or portions of States. Some illustrate articles; others were for coal, iron, lead, and zinc deposits; and many were State geological survey maps. During this period there was a transition from hand-colored maps to color printing by lithography.

Chromolithography for geologic maps was introduced in America in 1854 by Bowen and Company of Philadelphia when they printed a map of the Pennsylvania coal fields made by R. C. Taylor (Marcou, 1884). Taylor is credited as the first in America or Europe to construct a geologic model, which, of course, is a three-dimensional type of map. The model was made in 1841 to show the coal fields of Pennsylvania.

J. H. Colton and Son of New York printed a color lithograph of *Map of Alabama* made by Michael Tuomey in 1855 (Marcou, 1884). Marcou states that this is the first chromolithograph made in the United States, but Taylor's map antedates it.

Color printing was not used extensively in America until after 1867 when the maps of the Hayden, King, and other United States surveys were published.

The map of New York State by Hall *et al.* appeared in 1842. This map is hand-colored and in four sections, each done by one of the authors who had been assigned a section of the State. The map is one of the first in the second period of development in the United States.

The geologic map of the Upper Mississippi Valley made by Owen in 1839 was printed in 1845 by the Federal Government (Owen, 1845). Though the work was done before 1842, the character of the work as well as the date of publication place it in the second period of development. Owen's map is one of the earliest on American mineral areas and the second map made under commission of the Government. It is hand-colored, with several cross sections showing the Illinois-Wisconsin area of mineral deposits. The map is notable because of the results achieved in a little over 2 months of field work. Owen received his commission in August and was required to complete the survey by winter. He so effectively organized the assignment that he covered the whole area of 11,000 square miles in 2 months and 6 days.

Owen (1846) made a map of the Ohio Valley in 1842 which was published in England sponsored by Lyell. Owen shows the distribution of the Paleozoic rocks remarkably well, and few major changes have been made in the area, though much of the detail has been revised. The Illinois coal basin and the Cincinnati Arch are well outlined.

James Hall used the map by Owen to a great extent in making his map of the same area in 1843 (L.C.). Hall's map (32 by 23 inches on a scale of 3 miles to 1 inch) includes the area from Connecticut to the Mississippi River and from Mackinac Straits to about the Tennessee State line. The colors are light tints, well applied, and are in great contrast with the poor appearance of another map of the same area made during the same year by Byram Lawrence. The Lawrence map was

lithographed in Boston, but other information concerning it is unknown (L.C.).

A geologic map of the United States and Canada by Lyell (1845) appeared in his book on travels in the United States during 1841 and 1842 (L.C.). The map by Hall was one of the chief sources for Lyell's map. Lyell's map is a very important one because it is the first map of the United States to be based on a non-Wernerian classification. The map (20 by 15 inches on a scale of 130 miles to the inch) is hand-colored with rulings and stippling and is detailed, especially in the central part where the information from Owen's and Hall's maps was available. The geology is not shown beyond the continental divide along the Rocky Mountains, but areas as far north as James Bay and Cape Breton are included.

The work of Jules Marcou in the field of geologic cartography was very extensive, not only in the making of maps, but also in the study and collection of maps. Few have delved as deeply as he into the history of geologic maps, and his list of maps (Marcou, 1884) is a very important contribution. During 1852, he made a map of the United States and British Provinces east of the Rocky Mountains which was printed and hand-colored in Boston (Marcou, 1853). The two copies examined were poor with smeared blotchy colors (L.C.). The area mapped is similar to that mapped by Lyell in 1845, but more geology to the west is included. The sheet is 34 by 23 inches with a scale of about 100 miles per inch.

A review of Marcou's publication and map of the United States (Dana, 1854) criticized him severely for conceit, audacity, and ignorance. Though the map was largely a compilation, chiefly from Lyell's map, and had many inaccuracies based on questionable and inadequate information, it served a useful purpose.

In 1853, while still in his twenties, Marcou was appointed U. S. Geologist to the Whipple Expedition for the survey of a route for a railroad from the Mississippi River to the Pacific Ocean. Starting from Boston he made the trip across the United States to Los Angeles. Due to a misunderstanding with Jefferson Davis, then Secretary of War, he was not allowed to publish his report, and his notes were taken from him. However, in 1855 he published in Paris an account of the trip and a complete geologic map of the United States made from memory, personal notes, and use of his map of 1853. This was among the first chromolithographs printed anywhere and has a beautiful color register (Marcou, 1855a). Eight colors are used, but 12 patterns are obtained by colored overprints of ruled lines and dots. The scale is 180 miles to the inch, and the sheet is 24 by 16 inches. A colored cross section from Ft. Smith, Arkansas, to Los Angeles appears at the top of the map. Although inaccurate, it was the first United States map showing the geology to the Pacific Coast. A

German edition was printed at Gotha (Marcou, 1855), and an English one at Zürich (Marcou, 1858) with a few slight changes, chiefly in color arrangement. Marcou (1884) made additional maps of parts of the United States and published maps of small areas of Nebraska in 1863, of California in 1875, and of Arizona in 1877.

Early maps of the Lake Superior mineral deposits were made by C. T. Jackson, J. D. Whitney, and J. W. Foster. An excellent hand-colored map of the Keweenawan iron district of Michigan was made by Jackson (1849) under a Congressional act of 1847. Whitney and Foster (1850) completed a series of colored maps of the copper area, and a year later (1851) a series on the iron deposits of northern Michigan. Some of the same maps were published in France, as mentioned previously (Rivot, 1855).

In 1851, Owen, Norwood, and Whittlesey (1852) surveyed a large area in Iowa, Wisconsin, and Minnesota, including the north and south shores of Lake Superior. The map is well made, hand-colored, and has a number of excellent cross sections of a panoramic type, also in colors. The strata in the hills of the background are colored where the rock formations underlying the hills were known, so that the panorama of the topography gives a three dimensional appearance.

The gold rush of 1849 was one cause for a map of the California gold area made by Tyson (1850) and published by the Federal Government. It was also published privately (1851).

Blake (1855) drew a series of maps on California geology as part of the report of the Williamson Survey for the Pacific railway. In 1856 Blake published a strip map showing an area 50-100 miles wide along the 35th parallel, from Ft. Smith, Arkansas to Los Angeles. This was along the route of the Pope and Whipple Survey for the Pacific railway (Whipple, 1856). Blake was never in the area but made the map from notes taken by Marcou, who was geologist for that expedition in 1853.

Five maps of the United States were published in the 10 years between 1845 and 1855. The one by Edward Hitchcock (1853) appeared the same year as the one by Marcou (1853). Both men utilized the earlier map of Lyell (1845). Another map by Marcou and one by Rogers appeared in 1855. Both were chromolithographed, and it is not known which is the first color-printed map of the United States, but since the one by Marcou was printed in Europe, Rogers' map is the first United States map to be colored-printed in America.

The map by H. D. Rogers was compiled for the American edition of Johnston's atlas (1855). It is entitled *Geological map of United States and British North America* and it includes nearly all of North America from Newfoundland to the Gulf of Tehuantepec. The map shows much more

detail than the 1853 map of Marcou and is probably much more accurate. The sheet is 24½ by 20½ inches with a scale of 165 miles to the inch. A colored cross section from Niagara Falls to the Atlantic Ocean is included.

In 1857 James Hall and J. P. Lesley made a *Map illustrating the several geological features of the country west of the Mississippi River* which was compiled from the Emory Survey (1857), the Pacific railroad survey (Blake, 1855), and other sources. The map is not as good as the Rogers' map, and a duplicate, dated 1858, is very poorly colored (L.C.). Both copies are hand-colored (23 by 20 inches) with the scale not shown.

The author of the Colton *Geological map of the United States of America* is not indicated on the map. It was drawn, engraved, and printed in 1867 by G. W. and C. B. Colton and Co. of New York for John P. Morton and Co. of Louisville, Kentucky (L.C.). The color register of the map is not good, but the patterns are quite distinct, and on the whole it is an outstanding map. The scale is 250 miles to the inch on a sheet 13 by 8 inches. This was one of several maps of the United States placed on exhibition at the 1938 meeting of The Geological Society of America in New York.

F. V. Hayden, one of the pioneer geologists in the West published a geologic map of Nebraska (1857) dealing with the formations along the Missouri River from the mouth of the Platte to Fort Benton. He made several other maps covering the same general area from 1858 to 1867. The publications by Hayden in 1867 followed by other reports and maps of the Federal geological and geographical surveys mark the end of the youthful period of development of geology and geologic maps in the United States.

From 1842 to 1867 a large number of geologic maps of small areas in North America appeared which need not be mentioned here. Nearly all of them are listed by Marcou (1884). Most of them were based on reconnaissance data. The development of geologic exploration was not rapid due to the lack of transportation, hostile Indians, and the absence of topographic maps. In most cases, base maps of any kind were lacking.

THIRD PERIOD, 1867–PRESENT

The initiation of the Federal surveys in 1867 marks the beginning of the third period of the development of geologic maps in the United States. After the Civil War, expansion to the westward necessitated a survey of the area for settlement, for location of mineral deposits, and for the new transcontinental railway. For the first time geologists were put at the head of the surveys where they could direct and organize the work from a geological viewpoint. Until this time geologists merely accompanied

a topographic or exploring expedition and were directed by military officers. The expeditions were for a definite mission or along a given route so that no opportunity was presented for seeing other than that along the line of march. Many of the early geologists were surgeons attached to the organization, and their geological training and activity were incidental though often utilized. Surgeons were often chosen with their additional ability as geologists in mind. The distinct change in the organization of the Federal surveys opened the way for rapid advancement of the science, and geologic maps and writings appeared in rapid succession.

F. V. Hayden was one of the first to be connected with the Federal surveys. His report and map of the Yellowstone area in 1869 led to the establishment of the first National Park (Hayden, 1869). This map (42 by 27 inches) is hand-colored and includes the basin of the Yellowstone and upper Missouri rivers and their tributaries from central Nebraska to west of the Rocky Mountains on a scale of 19 miles to the inch. The base map was one made by the War Department in 1859-1860.

The first map of the United States Geological and Geographical Survey of the Territories appeared in 1875 (Hayden, 1875-1882). From then until 1882 other geologic maps of that survey by W. H. Holmes, F. M. Endlich, A. C. Peale, A. R. Marvine, C. A. White, and F. V. Hayden were published. *The geological and geographical atlas of Colorado and portions of adjacent territory* published in 1877 was one of these.

The Survey west of the 100th meridian under Wheeler (1875), the Exploration of the Colorado River of the west under Powell (1875), the Survey of the 40th parallel under King (1876-1878) and the Survey of the Rocky Mountains under Powell (1877) added to the rapidly mounting list of maps from 1875 to 1879.

A geological map of the United States was compiled for the ninth Census by C. H. Hitchcock and W. P. Blake in 1872 (L.C.). The scale is 90 miles per inch, on a sheet 33 by 21½ inches. The printed colors are deeply tinted, brilliant but well matched, and give a splendid though very contrasting appearance. Gaps and overlaps of color occur, and the shades of color are slightly different on two copies examined. The map is well detailed especially west of the Rocky Mountains which heretofore had been broadly generalized on more or less scant information. It was the best map of United States until 1884 and represents a transition to the period of more accurate maps based on information of the U. S. Geological Survey.

By 1879 it was desirable and necessary to unite the several government surveys, and so the U. S. Geological Survey had its birth with Clarence King as the first director. J. W. Powell succeeded him a year later.

The Second Annual Report by Powell (1882, p. 49-54) contains a set of color charts, prepared by Bailey Willis, designated for use on all geologic maps. From that time on definite, regular, uniform sets of maps were issued. The Geological Atlas of the United States in the form of folios was inaugurated, and the development of color printing advanced rapidly with advancement of the Survey. By 1885, areas covered by 46 folios were mapped, though the first folio did not appear for sale to the public until 1894. The Geological Survey had issued 106 folios by 1904, at which time a slight change was made in the color scheme. The revised arrangement is still used for all folios and colored maps printed by the U. S. Geological Survey.

The first geologic map of the United States published by the U. S. Geological Survey was made by McGee (1885) in 1884. It was color-printed with a scale of 110 miles to the inch. This is another outstanding and important map and was one of those exhibited by the Library of Congress at the New York meeting of The Geological Society of America in 1938. McGee (1893) compiled another map entitled *Reconnaissance map of the United States showing the distribution of the geologic systems.* It was derived from data of the Survey and was printed in color over a base map (100 miles to the inch) with contour lines.

Bailey Willis compiled a geologic map of the United States in 1903 and data from it was included on a preliminary map of North America in 1906 (U.C.). The map of 1906 was reprinted in French for the International Geological Congress held in Mexico City in 1906 (L.C.). The final map of North America, revised from the preliminary one by Willis in 1906, was prepared by G. W. Stose and Bailey Willis in 1911 (Willis, 1912). Each of the four sheets are 30 by 40 inches on a scale of 1:5,000,000. A reduction of the map was printed as a fold-in in the text-book by Pirsson and Schuchert (1924). The Geological Society of America has authorized the publication of a geologic map of North America, revised by G. W. Stose and Bailey Willis from their earlier map. It is probable that this will be ready for distribution in 1943.

The most recent map of the United States was prepared by G. W. Stose and printed in four sheets by the U. S. Geological Survey in 1932 shortly before the meeting of the Sixteenth International Geological Congress in this country.

Several glacial maps of portions of the United States and Canada were made prior to 1881, the one by Bigsby (1851) probably being the earliest. The first map showing regional glaciation is probably the small uncolored one by Shaler and Davis (1881). Chamberlin's maps (1883) of northern United States are thought to be the earliest glacial maps with color overprints showing the extent of the ice sheets. Maps by Warren Upham

(1895) and Frank Leverett (1902) are good examples of early color-printed glacial maps. Antevs (1929) published a large set of uncolored glacial maps for North America and other parts of the world. Many other glacial maps have been made since the turn of the century and are readily available in the literature.

A large glacial map of North America to be printed in colors is now being prepared by a group of prominent glacial geologists in Canada and the United States. It will be published in the near future by The Geological Society of America.

Before the U. S. Geological Survey was organized topographic maps of the United States were few. The need for topographic maps by the field geologists made it necessary for the U. S. Geological Survey to procure funds and make the basic maps. When these began to appear geologic maps became more accurate, the field data was easier to place, and maps appeared in rapid succession.

After 1880 the progress of geology and geologic mapping was so rapid that it would require a large volume to list the hundreds of high-class maps published by State surveys, by individuals, by government surveys over the world, and by the various geologic journals of America and foreign countries. The advance of petroleum and mining geology and the utilization of geologists by private companies has resulted in an enormous number of maps, most of which are retained for private use and rarely published. The systematic color and pattern introduced in the folios of the Geologic Atlas of the United States, has been followed in most of the maps printed by the U. S. Geological Survey and by other publishing organizations in America. The result has been uniformly high-class geological maps too numerous to describe in detail.

Until the U. S. Geological Survey developed its own plant for map reproduction the contracts for lithographic work were scattered among various firms whose excellent early work may be seen in many of the publications from 1868 to 1894. The colored maps of the Federal Surveys from 1869 to 1879 are excellent examples of the early lithographic technique before the organization of the U. S. Geological Survey. Several splendid detailed colored maps by Emmons and Becker in the Second Annual Report (Powell, 1882) illustrate the early maps published by the U. S. Geological Survey.

The chromolithographs of two of W. H. Holmes' beautiful color paintings in Monograph 2 of the U. S. Geological Survey (Dutton, 1882), though not geologic maps, merit attention. The reproduction in color of the Kanab Desert (Pl. 21) and Zion Canyon (Frontispiece) made in 1880 are splendid examples of the early art and technique of lithographic printing and are a tribute to the pioneer lithographic work of T. Sinclair.

Julius Bien of New York also reproduced a color sketch by W. H. Holmes showing the Garden of the Gods and Pike's Peak which appears in Hayden's report of 1878, published in 1883. A number of the same paintings by Holmes were reproduced in Germany and appeared in Neumayr's *Erdgeschichte* (1890).

In 1890, the U. S. Geological Survey originated its own map reproduction plant, now known as its Division of Engraving and Printing. Since its organization this plant has followed the old German process of copper-plate engraving for most of its standard geologic maps and folios. By this process the three basic topographic features—culture and lettering, drainage, and contours—are engraved on three separate copper plates for printing in black, blue, and brown, respectively. Geologic boundaries and letter symbols indicating formations are engraved on a fourth copper plate for overprinting in black, and such geologic features as faults and dikes are engraved on a fifth copper plate, for overprinting in a separate color, usually red. None of the printing is done from the copper plates, but the images are transferred to lithographic stones or metal plates, from which the actual printing is done in flat-bed or cylindrical presses, each color requiring a separate stone or plate. Various patterns are pulled from engraved plates and lithographic stones and transferred to proper color-printing stones or plates.

Each of the four sheets of the geologic map of the United States, printed in 1932, contained an average of 28 colors and required 28 printings. On some colored maps, such as land-classification maps, different tints are secured by combinations of colors, but this is seldom attempted on geologic maps where perfect registration of very narrow color bands is required. The 1932 geologic map of the United States compiled by Stose is considered the most perfectly registered map that has ever been printed and testifies to the beauty, technique, and accuracy of the present methods of printing. The geologic map of Belgium compiled by Andrés Dumont in 1855 was printed by hand in 42 colors and probably represents one of the best accomplishments of old hand printing.

The multicolored geologic maps of the present are the finest that can be produced, but many of them are little better than some of those printed at the close of the nineteenth century. This is a tribute to the technicians of that date and not a depreciation of the present technicians. The preparation of plates, methods of printing, the quantity printed, and the speed of production have been greatly improved. Line rulings, symbols, and stippling have been in continuous use. Those methods of representation are much less expensive to reproduce than color and with modern improvements are very satisfactory.

Data for geologic maps were secured on foot, horseback, canoe, boat, or wagon, and now by automobile and airplane as well. With the development of airplanes and photography, geologic mapping has taken a new significance. Wide areas may be covered rapidly and accurately, eliminating extensive topographic surveys. More regions which were inaccessible will be mapped as the need develops. However, the geologist must visit the areas which are seen from the air, in order to examine fossils, minerals, and types of rock formation that cannot be identified except at close range.

LIST OF MAPS OF THE UNITED STATES

1752 Jean Guettard, with English reprints and modifications in 1756 and 1760
1809 William Maclure, eastern United States, revised in 1811
1817, 1822 Parker Cleaveland, modified from Maclure
1818 John Melish, Maclure's map re-engraved and improved
1832 Hinton, after Maclure, but extended to the Rocky Mountains
1845 Sir Charles Lyell, modified from earlier maps, a new classification used
1853 Jules Marcou, covered as far west as the Rocky Mountains
1853 Edward Hitchcock, compiled from earlier maps
1855 Jules Marcou, first map of the entire United States, printed in Europe
1855 Henry Rogers for Johnston's *Physical atlas of natural phenomena*
1857 James Hall and J. P. Lesley, west of the Mississippi River
1867 Colton and Co., author not indicated
1872 C. H. Hitchcock and W. P. Blake, for the Ninth Census
1881 C. H. Hitchcock, wall map 13 by 8 feet
1885, 1893 U. S. Geological Survey, compiled by W J McGee
1903 U. S. Geological Survey, compiled by Bailey Willis
1906 U. S. Geological Survey, compiled by Bailey Willis, a preliminary map of North America, also printed in France for the International Geological Congress held in Mexico City
1912 U. S. Geological Survey, compiled by Bailey Willis and G. W. Stose: final map of North America
1932 U. S. Geological Survey, compiled by G. W. Stose: map of the United States

In preparation:

Glacial map of North America
New geological map of North America

LIST OF OUTSTANDING AND SOME OF THE MOST INTERESTING GEOLOGIC MAPS

1664 First map by Abbé Coulon
1743 First map in England by Christopher Packe
1746 First map in France by Jean Guettard
1752 First map of America by Jean Guettard
1762 First map in Germany by Christian Füchsel
1771 Map of the Auvergne region with the early use of contours by Nicholas Desmarest

1775 First hand-colored map by Gottlieb Gläser
1809 First map of United States by an American, William Maclure
1810 Map of the Paris Basin by Georges Cuvier and Alexandre Brongniart
1813 Map of France and Belgium by Jean d'Omalius d'Halloy
1815 Map of England and Wales by William Smith
1816 Map of northeastern Ireland by J. F. Berger
1819 Most widely used early map of England by George Greenough
1821 First map of any part of Russia by W. T. H. F. Strangeways
1821 Map of Antigua, first map of West Indies by Nicholas Nugent
1823 Map of Triassic in Connecticut Valley by Edward Hitchcock
1824 Map of European Russia by W. T. H. F. Strangeways
1827 Early map of South American area by M. de Rivero
1832 First map by a State survey (Massachusetts) by Edward Hitchcock
1832 Map of Germany by Leopold von Buch
1834 Early paleogeographic map and early map of Europe by Sir Charles Lyell
1835 Structure of the eastern Alps by Adam Sedgwick and Sir Roderick Murchison
1835 First map of all Scotland by John MacCulloch
1838 First map of all Ireland by Richard Griffith
1838 Map of the Silurian system by Sir Roderick Murchison
1839 Map of Germany and central Europe by Heinrich von Dechen
1841 Complete map of France by Élie de Beaumont and P. A. Dufrenoy
1842 Map of the Ohio Valley by D. D. Owen
1842 Map of the State of New York by James Hall, E. Emmons, W. W. Mather, and L. Vanuxem
1843 Maps of South America by Alcide d'Orbigny
1843 First map of the world by Ami Boué
1845 Map of the Permian System in the Ural Mountains by Sir Roderick Murchison, E. P. de Verneuil, and Alexander von Keyserling
1845 Map of United States by Sir Charles Lyell
1849 First map of the ore district of Lake Superior by C. T. Jackson
1851 First map of the Arctic by Sir John Richardson
1851 First chromolithograph of a geological map by E. Beyrich
1854 Chromolithograph of the map of France by Élie de Beaumont and P. A. Dufrenoy
1855 First complete map of the United States by Jules Marcou
1855 Map of Belgium in 42 printed colors by Andrés Dumont
1855 First map of all India by George Greenough
1860 Map of the world by Jules Marcou
1875-1882 Maps of the U. S. Geological and Geographic Surveys
1880 First colored maps of the U. S. Geological Survey
1885 Map of United States by W J McGee
1894 First folio of the Geologic Atlas of the United States
1912 Map of North America by Bailey Willis and G. W. Stose
1919 Map of Brazil by J. C. Branner
1922 Map of Asiatic Russia and most of European Russia issued by Thirteenth International Geological Congress, Brussels
1925 Map of Europe, with structure transparency by F. Beyschlag and W. Schriel
1925 Map of the Union of South Africa by Alexander du Toit
1931 Map of all Australia by Sir Edgeworth David

1932 Map of the United States by the U. S. Geological Survey
1932–1939 Map of the world (80 sheets) by W. Schriel (incomplete)
1937 Maps of Russia in the guidebook of the Seventeenth International Geological Congress
1943 Map of North America by Bailey Willis and G. W. Stose (In press)

REFERENCES CITED

Andress, Richard (1930) *Handatlas,* Bielefield und Leipzig.

Antevs, Ernest (1929) *Maps of Pleistocene glaciations,* Geol. Soc. Am., Bull., vol. 40, p. 631-720.

Bain, Andrew (1852) *On the geology of southern Africa,* Geol. Soc. London, Tr., 2d ser., vol. 7, p. 175-192, Pl. 20.

Bakewell, Robert (1829) *Introduction to geology,* 1st Am. ed., New Haven.

Bartholomew, John (1936) *Oxford advanced atlas,* Oxford.

Beaumont, Élie de, and Dufrenoy, P. A. (1869) *La stratigraphie, Paris.*

Beche, H. T. de la (1824) *On the geology of the north coast of France, and the inland country adjoining,* Geol. Soc. London, Tr., 2d ser., vol. 1, p. 73-89, Pl. 11.

——— (1829) *Remarks on the geology of Jamaica,* Geol. Soc. London, Tr., 2d ser., vol. 2, p. 143-194, Pl. 18.

Berger, J. F. (1814) *Mineralogic account of the Isle of Man,* Geol. Soc. London, Tr., 1st ser., vol. 2, p. 29-65, Pl. 1.

——— (1816) *On the geological features of the northeastern counties of Ireland,* Geol. Soc. London, Tr., 1st ser., vol. 3, p. 121-195, Pl. 8, 9.

Berghaus, Hermann (1892) *Atlas der Geologie Physikalisches,* vol. 1, Justus Perthes, Gotha.

Berkey, Charles P., and Morris, F. K. (1932) *Geology of Mongolia, Natural History of Central Asia,* vol. 2, Am. Mus. Nat. Hist., Putnam's, New York and London, 475 pages.

Beyrich, E. (1849) *Ueber der Zusammensetzung und Lagerung der Kreideformation in der Gegend zwischen Halberstadt, Blankenburg, und Quedlinburg,* Zeit. Deutschen Geol. Gesell., vol. 1. p. 288-339, Pl. 4.

——— (1849a) *Erläuterung zu der geognostischen Karte der Umgegend von Regensburg,* Zeit. Deutschen Geol. Gesell., vol. p. 411-423, Pl. 5.

——— (1851) *Bemerkungen zu einen geognostischen Karte des nördichen Harzrandes von Langelsheim bis Blankenburg,* Zeit. Deutschen Geol. Gesell., vol. 3, p. 567-569, Pl. 15.

Bigsby, J. J. (1821) *Geological and mineralogical observations on the northwest portion of Lake Huron,* Am. Jour. Sci., 1st ser., vol. 4, p. 1-16, Pl. 2.

——— (1824) *Notes on geology and geography of Lake Huron,* Geol. Soc. London, Tr., 2d ser., vol. 1, p. 175-209, Pl. 31.

——— (1851) *On the erratics of Canada,* Geol. Soc. London, Quart. Jour., vol. 7, p. 215-238, Pl. 14.

——— (1852) *On the geology of the Lake of the Woods south of Hudson's Bay,* Geol. Soc. London, Quart. Jour., vol. 8, p. 400-406, Pl. 22.

——— (1853) *On the geology of Quebec and its environs,* Geol. Soc. London, Quart. Jour., vol. 9, p. 82-101, Pl. 6.

Blake, W. P. (1855) *Report of explorations and survey for a railroad from the Mississippi River to the Pacific Ocean under the Secretary of War,* 33d Cong., 1st sess., House Ex. Doc., No. 129, vols. I-IV, Washington, D. C.

Bloom, Sol (1937-1938) *Early maps in the Library of Congress reproduced by the U. S. Geol. Survey in 1937-1938 under the direction of Lawrence Martin,* U. S. Constitution Sesquicentennial Commission, Sol Bloom, Director, Washington, D. C.

Boisse, Ad. (1852) *Recherches sur les gîtes métallifères de lAveyron, et sur leurs relations avec les divers produit plutoniques,* Ann. des Mines, ser. 5, vol. 2, p. 467-520, Pl. 9.

Boll, Ernst (1851) *Geognostische Skizze von Meklenburg,* Zeit. Deutschen Geol. Gesell., vol. 3, p. 436-477, Pl. 19.

Branner, J. C. (1919) *Outline of the geology of Brazil to accompany a geologic map of Brazil,* Geol. Soc. Am., Bull., vol. 30, p. 189-337.

Buch, Leopold von (1797) *Versuch einer Mineralogischen Beschreibung von Landeck,* Breslau.

Chamberlin, T. C. (1883) *Preliminary paper on the terminal moraines of the second glacial epoch,* U. S. Geol. Survey, Third Ann. Rept., 1881-1882, p. 291-402.

Cist, Zachariah (1822) *Account of the mines of anthracite in the region about Wilkesbarre, Pennsylvania,* Am. Jour. Sci., 1st ser. vol. 4, p. 1-16, Pl. 2.

Claussen, P. (1841) *Notes géologique sur la Province de Minas Geraes au Brésil,* Acad. Roy. de Belgique, Bull. vol. 8, p. 322-343.

Cleaveland, Parker (1817) *Elementary treatise on geology and mineralogy,* vol. 1, Boston; 2d ed. 1822.

Cole, Grenville A. J. (1924) *Handbook of the geology of Ireland,* T. Murby and Co., London, 82 pages.

Collomb, Edouard (1846) *Carte du terrain erratique de la Vallée de St. Amarise,* Soc. Géol. France, Bull., 2d ser. vol. 3, p. 196, Pl. 3.

Conybeare, William (1816) *Descriptive notes referring to the outline of sections presented by a part of the coasts of Antrim and Derry,* Geol. Soc. London, Tr., 1st ser., vol. 3, p. 196-216, Pl. 10.

——, and Buckland, William (1824) *Observations on the southwest coal district of England,* Geol. Soc. London, Tr., 2d ser., vol. 1, p. 210-316, Pl. 38.

Cuvier, Georges, and Brongniart, Alexandre (1810) *Essai sur la géographie minéralogique des environs de Paris,* Paris.

Dana, J. D. (1854) *Nature of a geological map of the United States and the British provinces of North America,* Am Jour. Sci., 2d ser., vol. 17, p. 199-206.

Dawson, J. W. (1845) *On the lower Carboniferous rocks or Gypsiferous formations of Nova Scotia,* Geol. Soc. London, Quart, Jour., vol. 1, p. 26-35, Pl. 34.

Degenhardt, Carl (1839) Archiv für Mineralogie, Geognosie, Bergbau, und Küstenkunde, vol. 12.

Dewalque, Gustave (1884) *Catalogue des ouvages de géologie de minéralogie, et de paléontologie,* Soc. Géol. de Belgique, Liege.

Dewey, Chester (1824) *A sketch of the geology and mineralogy of a part of Massachusetts and parts of the adjoining states,* Am. Jour. Sci., 1st ser., vol. 8, p. 1-60.

Domeyko, Ignace (1846) *Mémoire sur la constitution géologique du Chili,* Ann. des Mines, ser. 4, vol. 9, p. 365-540, Pl. 4.

—— (1848) *Mémoire sur le terrain tertiare et les lignes d'ancien niveau de l'Ocean du Sud, aux environs de Coquimbo (Chili),* Ann. des Mines, ser. 4, vol. 14, p. 153-162, Pl. 2.

Dutton, C. E. (1882) *Tertiary history of the Grand Canyon district,* U. S. Geol. Survey, Mon. 2, 264 pages.

Ebels, J. L. (1808) *Structure of the earth in Alpine mountain systems,* Zürich.

Elles, Gertrude (1931) *The study of geologic maps,* Cambridge Univ. Press, Cambridge, 76 pages.

Emory, W. H. (1857) *Report on the United States and Mexican boundary survey,* 34th Cong., 1st sess., House Ex. Doc. No. 135, vol. 1, pt. 2, Washington, D. C.

Enciclopedia Universal Illustrada (1924) vol. 21, Barcelona.

Encyclopedia Britannica (1929) 14th ed., vol. 14, pp. 836-845, Maps.

Featherstonehaugh, G. W. (1835) *Report of the mineralogical and geographical investigators to the Secretary of War,* 23d Cong., 2d sess., Senate Ex. Doc. 151, vol. IV, Washington, D. C.

Finch, John (1824) *A sketch of the geology of the country near Easton, Pa.,* Am. Jour. Sci., 1st ser., vol. 8, p. 236-240, Pl. 1.

Foetterle, Franz (1856) *Die Geologie von Süd-Amerika,* Petermann's Mittheilungen aus Justus Perthes' Geographischer Anstalt, Gotha.

Forbes, David (1861) *On the geology of Bolivia and southern Peru,* Geol. Soc. London, Quart. Jour., vol. 16, p. 460-470, Pl. 21.

Fordham, Herbert (1927) *Maps, their history, characteristics, and uses,* Cambridge Univ. Press, Cambridge.

Franklin, Capt. James (1835) *On the geology of a portion of Bundelcund, Boghelcund and the districts of Saugor and Jubulpore,* Geol. Soc. London, Tr., 2d ser., vol. 3, p. 191-200, Pl. 25.

Freiesleben, Johann K. (1807-1815) *Geognostic contribution to the knowledge of the Copper Slate series, with special reference to a part of Mansfeld and Thuringia,* Freiburg, 4 volumes.

Füchsel, Christian (1762) *Historia terrae et maris ex historia Thuringiae permontium descriptionem erecta,* Acta. Acad. Elect. Soc. Mayence, Erfurt.

Fuller, J. (1760) *Naval chronicle of voyages, travels, expeditions, remarkable exploits, and achievements of the most celebrated English navigators, travellers, and sea-commanders,* vol. II, London.

Galeotti, H. G. (1838) Acad. Roy. de Belgique, Bull., vol. 5, p. 739.

Geikie, Sir Archibald (1897) *Founders of geology,* Macmillan, New York, 297 pages.

Gesner, A. (1836) *Remarks on the geology and mineralogy of Nova Scotia,* Halifax, 273 pages.

Godfrey, J. G. H. (1878) *Notes on the geology of Japan,* Geol. Soc. London, Quart. Jour., vol. 34 p. 542-555.

Griesbach, C. L. (1871) *On the geology of Natal in South Africa,* Geol. Soc. London, Quart. Jour., vol. 27, p. 53-72, Pl. 2.

Guettard, Jean (1746) Mémoires de l'Académie Royale Française, Paris.

——— (1752) *Carte minéralogique, ou l'on voit la nature des terrains du Canada et de la Louisiane,* Mémoires de l'Académie Royales des Sciences, vol. 4, Paris. (The copy of the map in the Map Division of the Library of Congress lists the publication as *Histoire de l'Académie Royale des Sciences, année 1752,* Paris, 1756).

Hall, James, Mather, W. W., Emmons, Ebenezer, and Vanuxem, Lardner (1842) *Geology of New York,* Albany, Pt. I-IV.

Halloy, Jean d'Omalius d' (1822, 1835) *Éléments de géologie,* Paris.

Hardouin, M. L. (1868) *Sur le géologie de la subdivision de Constantine, Algerie,* Soc. Géol. France, Bull., 2d ser., vol. 25, p. 328-346, Pl. 5.

Hatch, F. H., and Corstorphine, C. H. (1905) *Geology of South Africa,* Macmillan, New York, 348 pages.

Hayden, F. V. (1857) *Notes explanatory of a map and section illustrating the geological structure of the country bordering on the Missouri River, from the mouth of the Platte River to Fort Benton,* Acad. Nat. Sci. Philadelphia, Pr., vol. 9, p. 109-116. (Map is a fold-in opposite p. 109.)

—— (1869) *Geological report of the exploration of the Yellowstone and Missouri Rivers,* 40th Cong., 2d sess., Sen. Ex. Doc. 77, Washington, D. C.

—— (1875-1882) *U. S. Geological and Geographical Survey of the Territories,* Washington, D. C.

Henslow, J. S. (1821) *Supplementary observations to Dr. Berger's account of the Isle of Man,* Geol. Soc. London, Tr., 1st ser., vol. 5, p. 482-505, Pl. 35.

Hislop, S., and Hunter, R. (1855) *On geology and fossils of the neighborhood of Nagpur, Central India,* Geol. Soc. London, Quart. Jour., vol. 11, p. 345, Pl. 10.

Hitchcock, Edward (1818) *Remarks on the geology and mineralogy of a section of Massachusetts on Connecticut River, with a part of New Hampshire and Vermont,* Am. Jour. Sci., 1st ser., vol. 1, p. 105-116.

—— (1818a) *A geological map of the northwest part of Massachusetts,* Am. Jour. Sci., 1st ser., vol. 1, p. 436.

—— (1823) *Geology, mineralogy, and scenery of the Connecticut,* Am. Jour. Sci., 1st ser., vol. 6, p. 1-86, Pl. 1.

—— (1824) *Notices of the geology of Martha's Vineyard and the Elizabeth Islands,* Am. Jour. Sci., 1st ser., vol. 7, p. 240-248, Pl. 4.

—— (1832) *Report on the geology of Massachusetts, examined under the direction of that State, during the years 1830 and 1831,* Am. Jour. Sci., 1st ser., vol. 22, p. 1-70. (Map is frontispiece.)

—— (1841) *Final report on the geology of Massachusetts,* Northampton.

—— (1853) *Outline of the geology of the globe and the United States in particular,* Phillips, Sampson, and Co., Boston.

Hochstetter, Ferdinand von (1864) *Geologie von Neuseeland,* Wien.

Holland, Henry (1811) *A sketch of the natural history of the Cheshire rock-salt district,* Geol. Soc. London, Tr., 1st ser., vol. 1, p. 38-61.

Isbister, A. K. (1855) *On the geology of Hudson's Bay Territory and portions of the Arctics and the northwestern regions of North America,* Geol. Soc. London, Quart. Jour., vol. 11, p. 497-520, Pl. 15.

Jackson, C. T. (1849) *Geological map of Lake Superior district,* 31st Cong., 1st sess., Senate Doc. No. 1, pt. III, Washington, D. C.

——, and Alger, Francis (1828) *A description of the mineralogy and geology of a part of Nova Scotia,* Am. Jour. Sci., 1st ser., vol. 14, p. 305-330. (Map opposite p. 209.)

Jacquot, E. (1857) *Étude géologique sur le pays Messin, ou nouvelles recherches sur le prolongement du bassin de la Sarre au-dessous de la partie centrale du département de la Moselle,* Ann. des Mines, ser. 5, vol. 11, p. 513-639, Pl. 8.

Johnston, Keith (1855) *Physical atlas of natural phenomena,* Edinburgh and Boston.

Judd, J. W. (1898) *The earliest engraved geological maps of England and Wales,* Geol. Mag., 4th decade, vol. 5, p. 97-103; and *The earliest geological maps of Scotland and Ireland,* Geol. Mag., 4th decade, vol. 5, p. 145-149.

Karsten, Hermann (1850) *Beitrag zur Kenntniss der Gesteine des nördlichen Venezuela,* Zeit. Deutschen Geol. Gesell., vol. 2, p. 345-361, Pl. 11.

King, Clarence (1876-1878) *U. S. Geological Exploration of the 40th parallel,* Washington, D. C., vol. 1, 1878; vol. 2, 1877; Atlas, 1876.

Leverett, Frank (1902) *Glacial formations and drainage features of the Erie and Ohio Basins*, U. S. Geol. Survey, Mon. 41, 802 pages.

Loftus, W. K. (1855) *On the geology of portions of the Turko-Persian frontier*, Geol. Soc. London, Quart. Jour., vol. 11, p. 247-344, Pl. 9.

Logan, W. E. (1852) *On the footprints occurring in the Potsdam sandstone of Canada*, Geol. Soc. London, Quart. Jour., vol. 8, p. 199-225, Pl. 6.

——— (1855) *Carte géologique du Canada*, Soc. Géol. France, Bull., 2d ser., vol. 12, p. 1316.

Lyell, Sir Charles (1834) *Principles of geology*, 3d ed., London.

——— (1841) *Principles of geology*, J. I. Kay and Co., Philadelphia.

——— (1845) *Travels in North America in 1841-1842*, London and New York.

Maclure, William (1809) Am. Philos. Soc. Philadelphia, Tr., vol. 6, pt. 2.

MacCulloch, John (1816) *Sketch of the mineralogy of Sky*, Geol. Soc. London, Tr., 1st ser., vol. 3, p. 1-111, Pl. 1.

McCormick, W. E. (1824) Edinburgh Philosophical Journal, vol. 10.

McGee, W J (1885) *Report of Mr. W J McGee*, U. S. Geol. Survey, Fifth Ann. Rept. 1883-1884, p. 34-41.

——— (1893) U. S. Geol. Survey, Fourteenth Ann. Rept. 1892-1893, pt. II. (Map in pocket.)

Marcou, Jules (1848) *Recherches géologique sur le Jura Salinois*, Mém. Soc. Géol. France, ser. 2, vol. 3, p. 1-151, Pl. 2.

——— (1853) *Geological map of the United States and British provinces of North America*, Gould and Lincoln, Boston.

——— (1855) *Über die Geologie ver Vereinigten Staaten und der Englischen Provinzen von Nord-Amerika*, Petermann's Mittheilungen aus Justus Perthes' Geographischer Anstalt, vol. I, Gotha.

——— (1855a) *Résumé explicatif d'une carte géologique de États-Unis et des provinces Anglaises de l'Amérique du Nord*, Soc. Géol. France, Bull., 2d ser., vol. 12, p. 813-936.

——— (1858) *Geology of North America*, Zurcher and Furrer, Zürich.

———, and John B. (1884) *Mapoteca geologica americana, a catalogue of the geological maps of America (North and South) 1752-1881, in geographic and chronologic order*, U. S. Geol. Survey, Bull. 7, 184 pages.

Maycock, J. D. (1821) Quart. Jour. Sci. Roy. Instit. Great Britain, vol. 11.

Merrill, G. P. (1906) *Contributions to the history of American geology*, Rept. of U. S. Nat. Mus. for 1904, Washington, D. C.

——— (1920) *Contributions to a history of American State geological and natural history surveys*, U. S. Nat. Mus., Bull. 109, Washington, D. C.

——— (1927) *First one hundred years of American geology*, Yale Univ. Press, New Haven.

Métherie, J. C. de la (1811) Jour. de Physique, de Chemie, d'Histoire Naturelle, et des Arts, vol. 62, Paris.

Mitchell, Elisha (1829) *On the geology of the gold region of North Carolina*, Am. Jour. Sci., 1st ser., vol. 16, p. 1-19.

Moussy, Martin de (1873) *Description géographique et statistique de la Confédération Argentine*, Atlas, Paris.

Murchison, Sir Roderick (1838) *The Silurian system*, J. Murray, London.

——— (1853) *Siluria*, London, 566 pages.

——— Verneuil, E. P. de, and Keyserling, Alexander von (1845) *The geology of Russia in Europe and the Ural Mountains*, J. Murray, London.

Neumayr, Melchior (1890) *Erdgeschichte,* Leipzig und Wien.

Nugent, Nicholas (1821) *A sketch of the geology of the Island of Antiqua,* Geol. Soc. London, Tr., 1st ser., vol. 5, p. 459-475, Pl. 32.

Orbigny, Alcide d' (1843) *Voyage dans l'Amérique méridional (le Brésil, l'Uruguay, la République Argentine, la Patagonie, Chili, Bolivia, Pérou) executé pendant les années 1826-1833,* vol. 3, pt. 3, Atlas de la géologie, Paris.

Owen, D. D. (1845) *Report of the geological exploration of part of Iowa, Wisconsin and Illinois.....in the year 1839,* Mineral Lands of the United States, Message from the President, 26th Cong., 1st sess., House Ex. Doc. 239, vol. IV, Washington, D. C.

—— (1846) *On geology of the western States of North America,* Geol. Soc. London, Quart. Jour., vol. 2, p. 433-447, Pl. 19.

——, Norwood, J. G., and Whittlesey, C. (1852) *Report of a geological survey of Iowa, Minnesota, Wisconsin, and a portion of Nebraska,* Lippincott, Philadelphia.

Phillips, John (1855) *Manual of geology,* R. Griffin and Co., London and Glasgow.

Pirsson, Louis V., and Schuchert, Charles (1924) *Textbook of geology,* vol. II, John Wiley, New York, 1026 pages.

Pissis, A. (1848) Mémoires présentés par divers savants à l'Académie des Sciences de l'Institute National de France, vol. 10, Paris.

—— (1873) *Sur la constitution géologique de la chaîne des Andes entre le 16° et le 55° degré de latitude sud,* Ann. des Mines, ser. 7, vol. 3, p. 402-426, Pl. 9. (Map between 22° and 42° S. Lat.)

Powell, J. W. (1875) *Exploration of the Colorado River of the west and its tributaries, 1869-1872,* Washington., D. C., 285 pages.

—— (1877) U. S. Geological and Geographical Survey of the Rocky Mountains, Washington, D. C., 195 pages.

—— (1882) U. S. Geol. Survey, Second Ann. Rept., 1880-1881, Washington, D. C., 588 pages.

Prestwich, Joseph (1888) *Geology,* Clarendon Press, Oxford.

Pumpelly, Raphael (1866) *Research in China, Mongolia, and Japan,* Smithson. Contr. No. 2, Washington, D. C.

Raisz, Erwin (1938) *General cartography,* McGraw-Hill, New York, 370 pages.

Reclus, Élisée (1868, 1871) *La terre,* Paris, 1868; New York, 1871.

—— (1893) *Nouvelle géographie universelle,* vol. 18, Amérique do Sud: Les regiones Andine, Paris.

Reed, F. R. C. (1921) *Geology of the British Empire,* Arnold, London, 480 pages.

Richter, Carl von (1851) *Erläuterung zu geognostiche Uebersichtskarte des östthüringische Grauwachen gebeits,* Zeit. Deutschen Geol. Gesell., vol. 3, p. 536-553, Pl. 20.

Rivero, M. de (1830) *Sketch of the rich mine of Pasco,* Am. Jour. Sci., vol. 17, p. 43-63. (Map opposite p. 216.) Original in Journ. Nat. Sci. and Nat. and Foreign Ind., vol. 1, no. 2, Lima, 1828.

Rivot, L. E. (1855) *Voyage au Lac Superieur (États-Unis d'Amérique),* Ann. des Mines, ser. 5, vol. 7, p. 173-328, Pls. 6, 7.

Roemer, Ferdinand (1854) *Die Kreidebildungen Westphalens,* Zeit. Deutschen Geol. Gesell., vol. 6, p. 99-236, Pl. 1.

Rouville, Paul de (1868) *Compte rendu de la course fait à La Valette, Montferrier, St. Gely, Grabels, Foncaude et Caunelles,* Géol. Soc. France, Bull., 2d ser., vol. 25, p. 879-888, Pl. 8, fig. 1.

Royal Geographical Society (1882) *Catalogue of the map room of the Royal Geographical Society,* London.

Sampaio, Theodoro (1911) *Atlas dos Estados Unidos do Brasil,* Bahia.

Saussure, H. B. de (1779) *Voyages dans les Alpes,* Neuchâtel.

Sawkins, J. G. (1871) *Geological observations on British Guiana, Geol.* Soc. London, Quart. Jour., vol. 27, p. 419-434.

Schauroth, Carl von (1853) *Uebersicht der geognostischen Verhältnisse des Hertzog thums Coburg und der anstossenden Ländertheile, als Erläuterung zur geognostische Karte,* Zeit. Deutschen Geol. Gesell., vol. 5, p. 698-742, Pl. 15.

Schlehan, Herr von (1852) *Versuch einer geognostischen Beschreibung der Gegend zwischen Amasry und Tyrla-asy und die nordküste von Klein Asien,* Zeit. Deutschen Geol. Gesell., vol. 4, p. 96-142, Pl. 1.

Sederhölm, J. J. (1932) Bull. Geol. Com. Finland, No. 98, Helsingford.

Sedgwick, Adam, and Murchison, Sir Roderick (1835) *On the structure and relations of the deposits contained between the Primary rocks and the Oölitic series in the north of Scotland,* Geol. Soc. London, Tr., 2d ser., vol. 3, p. 125-160, Pl. 13.

——— ——— (1835a) *A sketch of the structure of the eastern Alps,* Geol. Soc. London, Tr., 2d ser., vol. 3, p. 301-420, Pls. 35, 36.

Shaler, N. S., and Davis, W. M. (1881) *Illustrations of the earth's surface, Glaciers,* Boston.

Smith, Alfred (1832) *On watercourses, and the alluvial and rock formations of the Connecticut River valley,* Am. Jour. Sci., vol. 22, p. 205-231.

Smith, William (1815) *A map of the strata of England and Wales with part of Scotland,* Memoirs to a map of strata of England, London.

Strangeways, W. T. H. F. (1821) *Description of the rapids of Imatra, on the River Voza in Carelia; with an outline of the probable history of their formation; and a notice of the bursting of the Lake Souvando into the Lagoda, in the year 1818,* Geol. Soc. London, Tr., 1st ser., vol. 5, p. 340-345, Pl. 17.

——— (1821a) *Geological sketch of the environs of St. Petersburg,* Geol. Soc. London, Tr., 1st ser., vol. 5, p. 392-458, Pl. 28.

——— (1824) *Outline of the geology of Russia,* Geol. Soc. London, Tr., 2d ser., vol. 1, p. 1-39, Pl. 2.

Sullivan, Henry B. (1922) *Catalogue of the geologic maps of South America,* Am. Geog. Soc., New York, 191 pages.

Taylor, R. C. (1846) Am. Philos. Soc., Philadelphia, Tr., n. ser., vol. 9.

——— (1848) *Statistics of coal,* Philadelphia.

Thiele, Walter (1938) *Official map publication,* Am. Libr. Assoc., Chicago.

Toit, Alexander du (1926) *Geology of South Africa,* Oliver and Boyd, London and Edinburgh, 463 pages.

——— (1927) Carnegie Inst. Washington, Pub. No. 381, Washington, D. C.

Tyson, P. T. (1850) *Memoirs upon the geology and productive resources of California,* 31st Cong., 1st sess., Ex. Doc. 47, Washington, D. C.

——— (1851) *Geology and industrial resources of California,* William Minifie and Co., Baltimore.

Upham, Warren (1895) *The glacial Lake Agassiz,* U. S. Geol. Survey, Mon. 25, 658 pages.

Wadia, Dosabhai (1939) *Geology of India,* Macmillan, London, 460 pages.

Wall, S. P. (1860) *On the geology of a part of Venezuela and of Trinidad,* Geol. Soc. London, Quart. Jour., vol. 16, p. 460-470, Pl. 21.

Wappaeus, J. E. (1884) *Geographia physica do Brasil,* Rio de Janiero.

Weaver, Thomas (1821) *Memoir on the geological relations of the east of Ireland,* Geol. Soc. London, Trs., 1st ser., vol. 5, p. 117-304, Pl. 15.

Websky, Herr von (1853) *Ueber die geognostische Verhältnisse der Erzlagerstätten von Kupferberg und Rudelstadt in Schlesien,* Zeit. Deutschen Geol. Gesell., vol. 5, p. 373-428, Pl. 9.

Webster, Thomas (1814) *On freshwater formations in the Isle of Wight with some observations on the strata over the Chalk in southeastern part of England,* Geol. Soc. London, Tr., 1st ser., vol. 2, p. 161-254, Pl. 9, 10.

Wheeler, G. M. (1875) U. S. Geological and Geographical Survey west of the 100th Meridian, Geology, vol. III and Atlas, Washington, D. C.

Whipple, A. W. (1856) *Report on survey along 35th parallel,* 33d Cong., 2d sess., House Ex. Doc. 91, vol. III, pt. IV, Washington, D. C.

Whitney, J. D., and Foster, J. W. (1850) *Report on geology and topography of a portion of the Lake Superior land district, Pt. 1, Copper lands,* 31st Cong., 2d sess., House Ex. Doc. 69, Washington, D. C.

——, — ——— (1851) *Report on geology and topography of the Lake Superior district,* 32d Cong., Spec. Sessions, Senate Ex. Doc. 4, Washington, D. C.

Willis, Bailey (1907) *Research in China,* Carnegie Inst. Washington, Washington, D. C.

——— (1912) *Index to the stratigraphy of North America,* U. S. Geol. Survey, Prof. Paper 71, Pl. I.

Winch, N. J. (1817) *Observations on the geology of Northumberland and Durham,* Geol. Soc. London, Tr., 1st ser., vol. 4, p. 1-101, Pl. 1.

Woodward, H. B. (1911) *History of geology,* London.

Zittel, Karl von (1908) *History of geology and paleontology,* Scribner, New York, 562 pages.

BIBLIOGRAPHY OF SOURCE BOOKS AND CATALOGUES OF GEOLOGIC MAPS

Dana, E. S. (1918) *Century of science in America,* Yale Univ. Press, New Haven.

Dewalque, Gustave (1884) *Catalogue des ouvages de géologie, minéralogie, et de paléontologie,* Soc. Géol. Belgique, Liege.

Elles, Gertrude (1931) *The study of geologic maps,* Cambridge Univ. Press, Cambridge, 76 pages.

Encyclopedia Britannica (1929) 14th ed., vol. 14, p. 836-845, Maps.

Fordham, Herbert (1927) *Maps, their history, characteristics, and uses,* Cambridge Univ. Press, Cambridge.

Geikie, Sir Archibald (1897) *Founders of geology,* Macmillan, New York, 297 pages.

Geographical Board of Canada (1918) *Catalogue of maps in the collection of the Geographical Board,* Ottawa.

Holmden, H. R. (1912) *Catalogue of maps, plans, charts in the map room of the Dominion Archives,* Pub. Canad. Archives, No. 8, Ottawa.

Library of Congress (1904) *Check list of maps published by foreign governments,* Washington, D. C.

Marcou, Jules, and John B. (1884) *Mapoteca geologica americana, a catalogue of the geological maps of America (North and South) 1752-1881, in geographical and chronologic order,* U. S. Geol. Survey, Bull. 7, 184 pages.

Mather, K. F., and Mason, S. L. (1939) *Source book in geology,* McGraw-Hill, New York, 702 pages.

Merrill, G. P. (1906) *Contributions to the history of American geology,* Rep. of U. S. Nat. Mus. for 1904, Washington, D. C.

——— (1920) *Contributions to a history of American State geological and natural history surveys,* U. S. National Museum, Bull. 109, Washington, D. C.

——— (1927) *First one hundred years of American geology,* Yale Univ. Press, New Haven.

Raisz, Erwin (1938) *General cartography,* McGraw-Hill, New York, 370 pages.

Royal Geographical Society (1882) *Catalogue of the map room of the Royal Geographical Society,* London.

Sullivan, Henry B. (1922) *Catalogue of the geologic maps of South America,* Am. Geog. Soc., New York, 191 pages.

Thiele, Walter (1938) *Official map publications,* Am. Libr. Assoc., Chicago.

Woodward, H. B. (1911) *History of geology,* London.

Zittel, Karl von (1908) *History of geology and paleontology,* Scribner, New York, 562 pages.

447 N. Broadway, New Philadelphia, Ohio.

Manuscript received by the Secretary of the Society, December 19, 1942.

BULLETIN OF THE GEOLOGICAL SOCIETY OF AMERICA
VOL. 54, PP. 1281-1304, 1 PL., 6 FIGS. SEPTEMBER 1, 1943

PRE-CRETACEOUS OF COLOMBIA

BY D. TRUMPY

CONTENTS

	Page
Abstract	1282
Pre-Ordovician basement (Gansser)	1282
General statement	1282
Macarena basement	1282
Pre-Paleozoic basement in other areas	1284
San José-Guaviare	1284
Eastern Cordillera	1286
Central Cordillera	1286
Sierra Nevada de Santa Marta	1286
Cambro-Ordovician	1287
Macarena	1287
Uribe trail	1289
Quetame series	1290
Devonian	1291
General statement	1291
Perijá range	1291
Carboniferous	1293
Cachalá	1293
Bucaramanga	1293
Perijá range	1295
Permian	1295
Triassic and Liassic	1297
Marine Triassic	1297
Liassic of El Banco area and Cesar Valley red beds	1299
"Giron" of middle Magdalena Valley	1300
Other formations of unknown age	1301
Conclusions	1301
References cited	1302

ILLUSTRATIONS

Figure	Page
1. Key map showing the main pre-Cretaceous fossil localities of Colombia	1285
2. Stratigraphic sections of Macarena (Llanos)	1288
3. Generalized stratigraphic column along the west foot of the Cordillera Perijá	1292
4. Generalized stratigraphic column of west and east sides of Santander Massif	1294
5. Generalized column of pre-Cretaceous sediments between Rio Coello and Rio Luisa	1296
6. Geological section along the Uribe trail	1298

Plate	Facing page
1. Syenite and fossils from Colombia	1304

ABSTRACT

Drs. O. Renz, H. Hubach, and A. Gansser, geologists of the Cia. de Petroleo Shell de Colombia, have collected several small faunas of Paleozoic and Early Mesozoic age during the past few years. Some of these faunas are new, while the others give additional information on the distribution of the pre-Cretaceous formations in Colombia.

The basement rocks of the Macarena are briefly described. Cambro-Ordovician graptolite and trilobite faunules were found in the Macarenas and near Colombia, a small village about 80 kilometers northeast of Neiva. On the Colombian side of the Sierra de Perija, Devonian beds with a Floresta fauna overlap with sharp, angular unconformity upon slightly metamorphosed shale. Small Carboniferous faunas were collected on Cerro Cerrejón in the Rancheria valley, at Bucaramanga, and at Labateca. A good Leonard fauna was found near Manaure in the Sierra de Perija, and boulders of Permian *Fusulina* limestones occur in red beds near Chiriguaná. Marine Upper Triassic limestones are normally interbedded with porphyritic red beds at Payande near Ibague. Probably also of Upper Triassic age are black shales with *Estheria* exposed on the road between Duitama and Charala and in Quebrada de los Indios about 25 kilometers south of Fundación.

Black shales and limestones underlying red beds and porphyrites have recently furnished ammonites of Lower Liassic age at a locality on Laguna Morrocoyal southwest of El Banco. Some granites and porphyrites of the Cordillera Central are post-Liassic.

PRE-ORDOVICIAN BASEMENT (GANSSER)

GENERAL STATEMENT

The oldest fossils known in Colombia belong to the lowermost Ordovician or uppermost Cambrian. Sediments of this age overlie the igneous and basement rocks in the Macarena and Garzon massifs.

MACARENA BASEMENT

The Macarena is a range of mountains bordering the southern llanos and extends from 2°20′ to 3°35′ N. Lat. and from 73°25′ to 74° W. Long. They form a sharp angle to the main trend of the Cordillera and attain a maximum elevation of about 1200 meters. The basement is exposed in the central and southern part of the range and is considered a part of the old Guayana shield.

The oldest rocks are mica schists and alkali feldspar gneisses, hornblende gneisses, amphibolites, and injection gneisses with all intermediate types from sericitic schist to highly injected granosyenitic gneiss.

The injection of the granosyenites exposed in the Central Macarena did not affect the overlying Ordovician sediments, in contrast with the Ordovician formations of the Central Cordillera near Puerto Berria which are partly metamorphosed.

(1) In the southern Macarena, mainly sericitic schist and sericitic, alkali feldspar gneisses form the basement. All variation exists between the schists and gneisses, the latter predominating. At the east border of the uplift, the gneisses are highly kaolinized, with secondary sericite developed along the bedding. The basement rocks in the central part of the southern Macarena are more massive with alkali feldspar gneisses

containing little mica, usually chloritized. Microcline and perthitic orthoclase are abundant, with only traces of acid plagioclase, while quartz is subordinate. The quartz grains are remarkably free from undulatory extinction and cataclastic effects. Even slightly injected gneisses show augen development. Chloritized amphibolite intercalations, usually *lit-par-lit*, seem primarily related to the above-mentioned rocks.

(2) In the Central Macarena, in the southern part, injection gneisses predominate, with granosyenites and some quartz porphyries in the north. The injection gneisses are very complex but are generally syenitic.

In the south-central Macarena, the coarse, alkali feldspar, augen gneisses contain large, gray phenocrysts of microcline and microperthite up to 5 centimeters in diameter, showing beautiful quadrille structure. Microcline is also present in the groundmass with olive-brown biotite and small muscovite lamellae. The quartz forms lenses with typical "mosaic" structure but with no marked stress indication. Microscopically the quartz is violet blue. The greenish augen gneisses are characterized by conspicuous pink feldspar phenocrysts. Injection is very irregular. Orthoclase predominates in the groundmass, with quartz and acid plagioclase subordinate. The color of the rock is mainly due to a green biotite, with pale yellow-green to dark-green pleochroism. Large apatite grains, sphene, and epidote, the last partly concentrated in layers, are secondary constituents. The predominance of the alkali feldspar reflects clearly the syenitic injection. Gneisses with less injection are regularly granoblastic without porphyritic structure. Microcline and quartz are abundant, plagioclase only rare and usually altered. Fine laminae of muscovite and biotite occur mainly on the bedding. The sedimentary origin of the gneisses is partly confirmed by garnet which appears occasionally as irregular grains. Some of these gneisses contain phlogopite in place of biotite.

The amphibolites are rare in south Central Macarena. The hornblende is of the normal greenish type. Quartz and especially microcline with typical quadrille structure show that the amphibolitic rocks have also been injected. Some diopsidic augite appears with the injections. A few amphibolites seem of ortho character, and these have a pronounced ophitic texture. Uninjected amphibolites are schistose, the hornblende often with a pale-green, partly actinolitic pleochroism. Epidote and clinozoisite are alteration products of the hornblende.

In the northern part of the Central Macarena, massif intrusives predominate. Marginally some dikes can be observed. Old diabase dikes are highly altered. The hornblende is mainly actinolite, with a very irregular and, for this type of hornblende, often typical, a fibrous

texture. Xenomorph calcite is the alteration product of basic plagioclase. With the granosyenites are gray porphyries with reddish orthoclase phenocrysts, typical of the main rock. The main intrusive body of the Central Macarena is a rather coarse-grained granosyenite. Striking is the flesh-colored orthoclase which is slightly perthitic and rather idiomorphic. The hornblende is altered to chlorite, epidote, and small plagioclase grains. The primary plagioclase is only subordinate and highly altered. There is no microcline in the syenitic main body, which is unusual, especially when it is compared with the syenitic basement near San José del Guaviaré.

PRE-PALEOZOIC BASEMENT IN OTHER AREAS

SAN JOSÉ DEL GUAVIARÉ (Fig. 1)

South of San José the exposed basement is overlain by complex pre-Tertiary sandstones. The transgressively covered syenitic rocks seem therefore part of the old pre-Paleozoic basement of the Guayana shield.

The basement, which covers a rather wide area south of San José (headwaters of the Caño Grande), consists in general of nepheline syenites with a variable amount of nepheline. The rocks are more basic than the granosyenitic basement of the Macarena, and quartz is practically absent. The following rock types can be distinguished: Coarse- and fine-grained biotite syenites, nepheline-biotite syenites, cancrinite-biotite-nepheline syenites, and hornblende syenite to hornblende-quartz syenite, the last only subordinate. In addition to massive rocks, very coarse nepheline syenite pegmatites as well as fine-grained syenite aplites occur.

The grain size of the rock varies considerably. Pegmatites increase toward the west where they contain inclusions of gneissoid biotite-nepheline syenites, often with a distinctive angular shape. The latter gneissic rocks seem fully assimilated toward the east and are responsible for the variable grain size of the massive rocks.

The feldspars consist mainly of perthitic orthoclase, microcline, and microcline perthite; the last two often show a clear quadrille structure. The nepheline is macroscopically gray to slightly oily greenish. Marginally, some crystals are somewhat altered to sericite, haüynite, and sodalite. Cancrinite seems to be primary and does not replace nepheline.

An important feature of the San José syenite is the abundance of magnetite ore. Within the medium-grained rocks magnetite is evenly distributed, often with the olive-brown biotite. In the coarser rocks and mainly in pegmatite, the magnetite forms a surprisingly large part of the rock, occurring often in octahedrons up to 20 centimenters.

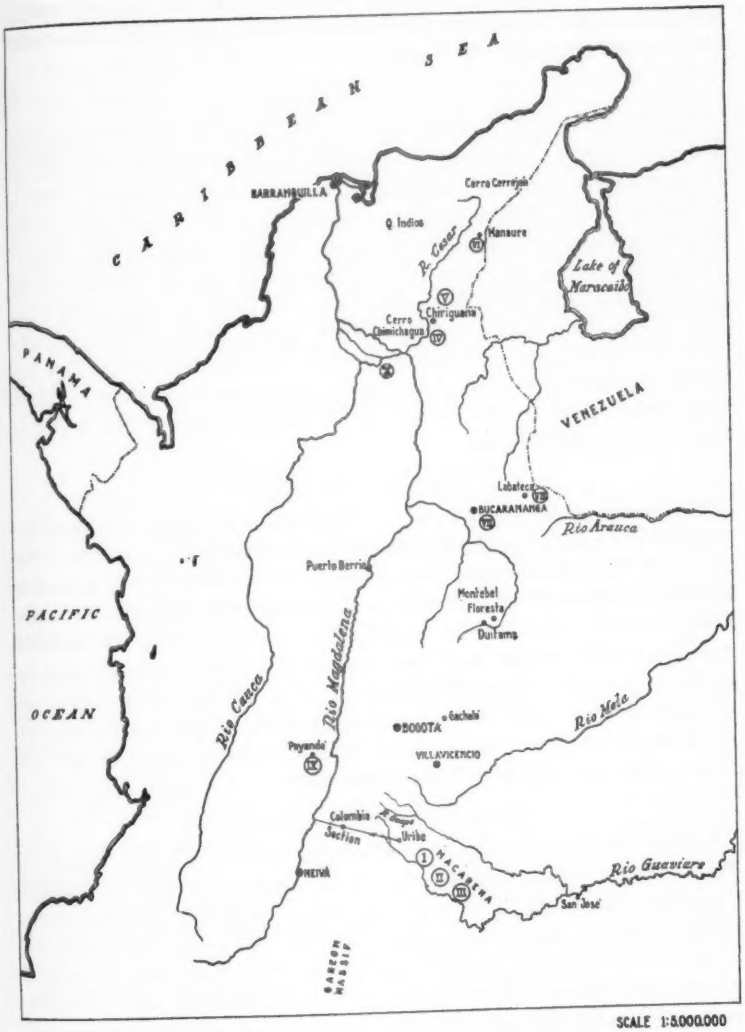

FIGURE 1.—*Key map showing the main pre-Cretaceous fossil localities of Colombia*
Roman numerals indicate location of sections (Figs. 2-6). Scale, *ca.* 1 : 8,000,000

Because of the abundant pegmatite, the amount of ore in the basement is considerable. It is strongly magnetic, with only a low percentage of titanium (fine ilmenite lamellas).

EASTERN CORDILLERA

The Garzon massif, forming the range between the River Magdalena and the Caquetá lowland, is definitely older than the Ordovician. Little is known about its petrology, except some notes by Grosse (1935). A biotite alkali feldspar gneiss is widespread and is usually cut by pegmatite dikes. The injection gneisses are very irregular; the feldspar and quartz grains are concentrated in lenticular layers, surrounded by biotite seams with subordinate muscovite. Aplitic to pegmatitic dikes may contain a rather complex mineral association. Macroscopically violet-red garnet, green diopside crystals, and large biotite flakes are readily recognizable. Interesting is the presence of molybdenum, with large basal flakes in the coarse-grained pegmatites and fine scales in the strongly injected rock.

CENTRAL CORDILLERA

The presence of a pre-Paleozoic basement is largely obscured by younger intrusions, predominantly of a granodioritic character. The age of the batholiths varies from Caledonian to post-Liassic, and more detailed surveys will be necessary to distinguish the different intrusions. Scheibe (1933) considers the amphibolites east and south of Medellin Archean. The gneisses south and east of the Puracé volcano may be of the same age. Younger intrusives of a similar granodioritic to biotitic? granitic type are concentrated mainly in the central part of the Central Cordillera (for example, Manizales biotite granite), and the young volcanism seems connected with them.

SIERRA NEVADA DE SANTA MARTA

Gneisses and amphibolites may belong to the pre-Paleozoic basement. Very probably the Central batholith is Paleozoic, similar to the Central Cordillera batholiths, with a predominance of biotite granites, hornblende granites, and granodiorites. Similar rocks were also observed at the west margin of the Santa Marta uplift intruded into a complex metamorphic series. Amphibolites, hornblende gneisses, and muscovite gneisses are strongly injected and traversed by aplitic quartz veins, aplites, and pegmatites, all probably in connection with the granites and granodiorites. Some garnet amphibolites and plagioclase eclogites, with thin layers of hornblendites, are the most basic rocks found in this area.

The dikes at the west margin of the Santa Marta Mountains trend mainly north-south in contrast to the east-west trend of the main uplift.

A small outcrop of doubtful pre-Paleozoic basement occurs at Cerro de Chimichaguá. A phlogopite-hornblende schist is traversed by several small dikes of syenitic hornblende pegmatite. Slightly pink dikes of granosyenite aplite are remarkable for the predominance of microcline, with little quartz and evidently no plagioclase. Small chloritized biotite flakes are only accessory. Near by are outcrops of fresh-looking biotite-hornblende granite. Some of the orthoclase shows a slight microcline lamellation at the margins. Plagioclase is abundant with clear twin lamellae. The biotite has an olive-brown pleochroism; the hornblende is of the normal green type. These granites seem to be similar to those south of Santa Marta town and are believed not to be older than Paleozoic.

CAMBRO-ORDOVICIAN

MACARENA

(Hubach, Gansser, Fig. 2)

On the east flank of the southern Central Macarena the basement is overlain by ±150 meters of thin-bedded to shaly micaceous sandstones and quartzite, followed by 150 meters of well-bedded quartzitic sandstone. The lower part furnished the following faunule determined by G. Marshall Kay.

Apheoortis (?) sp.
cystid plate
"Bucania" sp.
Ampyx sp. aff. *A. linnarssoni* Schmidt
"Orthoceras" sp.
Megalaspis sp. cf. *M. planilimbata* Angelin
sp. cf. *M. extenuata* Dalman
cf. *Ptychopyge* sp.

The age is Arenigian or Canadian in North America.

Later collections from the same locality furnished graptolites and trilobites, but they have not been determined. The upper part of the series is barren.

In the Central Macarena 45 kilometers north of the above locality the series is locally reduced tectonically and by overlap to a thickness of 15 meters. A thin limestone on the Caño Guapayito furnished the following faunule also determined by G. Marshall Kay.

Za-81 "Caño Guapayita"
Dark, crystalline limestone with fossils in fine-textured interbeds
Lingula sp. cf. *Obolus elongatus* Harrington
Obolus sp. cf. *O. salteri* (Hall)
"Orthis" sp. cf. *Finkelnburgia samensis* Kobayashi
Asaphellus (?) sp., pygidium
Kainella meridionalis Kobayashi
K. sp. cf. *K. lata* Kobayashi
cf. *Protopliomerops primigenus* (Angelin)
cf. *Peltura* sp., pygidium
Shumardia (?) sp.

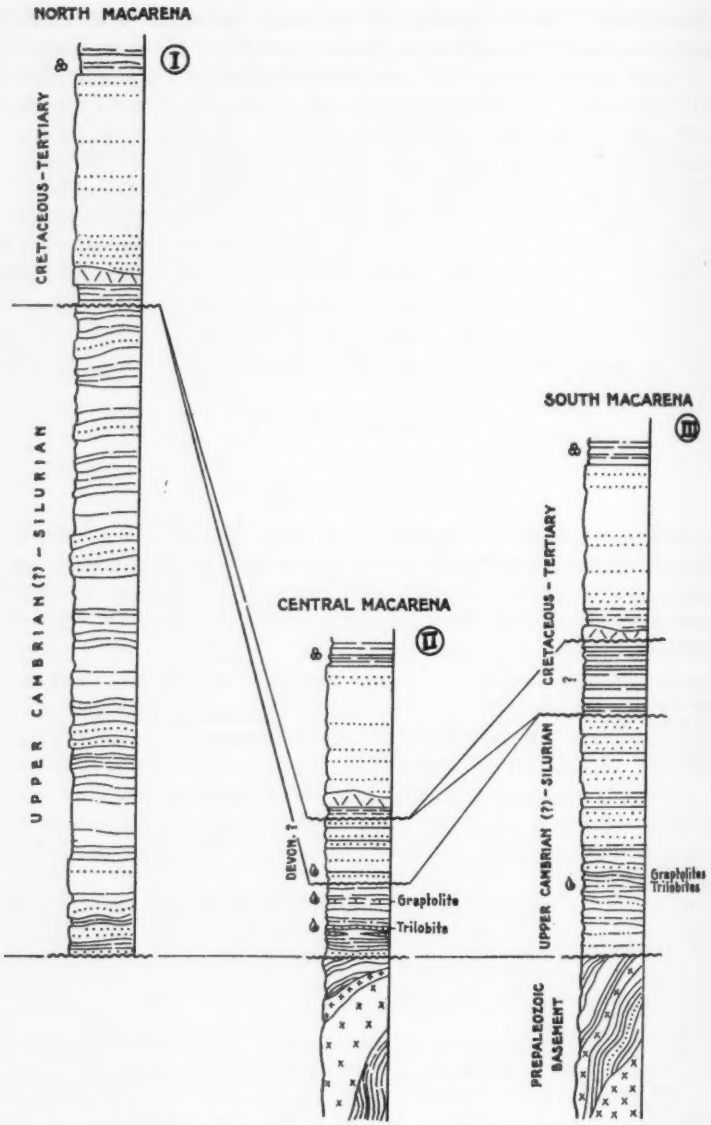

FIGURE 2.—*Stratigraphic sections of Macarena (Llanos)*
After H. Hubach and A. Gansser. Scale, 1 : 5000. *See* Figure 1 for locations.

Kay comments as follows:

"The faunule seems of Tremadocian age and would be classed as uppermost Cambrian in Britain but basal Ordovician in N. America and Scandinavia. The *Peltura* suggests that the age may be uppermost Cambrian as in Scandinavia."

At a locality midway between the above two the series is more shaly and 160 meters thick. It furnished the following faunule determined by the same authority.

Za-144 "Caño 40½ tributary"
Dark, somewhat phyllitic, silty shale
Dichograptus octobrachiatus (Hall)
Tetragraptus sp. aff. *T. bigsbyi* (Hall)
Didymograptus sp.
"Obolus" sp. cf. *Elkania ambigua* (Walcott)
"Lingula" sp. cf. *Obolus elongatus* Harrington
Caryocaris sp.

"The faunule is lower Arenigian—lower Deepkill Ordovician of the Canadian series in North America."

Another sample from the Central Macarena contains *"Archaeorthis* sp. cf. *Eoorthis grandis* Harrington also of Lower Ordovician age".

In the northern Macarena the series is at least several hundred meters thick and consists of gray-black shales or slates with banks of quartzitic sandstones. No good fauna was collected, and the base has not been seen, though basement is believed to outcrop in the interior. The Güéjar River has cut a gorge in this formation which was therefore called Güéjar series in Shell reports.

URIBE TRAIL

(Renz, Fig. 6)

The trail crosses the East Cordillera at Lat. 3°20′ N. at the lowest depression (±2000 meters above sea) of the whole range. Figure 5 shows roughly the structure along this trail.

Northwest of Uribe in a small tributary (Quebrada Agua Bonita) of the Rio Duda some boulders of gray sandy limestone contained trilobites. They probably originated in the Lower Güéjar series.

Kay determined the fossils as follows: *"Plethopeltis* (?) aff. *Bathyurus orbignianus* Kayser" and considers the age as probably Cambrian—Upper St. Croixan.

The crest of the Cordillera is formed by a complex syncline of Cretaceous and Tertiary formations. West of this syncline a zone of Paleozoic formations is exposed in the Rio Ambica as far as the Rio Blanco and consists mainly of light-brown and greenish, soft, micaceous shales with some sands. On Cueva Creek the shales contain cf. *Didymograptus murchisoni* (Beck). Kay considers its age as "Ordovician, probably late Arenigian (Llanvirnian)."

The shales are overlain by a thick (±1000 meters) quartzite series, well exposed along the Ambica. The contact appears to be an unconformity, but this may be due to different reaction to tectonic movements.

The quartzites have furnished no fossils; they are overlain by shales, sandstones, and limestones containing Aptian ammonites. Whether the "Ambica" quartzite is still Paleozoic or basal Cretaceous cannot be decided on present evidence.

The Ordovician of the Rio Ambica covers apparently the north plunge of the Garzon massif.

The only other known Ordovician locality in Colombia is that described by Harrison (1930) from near Puerto Berrio.

QUETAME SERIES

The Quetame series has often been mentioned in the literature. Its type locality is at Quetame, a small village on the Bogota-Villavicencio road, its exposures extending along the road toward Villavicencio for about 38 kilometers. It consists mainly of chloritic to sericitic schists and phyllites with quartzitic sandstones and quartz conglomerates. A zone of yellow quartzites, ± 800 meters thick, together with thin, gray, graphitic shale intercalations, is interbedded in the series, but the intense folding makes it impossible to determine the true stratigraphic sequence. On the west flank of the massif, the Quetame is overlain by a very thick Lower Cretaceous series containing Valanginian ammonites. This Cretaceous series begins with a coarse, basal conglomerate.

On the east flank of the massif near Villavicencio, the Quetame phyllites pass gradually into brick-red shales of lower Carboniferous or Devonian age ("Pipiral series"). In the Uribe area and on the Guape, the Güéjar series becomes regionally metamorphosed, and the main part of the Quetame undoubtedly corresponds to the Güéjar series, but the regional metamorphism has also affected younger formations. On the Guape and the Ariari, a large gabbro massif has intruded the Quetame schists, but the regional metamorphism is not due to this intrusion but to deep burial and very intense folding, mostly Tertiary in age. The lower Cretaceous near Caqueza has also been affected by metamorphism, but to a lesser degree.

The Quetame massif extends about 220 kilometers from the Uribe trail to the Garagoa River. Except for plant remains, the schists are not fossiliferous but grade into fossiliferous formations, from which boulders containing a few Devonian and Silurian fossils mentioned by Schuchert (1935) and Scheibe (1933) were derived.

The term Quetame does not indicate a stratigraphic unit but a facies.

Similar metamorphic Paleozoic formations occur in the Cordillera Central, the Sierra de Santa Marta, and the Perijá range. In the Perijá range metamorphism is locally so slight that the rocks more closely resemble the Güéjar series than the Quetame.

DEVONIAN (Renz)

GENERAL STATEMENT

The fauna of the Floresta Devonian has been recently monographed by Caster (1939). The formation consists of 400 meters of light-gray shale weathering brownish yellow. A basal sandstone member, 40 meters thick, overlies altered chloritic garnet schists. Above the gray shales are vivid red shales overlain by quartzitic sandstones and dark-red conglomerates. Our collections did not have any species not already recorded by Caster.

PERIJÁ RANGE (Fig. 3)

The Devonian of the Venezuelan side has been known for a long time (Cachirí fauna). On the Colombian side two new areas were found, with faunas more closely allied to Floresta than Cachirí: (1) Curumaní-Santa Isabel region east of Chiriguaná, and (2) east of Manaure, in the upper Cesar Valley.

(1) A complete section of the Devonian was studied in the region of Rio Simití 5 kilometers south of Santa Isabel. The Devonian is transgressive with a very pronounced unconformity over slightly metamorphosed gray slates, arkosic sandstones, and fine arkosic conglomerates, similar to the Güéjar series of the Macarena but without fossils. The Devonian begins with quartz conglomerates, about 1 meter thick, which are overlain by approximately 5 meters of light brown-gray chert containing a good Middle Devonian fauna. The following fossils were determined by Emeis, Shell paleontologist:

Arcospirifer olssoni Caster
A. sp. (n. sp. ?)
Atrypa sp. (*A. harrisi* Caster)
Elytha colombiana Caster
Strophonella meridionalis Caster
Anaplotheca (?) *silvetti* (Ulrich)
7 different species of *Spirifer*

The chert is overlain by 20 meters of reddish-gray claystone shale passing into fine light-gray banded sandstone about 10 meters thick. Then follows a thick formation of fine- to medium-grained green-brown sandstone with intercalations of micaceous gray-brown shaly layers and a few thin gray shale intercalations. In sandy shales which are poorly exposed in a small creek, 2.5 kilometers east-southeast of Santa Isabel, a Devonian fauna was found. Particularly abundant are *Atrypa* sp., *Meganteris australis* Caster, *"Spirifer" kingi* Caster.

The Devonian is overlain by Triassic red beds.

(2) East of Manaure the Cretaceous sediments are cut off from Paleozoic, which forms a large part of the Perijá, by a fault of considerable displacement. The Devonian is composed mainly of whitish-brown sandstone and quartzites with intercalations of silky, gray shales. About 1.5 kilometers east of Manaure a rich fauna was collected in a fine

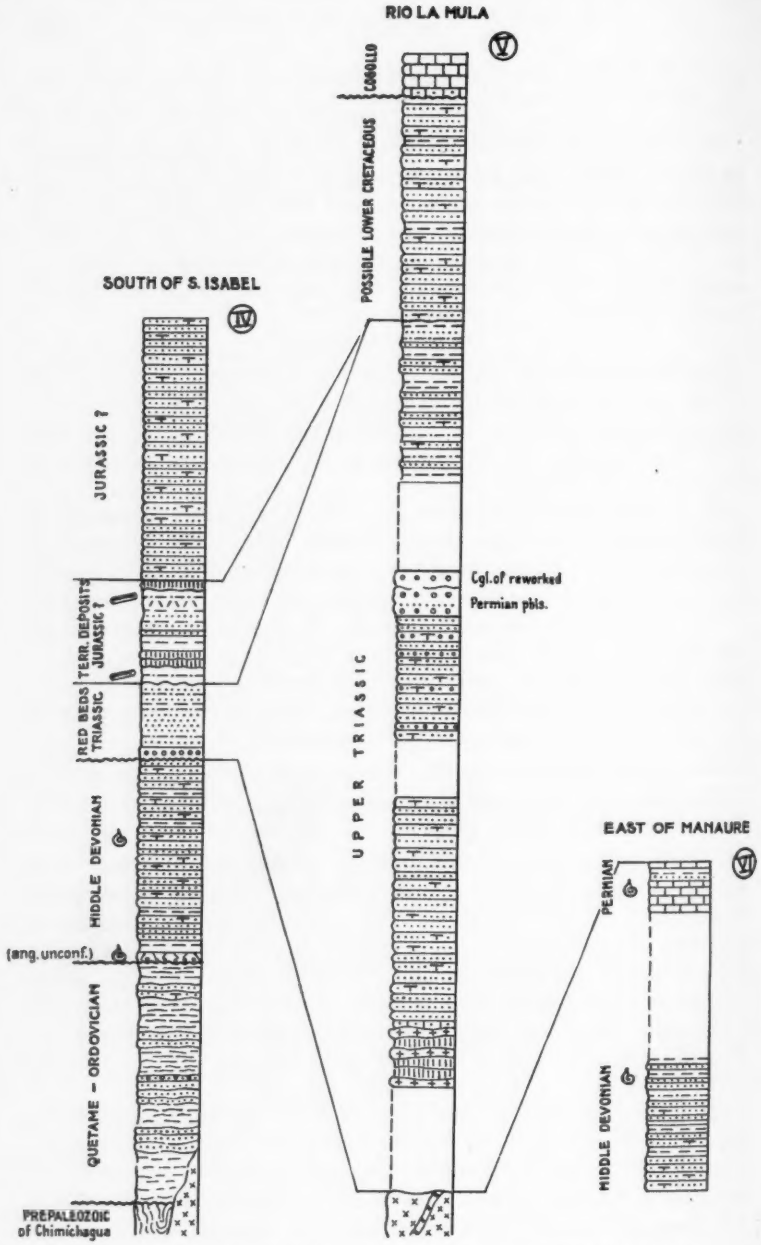

FIGURE 3.—*Generalized stratigraphic column along the west foot of the Cordillera Perijá*

After O. Renz. Scale, 1 : 20,000. *See* Figure 1 for locations.

ferruginous sandstone. The most important forms, according to determinations by James Steele Williams, of the U. S. Geological Survey, are:

Crinoid columnals
Fenestrellinoid bryozoans, probably largely belonging to *Polypora*
Leptaena ? cf. *L. boyaca* Caster
Stropheodonta ? cf. *S. concava* Hall
S. ? *koslowskii* Caster
Stropheodonta (*Cymostrophia*) cf. *S. dickeyi* Caster
Chonetes ? sp. undet.
Delthyris ? cf. *"Spirifer" duodenarius* Hall
Spirifer (*Australospirifer*) cf. *S. antarcticus* (Morris and Sharp)
Spirifer (*Australospirifer*) *iheringi* Kayser
"Spirifer" kingi Caster
Spirifer ? sp. undet.
Other brachiopods, fragmentary, undetermined
Gastropods 1 or 2 fragments of indeterminate forms, trilobite pygidium, undetermined.

This fauna is Middle Devonian.

Along the eastern slope of the Cordillera Oriental, Devonian sediments are not so well developed as in the Sierra de Perijá. In the upper Rio Ariari, pebbles of dark-gray sandy, slightly micaceous shales containing Devonian fossils (fragment of a trilobite, *Stropheodonta*, and *Chonetes* sp. *concava* Hall) were observed.

CARBONIFEROUS

GACHALÁ

Best known is the Carboniferous from the east flank of the Quetame massif, first found by Stutzer (1927), and studied more in detail by Kehrer (1933). The formation is in part highly fossiliferous, but the fauna is still insufficiently collected and studied. Lower to Upper Carboniferous is present.

BUCARAMANGA

(Hubach, Fig. 4)

The Carboniferous of Bucaramanga was first found by Merritt, but his report is unpublished. Dickey (1941) gives a short description but lists no fossils. The series is overthrust by granites and schists of the Santander massif, and part of the sequence may be structurally reversed. The apparent top is formed by limestones and primary limestone breccias with crinoid stems, underlain by red and black shales and sandstones.

A very thin fossil bed furnished the following species determined by James Steele Williams:

Crinoid columns
Schuchertella ? sp. indet.
"Productus" sp. indet.
"Productus" sp. indet. may be *Diaphragmus* sp.
Spirifer increbescens trigonalis Martin
Punctospirifer sp. indet.
Composita subquadrata (Hall) var.
Aviculopecten ? sp. indet. fragment.

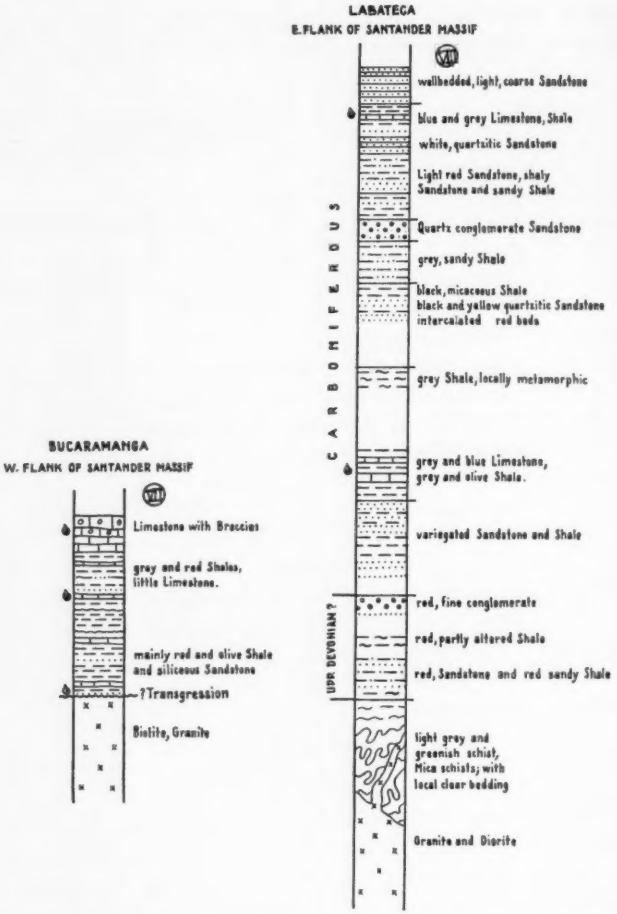
LABATECA
E. FLANK OF SANTANDER MASSIF
VIII
wellbedded, light, coarse Sandstone
blue and grey Limestone, Shale
white, quartzitic Sandstone
Light red Sandstone, shaly Sandstone and sandy Shale
Quartz conglomerate Sandstone
grey, sandy Shale
black, micaceous Shale
black and yellow quartzitic Sandstone intercalated red beds
grey Shale, locally metamorphic
grey and blue Limestone, grey and olive Shale.
variegated Sandstone and Shale
red, fine conglomerate
red, partly altered Shale
red, Sandstone and red sandy Shale
light grey and greenish schist, Mica schists, with local clear bedding
Granite and Diorite
CARBONIFEROUS
UPR DEVONIAN ?
BUCARAMANGA
W. FLANK OF SANTANDER MASSIF
VIII
Limestone with Breccias
grey and red Shales, little Limestone.
mainly red and olive Shale and siliceous Sandstone
?Transgression
Biotite, Granite

FIGURE 4.—*Generalized stratigraphic column of west and east sides of Santander Massif*

After H. Hubach. Scale, 1 : 31,250. *See* Figure 1 for locations.

The fauna is either Mississippian or early Pennsylvanian. The Carboniferous overlaps on granite. Hettner (1892) included this series in his Giron *Labateca* (Hubach) (Fig. 4).

Carboniferous sediments, ±2400 meters thick, were found on the Páramo de Tierra Negra near Labateca at the Venezuelan border. They

consist mainly of thick sandstone members, partly gritty, alternating with shales, marly shales, and few limestones. Red sediments prevail especially in the lower and middle parts. The following fossils from the lower part have been provisionally determined by Barker:

Fenestella retiformis von Schlotheim
Spirifer cf. *increbescens* (Hall)
Derbya buchi d'Orbigny
Spiriferina campestris White
Aviculopecten sp.
Corals
Strophomena ?
Productus sp.

The age is probably Upper Carboniferous.

The basal part consists of red shales and conglomerates, partly altered to schists by a granitic intrusion. They may be partly Devonian.

A still thicker series (±4000 meters) of probable Carboniferous occurs in the Murillo range east of Labateca, but no determinable fossils have been found. Plant remains are common. The lower 1200 meters contains red beds intruded by granites.

PERIJÁ RANGE

(Fig. 3)

At Manaure Carboniferous was not found *in situ*, but gray limestone boulders with abundant *Spirifer* and *Productus* are common in the streams.

At Cerro Cerrejón in the Ranchería valley, the Tertiary (Eocene) is overthrust by green-brown shales and sandy shales with brown sandstones and some limestones. The latter contain many brachiopods, *Spirifer*, and *Productus*. The Carboniferous is again overthrust by red beds covered unconformably by the Cogollo limestone which forms the top of the mountain.

PERMIAN

(Renz) (Fig. 3)

The best Permian fauna was found east of Manaure in the Perijá, in a fault block between Upper Cretaceous and Devonian. The formation is a gray, slightly dolomitic limestone with layers and nodules of black chert. Fossils are common and were determined by James Steele Williams and A. K. Miller.

Sponge ? indet.
Crinoid columns
"Productus" inca d'Orbigny
Rhynchonelloid brachiopod, possibly a *Leiorhynchus*
Pugnoides swallovianus ? (Shumard).
Spiriferina campestris White, n. var.
Schizodus ? cf. *S. cuneatus* Meek
Astartella sp. undet., small form
Bellerophonids, several indeterminate forms
Bellerophon ? cf. *B. crassus*
Euphemites ? sp. undet., small form
"Pleurotomaria" sp. undet., very incomplete
"Murchisonia" ? sp. undet.
Baylea ? sp. undet.
Titanoceras ? sp. undet.
Medlicottia sp. undet. of the type of *Medlicottia whitneyi* Böse
Perrinites cf. *hilli* (Smith)

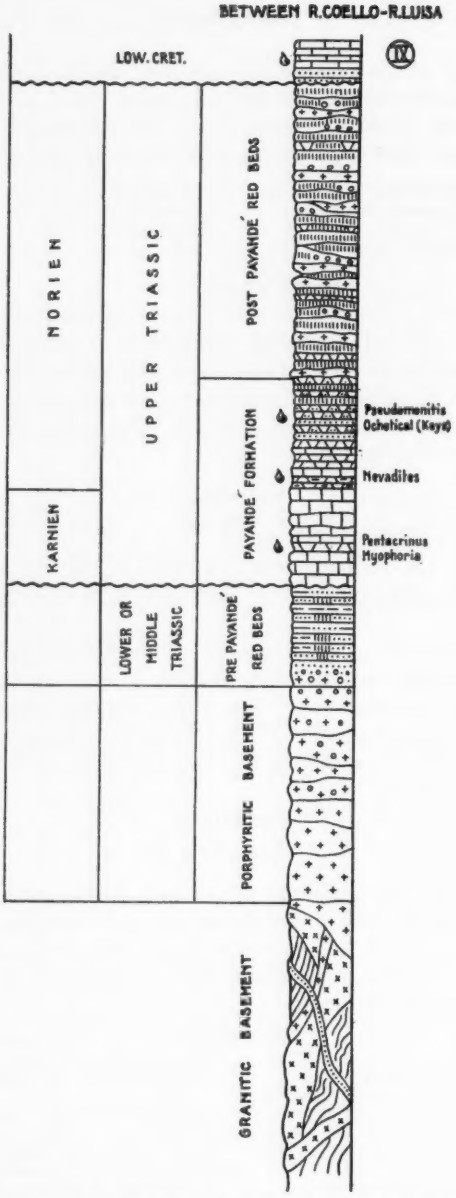

FIGURE 5.—*Generalized column of pre-Cretaceous sediments between Rio Coello and Rio Luisa*

After O. Renz. Scale, 1 : 10,000. *See* Figure 1 for locations.

The fauna, especially *Perrinites*, is typical for the Leonard of West Texas.

Farther south in the Perijá range, on the Rio Mula, volcanic red beds contain conglomerates with limestone boulders, in which Permian Fusulinae occur, and from which Emeis determined *Paraschwagerina yabei* (Staff). The limestone has not been found in place and may have been removed by post-Permian erosion.

Elsewhere in Colombia, the Permian has not yet been proven by fossils, but quite possibly the top of the Gachalá and Labateca sections extend into this period.

TRIASSIC AND LIASSIC

MARINE TRIASSIC

(Renz) (Fig. 5)

Pseudomonotis ochotica had been reported by Diener and Jaworski (1922) from Chaparral in the upper Magdalena valley, but the locality could not be found. The Triassic locality mentioned by Schuchert (1935) after Rollot at Utica does not exist since only Lower Cretaceous outcrops in that region.

Marine Triassic was found north of Chaparral at Payandé. Between the Coello and Luisa rivers the basement of the Central Cordillera is unconformably overlain by a series of porphyritic red beds with a 400-meter-thick limestone chert formation between. This formation has been called the Payandé.

Conspicuous is a gray limestone, partly sandy or siliceous, with intercalations of brown, partly tuffaceous cherts. It is cut by many dikes of gray-green porphyrite, causing strong contact metamorphism. The limestone is altered locally to marbles, and wollastonite needles are common. The lower part furnished well-preserved gastropods, bivalves, crinoids (mostly *Pentacrinus*), and echinoids. Emeis determined from the lower part *Myophoria jaworski* Steinmann, well known from the Karnian of Perú. Gastropods and brachiopods have not yet been determined.

In the middle of the formation, a gray cherty shale overlying the limestone furnished several ammonites identified as:

Nevadites sutanensis Jaworski
N. cf. *lissoni* Jaworski
Anolcites dieneri Jaworski

In the upper part a light-brown, cherty tuff contains abundant well-preserved *Pseudomonotis ochotica* Keyserling (Pl. 1, fig. 2). The upper part of the Payandé is therefore definitely Norian. The fauna is evi-

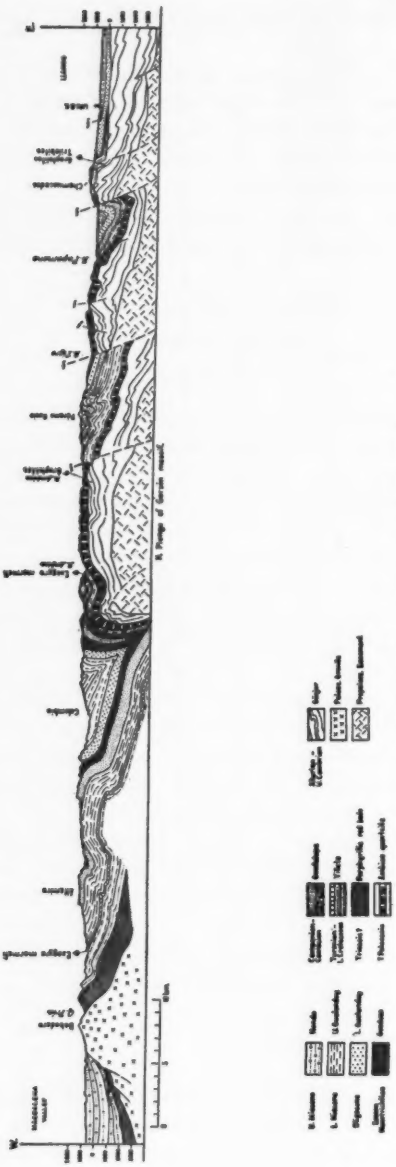

FIGURE 6.—*Geological section along the Uribe trail*
After O. Renz. *See* Figure 1 for location.

dently the same as that described by Jaworski from the Suta limestone of Perú.

The marine Payandé is transitional with a red-bed series composed mostly of porphyritic flows, tuffs, and volcanic breccias which must be Upper Triassic, but possibly extending into the Rhaetic. The formation is unconformably overlapped by Lower Cretaceous.

Other remnants of marine Triassic probably occur in the Quebrada de los Indios and at Montebel.

LIASSIC OF EL BANCO AREA AND CESAR VALLEY RED BEDS

(Hubach, Renz) (Fig. 1, loc. X)

Geologists of the Texas Company discovered a fossil locality at Laguna Morrocoyal, about 45 kilometers southwest of El Banco. The locality was studied in greater detail by Hubach who collected a small fauna of ammonites, bivalves, and plants. These fossils occur in black shales and thin limestones in the lower part of a thick series (over 2600 meters) of red beds, shales, sandstones, and conglomerates with very thick, generally acid flows, volcanic tuffs, and gray, yellow, or purple agglomerates. The series is intruded and overlain by a chaotic assemblage of intrusive volcanic breccias, mostly acid to intermediate. The youngest rocks seem to be strongly differentiated intrusives—granites, diorites, and gabbros. Lower Cretaceous (Barremian or older) overlaps onto the upper igneous series on the east side of the Central Cordillera about 40 kilometers east-southeast of Morrocoyal.

The fossils from the Morrocoyal beds have not been fully determined. The most common forms are ammonites belonging to the Liassic genus *Arietites*, but *Psiloceras* is probably also present. One bivalve species is common. Fish remains and well-preserved plants are likewise found in the black shale member.

Another fossil locality was found previously by Shell geologists R. Martin and O. Renz in Quebrada de los Indios, about 32 kilometers southeast of Fundacion at the southwest side of the Santa Marta Mountains. A 200-meter-thick series of black, partly siliceous shales and quartzitic sandstones, with occasional thin sandy limestones, is in fault contact with schists of the Santa Marta massif. It is normally overlain by greenish quartzites and claystones alternating with green and red porphyries and tuffs. In the upper part, dark-red quartz porphyries predominate. The fauna of the Indios beds consists of poorly preserved gastropods and bivalves and one possible ammonite impression. Most common are small species of *Estheria* apparently allied with those from the Montebel series. Whether the Indios beds should be correlated with the Liassic of Morrocoyal or the Upper Triassic of Montebel is uncertain.

A third fossil locality found by O. Renz near Manaure in the Cesar Valley is near the top of the red beds. It furnished only indeterminable mollusks and possibly some ammonite fragments from thin (20-30 centimeter) beds of nodular limestones interbedded with red sandstones, conglomerates, and sandy shales containing silicified wood. This locality is 20 kilometers south-southwest of Urumita, where Karsten recorded lower Cretaceous ammonites in red beds. Karsten's report gave rise to the formerly generally accepted Lower Cretaceous age of all "Giron red beds" in Colombia. No fossils were found by Shell geologists in the Urumita red beds, but Karsten's record cannot be dismissed without further evidence, and the presence of Lower Cretaceous red beds in the upper Cesar Valley must be still considered a possibility.

The red beds in the Cesar Valley are more than 4000 meters thick but vary widely, partly because of pre-Cretaceous erosion. The amount of volcanic material, such as interbedded flows and agglomeratic tuffs, is subject to rapid change and is greatest on the flanks of the Santa Marta and the Cordillera Central, but even in the Perijás there are rhyolite and liparite flows. Conglomerates with boulders of Permian *Fusulina* limestone were found by Renz in the Chiriguana area where horizons of fossil plants also occur.

In the southeastern Cesar Valley along the front of the Perijás, the red beds are overlain by 600 meters of brown and green quartzitic sandstones with thin, gray unfossiliferous shales. Overlying them is 600 meters of coarse, white massive sandstone with light-gray, unfossiliferous shale. The upper sandstone may belong to the Lower Cretaceous and be the equivalent of the Tomon of Venezuela.

The age of the red beds in northern Colombia may therefore range from upper Triassic to lower Cretaceous, but only the lower Jurassic (Liassic) is well established.

"GIRON" OF THE MIDDLE MAGDALENA VALLEY

From Hettner's description of the Giron, it is clear that he included within this series the red beds near the city of Giron as well as the Carboniferous of Bucaramanga and referred these rocks to the lower Cretaceous, largely from Karsten's record of ammonites from Urumita. The name is now generally restricted to the series of sandstones, grits, and conglomerates alternating with red and green siltstones and shales, over 2000 meters thick, outcropping in the Lebrija gorge north of Giron. Dickey (1941) and De Böckh (1929) have given good descriptions of the formation. It apparently overlies Carboniferous Bocas shales and is overlain by basal Cretaceous fossiliferous sandstones and limestones

with no visible unconformity. In the Chicamocha gorge, 35 kilometers south of Giron, it overlaps with pronounced unconformity upon crystalline schists intruded by granites, and it thins rapidly toward the old massif. No fossils except plant remains have been found near the type locality.

About 130 kilometers south of Giron at Montebel (on the road between Duitama and Charala), upper Giron sandstones and grits are overlain by black, partly massive shales, several hundred meters thick, containing remains of plants, *Estheria*, and small gastropods. A. A. Olsson (personal communication), who collected at the same locality, considers the formation upper Triassic. The Giron in its type region contains no volcanic or effusive material.

West of the Magdalena (on the Anacué) red and green siltstones with a few banks of tuffaceous sandstones and tuff breccias are correlated with the Giron. They are intruded by a red, generally coarse granite (hornblende-biotite granosyenite to quartz monzonite according to Gansser). This intrusive body is cut by dikes of monzonitic to gabbro porphyries (diabase) and aplitic granodiorites. Young porphyries cover a great extension in the headwater of the Anacué. The youngest porphyries (the most basic ones) in the red beds are possibly of Lower Cretaceous age since, in the Muzo emerald district, Gansser found ultrabasic intrusions in Albian rocks.

OTHER FORMATIONS OF UNKNOWN AGE

A limestone several hundred meters thick, intruded by gabbro and greatly altered, outcrops between the rivers Guape and Ariari in the Llanos front. Its age is unknown, and there are no limestones of similar thickness known in the Paleozoic sections in the Macarena or at Villavicencio.

A very thick (over 2000 meters) sandstone conglomerate section overlain by red shales occurs on the Rio Ele in Arauca. Only indeterminable plant remains have been obtained from these beds. It may represent a near-shore facies of the Murillo formation, also of unknown age.

CONCLUSIONS

Our knowledge of the pre-Cretaceous is still too scanty for sweeping generalizations and conclusions.

An early Paleozoic (mainly Ordovician) geosyncline was probably present in the area of the East Cordillera, but its sediments were to a large extent greatly metamorphosed or eroded in later periods. Caledonian folding is indicated in the Perijá range.

Thick Devonian, Carboniferous, and Permian marine deposits were folded in late Permian or more likely lower Triassic orogenic phases, and to a large extent they were eroded.

Marine upper Triassic with strong affinities with the Peruvian Triassic has been found in the upper Magdalena Valley but may have extended to the Caribbean coast. Marine lower Jurassic is known only from the El Banco district. Triassic and Jurassic are chiefly red beds with variable amounts of effusive and intrusive igneous rocks.

REFERENCES CITED

Caster, K. E. (1939) *A Devonian fauna from Colombia,* Bull. Am. Paleont., vol. 24, no. 83.

De Böckh, H. in Gregory, J. W. (1929) *The structure of Asia,* London, p. 164

Dickey, P. A. (1941) *Pre-Cretaceous sediments in Colombia,* Am. Assoc. Petrol. Geol., Bull., vol. 25, p. 1789-1795.

Gerth, H. (1932) *Geologie Südamerikas,* Berlin.

Grosse, E. (1935) *Compilación de los estudios geológicos oficiales en Colombia,* tome 3, Bogotá, p. 54-58.

Harrison, J. T. (1930) *The Magdalena Valley, Colombia, S. A.,* 15th Intern. Geol. Cong. S. Africa, C. R., vol. 2.

Hettner, A. (1892) *Die Kordillere von Bogotá,* Petermanns Mitt., Ergänzungsheft 104, Gotha.

Jaworski, E. (1922) *Die Marine Trias von Süd Amerika,* Neues Jahrb., Beil.-Bd. 47.

Karsten, H. (1886) *Géologie de l'ancienne Colombie Bolivarienne,* Berlin.

Kehrer, W. (1933) *El Carboniano del borde, llanero de la Cordillera Oriental,* Bol. Minas, nos. 49-54, p. 105-121, Bogotá.

Oppenheim, Victor (1940) *Jurassic Cretaceous (Giron) beds in Colombia and Venezuela,* Am. Assoc. Petrol. Geol., Bull., vol. 24, p. 1611-1619.

Scheibe, R. (1933) *Compilación de los estudios geológicos oficiales en Colombia,* tome 1, Bogotá.

Schmidt, W. E. (1938) *Fósiles paleozoicos de la Cordillera Oriental de Colombia,* Ministerio de Industrias y Trabajo, Bogotá (publ. also Berlin, 1934).

Schuchert, Charles (1935) *Historical geology of the Antillean-Caribbean region,* New York.

Stutzer, O. (1927) *Beiträge zur Geologie der Kolumbianischen Ostkordillere in der naeheren u. wieteren Umgebung von Bogotá,* Neues Jahrb. Beil.-Bd. 57.

Shell Petroleum Company, Bogota, Colombia.

Manuscript received by the Secretary of the Society, July 7, 1942.
Published with permission of Anglo-Saxon Petroleum Company.

EXPLANATION OF PLATE I

PLATE 1.—SYENITE AND FOSSILS FROM COLOMBIA

Figure

1. Nepheline-Cancrinite-Biotite Syenite
   1. Nepheline slightly altered by sericite, hauynite
   2. Microcline-microcline perthite (clear quadrille structure)
   3. Orthoclase (perthitic)
   4. Perthite
   5. Cancrinite

   Biotite and magnetite are present but do not show in photograph; holocrystalline texture; massive structure.

2. *Pseudomonotis ochotica* Keyerling
   Upper Triassic: Locality Payandé.

3. *Estheria* sp. greatly enlarged.
   Probably Upper Triassic; Locality Quebrada de los Indios.

4-6. Liassic ammonites from Laguna Morrocoyal
   Impressions of *Arietites* and *Psiloceras*.

1

4

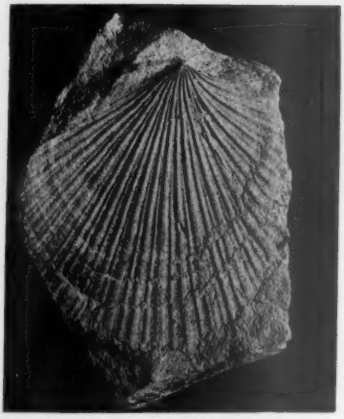

2

5

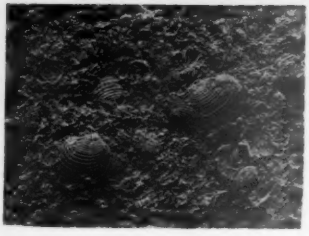

3

6

SYENITE AND FOSSILS FROM COLOMBIA

BULLETIN OF THE GEOLOGICAL SOCIETY OF AMERICA
VOL. 54, PP. 1305-1374, 28 FIGS. SEPTEMBER 1, 1943

PACKING IN IONIC MINERALS

BY H. W. FAIRBAIRN

CONTENTS

Page

Abstract 1306
Introduction 1307
Acknowledgments 1308
Concept of packing index 1308
  Development of methods of volume determination 1308
  The packing index 1310
  Sources of error 1311
  Selection of ion radii 1311
  Degree of accuracy of packing index 1315
  Correlation of crystal packing with packing of uniform spheres 1316
Mineralogic correlations of packing index 1320
  Correlation of refractive index and density with packing index 1320
    Introduction 1320
    Discussion of data 1322
  Correlation of hardness with packing index 1331
    Introduction 1331
    Discussion of data 1335
    Conclusion 1345
  Correlation of packing index with polymorphic phases 1347
    General statement 1347
    Thermal inversion (fixed composition) 1347
    Thermal inversion (variable composition) 1347
    Pressure inversion 1348
  Correlation of packing index with phases showing incongruent melting 1349
  Correlation of packing index with size of minor ions 1350
  Summary of mineralogic correlations 1353
Geologic aspects of ion packing 1353
  Introduction 1353
  General correlation with temperature of formation of minerals 1354
  Correlation with silicate crystallization 1355
  Correlation with incongruent phases in magma 1356
  Rock density and rock-packing index 1357
  Packing index of metamorphic rocks 1361
  The eclogite problem 1363
  Glaucophane schist 1364
  Correlation of packing index with thermal and stress environment of metamorphic silicates 1365
  Correlation of packing index with morphological development of porphyroblasts 1369
  Correlation of packing index with rates of mineral alteration 1370

Page

Possible inversions in stony meteorites 1372
Summary of geologic applications 1372
References cited 1373

ILLUSTRATIONS

Figure Page

1. Contrast of type of packing and closeness of packing 1311
2. Relative diameters of selected ions 1315
3. Range of packing indices 1316
4. Atomic number—ion refractivity relations 1321
5. Packing index—density—refractive index relations of Al-rich silicates 1325
6. Packing index—density—refractive index relations of K-rich silicates 1327
7. Packing index—density—refractive index relations of Ca-rich silicates 1327
8. Packing index—density—refractive index relations of Na-rich silicates 1329
9. Packing index—density—refractive index relations of Mg-rich silicates 1329
10. Packing index—density—refractive index relations of miscellaneous silicates. 1330
11. Packing index—density—refractive index relations of unclassified silicates... 1331
12. Packing index—density—refractive index relations of oxides 1332
13. Packing index—density—refractive index relations of sulphates, phosphates, chlorides, fluorides 1333
14. Packing index—density—refractive index relations of carbonates, nitrates, borates, tungstates, nonionic minerals 1334
15. Packing index—hardness—bonding index relations for chlorides, oxides and hydroxides 1337
16. Packing index—hardness—bonding index relations for ZO_4 silicates 1338
17. Packing index—hardness—bonding index relations for Z_2O_7, ZO_3, Z_4O_{11} silicates 1339
18. Packing index—hardness—bonding index relations for $Z_3O_8(?)$, Z_4O_{10} silicates 1340
19. Packing index—hardness—bonding index relations for ZO_2 silicates and miscellaneous phosphates 1341
20. Packing index—hardness—bonding index relations for carbonates ,tungstates, sulphates 1342
21. Packing index—density relations of common igneous rocks 1358
22. Chemical relations of selected constituents of rocks of Figure 23 1359
23. Packing index—density relations of an approximately isochemical rock series 1360
24. Packing indices of common metamorphic rocks 1362
25. Comparison of packing indices of minerals in gabbro and eclogite, hornblende schist and glaucophane schist 1363
26. Packing indices of metamorphic minerals based on thermal characteristics... 1366
27. Relation between packing and bonding indices and position in "crystalloblastic" series 1368
28. Comparison of packing indices with rate of mineral alteration 1371

ABSTRACT

An attempt is made to give approximate quantitative values to the ratio ion volume/unit cell volume for a selected group of about 200 minerals. A "packing index" is proposed to express this relationship. The general correlation of this packing index with specific gravity, hardness, and mean refractive index, whereby increase or decrease in one is paralleled by changes in the same direction in the others, is shown in some detail. Unexplained discrepancies in this correlation are

mostly confined to refractive index data for minerals containing much Ti^{4+}, Zr^{4+}, B^{3+}, Fe^{2+}, and K^{1+}. Ti^{4+} is likewise dominant in certain minerals with unexplained hardness anomalies. These correlations demonstrate the superiority of the concept of packing index for much of this comparative work.

The role of packing index in thermal inversion and incongruent melting is believed to be accessory for the most part; in pressure inversion, however, it plays a vital part. It is also an important factor in controlling the maximum size of the minor ions which may enter a crystal structure.

Consideration is given to packing index in its possible effect on order of crystallization in rocks. A general correlation is evident, but it is concluded that other factors control these processes. Comparison of the packing indices of a selected group of rocks with their respective specific gravities shows the superiority of the former, especially for comparisons involving varying quantities of iron-rich minerals. The eclogite problem is discussed briefly in terms of packing index, and the general conclusion of leading investigators is confirmed that pressure probably played a leading part in the genesis of these rocks. The origin of glaucophane schist is shrouded in more uncertainty. Attention is also directed to packing index in its relation to metamorphic silicates in general, and issue is taken with the misleading "oxide volume law". In an attempted correlation of packing index with temperature of formation of metamorphic silicates it is disclosed that "anti-stress" minerals are high temperature-low index types, whereas "stress" minerals show the opposite relation in general.

There is fairly direct correlation between packing index and the degree of development of porphyroblast crystal faces ((high index = good crystal development). The rate of mineral alteration, on the other hand, seems to vary inversely with packing index.

The possibility of mineral inversions in stony meteorites due to release of pressure is considered briefly from the standpoint of packing index. Speculations concerning the derivation of some chondrules from garnet and of graphite from diamond are mentioned.

INTRODUCTION

The role played by pressure in the formation of igneous and metamorphic rocks has long been a fertile field for speculation among geologists. Until recently, mineralogists could offer but few facts in support or negation of such speculations. Relative rock densities were used to some effect, as many foliated rocks such as schists have higher specific gravity than chemically analogous igneous rocks. As the majority of the schist minerals occur commonly also in hydrothermally altered rocks, which are neither igneous nor foliated, it has proved difficult, however, to assign a specific role to pressure. Of late years, too, the justifiable emphasis on temperature has relegated pressure effects to a lesser part in geologic processes. The writer has approached this subject through investigation of a more fundamental characteristic than density—namely, the ion packing of minerals. As the study developed it was found desirable to expand the problem to include all possible mineralogic as well as geologic aspects of ion packing. This has resulted in a better-balanced perspective of crystal packing than could otherwise have been obtained and has disclosed some unexpected problems.

The investigation of ion packing first became a practical problem with the development of modern structural crystallography. In this paper discussion is restricted to geologically important crystals and deals with the

packing problem for the so-called "ionic" minerals, which embrace roughly all except the native elements and sulphides.[1] Reasonably reliable data on ionic radii and unit cell volumes make possible the determination of the ratio ion volume/unit cell volume, correlation of this quantity with mineralogical constants such as refractive index, and some attempt at explanation of geological relations. As far as the writer is aware, no quantity other than "molecular volume" has ever been used in this connection. The limited usefulness of molecular volume will become apparent as the discussion proceeds.

ACKNOWLEDGMENTS

In the preparation of the paper the writer has been stimulated and guided in many ways by M. J. Buerger and Harry Berman (crystal-structural and mineralogic aspects of the problem) and by W. J. Mead and W. H. Newhouse (geologic correlations). No small service has been rendered by students through their incidental criticism at various stages of the work. To all concerned in any way with its development and presentation, grateful acknowledgment is made at this time.

CONCEPT OF PACKING INDEX

DEVELOPMENT OF METHODS OF VOLUME DETERMINATION

In the early days of theoretical chemistry, when the molecular weight and density of compounds comprised the only data relating to volume, and ionic radii were entirely unknown, the determination of molecular volume (molecular weight/density) was an important calculation, as it permitted comparison of cell volume relations. Various aspects of this relationship were thoroughly explored, under the leadership of Hermann Kopp (Mellor, 1922), during the second quarter of the last century. It still serves in petrologic work as a basis for discussion of rock chemistry. A compilation of molecular volumes has recently been made by Blitz (1934) which includes all classes of compounds. Molecular weight and consequently molecular volume are, however, relative, not absolute quantities and have limited application. Moreover, they yield no information concerning the closeness of packing of the crystal units. The next stage therefore was the determination of absolute values for molecular weights and volumes. In 1865 Loschmidt (Mellor, 1922) bridged this gap for the first time, applying the long-neglected law of Avogadro to the problem. Omitting details, he determined a constant N, usually known as Avogadro's number, which permits the transition to be made. In recent years this constant has been redetermined by almost a dozen different

[1] It is realized that bonds other than those of ionic type occur in many of these minerals, but as they are believed to be a minority, the modifier "ionic" may be used in absence of a better term.

methods, all of which show remarkable agreement. The approximate value of N ($= .6 \times 10^{24}$) is adequate for all computations in this paper. That is,

$W_{abs.}$ (in grams) $= \dfrac{W_{mol.}}{.6 \times 10^{24}}$ where $W_{abs.}$ = absolute weight

$V_{abs.}$ (in cc.) $= \dfrac{W_{mol.}}{(.6 \times 10^{24})D}$ $W_{mol.}$ = molecular weight

$V_{abs.}$ (in cu. A) $= \dfrac{W_{mol.}}{.6\,D}$ $V_{abs.}$ = absolute volume

D = density

1 cc. $= 10^{24}$ cu. A

A third stage of development, confined to crystalline substances, commenced in 1914 with W. L. Bragg's pioneer X-ray diffraction studies. With this searching technique it is possible to determine independently the dimensions and consequently the volume of a unit cell of a substance. (*See* Table 1 for volumes of various cells.) The correctness of the premises

TABLE 1.—*Volumes of unit cells*

(a, b, c, α, β, γ, are the standard crystallographic symbols)

Isometric	a^3
Tetragonal	$a^2 c$
Rhombohedral	$a^3 \dfrac{(1 - \cos\alpha)^2}{\sin\alpha\,(1 + \cos 2\alpha)}$
Hexagonal	$\dfrac{\sqrt{3}}{2} a^2 c$
Orthorhombic	abc
Monoclinic	$abc \sin\beta$
Triclinic	$abc\sqrt{1 - \cos^2\alpha - \cos^2\beta - \cos^2\gamma + 2\cos\alpha\,2\cos\beta\cos\gamma}$

of this method and the preceding one is shown by the close correspondence in values which may be obtained for any substance, where cell dimensions, chemical composition, and density are accurately determined (Table 4). As the unit cell usually contains more than one formula unit of the material, the relation between the chemical and X-ray methods is expressed as follows— $\dfrac{V\text{ (unit cell)}}{Z} = \dfrac{W\text{ (mol.)}}{.6D}$, where Z = the number of formula units in the cell. Thus $V_{abs.}$ may be obtained by two methods.[2]

A final stage, and one with which this paper is particularly concerned, was the determination of ion dimensions (Stillwell, 1938), first by Wasastjerna in 1922, later by Goldschmidt (1926), Pauling (1927), Zachariasen (1931), and Kordes (1939). Empirical and theoretical

[2] For data on dimensions of unit cells the reader is referred to Bragg (1937) and the comprehensive Strukturbericht (Ewald, Hermann, *et al.*, 1931).

methods yielded essentially similar results. In consequence of these advances it is possible to calculate approximately the percentage of the total volume of a unit cell which is occupied by ions and thus compare crystals with one another on the basis of their packing. That is—

$$V_{\text{abs.}} = \frac{V \text{ unit cell}}{Z} = \frac{W_{\text{mol.}}}{.6\,D} = \text{Vol. ions} + \text{Vol. "interstices"}.$$

Calculations based on these quantities give the closeness of ion packing in a crystal.

THE PACKING INDEX

Probably the first attempt to determine closeness of ion packing was made by Sollas in 1898, on cubic crystals of the NaCl type. Although nothing was known definitely of the sizes of atoms at that time, it was his belief that NaCl molecules did not exist but that in their stead small sodium ions and larger chlorine ions were stacked together in compact cubical form. By assuming certain values for ion radius, Sollas calculated the closeness of packing for a number of simple crystals. Although this work is now only of historical interest, his discussion was astonishingly prophetic and ranks high in the literature of crystal chemistry which antedates the X-ray diffraction period.

In the present investigation calculations of closeness of packing are confined to those mineral crystals displaying mainly ionic bonds. Substances showing predominant homopolar (covalent) bonding are omitted as some uncertainty exists concerning the absolute size of their atoms. This group consists largely of sulphides, arsenides, and antimonides, leaving as ionic minerals [8] the silicates, oxides, carbonates, sulphates, etc.

At the outset, distinction must be made between closeness of packing and type of packing. Structural crystallographers use the latter term to denote a purely geometrical arrangement of atoms or ions, a conception which permits considerable latitude in relative size of adjacent ions. Thus in Figure 1 the same *type* of packing is shown by both (a) and (b). The *closeness* of packing differs in each example, as may be seen by inspection of the interstices, (b) being more closely packed than (a). The term *packing index* is proposed to denote closeness of packing. It is derived from the expression $\frac{V \text{ ions}}{V \text{ unit cell}} \times 100$, which represents the percentage of the absolute volume of one formula unit of a crystal occupied by ions. The packing index is this quantity arbitrarily divided by 10 — $P.\,I. = \frac{V \text{ ions}}{V \text{ cell}} \times 10$. The packing index of a substance therefore lies

[8] For details of ionic and other types of bonds the reader is referred to standard texts on crystal chemistry (Stillwell, 1938; Evans, 1939).

between 0 and 10, a convenient numerical range analogous to that expressing specific gravity or hardness.

SOURCES OF ERROR

As already stated, the excellent agreement of the theoretical and experimental methods of calculating absolute volume removes all appreciable

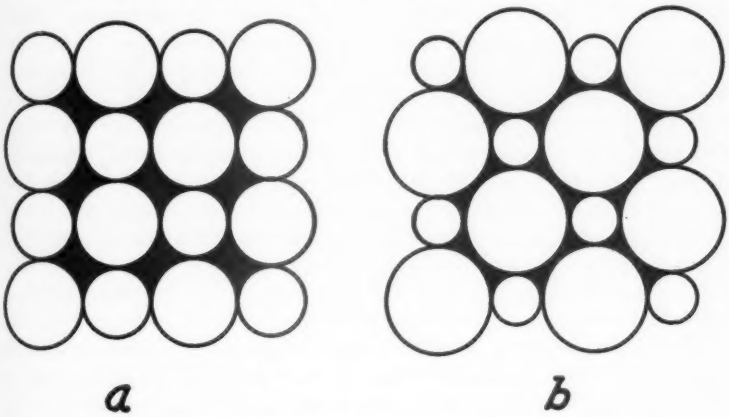

FIGURE 1.—*Contrast of type of packing and closeness of packing*

Shown by (a) where spheres are approximately of same size and relatively large interstices exist, and (b) where greater discrepancy in sphere size decreases interstitial space. Co-ordination of the spheres (type of packing) is identical in both cases.

error from this part of the packing index determination. For a number of minerals, indeed, where unit cell dimensions are undetermined, but composition and density are known, the latter quantities suffice to determine absolute volume. All error is restricted for practical purposes to calculation of the volume of the ions in the crystal cell.

SELECTION OF ION RADII

Two assumptions underlie the computation of ion volume: (1) The effective zone of influence of each ion is essentially spherical, and (2) an average radius can be determined for each. Regarding the first, most investigators agree that a sphere more nearly approximates the domain of an ion than any other geometrical form. The second point requires more extended discussion.

One of Sollas' most prescient statements (1898) was that there "does not seem to be any sound reason why the volume of an element should remain absolutely constant and independent of an element with which it is associated." As a generalization this is still true today. Although the

effective radius of an ion is fairly constant for structurally related compounds, important differences exist between certain groups of unrelated ones. (*Compare* O^{2-} in silicates, carbonates, etc.) The selection of average radii is therefore no mean task if volume relations of ionic minerals are to be intelligently discussed. Fortunately the problem is lightened considerably by the numerical predominance of oxygen in these compounds (halides and fluorides excepted). By any standard the oxygen ion is also much larger than the cations associated with it and in silicates forms over 90 percent of the total ion volume. Its radius is thus the critical dimension in the entire computation of packing index. For oxides Wasastjerna (Stillwell, 1938) determined empirically that $O^{2-} = 1.32$, a value used later by Goldschmidt as a basis for radius determination of associated cations in oxides. Some years later Pauling and Zachariasen (Stillwell, 1938) determined that $O^{2-} = 1.40$, the former on theoretical grounds, the latter empirically. Still more recently Kordes (1939a) calculated an empirical value of 1.37 and a theoretical value of 1.35. The writer has selected the Goldschmidt-Wasastjerna radius of 1.32 through the following indirect approach.

Structural analysis of a number of oxides indicates conditions of closest packing. This is particularly true of aluminum and beryllium oxides where the small cations lie in the interstices between approximately close-packed oxygen anions. If the cations are neglected and the anions considered geometrically as a framework of uniform spheres, it can easily be shown that the spheres occupy 74 percent of the total volume of any given unit of the framework. For corundum the following is then true:

Vol. of unit cell of corundum = 85 cu. Å (= $2Al_2O_3$)

" " 6 O^{2-} = $\frac{74}{100} \times 85 = 62.9$ cu. A

" " 1 O^{2-} = 10.5 cu. Å

Radius of O^{2-} = 1.36 A

This method of attack indicates that 1.36 is the maximum O^{2-} radius possible for corundum if Al^{3+} is small enough to permit O^{2-} to pack together with the minimum interstitial space. As perfect spheres and absolutely tight packing cannot be assumed, O^{2-} must be somewhat less than 1.36. Furthermore, if $Al^{3+} = .57$ (Goldschmidt's value), O^{2-} anions of radius 1.36 would not pack absolutely tightly, as it can be shown that the maximum radius of interstitial spheres is .56 where the main framework has spheres of 1.36 radius. For this reason also O^{2-} is probably less than 1.36.

By similar calculation it can be shown that in the close-packed structures assumed for chrysoberyl ($BeAl_2O_4$), diaspore ($HAlO_2$), and bromellite (BeO) the oxygen ions cannot exceed 1.34, 1.37, and 1.34 Å respec-

tively. For the same reasons as those mentioned for corundum it is highly probable that the true O^{2-} radius is less than these values.

In the silicates, the problem of an average O^{2-} radius becomes more complex because of increase in the kinds of cations present. An average made by the writer from seven published descriptions gives $O^{2-} = 1.34$, obtained

TABLE 2.—*Correlation of average O^{2-} radii in common radicles with co-ordination and valence*

Central element of the radicle	Cation	Co-ordination	Average radius of O^{2-}
Silicon	Si^{4+}	4	1.32Å
Phosphorus	P^{5+}	4	1.27
Sulphur	S^{6+}	4	1.22
Boron	B^{3+}	3	1.20
Carbon	C^{4+}	3	1.15
Nitrogen	N^{5+}	3	1.05

from O-O distances in the Si-O tetrahedra.[4] The range of values is 1.30-1.37. Additional data are obtainable from topaz and kyanite, both of which have approximately close-packed structures and predominant Al cations, thus permitting analysis similar to that for the selected oxides above. For kyanite the following is true under geometrical packing conditions.

Vol. of unit cell = 288 cu. Å ($=4Al_2SiO_5$)

" " 20 O^{2-} = $\frac{74}{100} \times 288 = 213$ cu. Å

" " 1 O^{2-} = 10.6 cu. Å

Radius of O^{2-} = 1.36 Å

The same value is obtained for topaz ($Al_2SiO_4F_2$) where O^{2-} and F^{1-} are assumed to have the same volume and form a close-packed structure consisting $\frac{2}{3}$ of O^{2-} and $\frac{1}{3}$ of F^{1-}. From these two examples the upper limit for O^{2-} is about the same as for the oxides. It seems reasonable, therefore, to assume a similar radius. It appears more prudent to use a small value for O^{2-} than a large one, and the writer's choice is the 1.32 radius of Wasastjerna and Goldschmidt.

Although comprehensive data are lacking for many phosphates, sulphates, borates, carbonates, and nitrates, there is fair agreement about the O-O distances in the PO_4, SO_4, CO_3, BO_3, and NO_3 radicals of those minerals already studied. Furthermore, the order of magnitude of the O^{2-} radii is correct, as may be seen in Table 2. In the first group, having 4-co-ordination, arrangement of the central elements in order of increasing

[4] Bragg (1937, p. 140) gives O-O = 2.6 ±, but no details as to the basis for this figure.

valence corresponds to the order of decreasing O^{2-} radius. This obtains also for the second group, showing 3-co-ordination. That is, for a given co-ordination and given anion, the attractive forces become greater with

TABLE 3.—*Effective radii, volumes and refractivity of ions of common elements**

Element Molecular Weight in ( )	Ion	Radius†	Volume ($V = 4.19r^3$)	Maximum Refractivity**
Aluminum (26.97)	Al^{3+}	.57	.80	.137
Barium (137.36)	Ba^{2+}	1.43	13.23	4.02
Beryllium (9.02)	Be^{2+}	.34	.17	.0167
Boron (10.82)	B^{3+}	.33	.15	.006
Calcium (40.08)	Ca^{2+}	1.06	4.99	1.182
Carbon (12.01)	C^{4+}	.2	.33	.0025
Cerium (140.13)	Ce^{3+}	1.18	6.87	1.77
Chlorine (35.46)	Cl^{1-}	1.81	24.85	8.17
Chromium (52.01)	Cr^{3}	.64	1.09	
Copper (63.57)	Cu^{1+}	.96	3.69	1.080
Fluorine (19.00)	F^{1-}	1.33	9.85	2.27
Hydrogen (1.00)	(a) $(OH)^{1-}$	1.40	11.48	4.8
	(b) H_2O molecule	1.38	11.02	3.71
Iron (55.85)	Fe^{2+}	.83	2.39	.109
	Fe^{3+}	.67	1.26	
Lead (207.21)	Pb^{2+}	1.32	9.64	1.777
Lithium (6.94)	Li^{1+}	.78	1.97	.060
Magnesium (24.32)	Mg^{2+}	.78	1.97	.238
Manganese (54.93)	Mn^{2+}	.91	3.14	.151
Nitrogen (14.01)	N^{5+}	.15	.01	.0013
Oxygen (16.00)	O^{2-}			6.84
in oxides		1.32	9.64	
silicates		1.32	9.64	
phosphates		1.27	8.59	
sulphates		1.22	7.63	
borates		1.20	7.24	
carbonates		1.15	6.37	
nitrates		1.05	4.86	
Phosphorus (30.98)	P^{5+}	.35	.18	.054
Potassium (39.10)	K^{1+}	1.33	9.85	2.07
Silicon (28.06)	Si^{4+}	.39	.25	.084
Sodium (23.00)	Na^{1+}	.98	3.94	.442
Sulphur (32.06)	S^{2-}	1.74	22.08	19.8
	S^{6+}	.34	.16	.036
Tin (118.70)	Sn^{4+}	.74	1.70	1.207
Titanium (47.90)	Ti^{4+}	.64	1.09	.463
Tungsten (183.92)	W^{4+}	.68	1.32	.371
Yttrium (88.92)	Y^{3+}	.93	3.41	1.37
Zinc (65.38)	Zn^{2+}	.83	2.39	.713
Zirconium (91.22)	Zr^{4+}	.87	2.87	.90

* Radii mostly from Evans (1939, p. 171), after Goldschmidt. Based on 6— co-ordination.

** Actual values, especially for large anions, less than these, due to polarization.

† Actual radii in compounds slightly less than theoretical effective radii of free ions.

increase in the charge on the cation and so reduce the effective radius of the anion.

Table 3 and Figure 2 include the results of the preceding discussion. The values for the cations and all anions except O^{2-} are those for 6-co-

ordination. No correction for other co-ordinations has been made in the packing index determinations, as the common cations are small relative to O^{2-} and the anions F^{1-} and Cl^{1-} vary little in any case. The average variation in radius is estimated as less than 5 percent from the value given,

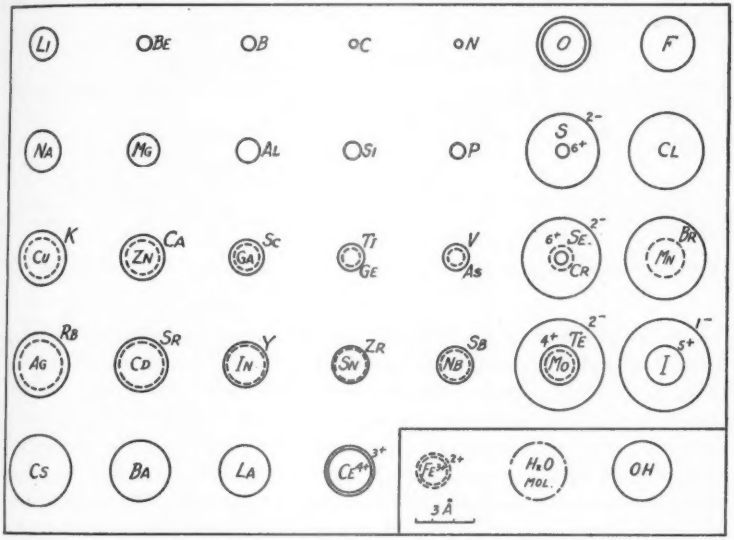

FIGURE 2.—*Relative diameters of selected ions*

Arranged as in the periodic table. Double circle for O^{2-} indicates its varying radius in silicates, sulphates, nitrates, etc. Water molecule (not an ion) included in lower right of table.

which, in the light of other uncertainties about the shapes and sizes of ions, is too small to justify additional arithmetic in calculating packing index.

DEGREE OF ACCURACY OF PACKING INDEX

It is necessary to emphasize that values given for packing index are not to be taken too literally. The writer regards them as semiquantitative only, and no pretense is made that this index can be determined as yet with the same average precision as a quantity such as specific gravity. Revisions up or down of at least 5 percent are to be expected for some minerals, which, in terms of packing index, would be expressed by $\pm .5$. Correlations limited to minerals of the same type (*e.g.*, silicates) can be made, however, with considerable confidence; comparison of species in different groups must be made with some reservations. In time, as better average values for ion radii become available, the packing index should

become a relatively fixed value, taking its place with other accepted quantities—refractive index, hardness, etc.—as part of the necessary description of a mineral. The advantages of discussion without further delay of the concept of packing index far outweigh in the writer's opinion the disadvantages arising from lack of precision in certain of the determinations.

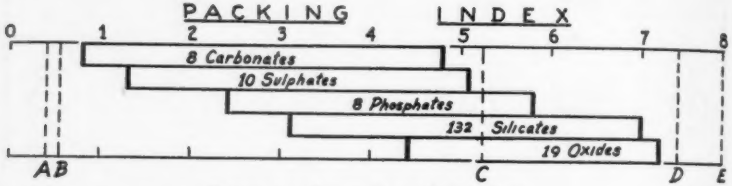

FIGURE 3.—*Range of packing indices*

Of minerals included in Table 4. A, B, C, D, E refer to packing indices of a series of artificial geometrical systems described in the text.

Table 4 lists alphabetically about 200 ionic minerals for which packing index has been determined. Silicates form approximately two-thirds of these, as the known species are numerous, and the group is of great geologic importance. Rare species are arbitrarily included wherever they appear to be useful for interpretation. The reader may add as many as desired following the method given. In this first presentation the writer considers that sufficient computations have been made to indicate the possibilities of the packing index. Complete tabulation can await later developments.

CORRELATION OF CRYSTAL PACKING WITH PACKING OF UNIFORM SPHERES

It is instructive to compare the packing indices of Table 4 with values computed for specific geometric systems of spheres. This has been done in Figure 3. The range in packing index for various groups of substances is depicted by horizontal columns arranged in order of increasing average packing index. It is interesting to note in passing that this is also the order of increasing average co-ordination of the ions—*i.e.*, 3-co-ordination is characteristic of carbonates, 4-co-ordination is prevalent in sulphates, phosphates, and silicates, 6-co-ordination dominates most oxide structures.

A and B (indices .42 and .56) represent attempts by Melmore (1942) and Heesch and Laves (1933) to discover the most open packing possible in a system of uniform spheres. The limit has probably not yet been reached. Of the minerals in Table 4, the packing index of natrite, computed minus its 10 molecules of H_2O, is the closest approach to A and B. C (index of 5.24) represents the cubic open packing of uniform spheres. It is seen that carbonate and sulphate ions are packed much less tightly than this, that the average phosphate and silicate packing index is almost

TABLE 4.*—*Reference list of minerals*

Mineral	Formula used	Cell vol. (calc.)	Cell vol. (expt.)	Ion vol.	Packing index	Remarks
Acmite	$NaFe(SiO_3)_2$	110	.....	64	5.8	
Actinolite	$Ca_2(Mg_{2.5}Fe_{2.1})(Si_4O_{11})_2(OH)_2$	458	444	258	5.6	
Akermanite	$Ca_2MgSi_2O_7$	143	150	80	5.4	
Albite	$NaAlSi_3O_8$	167	168	83	4.9	
Almandite	$Fe_3Al_2(SiO_4)_3$	195	190	125	6.6	
Alunite	$KAl_3(SO_4)_2(OH)_6$	263	.....	133	5.1	
Amblygonite	$LiAl(PO_4)F.1/4H_2O$	82	.....	47	5.8	6.7 incl. H_2O
Analcite	$NaAlSi_2O_6.H_2O$	163	161	61	3.7	4.5 incl. H_2O
Anatase	TiO_2	34	33	21	6.3	
Andalusite	$(Na_{.4}K_{.2}Al_{7.4})(SiO_4)_4[O_{2.2}(OH)_{1.2}]$	348	344	205	6.0	
Andradite	$Ca_3Fe_2(SiO_4)_3$	225	217	134	6.1	
Anhydrite	$CaSO_4$	77	75	36	4.7	
Anorthite	$Ca(Al_2Si_2O_8)$	168	.....	84	5.0	
Anorthoclase	$Na_{.75}K_{.25}(AlSi_3O_8)$	174	.....	85	4.9	
Anthophyllite	$Mg_7Fe_2(Si_4O_{11})_2(OH)_2$	443	436	252	5.7	
Apatite	$Ca_5(PO_4)_3F$	266	260	138	5.3	
Apophyllite	$K_{.5}Ca_2(Si_4O_{10})F_{.5}4H_2O$	322	320	117	3.6	5.1 incl. H_2O. Status of H undecided.
Aragonite	$CaCO_3$	57	56	24	4.3	
Astrophyllite	$(Na_2K_2Ca)(Fe_{10}Al_2Ti_2)(Si_2O_7)_6(OH)_8$	1009	1001	561	5.6	
Augite	$(Ca_{.6}Mg_{.6}Fe_{.2}Al_{.5}(Al_{.5}Si_{1.5}O_6)$	108	.....	64	5.9	
Axinite	$H(Ca_2Fe)BAl_2(SiO_4)_4$	290	282	169	5.9	
Babingtonite	$Ca_2Fe^{II}Fe^{III}Si_5O_{14}(OH)$	284	290	161	5.5	
Barite	$BaSO_4$	86	86	44	5.1	
Benitoite	$BaTi(Si_3O_9)_2$	189	183	102	5.6	
Bertrandite	$Be_4(Si_2O_7)(OH)_2$	153	149	92	6.1	
Beryl	$Be_3Al_2(SiO_3)_6$	334	365	177	5.1	
Biotite	$KMg_{1.25}Fe_{1.5}(Al_{1.5}Si_{2.5}O_{10})(OH)_2$	252	.....	138	5.5	
Bromellite	BeO	13.7	13.7	9.8	7.2	
Brookite	TiO_2	33	32	21	6.4	
Brucite	$Mg(OH)_2$	41	40	27	6.7	
Calcite	$CaCO_3$	61	61	24	4.0	
Cancrinite	$(Na_{4.2}Ca_{.9})(Al_{3.2}Si_{3.1}O_{12})(CO_3)_{1.1}.2H_2O$	676	.....	299	4.4	4.7 incl. H_2O
Cassiterite	SnO_2	37	35	21	6.0	
Celsian	$Ba(Al_2Si_2O_8)$	183	.....	92	5.0	
Chabazite	$(Ca_2Na)(Al_{12}Si_{17}O_{60}).40H_2O$	2652	.....	822	3.1	4.7 incl. H_2O
Chlorite	(See Prochlorite)					
Chloritoid	$(Fe_{1.5}Mg_{.5})Al_2(Al_2Si_2O_{10})(OH)_4$	240	.....	149	6.2	
Chondrodite	$2Mg_3SiO_4.MgF_2$	182	181	107	5.9	
Chromite	$FeCr_2O_4$	75	73	43	5.9	
Chrysoberyl	$BeAl_2O_4$	58	54	40	7.2	
Chrysotile	(See serpentine)					
Clinoenstatite	$MgSiO_3$	52	.....	31	6.0	
Clinohumite	$4Mg_2SiO_4.MgF_2$	327	326	196	6.0	
Clinozoisite	$Ca_2Al_3(SiO_4)_3(OH)$	225	232	140	6.1	
Clintonite	$MgCa_4Al_2(Al_2Si_4O_{20})(OH)_6$	687	.....	399	5.8	
Cordierite	$(Mg_{1.2}Fe_{.8})(Al_4Si_5O_{18})$	387	390	182	4.7	ZO_2 classification not established. Possibly allied with beryl (ZO_2).
Corundum	Al_2O_3	43	.....	31	7.2	
Cristobalite (high)	SiO_2	.....	45	19.5	4.3	
Cristobalite (low)	SiO_2	44	43	19.5	4.5	
Cronstedite	$Fe_3Fe_2(Fe_2Si_2O_{10})(OH)_6$	170	.....	89	5.2	
Cryolite	Na_3AlF_6	117	.....	72	6.2	
Cummingtonite	$(Mg_{.8}Fe_{2.2})(Si_4O_{11})_2(OH)_2$	447	456	249	5.5	
Cuprite	Cu_2O	80	77	34	4.4	
Cuspidine	$Ca_4(Si_2O_7)F_2$	210	.....	108	5.1	
Danburite	$CaB_2(Si_2O_7)O$	137	135	83	6.1	Z_2O_7 classification not definitely established
Datolite	$CaB(SiO_4)(OH)$	90	88	55	6.2	
Diamond	C	6.0	5.6	1.9	3.4	Non-ionic
Diaspore	$HAlO_2$	29	29	20	7.0	
Dickite	$Al_2(Si_2O_5)(OH)_4$	164	.....	96	5.9	
Diopside	$CaMg(SiO_3)_2$	110	109	65	5.9	
Dolomite	$CaMg(CO_3)_2$	107	106	46	4.3	
Dravite	$NaMg_3B_3Al_2(Al_2Si_6O_{27})(OH)_4$	521	524	323	6.2	
Dumortierite	$Al_3B(SiO_4)_3O_3(OH)$	318	.....	202	6.4	
Enstatite	$MgSiO_3$	52	52	31	6.0	
Epidote	$Ca_2(Al_{1.8}Fe_{1.2})(SiO_4)_3(OH)$	233	.....	140	6.1	

* As H_2O in zeolites, montmorillonite, vivianite, etc., is a loosely held molecule, not an ion like $(OH)^{1-}$, it is excluded in the computation of true packing index of such minerals. The index which includes H_2O is given in the column headed "Remarks."

TABLE 4.*—*Reference list of minerals—continued*

Mineral	Formula used	Cell vol. (calc.)	Cell vol. (expt.)	Ion vol.	Packing index	Remarks
Epsomite	$MgSO_4.7H_2O$	244	.....	33	1.4	4.5 incl. H_2O
Euclase	$BeAl_2(SiO_4)_2(OH)_2$	159	.....	103	6.5	
Fayalite	Fe_2SiO_4	77	.....	44	5.7	
Ferrodolomite	$CaFe(CO_3)_2$	107	111	46	4.2	
Fluorite	CaF_2	.....	41	25	6.2	
Forsterite	Mg_2SiO_4	73	73	43	5.9	
Friedelite	$Mn_8Si_6O_{15}(OH)_{10}$	544	.....	286	5.3	
Gahnite	$ZnAl_2O_4$	66	66	42	6.4	
Gehlenite	$Ca_2Al(AlSiO_7)$	150	150	79	5.3	
Gibbsite	$Al(OH)_3$	55	53	35	6.5	
Glauberite	$Na_2Ca(SO_4)_2$	163	....	74	4.5	
Glauconite	$(K_{.78}Ca_{.14}Na_{.33})(Al_{1.47}Fe_{.97}Mg_{.46}Fe_{.10})(Al_{.88}Si_{3.65}O_{10})(OH)_2$	261	237	128	5.1	
Glaucophane	$Na_4Mg_3Al_4(Si_{16}O_{44})(OH)_4$	842	910	505	5.7	
Goethite	$HFeO_2$	35	34	22	6.3	
Graphite	C	9.3	8.8	1.5	1.7	Non-ionic
Grossularite	$Ca_3Al_2(SiO_4)_3$	213	207	133	6.4	
Gypsum	$CaSO_4.2H_2O$	124	123	36	2.9	4.7 incl. H_2O
Gyrolite	$Ca_4(Si_6O_{15})(OH)_2.3H_2O$	456	.....	189	4.1	4.9 incl. H_2O
Halite	NaCl	46	45	26	5.8	
Hambergite	$Be_2(BO_3)(OH)$	.....	66	34	5.1	
Hedenbergite	$CaFe(SiO_3)_2$	118	.....	65	5.5	
Helvite	$(Mn_{4.5}Fe_{2.4}Zn_{1.1})(Be_6Si_6O_{24})S_2$	564	549	301	5.4	
Hematite	Fe_2O_3	51	.....	34	6.6	
Heulandite	$(Ca_6Na)(Al_{11}Si_{29}O_{80}).25H_2O$	2322	.....	816	3.5	4.8 incl. H_2O
Hornblende	.....	.....	.....	.....	5.7	Not computed but undoubtedly close to this value
Humite	$3Mg_2SiO_4.MgF_2$	253	253	150	5.9	
Hypersthene	$Mg_{1.71}Fe_{.29}(SiO_3)$	53	.....	32	5.9	
Ice	H_2O	32	33	11	3.3	Non-ionic
Ilmenite	$FeTiO_3$	51	.....	32	6.4	
Ilvaite	$Fe_2Fe(SiO_4)_2(OH)$	155	166	95	5.9	
Jadeite	$NaAl(SiO_3)_2$	99	.....	63	6.4	
Kaolinite	$Al_2Si_2O_5(OH)_4$	167	163	96	5.8	
Kieserite	$MgSO_4.H_2O$	89	.....	33	3.7	4.9 incl. H_2O
Kornerupine	$Mg_{10}Al_{10}(SiO_4)_5O_7$	734	729	444	6.1	
Kyanite	$(Na_{.2}Al_{7.8})(SiO_4)_4[O_{2.5}(OH)_{.5}]$	301	288	202	7.0	
Lawsonite	$CaAl_2(Si_2O_7)(OH)_2H_2O$	168	172	98	5.8	6.4 incl. H_2O. Status of H not definitely established
Lazulite	$(FeMg)Al_2(PO_4)_2(OH)_2$	170	.....	96	5.7	
Lazurite	$Na_{10}(Al_6Si_6O_{24})S_2$	700	.....	321	4.6	
Leifite	$Na_4(Al_2Si_9O_{22})F_2$	511	.....	251	4.9	
Leucite	$K(AlSi_2O_6)$	147	143	69	4.8	
Leucophanite	$(CaNa)Be(Si_2O_6F)$	137	136	77	5.6	
Magnesite	$MgCO_3$	48	45	21	4.8	
Magnetite	$FeFe_2O_4$	75	74	44	5.9	
Margarite	$CaAl_2(Al_2Si_7O_{10})(OH)_2$	218	223	128	5.8	
Marialite	$Na_4(Al_3Si_9O_{24})Cl$	563	554	277	5.2	
Meionite	$Ca_4(Al_6Si_6O_{24})(CO_3)$	557	554	287	5.2	
Melilite	$Ca_2Mg_{.6}Al_{.8}(Al_{.6}Si_{1.4}O_7)$	145	150	80	5.3	
Merwinite	$Ca_3Mg(SiO_4)_2$	172	.....	94	5.4	
Microcline	$K(AlSi_3O_8)$	182	174	89	5.0	
Mirabilite	$Na_2SO_4.10H_2O$	359	.....	46	1.3	4.3 incl. H_2O
Monazite	$Ce(PO_4)$	76	.....	41	5.4	
Monticellite	$CaMg(SiO_4)$	83	85	46	5.4	
Montmorillonite	$Mg_2Al_4(Si_{12}O_{30})(OH)_{10}.12H_2O$	1149	.....	416	3.6	4.8 incl. H_2O
Mullite	$Al_6(SiO_4)_2O_5$	234	.....	131	5.6	Al always somewhat less than 6
Muscovite	$KAl_2(AlSi_3O_{10})(OH)_2$	238	234	132	5.5	
Natrite	$Na_2CO_3.10H_2O$	325	.....	27	.8	4.2 incl. H_2O
Natrolite	$Na_{16}(Al_{16}Si_{24}O_{80}).16H_2O$	2256	2238	856	3.8	4.6 incl. H_2O
Nephelite	$Na(AlSiO_4)$	92	93	44	4.8	
Niter (Saltpeter)	KNO_3	80	80	24	3.0	
Norbergite	$Mg_3SiO_4.MgF_2$	107	105	68	6.4	
Okenite	$Ca_2(Si_4O_{10}).4H_2O$	308	.....	107	3.5	4.9 incl. H_2O
Orthoclase	$K(AlSi_3O_8)$	182	174	89	5.0	
Pargasite	$Ca_4Na_2Mg_5Al(Al_3Si_{13}O_{44})F_4$	928	.....	542	5.8	
Pectolite	$Ca_4Na_2(Si_6O_{17})(OH)_2$	395	383	203	5.2	
Periclase	MgO	18.4	18.5	11.6	6.3	
Perovskite	$CaTiO_3$	57	.....	35	6.2	
Petalite	$Li(AlSi_4O_{10})$	213	.....	100	4.7	
Phenakite	Be_2SiO_4	62	62	39	6.3	
Phlogopite	$KMg_{2.25}(Al_{1.8}Si_{3.2}O_{10})(OH)_2$	252	247	140	5.6	

TABLE 4.*—*Reference list of minerals—continued*

Mineral	Formula used	Cell vol. (calc.)	Cell vol. (expt.)	Ion vol.	Packing index	Remarks
Polylithionite	$KLi_2Al(Si_4O_{10})F_2$	231	.....	132	5.7	
Prehnite	$Ca_2Al(AlSi_3O_{10})(OH)_2$	242	238	132	5.5	
Prochlorite	$(Mg_{3.8}Fe)Al_{1.2}(Al_{1.2}Si_{2.8}O_{10})(OH)_8$	337	348	200	5.8	
Pseudobrookite	Fe_2TiO_5	.....	91	52	5.7	
Pumpellyite	$Ca_2Al_2(SiO_4)_3(OH).H_2O$	246	.....	140	5.7	6.1 incl. H_2O
Pyrope	$Mg_3Al_2(SiO_4)_3$	192	191	124	6.5	
Pyrophyllite	$Al_2(Si_4O_{10})(OH)_2$	215	212	122	5.7	
Quartz (low)	SiO_2	38	37	19.5	5.2	
Rhodonite	$MnSiO_3$	61	60	32	5.3	
Riebeckite	$Na_4Fe_6Fe_4(Si_{16}O_{44})(OH)_4$	907	.....	509	5.6	
Rutile	TiO_2	32	31	20	6.6	
Sanbornite	$BaSi_2(Si_4O_{10})$	218	.....	124	5.7	
Sanidine (Na-rich)	$K_{.5}Na_{.5}(AlSi_3O_8)$	175	.....	86	4.9	
Saponite	$Mg_{3.25}Al_{.26}(Al_{.26}Si_{3.66}O_{10})(OH)_{2.25}.4H_2O$	361	.....	142	4.0	5.2 incl. H_2O
Sapphirine	$Mg_2Al_4(SiO_4)O_6$	168	174	104	6.1	
Sarcolite	$Ca_2Al_2Si_2O_{12}$	259	.....	133	5.1	Classification undecided
Scapolite (See Marialite)						
Scheelite	$CaWO_4$	78	78	45	5.8	
Schorl	$NaFe_3B_3Al_3(Al_3Si_6O_{27})(OH)_4$	540	524	324	6.0	
Scolecite	$Ca(Al_2Si_3O_{10}).3H_2O$	272	.....	104	3.8	5.0 incl. H_2O
Serendibite	$Ca_2Mg_4Al_6B_2(SiO_4)_4O_{10}$	433	.....	282	6.5	
Serpentine	$Mg_3(Si_2O_5)(OH)_4$	186	180	101	5.4	
Shattuckite	$2Cu(SiO_3).H_2O$	130	.....	77	5.9	6.8 incl. H_2O
Siderite	$FeCO_3$	50	50	22	4.4	
Sillimanite	$Na_{.1}Al_{7.9}(SiO_4)_4[O_{2.8}(OH)_{.2}]$	335	323	201	6.2	
Silver	Ag	.....	17.0	12.5	7.4	Non-ionic
Soda (see Natrite)	$Na_2CO_3.10H_2O$	325	.....	27	.8	4.2 incl. H_2O
Soda Niter	$NaNO_3$	63	66	18	2.8	
Sodalite	$Na_8(Al_6Si_6O_{24})Cl_2$	712	703	319	4.5	
Spessarite	$Mn_3Al_2(SiO_4)_3$	197	195	127	6.5	
Spinel	$MgAl_2O_4$	66	66	42	6.4	
Spodumene	$LiAl(SiO_3)_2$	98	.....	61	6.2	
Spurrite	$Ca_5(SiO_4)_2(CO_3)$?	245	.....	115	4.7	Classification undecided
Staurolite	$Na_{.4}Fe_{3.2}Mg_{1.8}Al_{18}(SiO_4)_8O_{16}.H_2O$	768	732	492	6.7	6.9 incl. H_2O (Jakob formula)
Stilbite	$Ca_4Na_2(Al_{10}Si_{26}O_{80}).30H_2O$	2433	2195	805	3.5	5.0 incl. H_2O
Stilpnomelane	$K_{.3}Ca_{.3}(Mg_{2.4}Fe_{.7}Fe_{5.2}Al_{.32})(AlSi_{11}O_{30})(OH)_{12}$	693	695	452	6.5	
Sylvite	KCl	.....	62	35	5.6	
Talc	$Mg_3(Si_4O_{10})(OH)_2$	230	225	126	5.6	
Thenardite	Na_2SO_4	89	.....	38	4.3	
Thermonatrite	$Na_2CO_3.H_2O$	136	.....	27	2.0	2.8 incl. H_2O
Thomsonite	$Ca_8Na_4(Al_{20}Si_{20}O_{80}).24H_2O$	2335	2248	847	3.7	4.9 incl. H_2O
Titanite	$(Ca_{2.8}Fe_{.4})(Ti_{2.8}Al_{.6})(Al_{.8}Si_{2.75}O_{16})O_4$	372	368	223	6.0	
Topaz	$Al_2(SiO_4)F_2$	87	85	60	7.0	
Tourmaline (See Schorl)						
Tremolite	$Ca_2Mg_5(Si_4O_{11})_2(OH)_2$	452	440	257	5.8	
Tridymite (low)	SiO_2	42.3	.....	19.5	4.6	
Variscite	$Al(PO_4).2H_2O$	103	.....	39.5	3.8	6.0 incl. H_2O
Vermiculite	$Mg_{3.2}Al_{.8}(Al_{.8}Si_{3.2}O_{10})(OH)_4.4H_2O$	355	.....	151	4.3	5.5 incl. H_2O
Vesuvianite	$Ca_{10}Mg_2Al_4(Si_2O_7)_2(SiO_4)_5(OH)_4$	707	722	433	6.1	Classification not definitely established
Vivianite	$Fe_3(PO_4)_2.8H_2O$	322	.....	76	2.4	5.1 incl. H_2O
Wavellite	$Al_3(PO_4)_2(OH)_3.5H_2O$	295	.....	106	3.6	5.4 incl. H_2O
Willemite	Zn_2SiO_4	93	94	44	4.7	
Witherite	$BaCO_3$	76	90	33	3.7	
Wolframite	$Fe_{.5}Mn_{.5}(WO_4)$	69	.....	43	6.2	
Wollastonite	$Ca_6(Si_2O_8)_2O_2$?	400	392	205	5.2	
Xenotime	YPO_4	67	71	38	5.3	
Xonotlite	$Ca_3(Si_2O_8)(OH)_2$	226	.....	116	5.1	
Zeophyllite	$Ca_6(SiO_3)_3(OH)_8F_2$	547	.....	298	5.4	
Zincite	ZnO	49	46	24	5.3	
Zircon	$Zr(SiO_4)$	68	64	43	6.7	
Zoisite	$Ca_2Al_3(SiO_4)_3(OH)$	227	229	140	6.2	
Zunyite	$Al_{13}(SiO_4)_5[(OH)_{18}F_3]Cl$	670	656	431	6.5	

* As H_2O in zeolites, montmorillonite, vivianite, etc., is a loosely held molecule, not an ion like $(OH)^{1-}$, it is excluded in the computation of true packing index of such minerals. The index which includes H_2O is given in the column headed "Remarks."

the same as C, and that the majority of the oxides are more closely packed than the cubic open packing type.

D (index 7.40) represents the closest packing of uniform spheres. E (index 8.00) represents still tighter packing in which the interstices of a system of close-packed uniform spheres are occupied by smaller spheres

TABLE 5.—*Summary of relations of some mineral constants to fundamental crystal-structure data*

Constant	Dependent on				Constant related to
	Ion radius	Ion co-ordination; (no. of touching neighbors)	Ion charge (valence)	Atomic number	
Packing index	x	x	.....	.....	Volume
Density	.....	x	.....	x	Relative mass
Refractive index (vectorial)	x	x	x	x	Light transmission
Hardness (vectorial)	x	.....	x	.....	Strength

of maximum volume. For practical purposes such a system possesses the maximum packing index. A number of the minerals listed in Table 4, consisting of ions of two contrasting volumes, are close packed in this way. In topaz and kyanite (index 7.0), corundum, chrysoberyl, and bromellite (index 7.2) is developed the maximum closeness of packing for silicates and oxides, respectively.

MINERALOGIC CORRELATIONS OF PACKING INDEX

CORRELATION OF REFRACTIVE INDEX AND DENSITY WITH PACKING INDEX

Introduction.—It has long been known that density and refractive index are closely related and that, in a series of compounds, variation in the one constant is accompanied by variation of the other in the same direction. It becomes obvious also that, in general, variation in packing index will be accompanied by variations in the same direction of both density and refractive index. In particular, however, packing index does not vary directly with these two associated quantities, except in the special case of polymorphous series where numbers and kinds of ions are the same. The magnitude of packing index, density, and refractive index is governed by a specific group of ion properties, as summarized in Table 5. The type of packing, or co-ordination of the ions, is the only common factor they possess. Density is characterized by dependence on the atomic number (and weight) of the elements in a compound. In contrast, ion volume, dependent on radius, is essential for determination of packing index.

Refractive index presents greater complications, especially in anisotropic crystals, where vectorial properties are important, and an adequate discussion is not attempted here.[5] The magnitude of the mean refractive index of an ionic crystal is governed to a considerable degree by the re-

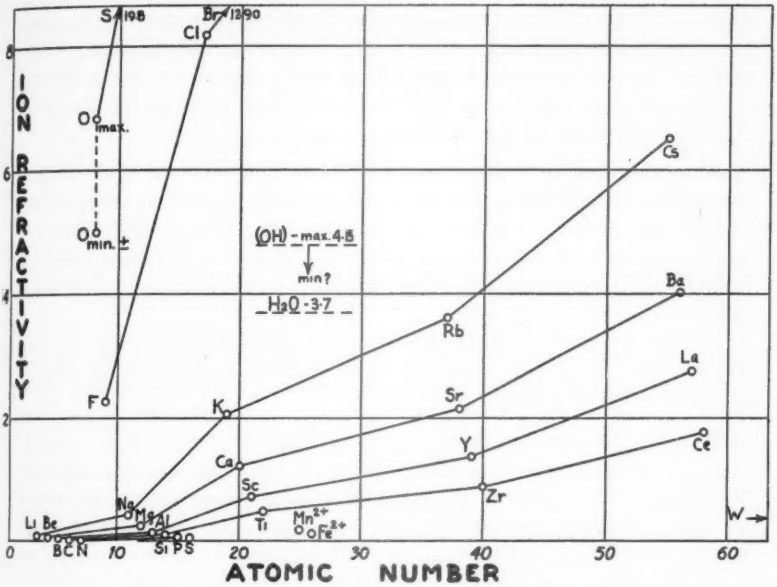

FIGURE 4.—*Atomic number—ion refractivity relations*
Based on H^{1+} refractivity = 0.

fractivity of the individual ions in the compound. (*See* Table 3.) Ion refractivity varies with atomic number in the same way as ion radius and is a periodic function; Figure 4 shows this clearly and also indicates that, quantitatively, the refractivity of the anions is more critical than that of the majority of cations, a parallel condition already noted for volumes of ions in any unit cell.

To illustrate the general dependence of packing index, density, and refractive index on each other, and at the same time to indicate specific points of independence, Figures 5 to 14 have been prepared which combine all three sets of data. The minerals have been subdivided as far as practicable into compositional groups and are arranged in order of in-

[5] For an introduction to crystal structure—refractive index relations *see* Evans (1939, p. 270) and Bragg (1937, p. 120).

creasing packing index (left). To the right, two-way horizontal columns indicate the magnitude of the corresponding density and mean refractive index. A preliminary glance at all of them shows a general increase of density and refractive index with increase in packing index. Detailed inspection shows marked prominences and indentions in the density-refractive index columns, which are in part explainable in terms of relative ion refractivity and atomic weight. The proportions of especially disturbing ions are indicated at the left as black sections of various sizes. The conspicuous features are listed in the captions to the figures and are further summarized in the following section.

Discussion of data.—The general characteristic of these figures—increase in density and refractive index with increase in packing index—has already been noted. This might be stated in more fundamental terms as total ion mass/unit cell and total ion refractivity/unit cell vary directly as total ion volume/unit cell. The modifying influence of individual ions will now be considered.

ANIONS: As most of the minerals under investigation are essentially oxygen compounds, comparison of the effect of other anions is best made in terms of O^{2-} as a base.

$(OH)^{1-}$ As far as the writer is aware, the effect of $(OH)^{1-}$ on the density and refractive indices of ionic substances has not previously been discussed. Of two substances of approximately the same packing index, one containing $(OH)^{1-}$ and the other none (or smaller quantities), the former has invariably lower density and refractive indices than the latter. (*Compare* kaolinite and pyrophyllite in Figure 5; zeophyllite and gehlenite in Figure 7; prochlorite and clintonite in Figure 9; friedelite and rhodonite in Figure 11; spinel and gibbsite in Figure 12; wavellite and variscite in Figure 13. The cause of the depression in density is obvious from valence considerations, as the following example illustrates.

The ratio of the anions $(OH)^{1-}$ and O^{2-} in pyrophyllite $Al_2(Si_4O_{10})(OH)_2$ is 2:10; in kaolinite $Al_2(Si_2O_5)(OH)_4$ it is increased to 8:10. As the univalent $(OH)^{1-}$ has essentially the same mass as O^{2-}, but requires only half as many of the heavier cations to neutralize its charge, the resulting density of kaolinite is notably less than pyrophyllite.

The cause of the relatively low refractive indices of OH-rich substances is undoubtedly related to the low refractivity of $(OH)^{1-}$ compared with O^{2-}. As it is also more readily polarized than O^{2-}, the difference between their refractivity as free ions (6.84 minus 4.8) is probably accentuated where they occur as ions in combination.

F^{1-} The influence of fluorine in depressing the refractive index and density of some substances relative to others richer in O^{2-} is well known. Notable contrasts of this kind where packing indices are approximately the same are: kyanite and topaz (Fig. 5); sarcolite and cuspidine (Fig. 7); enstatite and chondrodite (Fig. 8). The depression of density of topaz, cuspidine, and chondrodite is caused by the same factor as illustrated for $(OH)^{1-}$—*i. e.*, fewer cation charges are required in F-rich than in O-rich substances. Figure 4, showing the relative refractivities of O^{2-} and F^{1-}, indicates clearly the reason for the contrast in refractive indices.

The contrast in refractive index shown by the chlorides and fluorides of Figure 13 is particularly worthy of note. Despite the higher packing index of the fluorides, their refractive indices are much lower than those of the chlorides.

Cl^{1-} The influence of Cl^{1-} relative to O^{2-} is obscured in most ionic minerals because of the small amounts present. A positive effect seems clear, however, in albite and marialite (Fig. 8). The explanation of the lower density of marialite is similar to that for substances rich in $(OH)^{1-}$ and F^{1-}. The higher refractive indices are due to the high refractivity of Cl^{1-} relative to O^{2-} (Fig. 4).

CATIONS: Unlike O^{2-} among the anions, there is no omnipresent cation in these ionic minerals which will serve as a base for comparison of relative density and refractive indices. This raises no difficulty with respect to density, as, for substances with the same packing index, variations in density depend directly on the elements present. No further discussion of density is therefore necessary. The known values of ion refractivity, however, are correlatable only in part with refractive indices. For purposes of discussion the cations are divided arbitrarily into two groups based on ion refractivity $>$ or $<$ 1. Inspection of Figure 4 shows that H, Li, Na, Be, Mg, Fe^{2+}, Mn, B, Al, Sc, Si, Ti, Zr, N, P comprise a low refractivity division; K, Rb, Cs, Ca, Sr, Ba, Y, Ce form a high refractivity group. As most of the minerals under investigation contain a number of cations, the specific effect of the refractivity of any one is not always easy to determine. This contrasts with the anions, which are few in number and predominantly oxygen. Only those cations therefore which seem to influence the refractive indices conspicuously are singled out for special mention. The low refractivity group is discussed first.

B^{3+} Although the refractivity of B^{3+} is low, its presence in ionic compounds seems to lower refractive indices to a greater degree than other ions such as Be^{2+} of comparable refractivity. Examples showing

the influence of B^{3+} are: kornerupine compared with sapphirine in Figure 5; datolite and danburite compared with zoisite and vesuvianite in Figures 7 and 8, etc. It cannot yet be claimed definitely that borates have relatively low refractive indices, as too few structural data are available for computation of packing indices.

Ti^{4+} The role of Ti^{4+} seems to be anomalous, as its refractivity is incompatible with the abnormally high refractive indices of its compounds. (*Compare* titanite with diopside in Figure 7; benitoite with sanbornite in Figure 11; rutile with spinel in Figure 12, etc.) The refractive indices of these Ti-bearing substances are much higher than those of many minerals containing ions in the high refractivity group. Some other factor must operate which is not yet taken into account.

Zr^{4+} This ion presents the same problem as Ti^{4+}—low refractivity and conspicuously high refractive indices (zircon in Figure 11, and other rare zircon minerals not listed in Table 4).

Li^{1+} The correlation of Li^{1+} refractivity with the refractive indices of its compounds is not very definite as far as the present study goes. Of the Li-rich minerals included in Table 4—petalite, spodumene, amblygonite, polylithionite—all have low refractive indices with respect to their packing indices. Comparison of jadeite with spodumene (packing index of jadeite $>$ packing index of spodumene) indicates no particular influence of lithium compared with sodium, as the refractive indices of the two minerals are about the same. This does not correspond with Figure 4. On the other hand, petalite, having lower refractive indices and packing index than nepheline (Fig. 5) possibly indicates lower refractivity of lithium compared with sodium. Inspection of the slope of the refractive index columns as a whole in Figure 5 seems to show that the difference in refractive indices of petalite and nepheline is greater than that demanded by the difference in packing index of the minerals.

Comment on amblygonite and polylithionite would add little to the above, as the effect of fluorine and possibly of water in the former, and of potassium and fluorine in the latter, is difficult to evaluate. In summary, it may be said that presence of Li^{1+} in appreciable quantities permits general correlation of refractive indices with refractivity but shows little correspondence in some of its details.

Fe^{2+} Numerous examples show that the low refractivity of Fe^{2+} is not in accord with the refractive indices of Fe^{2+}-rich substances as a whole. Selected pairs of minerals of approximately equal packing index

GENERAL NOTE REGARDING FIGURES 5 TO 14

Compositional groups arranged in order of increasing packing index (left). Variation of density and refractive index shown in double column (right). The packing index of minerals containing H_2O molecules is computed both with H_2O (broken line extension of the columns) and without H_2O (heavy unbroken line). The refractive index and density of such minerals refer only to those with the normal content of water. Proportions of selected cations and anions shown in the packing index columns.

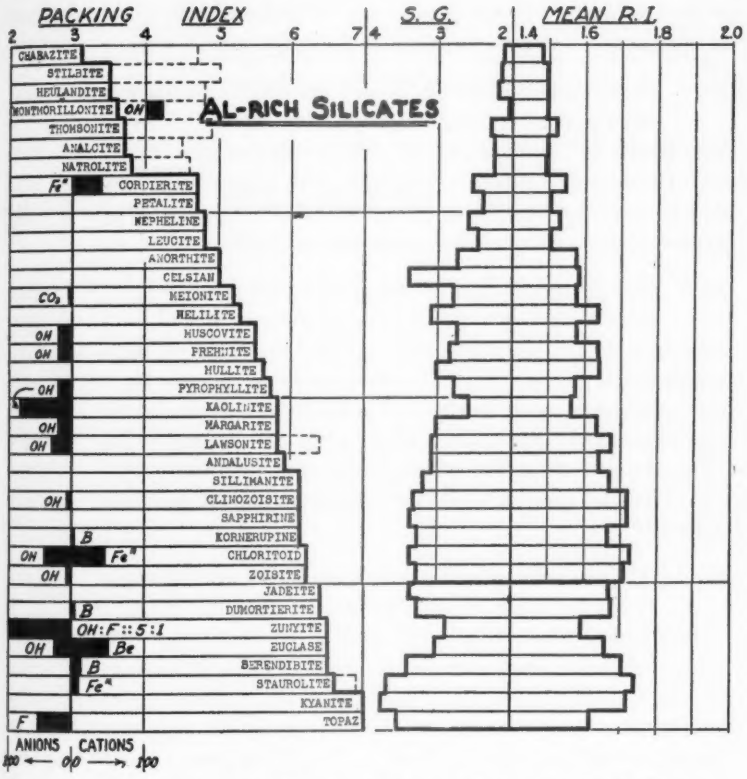

FIGURE 5.—*Packing index-density-refractive index relations of Al-rich silicates*

Montmorillonite—The relatively low density and refractive index are probably related to Mg^{2+} and $(OH)^{1-}$, neither of which is present in the neighboring Ca-rich zeolites.

Cordierite—Sharp increase in density and refractive index due largely to presence of Fe^{2+}, absent in immediate neighbors.

Celsian—Ba^{2+} is undoubtedly the disturbing element here.

Kaolinite—Both density and refractive index are relatively depressed. Referable to $(OH)^{1-}$ (45% of total anions)

Zunyite—Indentation in density and refractive index columns referable to (OH^{1-} and F^{1-}). No other anion except a single Cl^{1-}.

Topaz—High F^{1-} content seems to be related to the relatively low density and refractive index.

—chloritoid-zoisite (Fig. 5), tremolite-actinolite and enstatite-hypersthene (Fig. 9)—indicate the effect of Fe^{2+} in raising refractive indices relative to Mg^{2+}, Ca^{2+}, etc. It is to be noted that the refractivity of Fe^{2+} is less than that of K^{1+}, yet the refractive indices of Fe^{2+}-rich compounds exceed without exception those of K^{1+}-rich substances.

The remaining cations of the low refractivity group—Na^{1+}, Be^{2+}, Mg^{2+}, Al^{3+}, Si^{4+}—are not conspicuous in any way with respect to the refractive indices of their compounds. More complete study of groups of compounds, not necessarily minerals, might permit closer correlation.

K^{1+} The refractive indices of K-rich minerals are uniformly low compared with others of the same packing index. (*Compare* nepheline with leucite in Figure 5; prehnite with muscovite, also in Figure 5; talc with phlogopite in Figure 9; actinolite with biotite in Figure 11.) This does not accord with the high refractivity of K^{1+} relative to the prominent cations in prehnite, nepheline, talc, and actinolite.

Fe^{3+} No information is at hand concerning the refractivity of Fe^{3+}, but, from all indications based on refractive indices of Fe^{3+}-rich compounds, its value should be high. This has long been appreciated by mineralogists. Using similar packing index as a basis for comparison, the following serve to illustrate the important influence of Fe^{3+}; acmite and hypersthene, ilvaite and schorl (Fig. 11), magnetite and chromite (Fig. 12). Birefringence increases also with increase in Fe^{3+}, but it is not considered necessary for present purposes to give details of this characteristic.

Ba^{2+} The refractivity of Ba^{2+} is anomalous with respect to the mean refractive index of those barium compounds included in Table 4. Comparison of celsian with anorthite (Fig. 5) shows conformity of relative refractive indices and refractivity, although the difference in refractive indices is possibly smaller than might be expected. In contrast, sanbornite and fayalite show a strong reversal of refractive indices compared with the refractivities of Ba^{2+} and Fe^{2+}. No explanation of this is apparent.

In conclusion, positive correlation of refractivity and refractive indices is possible for one cation only, B^{3+}. Others such as Ti^{4+}, Zr^{4+}, K^{1+} show complete reversal of the expected correlation. Of these latter, all except K^{1+} have high valency and are either transition or rare-earth elements (Evans, 1939, p. 17). What significance, if any, may be attached to this circumstance is unknown.

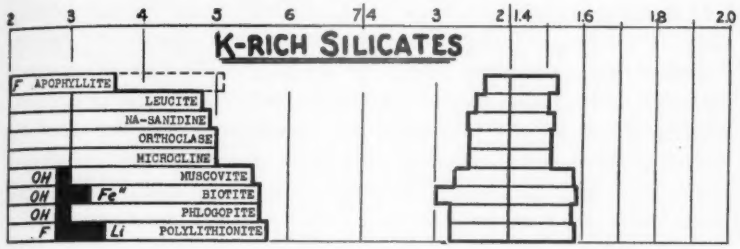

FIGURE 6.—*Packing index-density-refractive index relations of K-rich silicates*
Projection of the density column of biotite undoubtedly related to Fe.

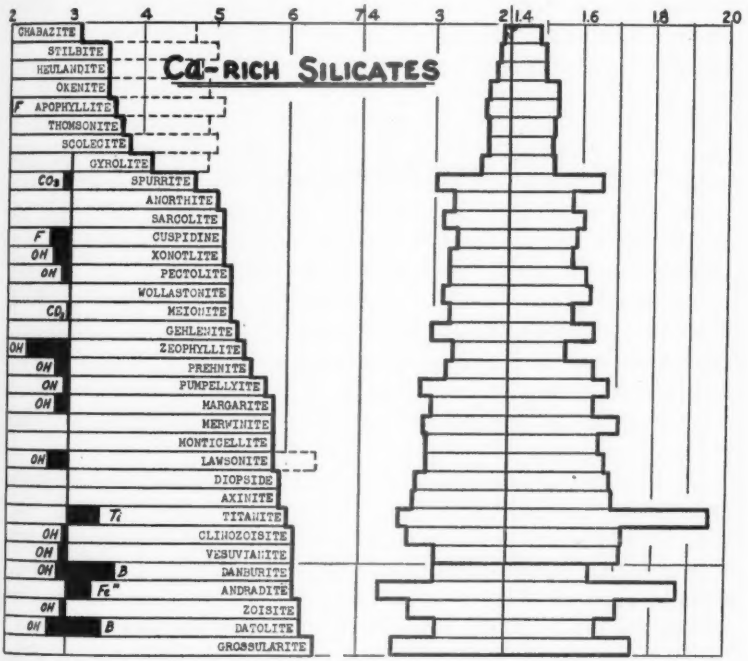

FIGURE 7.—*Packing index-density-refractive index relations of Ca-rich silicates*

Spurrite—High refractive index and density probably dependent on presence of $(CO_3)^{2-}$.
Zeophyllite—Conspicuous indentations due to abundant $(OH)^{1-}$.
Titanite—Disproportionately high refractive index related to Ti^{4+}.
Vesuvianite, Danburite, Datolite—As B^{3+} is common to all three, and is absent in neighboring minerals of similar packing index, it is undoubtedly the disturbing factor in the low density and refractive index.
Andradite—Presence of Fe^{3+} is significant as the cause of the high density and refractive index.

Comparing anions and cations, the refractivity-refractive index correlation of the former is much more satisfactory than that for the cations. As mentioned on a previous page, a fair comparison of cations is hampered by the numbers of these present in many minerals, particularly in silicates, whereas anions are few in number, with predominant oxygen (fluorides and chlorides excepted). Nevertheless, there are fundamental discrepancies in the refractivity-refractive index correlation for certain substances which demand further explanation than the author is able to give at the present time.

WATER MOLECULES: In addition to the above discussion of ions, the role of water molecules merits brief attention. With a few exceptions H_2O in ionic minerals is confined to those of low packing index, and only these are considered here. Density and refractive indices for these minerals are referable, however, to that packing index which includes the water content (broken line extensions of packing index columns).

The refractive indices of the zeolites (Figs 5, 7, 8) indicate no conspicuous influence of H_2O compared with H_2O-free substances of slightly higher packing index. Apophyllite (Fig. 6) shows normal relations with leucite, the difference in refractive index being referable to differences in packing index alone. The similar refractive indices of vermiculite and cordierite relative to their dissimilar packing indices (Fig. 9) are explainable in terms of Fe^{2+}, which raises refractive index, and OH^{1-}, which lowers it. The water-bearing sulphates of Figure 13 show apparently normal relations. In the phosphate group (also in Figure 13) all apparent discrepancies among the water-bearing minerals may be explained in terms of particular ions—Fe^{2+} in vivianite, $(OH)^{1-}$ in wavellite, Li^{1+} and F^{1-} in amblygonite.

The single conspicuous exception to the above is found in the carbonate group (Fig. 14), where the difference in refractive indices of natrite and thermonatrite seems to be referable to the packing index computed for ions only, and not to the index which includes water molecules. In general, however, presence of H_2O molecules does not seem to influence refractive indices conspicuously for substances of about the same packing index.

As the refractivity of free O^{2-} is considerably higher than that of H_2O it may be assumed in explanation of the above that polarization of O^{2-} in these water-bearing compounds is sufficient to reduce O^{2-} refractivity to values comparable with that for H_2O (3.7). Following a method recently used by Kordes (1939b) it is possible to determine the actual refractivity of O^{2-} in ionic oxygen compounds and to compare this

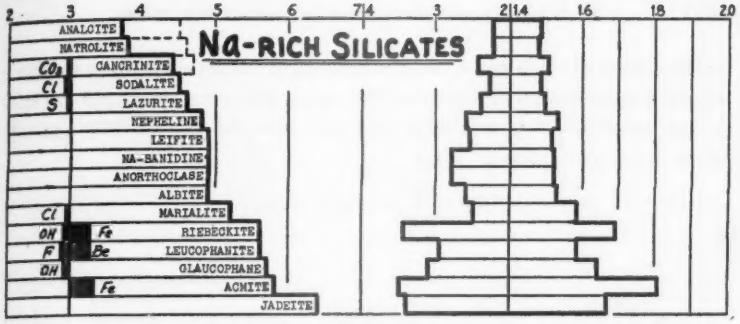

FIGURE 8.—*Packing index-density-refractive index relations of Na-rich silicates*

Cancrinite—The slightly excessive projections may be attributed to $(CO_3)^{2+}$.
Riebeckite—The influence of Fe^{2+} is probable here.
Marialite—Only chlorine could be responsible for contrast in density and refractive index with albite.
Acmite—The disturbing ion is probably Fe^{3+}.

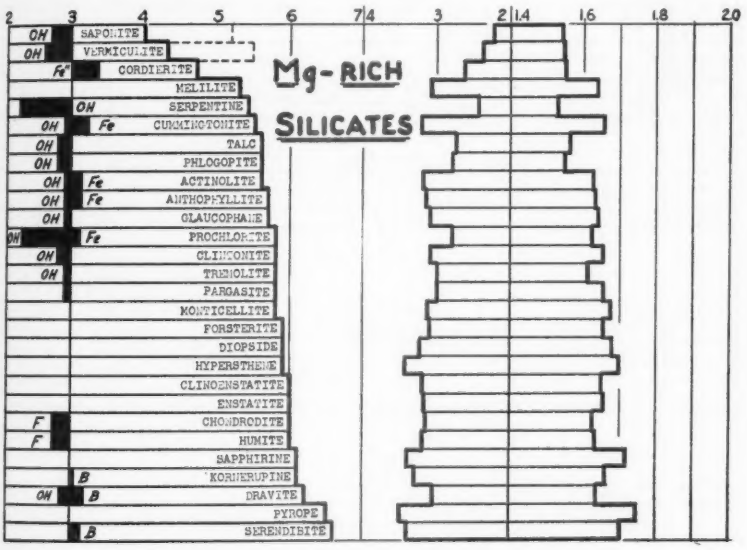

FIGURE 9.—*Packing index-density-refractive index relations of Mg-rich silicates*

Serpentine—High content of $(OH)^{1-}$ is undoubtedly related to indentations in refractive index and density columns.
Phlogopite—Slight indentation in refractive index column relative to talc column is probably due to K^{1+}.
Prochlorite—Indentations not as pronounced as serpentine, although $(OH)^{1-}$ content just as large. Presence of iron is probably a contributing factor.
Chondrodite, Humite—Slight depression of refractive index and density probably related to fluorine content.
Kornerupine, Serendibite—Boron is probably the significant element here.
Dravite—B^{3+} and $(OH)^{1-}$ probably responsible for the even greater indentations in refractive index-density columns than shown by kornerupine and serendibite.

value with that of free O^{2-}. The molecular refractivity MR of a substance is approximately equal to the sum of the refractivities of the ions of the substances. It is also related to molecular volume MV and the mean refractive index n. Thus—

$$MR = \sum IR = \frac{n^2 - 1}{n^2 + 2} \cdot MV$$

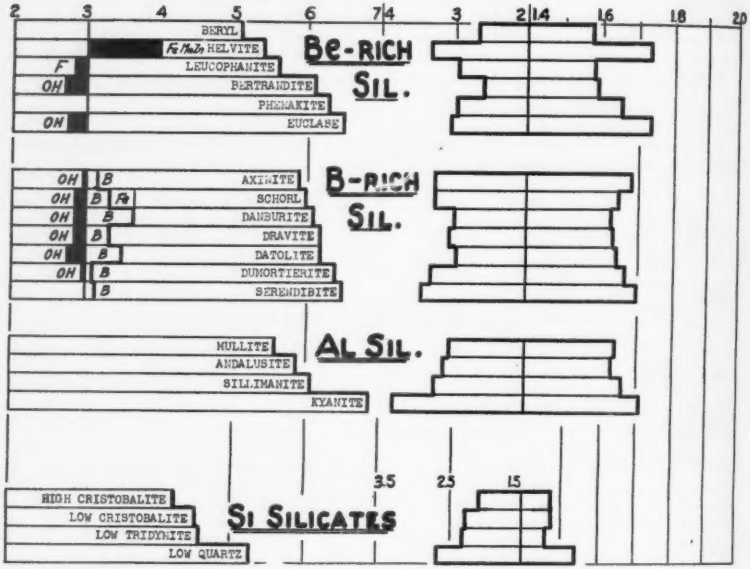

FIGURE 10.—*Packing index-density-refractive index relations of miscellaneous silicates*

Be-rich silicates

Helvite—Abundant heavy cations explain the high density and refractive index.

Bertrandite—Low density and refractive index relative to leucophanite probably dependent on presence of calcium in the latter and the considerable amount of $(OH)^{1-}$ in bertrandite.

B-rich silicates

Density-refractive index columns have a definite concave outline. This seems due to the presence of more B^{3+} and $(OH)^{1-}$ in the middle group—danburite, dravite and datolite—than in other minerals of the series.

Al silicates

This is a polymorphous group. The expected gradual increase in density and refractive index with increased packing index is clearly shown. The slightly different composition of mullite is probably responsible for the protuberance of its refractive index column.

Si silicates

This is likewise a polymorphous group. Density increases regularly with packing index; the refractive indices are somewhat irregular.

By assuming the refractivity of each small cation in a compound to have the same value as that of the corresponding free cation (no polarization), the value for O^{2-} can be determined without difficulty:

$$MR = \sum IR_{\text{cations}} + \sum IR_{\text{anions}} \; (= O^{2-})$$

Calculation of a few representative examples shows that O^{2-} refractivity in compounds is ordinarily much less than the free ion value (in quartz 3·55, diopside 3·94, periclase 4·22, titanite 5·04, etc.). It seems possible, therefore, to interpret at least approximately the above conclusion regarding water-bearing substances in terms of actual refractivities of O^{2-} and H_2O.

CORRELATION OF HARDNESS WITH PACKING INDEX

Introduction.—Hardness, as defined by the Mohs scale, is the least precise mineralogical "constant" in current use. It is determined on a

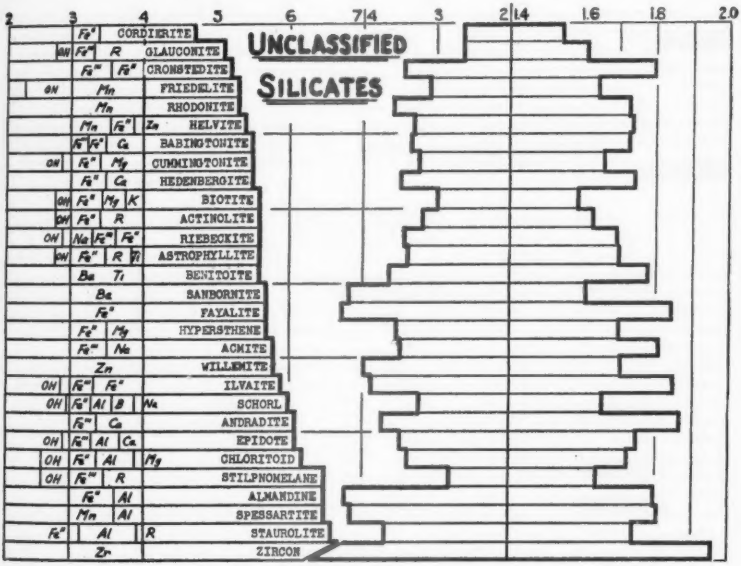

FIGURE 11.—*Packing index-density-refractive index relations of unclassified silicates*

The irregular density-refractive index double column contrasts with the more regular columns in the classified compositional groups just described. Kinds and proportions of the chief cations (except silicon) and anions (except oxygen) are indicated at the left of the table. Large amounts of Fe^{3+} seem to raise the refractive index disproportionately, except in stilpnomelane, which contains a considerable amount of $(OH)^{1-}$. Titanium has a similar tendency, as shown by the contrast in benitoite and sanbornite. Zirconium (in zircon) also influences density and refractive index rather strongly compared with the effect shown by other elements. R-unclassified ions.

relative, not an absolute, basis, with very large inequalities in the intervals between successive steps in the scale. Various attempts to standardize the determination and to obtain consistent quantitative results have not been particularly successful. One obvious difficulty, especially in optically anisotropic crystals, is the variable hardness on different planes and in different directions within a plane. A second is the interfering effect of cleavage planes which happen to intersect the surface being tested. In addition to a general lowering of hardness, the interference of such planes may yield two discrepant values where tests are made in the same crystal direction, but with opposite direction-sense. A third, true for all materials, is the possible occurrence of abundant alteration products or inclusions, which may easily escape notice if no microscopic examination is made. In the discussion to follow only the

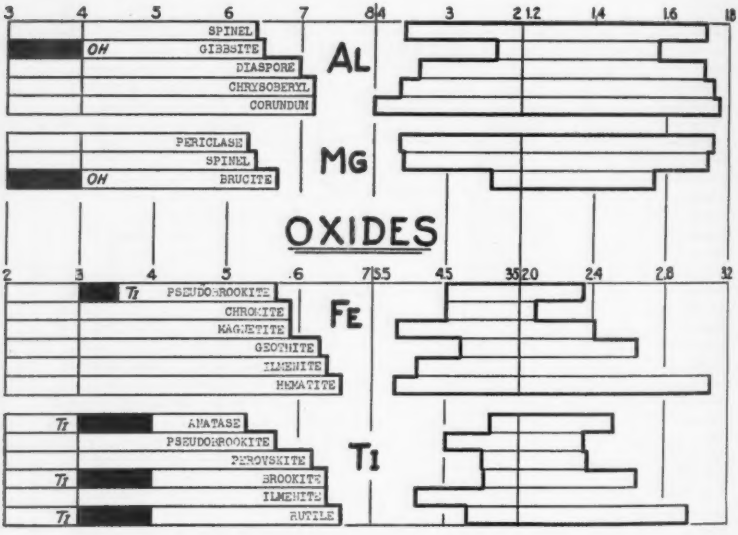

FIGURE 12.—*Packing index-density-refractive index relations of oxides*

Gibbsite, Brucite } —Indentation in refractive index-density columns undoubtedly related to presence of $(OH)^{1-}$ as the only anion.

Chrysoberyl—Higher refractive index and density than bromellite (see Table 4) for same packing index apparently related to absence of Al in bromellite.

Hematite—Disproportionately high refractive index related to abundant Fe^{3+}. Contrast this with refractive index of chromite, which contains only Fe^{2+}.

Rutile, Brookite, Anatase } —Polymorphous series with regular increase in density and refractive index.

first two effects will be considered, as the third one can be eliminated by selection of unaltered material.

The hardness "scratch" test is one of the many methods of determining the strength of a crystal. From the previous discussion of ion packing it might be expected that a cell composed of closely packed ions would be stronger (and harder) than another less tightly packed. This is strictly

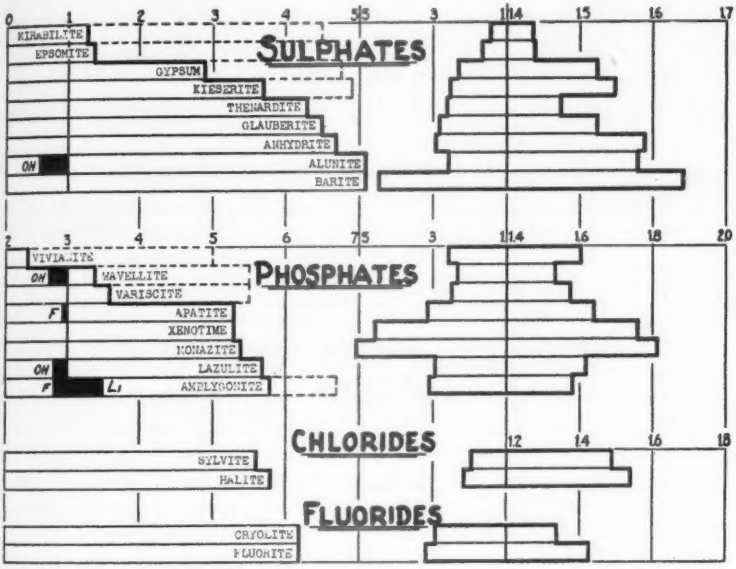

FIGURE 13.—*Packing index-density-refractive index relations of sulphates, phosphates, chlorides, fluorides*

Sulphates

The indentations in the refractive index columns correspond well with those of the packing index columns if the broken line extensions (computed for water) of mirabilite, epsomite, gypsum, and kieserite are used for comparison. Alunite does not show the anticipated relative increase in refractive index, probably due to its $(OH)^{1-}$ content.

Phosphates

Vivianite } —Reversed position of density-refractive index columns relative to packing undoubtedly
Wavellite } related to Fe^{2+} in the former and to $(OH)^{1-}$ in the latter.

Xenotime } —Increase in density and refractive index seems disproportionate. Y and Ce are the
Monazite } significant ions.

Lazulite—Lower density and refractive index compared with apatite probably related to $(OH)^{1-}$.

Amblygonite—Density and refractive index do not show increases compatible with the packing index (water content included). Undoubtedly related to lithium and fluorine content.

Chlorides

No comment necessary.

Fluorides

Presence of calcium in fluorite is probably related to its relatively high density and refractive index.

true for polymorphous substances and appproximately true for chemically dissimilar compounds, but is modified by other factors outlined by Goldschmidt (1926, p. 102). In simple binary compounds it has been shown that the hardness of compounds of the same structure type varies inversely with interionic distance and directly with valence (Table 5). That is, the relative hardness of two ionic compounds such as MgO and NaCl may be predicted with certainty, as on both the above-mentioned grounds MgO should be, and is, much harder than NaCl. As most of the minerals treated in this paper contain more than two ions, the combination of multiple interionic distances and valences is more difficult to reconcile with mean hardness. An attempt has been made to neutralize the valence

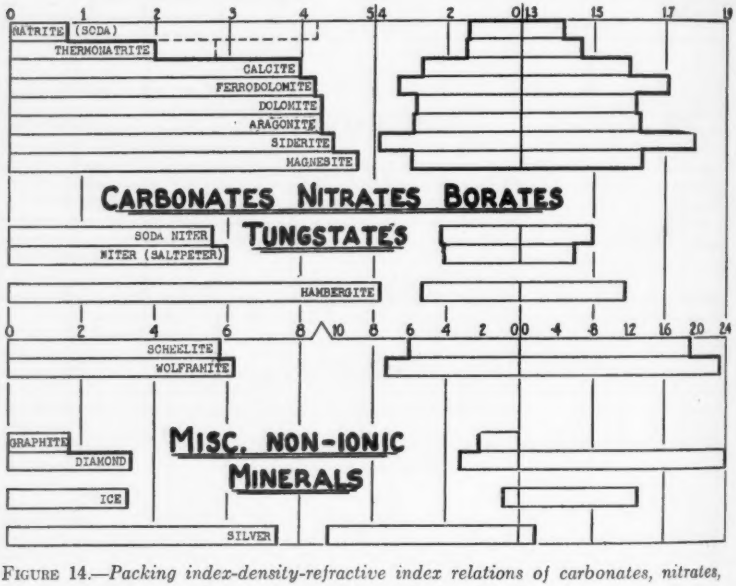

FIGURE 14.—*Packing index-density-refractive index relations of carbonates, nitrates, borates, tungstates, nonionic minerals*

Carbonates

Natrite, Thermonatrite } —The reason for the reversal from the expected conditions (using packing index computed with water) is not apparent on compositional grounds.

Ferrodolomite, Siderite } —The protuberances in the density-refractive columns of these minerals are clearly referable to Fe^{2+}.

Nitrates

As will be shown, the reversal in the packing index-density columns is probably not due to the compositional difference of the two minerals concerned.

Tungstates

No comment required.

variable by computing for each mineral an average bond content per cu. Å, a quantity which is obviously dependent on the valence of the component ions. Thus in orthoclase, $KAlSi_3O_8$, there are 16 bonds between anions and cations per formula unit. As there are four formula units in the unit cell of orthoclase, these 16 bonds are distributed over $\frac{696}{4} = 174$ cu. Å, and the number of bonds per cu. Å $= .092$. It is convenient to use the expression "bonding index" for this quantity.[6] In optically anisotropic crystals the bonds are not evenly distributed throughout the structure, and the value obtained by the above method is a mean which does not hold strictly for individual cubic Ångstrom units. This is particularly true of minerals with micaceous cleavage in which the number of bonds per unit area parallel to such planes is conspicuously less than along other planes. This matter is considered in more detail on a subsequent page. For most minerals, however, this extreme maldistribution of bonds is not an important factor, and it is possible to correlate mean hardness with bonding and packing indices.

Figures 15-20 are drawn similarly to Figures 5-14, with minerals arranged in order of increasing packing index. Structural instead of compositional grouping is the basis of this set of figures wherever possible (phosphates and sulphates excepted, owing to absence of complete structural data). Hardness and bonding index are shown exactly as were density and refractive index in Figures 5-14. The hardness subdivisions represent an approximate quantitative scale, for, despite the lack of complete agreement concerning methods and results, most of the scales so far determined are similar in broad outline, and any one of them is superior to the Mohs scale for graphic illustration. The writer has therefore selected a recent scale set up by Hodge and McKay (1934), in which an average absolute value of hardness for each mineral of the Mohs scale has been determined. The hardness of other minerals not determined quantitatively may then be plotted with approximate accuracy by interpolation.

Discussion of data.—Inspection of this group of figures indicates a general correlation among hardness, bonding index, and packing index and shows that most of the discrepancies are found in the hardness columns. As might be expected, the simpler binary compounds (Fig. 15) show the best agreement.

Halite group (Fig. 15)—Periclase contrasts strongly with sylvite and halite owing to (1) discrepancy in size of its cation and anion, which per-

[6] This mode of attack is not so fundamental in character but is much simpler to grasp than the method used by Fersman (1937, p. 159) in his analysis of the mechanical stability of crystal lattices.

mits relatively tight packing, (2) divalent instead of monovalent ions, which increases bonding index and hardness, (3) small interionic distance, which increases hardness and packing index.

Corundum group (Fig. 15)—No comment required other than to note the inadequacy of the Mohs hardness scale to represent the true hardiness of corundum.

Rutile group (Fig. 15)—The anomaly in the comparison of hardness of cassiterite and rutile with respect to their packing and bonding indices is unexplained. Goldschmidt (1926, p. 108) refers to the unlike ion structure of the cations represented in this group but does not discuss the matter further. (*Compare* titanite and andalusite below.)

Zincite group (Fig. 15)—The relations of packing index, hardness, and bonding index are normal.

Spinel group (Fig. 15)—Normal relations.

Hydroxide group (Fig. 15)—The explanation of the reversal in bonding index of gibbsite and brucite is to be found in the cations. In gibbsite three bonds are concentrated in one cation; in brucite only two occur, and, despite the greater radius of Mg^{2+} in the latter, the bonding index of gibbsite is somewhat larger than that of brucite. As the packing and bonding indices influence the hardness in different directions in this case, only a small difference is to be expected, the bonding index apparently exerting the greater effect. It should be noted in passing that, as these are layer lattice minerals, the hardness given here is the result of determinations made on basal cleavage surfaces and represents a minimum value. (*Compare* with Z_4O_{10} silicates.)

Diaspore group (Fig. 15)—Normal relations obtain among packing index, hardness, and bonding index.

Miscellaneous group (Fig. 15)—Normal relations prevail despite the mixed character of the structure types represented. The contrast between cuprite and chrysoberyl is particularly noteworthy.

Silicates (ZO_4 subdivision, Fig. 16)—Variations in hardness given by the Mohs scale become greatly magnified for this group of minerals, when plotted on an absolute scale, and indicate clearly the need for a quantitative standard. Indentations in the bonding index columns for chondrodite, datolite, zunyite, topaz, etc., may be explained by the same method as used for the sulphates and phosphates. Of greater interest is a comparison of hardness of certain pairs of minerals.

Willemite
Monticellite

Assuming that the hardness determinations are reliable, there is nothing exceptional in the cleavage properties of these two minerals which would explain their lack of contrast in hardness. However, as willemite has trigonal and monticellite orthorhombic sym-

GENERAL NOTE REGARDING FIGURES 15 TO 20

Groups of minerals arranged as far as possible according to structure type and in order of increasing packing index. Hardness plotted on an approximate quantitative scale using the Mohs mumbers.

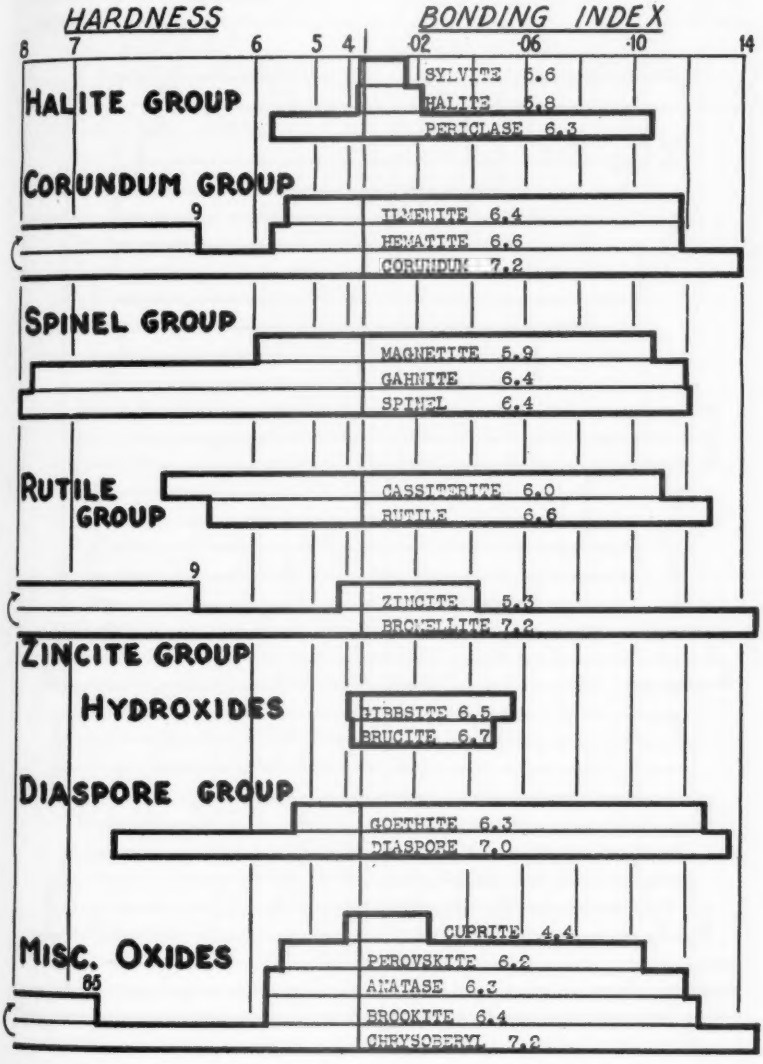

FIGURE 15.—*Packing index-hardness-bonding index relations for chlorides, oxides, hydroxides*

metry elements, it is possible that the ambiguity in hardness relations will find its explanation here.

Merwinite Pumpellyite

As each of these minerals has one excellent cleavage the reversal in hardness from the expected relation seems anomalous. As with willemite and monticellite, however, the difference

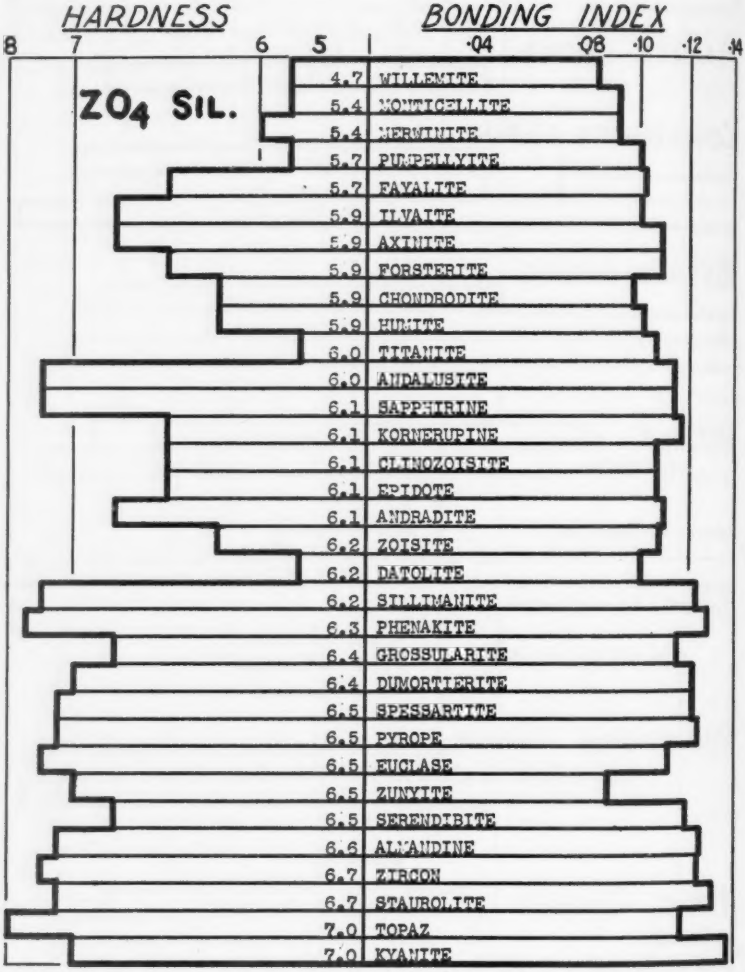

FIGURE 16.—*Packing index-hardness-bonding index relations for ZO_4 silicates*

in crystal symmetry (orthorhombic in merwinite, monoclinic in pumpellyite) may play a part.

Titanite
Andalusite

The serious discrepancy in hardness of these two minerals relative to their packing and bonding indices remains an

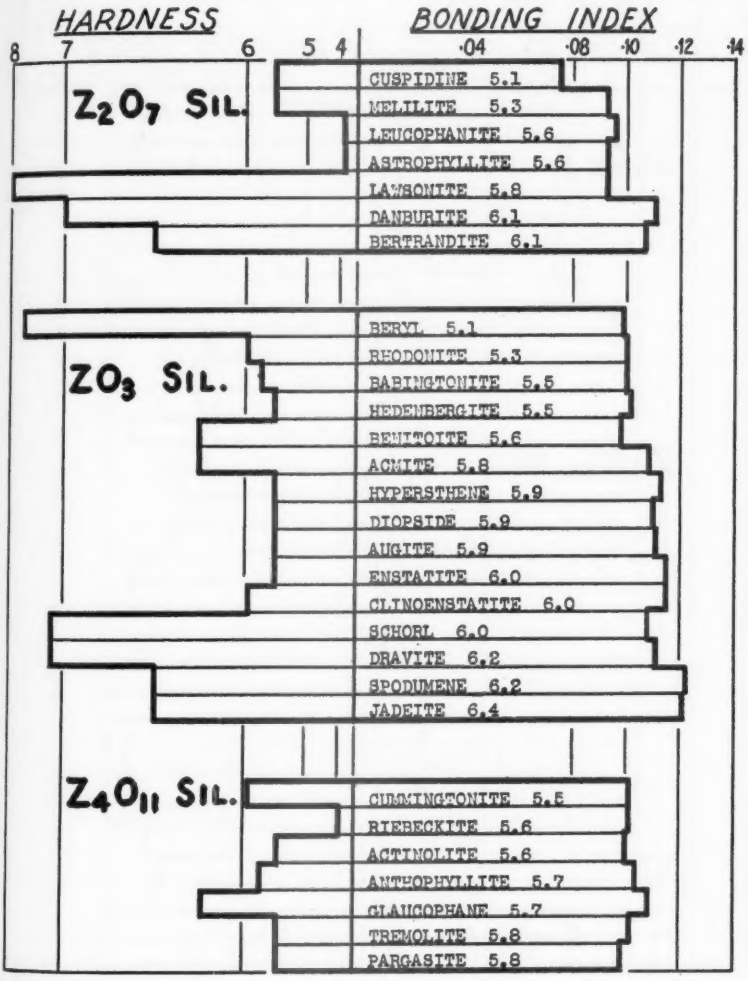

FIGURE 17.—*Packing index-hardness-bonding index relations for Z_2O_7, ZO_3, Z_4O_{11} silicates*

anomaly. It is unlikely that much of the difference is due to faulty hardness determination, as both minerals are obtainable in large, unaltered crystals. Each has fairly good cleavage, so that this factor is removed from the discussion. The role of the monoclinic symmetry elements of titanite relative to the orthorhombic elements of andalusite is unknown.

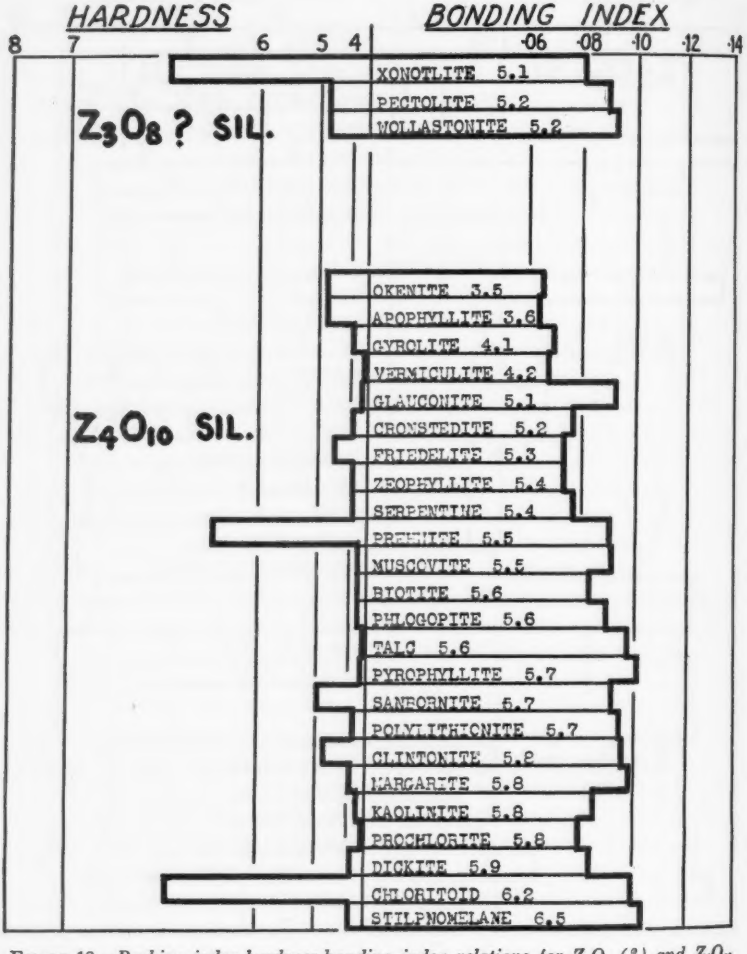

FIGURE 18.—*Packing index-hardness-bonding index relations for Z_3O_8 (?) and Z_4O_{10} silicates*

Sapphirine Kornerupine — The discrepancy in hardness in this pair could be ascribed to the lack of cleavage in sapphirine and its presence in kornerupine, thus lowering the hardness of the latter.

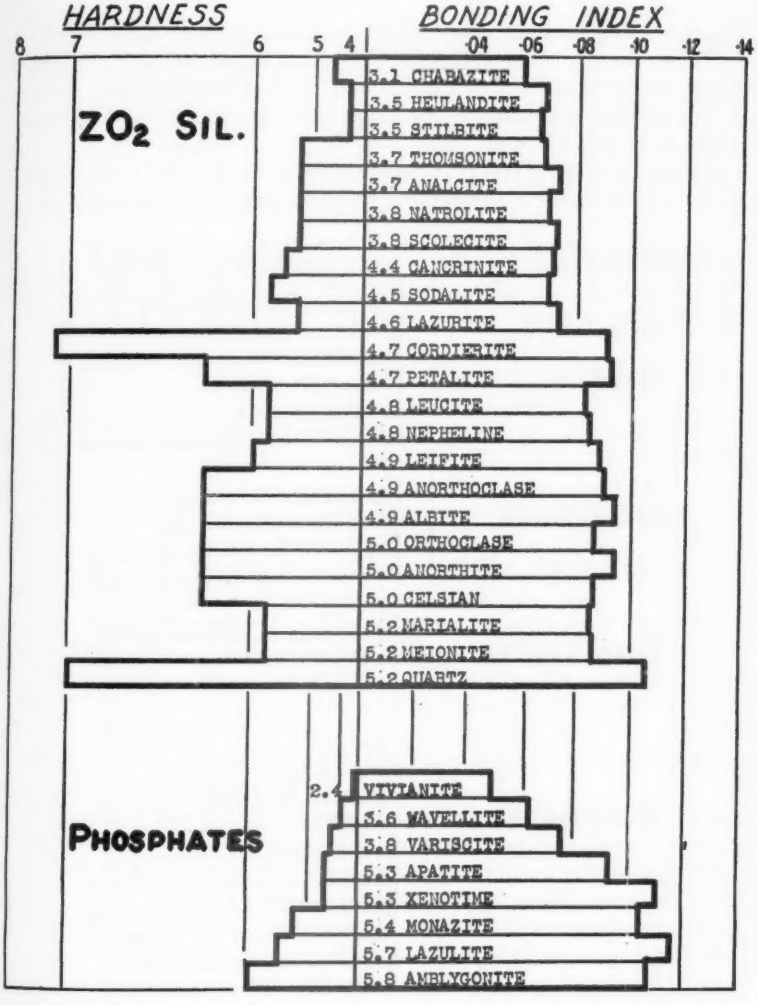

FIGURE 19.—*Packing index-hardness-bonding index relations for ZO_2 silicates and miscellaneous phosphates*

Zunyite
Serendibite

The superior hardness of zunyite relative to its low bonding index, and the hardness of serendibite remain unexplained at present. Serendibite is reported to have no cleavage; zunyite poor cleavage only.

Topaz
Kyanite

The hardness determination of topaz possibly needs revision. Earlier investigators have not been unanimous as to its position in the Mohs scale, some finding its hardness inferior to that of quartz. If this should prove true the hardness anomaly for kyanite and topaz would be largely removed.

Z_2O_7 subdivision (Fig. 17)—The hardness of the silicates in this group cannot be correlated satisfactorily with packing index and bonding index.

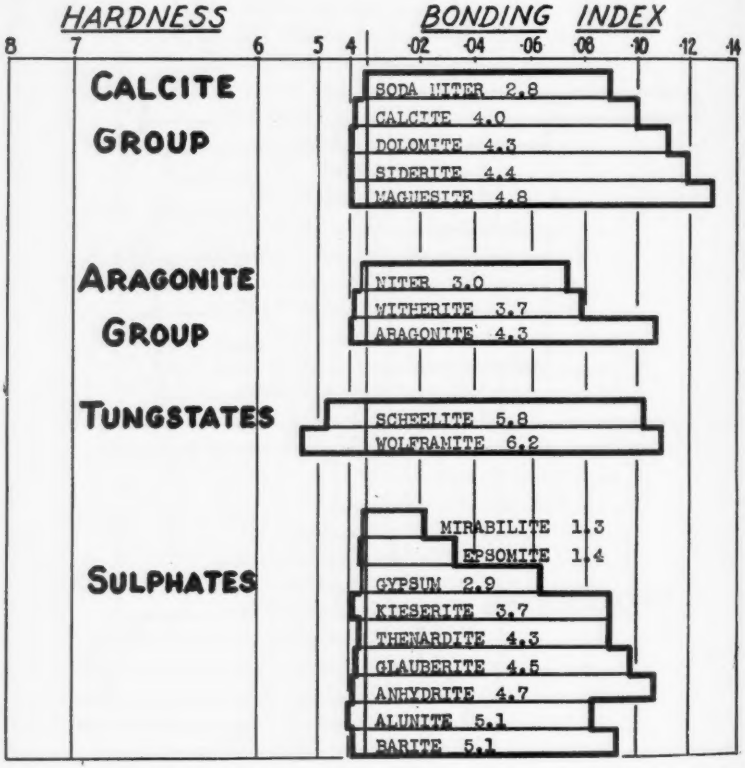

FIGURE 20.—*Packing index-hardness-bonding index relations for carbonates, tungstates, sulphates*

This may be partly due to the uncertain classification of lawsonite and danburite. Their absence from the Z_2O_7 group would improve the possibilities of correlation considerably. However, notable discrepancies would still remain, particularly the relative hardness of melilite and leucophanite.

ZO_3 subdivision (Fig. 17)—The silicates of this group permit a greater degree of correlation than the preceding one.

Beryl
Benitoite
Tourmaline

The superior hardness of beryl, benitoite, and tourmaline (schorl and dravite) is undoubtedly related to the ring structure which characterizes them, as contrasted with the chain structure of the remaining minerals.

Acmite
Hypersthene

The principal anomaly in the chain minerals is the unexpectedly high hardness value for acmite compared with hypersthene. No explanation is offered, unless it is assumed that the hardness is incorrectly determined.

Z_3O_8(?) subdivision (Fig. 18)—This group was proposed by Berman (1937) to accommodate wollastonite and structurally allied minerals. Xonotlite offers a conspicuous hardness anomaly for which no explanation is apparent, especially as each member of the group has pronounced cleavage.

Z_4O_{11} subdivision (Fig. 17)—Correlation is reasonably good in this group. The principal exception is the low hardness of riebeckite compared with either of its neighbors. Careful quantitative study of hardness in the amphibole family might rectify this anomaly.

Z_4O_{10} subdivision (Fig. 18)—Packing index and bonding index relations are normal here, the discrepancies in the latter being easily explained in terms of relative ion size and valence. Hardness on the other hand does not increase even in a general way with increase in packing and bonding indices. This is primarily because it is determined in these minerals almost invariably on the basal planes of easy cleavage, characteristic of this group of silicates.

Hardness is at a minimum along cleavage planes, and, as these are by definition planes containing a minimum concentration of bonds per unit area, the lack of correlation between bonding index (computed for the entire crystal) and hardness (referable here to minimum values on cleavage planes) is not surprising. In absence therefore of any values even approaching the mean hardness for these minerals (prehnite and chloritoid possibly excepted) it would be pointless to pursue the hardness problem further in relation to crystal packing for these layer lattice structures. An excellent analysis of layer lattice bonding in its relation

to hardness and cleavage has been made by Pauling (Bragg, 1937, p. 217), but its details are not relevant to the main thesis of this paper.

ZO_2 subdivision (Fig. 19)—In contrast with the preceding group, normal correlation of the three quantities is permissible here, with a few exceptions in the hardness columns. No mineral in this group possesses a cleavage which dominates the crystal habit completely, as in the Z_4O_{10} subdivision, where (001) practically eliminates other planes for the hardness test. A mean hardness may therefore be obtained in ZO_2 silicates which permits correlation in most cases with packing and bonding indices.

Heulandite
Stilbite
Chabazite — The hardness of these minerals is low with respect to chabazite. Determinations have possibly been made on cleavage faces or have been affected by them. This would be a less likely circumstance for chabazite, which has no well-developed cleavage.

Sodalite
Lazurite — The low hardness of lazurite seems anomalous, as its physical properties are similar to those of sodalite. The hardness values may possibly be inaccurate.

Cordierite
Petalite — As cordierite lacks well-developed cleavage, its hardness is probably a reliable mean value. In comparison, the unduly low hardness of petalite indicates the probable influence of its two cleavages.

Phosphates (Fig. 19)—Correlation is in general excellent for these phosphates. In the bonding index columns the indentation for monazite is due to Ce^{3+} being larger than the Y^{3+} in xenotime, with consequent lower concentration of bonds per cu. Å. In amblygonite only 9 bonds are needed for 3 cations, whereas in lazulite 18 bonds are needed for 5 cations. No explanation of the anomalous hardness relations of xenotime and monazite is apparent, as each has one perfect cleavage. Similarly for amblygonite (perfect cleavage) and lazulite (poor cleavage) the hardness relations appear ambiguous.

Calcite group (Fig. 20)—Revision of the hardness determinations in this group might result in a scale of values in better correspondence with the packing and bonding indices. It is probable that the present hardness values are in part based on tests on cleavage fragments; to that extent such values are lower than average.

Aragonite group (Fig. 20)—No comment required.

Tungstates (Fig. 20)—No comment required.

Sulphates (Fig. 20)—Bonding and packing indices increase uniformly as far as anhydrite but are divergent for alunite and barite. This is

easily explained in terms of the cations, as the presence of K^{1+} in alunite and Ba^{2+} in barite necessitates larger cells than required for anhydrite, with consequent lower concentration of charge per cu. Å. The contrast in bonding index may be traced to the monovalent K^{1+} and $(OH)^{1-}$ in alunite, where only 22 bonds are needed for 6 cations, compared with the 8 needed for 2 cations in barite.

As the hardness differences (absolute scale) are small for these particular sulphates, detailed comment on the discrepancies with bonding and packing indices may prove to be unwise. Assuming the hardness differences to be real, however, the following points deserve mention.

The low hardness of gypsum compared with epsomite may be due to the extremely easy (010) cleavage in gypsum, caused by the weak molecular H_2O bonds concentrated in this plane. Thus hardness tests in almost any plane or direction in gypsum may be modified so that no exact correlation with the bonding index is possible.

The superior hardness of kieserite compared with thenardite remains anomalous, especially as the former is noted for its five good cleavages, which might be expected, if anything, to lower the hardness. Thenardite possesses only one cleavage.

The greater hardness of alunite compared with barite may be explained on cleavage grounds. Barite possesses three excellent cleavages, whereas alunite has a single imperfect one. Thus, as in gypsum, the true average "strength" of barite may not be indicated by the hardness test as accurately as that for alunite.

Conclusion.—The well-known direct variation of packing index with hardness is confirmed by the present analysis. Individual aberrations are explainable for the most part (1) by study of the bonding conditions of the crystal (bonding index), (2) by consideration of the influence of cleavage planes in lowering hardness, (3) by possible faulty hardness determinations. As in the refractive index correlations, Ti^{4+} shows anomalous behavior with respect to the hardness of some of its compounds. Titanite and rutile show this clearly, and as before no explanation is offered.

The keynote of the hardness correlation may be said to be the inadequacy of the standard used for its determination. The convenience of a relative hardness scale such as that of Mohs is unquestioned, but the gross inequalities of the intervals on this scale should be remedied. Improved correlation with packing index and bonding index would undoubtedly result, and the influence of disturbing cleavage planes could be better evaluated.

TABLE 6.—*Thermal inversion (fixed composition*)*

Compound	Low ← Phases → High (mineral names, if any)			Transformation low → high produces		
				Density	Mean Refractive index	Symmetry
Al_2O_3	Corundum	β–Al_2O_3	α–Al_2O_3	Decr.†	Decr.	High
TiO_2	Anatase		Rutile	Incr.	Incr.	No change
	Brookite		Rutile	Incr.	Incr.	High
SiO_2	Quartz	Tridymite	Cristobalite	Decr.	Decr.**	High
$Na(AlSi_3O_8)$	Albite		α–$NaAlSi_3O_8$	?	Decr.	?
$K(AlSi_3O_8)$	Adularia		Sanidine	Incr.	Decr.	No change
$Na(AlSiO_4)$	Nepheline		α–$NaAlSiO_4$	?	Decr.	High
$K(AlSi_2O_6)$	β–leucite		α–leucite	?	Decr.	High
$Mg_2(Al_4Si_5O_{18})$	μ–$Mg_2Al_4Si_5O_{18}$		Cordierite	?	Decr.	?
$Li(AlSi_4O_{10})$	Petalite	β–$LiAlSi_4O_{10}$	α–$LiAlSi_4O_{10}$	Decr.	?	High
$Ca_6(Si_3O_9)O_2$	Wollastonite		Pseudo-wollastonite	Decr.	Decr.	?
$Mg(SiO_3)$	Enstatite		Clinoenstatite	Decr.	Incr.‡	Low
$LiAl(SiO_3)_2$	Spodumene		α–$LiAl(SiO_3)_2$	Decr.	Decr.	High
$Ca_2(SiO_4)$	γ–Ca_2SiO_4	Shannonite	Larnite	Incr.	Incr.	Low
$CaSO_4$	Anhydrite		α–$CaSO_4$	?	Decr.	Low
Na_2SO_4	Thenardite and fo	ur higher phases		Both incr.	and decr. found	
$CaCO_3$	Aragonite	Calcite	α–$CaCO_3$	Decr.***	Decr.	High
	μ–$CaCO_3$	Calcite	α–$CaCO_3$	Incr.***	Incr.	No change
KNO_3	Niter		α–KNO_3	?	?	High

* Data from Winchell (1931).

† Density of α–Al_2O_3 < density of β–Al_2O_3.

** Mean n of low cristobalite > low tridymite.

‡ Difference in mean n is only .001.

*** Refers only to the two lower phases, as data are lacking for α–$CaCO_3$.

CORRELATION OF PACKING INDEX WITH POLYMORPHIC PHASES

General statement.—Changes in type and closeness of packing have long been recognized as essential to polymorphic transformations. Such transformations may be produced thermally (the better known method) or under suitable pressure. Each will be considered in the discussion to follow. Polymorphism is used here in a broad sense to include inversions which involve compositional changes as well as those where the composition remains fixed.

Thermal inversion (fixed composition).—Seventeen compounds included in Table 4 show thermal inversion involving no change in composition. These are listed in Table 6 from data compiled by Winchell (1931). As the numbers and kinds of ions remain fixed for this inversion type, increase or decrease in packing index can be inferred directly from comparison of densities or mean refractive indices. Inspection of the table indicates that in general the transformation from a low to a higher phase involves decrease in packing index, in spodumene attaining a 30 percent volume increase. This trend might be predicted because of the need for greater "Lebensraum" in the cell as heat accretions cause greater vibrations of the ions. The opposite trend, however, is shown by all TiO_2 and Ca_2SiO_4 inversions and by some Al_2O_3, Na_2SO_4, and $CaCO_3$ transformations. The data are ambiguous for $KAlSi_3O_8$ and $MgSiO_3$ and involve only small changes in density and refractive indices. The $KAlSi_3O_8$ inversion is known to be sluggish, however, and contrasts sharply in this respect with transformations of the SiO_2 type. Apparently, therefore, ion packing explains these inversions only in part.

Table 6 shows in addition the well-known change to higher symmetry for most low → high transformations. Many of the high phases are isometric. In practically all cases decrease in packing index (= decrease in density and refractive index) is accompanied by the change to higher symmetry, the exceptions being TiO_2 and $CaSO_4$. Apparently this factor, like ion packing, is merely accessory to a more fundamental issue which determines the structure of each stable phase.

Buerger (1936) believes that the stable phase at a given temperature is that one leading to least vapor pressure. This hypothesis is superficially very plausible and merits thorough examination on specific compounds. Until further thermodynamic work is carried out the real significance of ion packing and crystal symmetry in thermal inversions will remain in doubt.

Thermal inversion (variable composition).—The older, rigid definition of polymorphism would exclude the examples to be described under this heading. No defense of the acceptance of the broader usage of the term

is offered here other than convenience in classifying the various kinds of inversions.

Three inversions involving change in composition have been selected. Others are known but most of these are incompletely investigated. Table

TABLE 7.—*Thermal inversion (variable composition)*

Low phase	Intermediate phase	High phase	Transformation low⟶high produces	
			Packing index	Symmetry
$Al_2Si_4O_{20}$ (Andalusite) (Sillimanite) (Kyanite)		$Al_2Si_3O_{19.5}$ (Mullite)	Decrease Decrease Decrease	No change No change High
$(XYZ)_7(Si_8O_{22})(OH)_2$ (Amphibole)		$(XYZ)_2(Si_2O_6)$ (Pyroxene)	No significant change	No change
$CaSO_4.2H_2O$ (Gypsum)	$CaSO_4.1/2H_2O$ ("Plaster of Paris")	$CaSO_4$*	Decrease†	High

† Comparison made on basis of ions + water.
* Not aragonite. Data from Winchell (1931).

7 shows the pertinent facts of interest in a correlation with packing index. The mullite transformation passed unrecognized until recently, as the high phase was long thought to be sillimanite. There is consistent decrease in packing index and, for the kyanite inversion, higher symmetry as well. The amphibole-pyroxene inversion is typical of (OH)-bearing compounds, but thoroughly investigated examples are few in number. The transformation neither supports nor negates the attempted correlation with packing index. The $CaSO_4$ inversions are accompanied by loss of water and show decrease in packing index and change to higher symmetry.

This type of inversion, as far as indicated in Table 7, supports the general condition of decrease in packing index and change to higher symmetry for transformations low → high. The same remarks apply here concerning the accessory role of these correlations as were made with regard to Table 6.

Pressure inversion.—Most of the information regarding inversions of this type stems from work on elements and the weaker binary compounds. Where structural determinations have been possible, it is known that low → high pressure inversion increases the co-ordination of the ions and consequently the packing index. Little success has attended efforts,

chiefly by Bridgman (1938, 1939), to produce inversions of this type in oxides and silicates. The experiments carried out involved either strong shearing stress combined with confining pressure, or compression alone. Partial results of shearing experiments of interest here are:

(1) No trace of kyanite was found in a sheared disc of andalusite powder. This transition should be attempted again either with or without a shearing component, as the relative packing indices—andalusite (6.0) and kyanite (7.0)—strongly suggest the possibility of a pressure transformation.

(2) Sheared cristobalite yields probable traces of tridymite. The packing index trend is in the anticipated direction.

(3) Sheared opal yielded unquestioned quartz in one experiment. As opal consists in part of cristobalite (packing index 4.3), formation of quartz (packing index 5.2) by inversion is to be expected.

(4) Sheared gypsum yields a new substance (properties incompletely known) which is neither plaster-of-paris nor anhydrite. The former would not be expected (*see* Table 7); the latter, however, could be a possibility as its packing index is greater than that of gypsum.

Compression experiments on ionic minerals have with few exceptions yielded negative results thus far. Two marked transitions are known for calcite, but the structure of the high-pressure forms is apparently unknown.

In summary, inversions dependent on pressure seem likely to permit closer correlation with packing index than transformations dependent on heat. Owing to the relatively great strength of many ionic minerals, however, experimental difficulties have thus far hindered accumulation of adequate data.

CORRELATION OF PACKING INDEX WITH PHASES SHOWING INCONGRUENT MELTING

The incongruent melting characteristic of many silicates provides a further test of the role of the packing index. Unfortunately the solid phases appearing during the incongruent melting interval have not been identified accurately in many cases, and useful data are lacking. Eight well-known examples are shown in Table 8. No attempt is made to show the complete reaction, as only the solid phases are of interest in the present analysis. Inspection of the new compounds, however, shows that Si and O are released into the melt in each case. The packing indices of the incongruent phases, leucite, forsterite, mullite, etc., show neither uniform decrease nor increase and indicate, for this incomplete tabulation at leaat, that the closeness of ion packing is not a decisive factor in their development. In contrast, these new phases show, with one exception (garnet), either higher symmetry or no change. It is of some interest to note that

suitably high pressure applied to a cooling melt of the composition of orthoclase will inhibit formation of the incongruent leucite phase and cause direct crystallization of orthoclase. This appears significant in

TABLE 8.—*Incongruent melting*

Stable phase below initial melting	Stable solid phase during melting interval	With rising temperature	
		Packing index of new phase shows	Symmetry of new phase becomes
Sanidine $K(AlSi_3O_8)$	Leucite $K(AlSi_2O_6)$	Decrease	Higher
Clinoenstatite $MgSiO_3$	Forsterite Mg_2SiO_4	Slight decrease	Higher
Cordierite $Mg_2(Al_4Si_5O_{18})$	Mullite $Al_6Si_2O_{13}$	Increase	No change
	Spinel MgO	Increase	Higher
Dumortierite $Al_6B(SiO_4)_3O_7(OH)$	Mullite $Al_6Si_2O_{13}$	Decrease	No change
Mullite $Al_6Si_2O_{13}$	Corundum Al_2O_3	Increase	Higher
Jadeite $NaAl(SiO_3)_2$	Nepheline $Na(AlSiO_4)$ Albite $Na(AlSi_3O_8)$	Decrease	Higher
Acmite $NaFe(SiO_3)_2$	Hematite Fe_2O_3	Increase	Higher
Garnet $X_3Y_2(SiO_4)_3$	Anorthite $Ca(Al_2Si_2O_8)$		
	Diopside-Hedenbergite $Ca(Fe,Mg)(SiO_3)_2$	Decrease	Lower
	Melilite $Ca_2Mg_{.5}(AlSi_{1.5}O_7)$ etc.		

view of the higher packing index of orthoclase. The writer will leave to others, however, the thermodynamic problems connected with incongruent melting and the investigation of the exact status of the packing index.

CORRELATION OF PACKING INDEX WITH SIZE OF MINOR IONS

Modern techniques in chemical and spectrographic analysis have shown the common occurrence of many unsuspected minor elements in minerals

normally regarded as "pure" compounds. Insofar as these accessory ions substitute for other ions of approximately the same size—Ga for Al, Fe for Si, Ba for K, Y for Ca, etc.—and therefore do not distort the crystal lattice unduly, the packing index of the mineral has no bearing on the problem. Where substituting ions are abnormally large, however, it is reasonable to assume the presence of accessory openings in such lattices which would provide adequate accommodation. Minerals of low packing index are most likely to harbor such openings. Data at present are inadequate for a complete correlation of this kind, and attention is directed merely to a few ionic minerals of markedly low packing index, some of which are already known to be the home of "over-size" minor elements, others of which seem to possess potentialities in this regard.

Table 9 summarizes information relating to a selected group of this kind. No attempt is made to state even approximate dimensions of the openings. Their shapes and relative orientations are given where known. A few of these minerals have immediate interest because of their known capacity to harbor cations much larger than they could possibly accommodate without the aid of inter-ion channels and pockets. Beryl is perhaps the best known of these, and its ability to take up several per cent of alkalis is general knowledge. Even the smallest alkali ion (Li^{1+}), however, would require considerable additional space over that required for Be^{2+} (Fig. 2). Caesium-rich beryl is well known, although the radius of Cs^{1+} is five times that of Be^{2+} and three times that of Al^{3+}. Undoubtedly the ample channels in the beryl lattice are the means of entrance of these large ions.

Cordierite may also contain appreciable amounts of alkalis. Although Li^{1+} might substitute for Mg^{2+} and Fe^{2+} without the aid of large openings, the commoner Na^{1+} and K^{1+} would require additional space. (*See* Figure 2). The nature of these openings is not yet definitely known, but if cordierite is isostructural with beryl, as suspected by Folinsbee (1941) and others, there would be no problem concerning the entrance of large alkali ions into its lattice. In any case its packing index is so much lower than that of any other Mg-rich silicate that large openings of some kind must be assumed.

The andalusite lattice contains pockets which could admit large ions (*i.e.*, relative to Al^{3+}). Jakob's recent work (1940, 1941) on andalusite and kyanite shows clearly that the omnipresent alkalis (principally sodium) and water occur in stoichiometric proportions and are an essential part of these minerals. Even a gem variety of andalusite contains an appreciable amount of these "impurities." The close-packed kyanite lattice might be expected to refuse entrance to any ion as large as Na^{1+}; nevertheless, Na^{1+} occurs consistently in amounts greatly exceeding

spectroscopic proportions. It will be interesting to discover, however, if andalusite has a higher per cent average of alkalis than kyanite, as Jakob's results now seem to suggest. If so, the pockets and relatively low packing index of andalusite would indicate the reason for such a relation.

The chemistry of the silica minerals is very suggestive of the utilization of large openings by "oversize" ions. For example, the substitution

TABLE 9.—*Partial list of ionic minerals possessing relatively open packing*

Mineral	Packing index	Character of principal lattice openings	Remarks
Cuprite	4.4	Nonintersecting channels	Unique structure. Low packing index for an ionic binary oxygen compound.
Anatase	6.3	Pockets	Included because of contrast with rutile (packing index 6.6).
Brookite	6.4	Nonintersecting channels	
Tridymite	4.6	Intersecting channels	May contain notable amounts of Na, Ca, Al, etc.
Cristobalite	4.5	Intersecting channels	Minor elements less well known than tridymite.
Sodalite	4.5	Probably intersecting channels	Contrast with feldspar (packing indices 4.9–5.0).
Cordierite	4.7	Possibly like beryl	Packing index very low in comparison with other (Mg, Fe) silicates. May contain several per cent alkalis.
Beryl	5.1	Nonintersecting channels	Packing index very low in comparison with euclase (6.5). May contain several per cent alkalis.
Melilite	5.3	Pockets	Packing index low relative to position in silicate structural classification (between ZO_4 and ZO_3).
Phenacite	6.3	Nonintersecting channels	Packing index low for a Be silicate of ZO_4 type.
Willemite	4.7	Nonintersecting channels	Isostructural with phenacite. Lower packing index because vol. Zn > vol. Be.
Mullite	5.6	Probably channels as in sillimanite, plus pockets	Included because of contrast with kyanite (packing index 7.0). Andalusite may contain notable amounts of alkalis, easily determinable by chemical analysis. (*See* Table 4).
Andalusite	6.0	Pockets	
Sillimanite	6.2	Nonintersecting channels	
Soda Niter	2.8	Planar openings	Contrast with magnesite (packing index 4.8), which is isostructural with these minerals.
Calcite	4.0	Planar openings	
Dolomite	4.3	Planar openings	
Siderite	4.4	Planar openings	

$Si^{4+} \rightarrow Al^{3+}$, common in ZO_2 silicates, requires the entrance of other ions to neutralize the modification in the valence from 4+ to 3+. For tridymite Lukesh (1942) has recently reported the formula $NaCa(Al_3Si_{15}O_{36})$, in which it must be assumed that the Na^{1+} and Ca^{2+} occupy the openings in the structure. Little is known of the "impurities" in cristobalite (other than water molecules), as suitable material for analysis is difficult to obtain. In one analysis quoted by Buerger (1935) several per cent of Fe^{3+} and Al^{3+} were found. In contrast, quartz shows only spectroscopic traces of "foreign" elements, and no great variety of these, a circumstance in harmony with its relatively high packing index.

No comment on the remainder of Table 9 can be made as the author has no data available for discussion. The correlation of degree of packing with the occurrence of "oversize" minor elements seems established, however, on the basis of the few minerals already described.

SUMMARY OF MINERALOGIC CORRELATIONS

A résumé of the preceding pages shows considerable correlation of the concept of packing index with mineralogic constants such as density, refractive index, and hardness. In a few examples, particularly where refractive indices are concerned, the correlation is elusive and unsatisfactory. Revision of the hardness scale is sorely needed. Correlations with density are generally excellent, all discrepancies being explained in terms of the atomic weights of the elements concerned. The superiority of the packing index concept over hardness, density, and refractive index for general comparative purposes is pointed out.

Correlation with phenomena relating to polymorphic inversions is incomplete and is most satisfactory in the case of transformations initiated by pressure. The status of the packing index with respect to incongruent melting phenomena is likewise somewhat nebulous.

As far as present facts permit analysis, a definite relation exists between packing index and the size of minor ions which may be admitted to a crystal lattice.

GEOLOGIC ASPECTS OF ION PACKING

INTRODUCTION

The transition from purely mineralogical to geological aspects of ion packing is a passage from quantitative (or semi-quantitative) to qualitative values, none the less important, however, because of this contrast. A survey will be made in the following pages of those geological relations which are of interest in a study of the packing index of minerals. Familiarity with the current status of these relations is expected of the reader, as space forbids their recapitulation here. Although more prob-

lems will be raised than solved, no apology for this situation is required, as the present study is admittedly exploratory in character.

GENERAL CORRELATION WITH TEMPERATURE OF FORMATION OF MINERALS

The compilation in Figure 3 of the range of packing indices of the various mineral groups, arranged compositionally, corresponds in a general way with geological experience regarding their relative temperatures of formation. That is, among minerals which crystallize from solutions of whatever kind, silicates and oxides are as a whole of higher thermal grade than sulphates and carbonates. It has commonly been observed that this temperature grouping is reflected in the relative hardness of silicates and oxides compared with sulphates and carbonates. Insofar as hardness is a function of the closeness and type of ion packing, the above correlation between packing index and temperature of formation could therefore have been predicted. Within each group, moreover, the minerals of lowest packing index are, quite generally, those whose temperature of formation is lowest. For example, cuprite (4.4) develops at a much lower temperature than corundum (7.2); zeolites (3.1-4.6) are low-temperature silicates compared with olivine (5.9); vivianite (2.3) crystallizes in a cool environment compared with amblygonite (5.8); mirabilite (1.3) develops in cold solutions, whereas alunite (5.1) requires considerable heat; natrite (.8) forms from cold carbonated waters in contrast to the higher temperature required for development of magnesite (4.8).

These differences in packing index are but a superficial expression of more fundamental causes governing the temperature of formation of minerals of this kind. To examine all these would lead too far from the central topic under discussion here. One, however, will be mentioned, because of its intimate relation to variations in packing index. Inspection of the dominant cations in the minerals from which Figure 3 is compiled shows the following:

Oxides—trivalent and tetravalent cations are dominant.
Silicates—trivalent and tetravalent cations are common.
Phosphates—trivalent cations are fairly common.
Sulphates—trivalent cations occur only with monovalent cations (as in alum).
Carbonates—trivalent cations absent.

In this compilation the central cations, Si, P, S. C in the silicate, phosphate, and sulphate tetrahedra, and in the carbonate planar groups, are not taken into account. Reference is only to the cations linking these units to each other. The progressive decrease in abundance of cations of high valence (Al, Ti, Si, Fe, Cr) relative to monovalent cations (Na and K chiefly) parallels a transition to ions of larger volume (*see* Figure 2) which, quite generally, lowers the packing index. This is in accord with Figure 3. That is (central cations excepted), highly charged cations tend

to leave solution and form solid phases at higher temperatures than cations with small charges. Although the further links in this chain of reasoning are not germane to the present discussion, their future analysis is of the utmost significance.

It should be pointed out that (oxides excepted) the members of each group in Figure 3 with lowest packing index contain water molecules, with the result that their ions are stacked together much less tightly than would be necessary if the water were absent. The relative absence of small cations outside the tetrahedra in zeolites, vivianite, thenardite, natrite, etc., is therefore not the sole cause of lower packing index. The affinity of these substances for water is apparently so great that excessively open-packed structures must form to accommodate it.

CORRELATION WITH SILICATE CRYSTALLIZATION

The crystal structural significance of the silicate sequence in a cooling magma has been discussed at some length by Fersman (1937, p. 85) as part of the general topic of lattice energy. There is an overall decrease in lattice energy of successive minerals as crystallization proceeds, and with it a general decrease in hardness and in the number of crystal symmetry elements. This is in turn related to net increase in ion size and net decrease in valence. Although no specific mention is made of the degree of ion packing in terms of lattice energy, it is obvious that the packing index must be one of the fundamental elements in the rather complicated formula used by Fersman. As the lattice energy is accurately known at present only for simple compounds, no further use of this quantity will be attempted here. Its fundamental importance, however, is unquestioned.

Table 10 shows the packing indices of the individual minerals in normal igneous crystallization, the sequence with falling temperature being indicated by arrows. The so-called discontinuous series at the left shows, with the exception of olivine, undoubted decrease in packing index. The continuous plagioclase series, crystallizing contemporaneously, shows little change and has a relatively low range of values. The final crystallization of zeolite minerals shows marked decrease in packing index.

These changes are governed by two important variables—the arrangement of the dominant tetrahedra in the crystal structure and the size of the cations linking the fundamental tetrahedra to each other. With falling temperature the numerical ratio central cation/oxygen increases in the successive silicates from ¼ to ½. The central cations (always Si, with or without Al) are designated by Z in Table 10. Increase in the ratio Z : O is a result of progressively greater sharing of O^{2-} by adjoining Z-O tetrahedra, which in turn is related generally to more open lattices (quartz excepted). In addition, monovalent ions first appear in the later crystal-

lizing phases and, as these (Na, K) are large in comparison with the prevalent ions appearing at earlier stages (Mg, Ca, etc.), silicates containing them tend to have relatively low packing indices. The packing index thus plays an interesting but accessory role in silicate crystallization.

TABLE 10.—*Relation of packing index to crystallization sequence in cooling magmas*

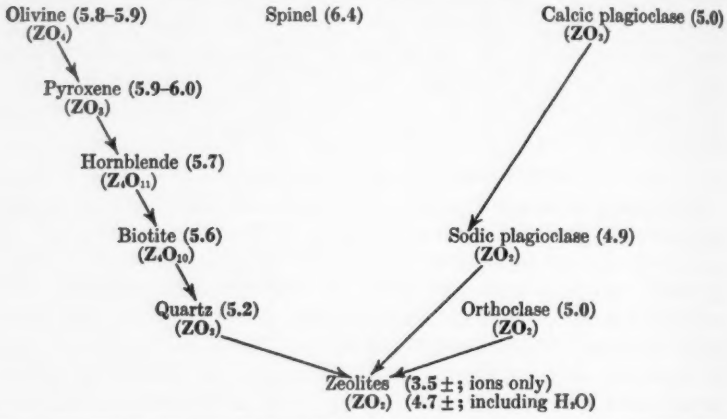

CORRELATION WITH INCONGRUENT PHASES IN MAGMA

The solidification of a melt of the composition of orthoclase involves the appearance and disappearance of an intermediate phase, leucite (*see* Table 8), over a temperature interval which substitutes for the fixed melting point characteristic of most compounds. It is well established that the normal habitat of leucite is in silica-poor mafic rocks and particularly in recent extrusives of this type. Deficiency in silica prevents exclusive formation of potash feldspar and is readily explained by the leucite-silica phase diagram. The abundance of leucite in some lavas and its absence in all plutonic rocks of equivalent composition are facts, however, not so easily explained. Barth (1937) quotes some recent experiments by Goranson which may shed light on the problem. At 2000 atmospheres pressure a melt ordinarily showing the incongruent leucite phase crystallizes directly as orthoclase. That is, over the normal incongruent temperature range the packing economy of orthoclase is stable, whereas that of leucite is not. The slightly higher packing index of orthoclase compared with leucite may therefore be geologically significant, as 2000 atmospheres is not an improbable pressure during emplacement of many magmas. Extruded rocks, not subject to pressures of this magnitude, would permit

crystallization of leucite, and, cooling rapidly, prevent its immediate inversion to orthoclase. Of possible significance also is the total absence of leucite from metamorphic rocks, where, presumably, pressures of some magnitude have operated. It is recognized of course that the abundance of silicon in the majority of such rocks, as well as the relatively low temperatures involved, are also potent factors. Again, the difference in packing index of the two minerals may possibly be traced to their relative proportions of Si and Al. In orthoclase and leucite all the Al, as well as Si, is housed as central cations in the O tetrahedra. It can be computed that the radius used for O^{2-} in silicates (1.32Å) restricts the central cation of a tetrahedron to a maximum radius of .18 Å, assuming perfect spheres in contact with each other. As Si^{4+} (.39Å) is twice and Al^{3+} (.57Å) three times this radius the tetrahedra are undoubtedly distorted. As more Al-O tetrahedra are present in leucite than in orthoclase it may be contended that the inferior packing index of leucite is due to the larger Al^{3+} ions. However, as the degree of packing in silicates is almost entirely a matter of oxygen size and arrangement, the nature of the tetrahedral distortion would need to be known before a decision could be made.

An obvious sequel to discussion of the leucite-orthoclase problem is the forsterite-clinoenstatite system, where similar uncongruent melting and packing index relations are found (Table 8). The geological aspect of the picture differs, however, as clinoenstatite is rare in igneous rocks, and forsterite as such is limited to metamorphosed limestones. The most nearly comparable minerals are olivine and pigeonite. Olivine, however, is more abundant in plutonic than in extrusive rocks, in the latter occurring mostly as phenocrysts and therefore being intratelluric in origin. Compared with orthoclase and leucite, the geologic occurrences are thus reversed. Moreover, no experimental data at elevated pressure for an $MgSiO_3$ melt are at hand. In view of the geological evidence it can only be assumed that pressure greater than that prevailing during the crystallization of Mg-rich magma would be necessary to inhibit the olivine stage, if indeed this is a possibility at all.

ROCK DENSITY AND ROCK-PACKING INDEX

It has previously been shown for individual minerals (Table 5) that density is a function of two variables, ion packing and atomic weight. For rocks, on the other hand, a third variable, porosity, must be taken into consideration and eliminated by various means before the density determination is complete. Determination of a packing index for the rock avoids the matter of porosity altogether, as ions only are concerned.

Furthermore, as with the packing index of minerals, the atomic weight variable is eliminated, and comparison of various rocks can be made on the basis of one variable only (closeness of ion packing). Figure 21

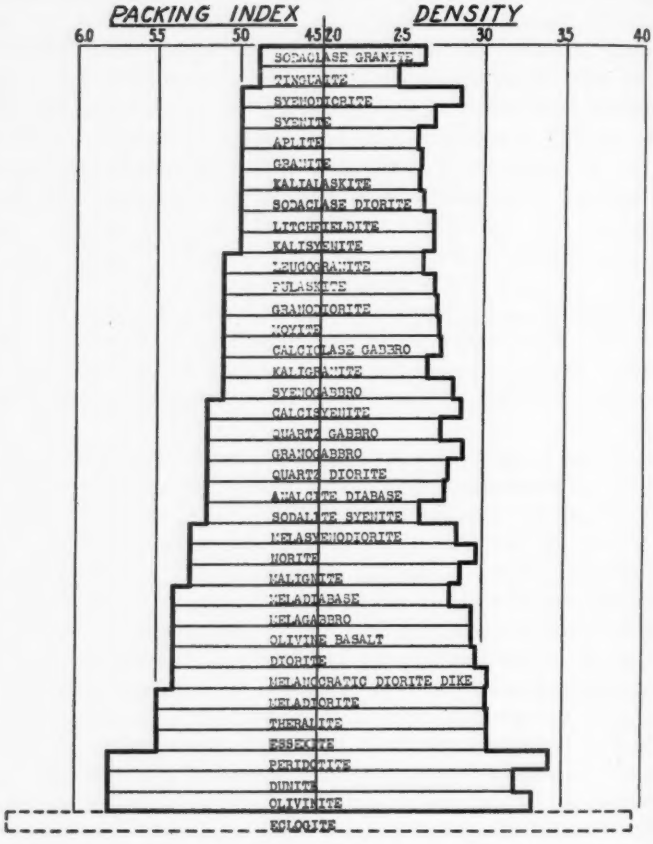

FIGURE 21.—*Packing index-density relations of common igneous rocks*
Eclogite (broken lines at bottom) added for comparative purposes.

shows a tabulation of the packing indices and densities of a number of igneous rocks selected more or less at random from Johannsen's compilation (1931-1938). Extrusive rocks were avoided (except for one olivine basalt) as the modes of such types may be relatively inaccurate, and small amounts of interstitial glass may also have escaped notice. No

check of the original literature was made to ascertain if the densities take account of porosity or not. However, this is not a serious matter for general comparison of all types of intrusives. The rock names are those used by Johannsen.

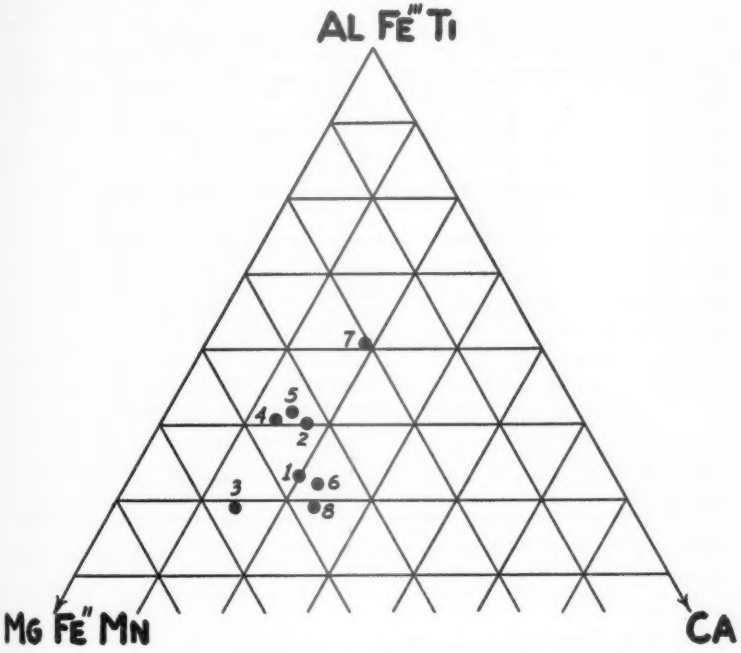

FIGURE 22.—*Chemical relations of selected constituents of rocks in Figure 23*
Numbering is from top to bottom as in Figure 23—*i.e.*, 1-norite granulite, 8-eclogite.

The packing index of a holocrystalline rock is computed without difficulty by combining the mode of the rock with the packing indices of the minerals it contains. Thus in a leucogranite containing 20 per cent quartz (packing index 5.2) the contribution of quartz to the packing index of the rock is $\frac{20}{100} \times 5.2 = 1.0$. The total of the contributions from each of the remaining minerals, computed similarily, represents the ion packing of the rock.

Comparison of the packing index and density columns in Figure 21 shows the anticipated parallel increase in both quantities in passing from silica-rich to silica-poor rocks. Individual density values depart

rather widely from the norm, however, as with syenodiorite, kaligranite, sodalite syenite, and peridotite, to name a few conspicuous examples. Magnetite is a common cause of abnormally high density; unusual proportions of certain silicates may also raise or lower specific gravity dis-

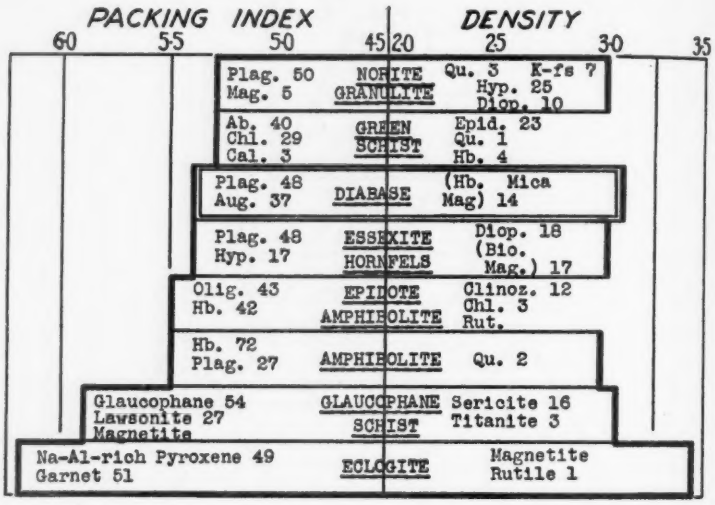

FIGURE 23.—*Packing index-density relations of an approximately isochemical rock series*

Kinds and proportions of the minerals in each rock are included.

proportionately. These factors are eliminated where a packing index is computed and comparison of various types is made without reference to density. Furthermore, the precautions required to neutralize the influence of porosity in a standard density determination are dispensed with; if required for other purposes, the porosity can easily be determined as an independent quantity.

The density of rock glass is somewhat less than that of completely crystallized igneous rock of similar chemical composition. Its packing index would be correspondingly less and of the same order of magnitude because of the identity in kinds and proportions of elements represented. Therefore, although a packing index cannot be computed directly for a glass, an approximation may be made indirectly where the density and packing index of the holocrystalline phase, and the density of the glassy phase, are known.

PACKING INDEX OF METAMORPHIC ROCKS

It has long been known that many metamorphic rocks, chemically similar to common igneous rocks, not only have distinctive mineral assemblages, but markedly different density from their igneous analogues. Eskola (1939, p. 346) has compiled a series of this kind, approximately isochemical with diabase, which is of considerable interest. Silica in these rocks varies between 46 and 52 per cent, three having 49 per cent. Variations in the remaining chief constituents (alkalis excepted) are shown in Figure 22. Subtraction of that part of the alumina in 7 (glaucophane schist) which combines with the high alkalis in this analysis to form feldspar would bring this point somewhat closer to the main group. The rocks are undoubtedly similar in a chemical sense, although unrelated in time and space.

Figure 23 shows diagrammatically the packing indices and densities of Eskola's series, and in addition the kinds and proportions of minerals in each. Two of the rocks have lower packing indices than diabase; four have higher packing indices. The inadequacy of density in indicating relative degrees of packing is clearly shown by the contrast between amphibolite and glaucophane schist, where marked difference in packing indices is accompanied by little change in density.

The packing indices of a number of miscellaneous foliated rocks have been computed and are assembled in Figure 24. Study of the packing indices of individual minerals in each rock substantiates the long-known observation that the rock density differs from that of an igneous or sedimentary rock of similar chemical composition. For example, although a mica schist may be approximately of the same chemical composition as an argillaceous sandstone (*i.e.*, isochemical with it) its packing index will tend to be somewhat higher; amphibolite, commonly isochemical with gabbro, likewise has a higher packing index.

Explanation of these packing relations as simply due to pressure without differentiating between two main types, or without reference to compositional and thermal factors, would be unjustified. It is true that certain minerals native to foliated rocks—chloritoid, glaucophane, staurolite, etc.—are unknown as crystallization products of magma. Others such as feldspar, quartz, and mica, however, are equally at home in either environment. Confining pressure is obviously not the only factor involved at any given temperature level. Stress (differential pressure) and concentration of particular ions are other factors of undoubted importance. The foliated character of many metamorphic rocks suggests that confining pressure is subordinate to stress during the main period of new mineral development. In massive metasomatic rocks neither stress nor confining pressure may be significant. Therefore the

circumstance that development of platy and prismatic minerals (mica, chlorite, amphibole, etc.) increases the bulk packing index of an unaltered rock seems in most cases to be incidental rather than casual. It

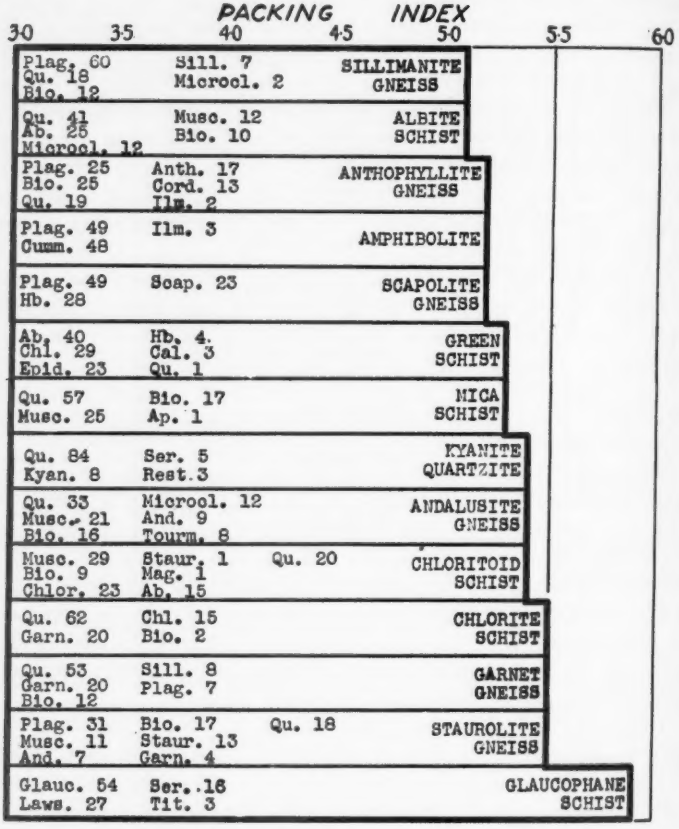

FIGURE 24.—*Packing indices of common metamorphic rocks*
Showing kinds and proportions of minerals in each.

is obvious that much remains to be done in this field, particularly in discovering if possible by synthetic means the phase relations in varying environments.

The conception of changes occurring within an isochemical system (in a geological sense) has its analogue in the isovolumetric (volume-for-volume) system first proposed by Lindgren (1912) to explain changes

due to metasomatic action. It is fairly obvious that the two types of system are mutually incompatible—*i.e.*, a rigidly isochemical system cannot at the same time be strictly isovolumetric, and vice versa. Only in cases where simple recrystallization occurs, as the metamorphism of limestone to marble, would it be possible for both isochemical and isovolu-

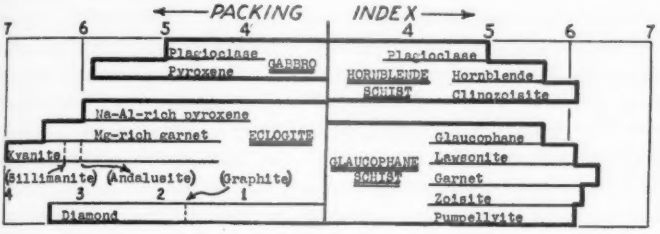

FIGURE 25.—*Comparison of packing indices of minerals in gabbro and eclogite (left), hornblende schist and glaucophane schist (right)*
Names in brackets (lower left) included for comparison only.

metric conditions to prevail. The role of packing index in isovolumetric systems related to ore deposits is not easy to evaluate as the replacing and replaced phases are commonly different structural types (*e.g.*, sulphides and silicates), thus making comparisons hazardous. It seems probable that chemical and thermal considerations are paramount here and that the closeness of packing exhibited by the minerals plays at best a secondary role.

THE ECLOGITE PROBLEM

A great deal has been written concerning these baffling but fascinating rocks, and it is not proposed here to make a review of the extensive literature. Eskola's discussion (1939, p. 363) is up to date and adequate. Eclogite is a massive garnet-pyroxene rock distinguished from all others by its high packing index (and density). It is variously considered as plutonic or as metamorphic, emphasis at present centering on the latter origin. Its gabbroic chemical composition permits its inclusion in Figure 23. The absence of plagioclase from eclogite (although an essential constituent of all rocks in Figure 23 except glaucophane schist) suggests special conditions of formation, as other plagioclase-free rocks (peridotite, dunite, etc.) are not isochemical with eclogite. The left half of Figure 25 is constructed to contrast the packing indices of the common constituents of gabbro with those of eclogite. It is notable that both essential constituents of most eclogites are distinguished by a high degree of ion packing. The aluminum which would ordinarily form plagioclase is taken up mostly by garnet, the excess going into the unusual pyroxene

variety omphacite. Sodium likewise goes with this pyroxene instead of into plagioclase. Omphacite is a clinopyroxene rich in the jadeite component and consequently has a higher packing index than common pyroxene varieties. All garnets are characterized by relatively high packing indices compared with other silicates. Furthermore, if aluminum is present in too great excess for inclusion in garnet and pyroxene, kyanite developes (not andalusite or sillimanite). Tilley (1936) recently found that so-called sillimanite in many eclogites is actually kyanite in every occurrence which he examined in detail. Finally, rare diamonds occur in rocks of eclogite character, not the less significant because of their rarity. Graphite appears to be unknown in these rocks.

In view of the high degree of packing of both main constituents and of two minor ones, it is difficult to attribute this unique mineral assemblage to thermal equilibrium alone. Laboratory studies provide indirect support for this conclusion. For example, although certain garnet varieties have been prepared synthetically, the mineral has never been found to crystallize at room pressure from melts approaching normal magmatic proportions. This might be possible under suitable high pressure. Moreover, its occurrence as an accessory mineral of certain igneous rocks is mostly confined to plutonic types, where it is reasonable to suppose that crystallization took place under considerable confining pressure. In experimental systems where jadeite would be expected to appear as a solid phase (*e.g.*, nepheline—albite—wollastonite) Foster (1942) and others before him have failed to obtain this compound. They believe that pressure is necessary for its crystallization. Furthermore it does not appear to be known as a constituent of igneous rocks. Kyanite is unknown in synthetic crystals or in igneous rocks; diamond has been produced in microscopic crystals, but only under high pressure. Circumstantial evidence therefore points to high pressure as a controlling factor in the formation of eclogite, as it would indeed be a coincidence if development of this unique mineral association were controlled by thermal or other factors alone. These facts have led a number of geologists to the belief that an eclogite layer may exist at depth within the earth's crust. However, it would lead too far afield to present the arguments for and against this hypothesis, and the interested reader is referred to Eskola (1939) for an introduction to the matter, and to Buddington (1943) for more recent critical comment.

GLAUCOPHANE SCHIST

Certain glaucophane rocks are as remarkable in their way as eclogite, especially those which are free of plagioclase and are chemically similar to gabbro. This latter type, shown in Figures 23 and 25, is in places

characterized by the unusual mineral lawsonite. Garnet, zoisite, and pumpellyite are the most interesting accessory minerals. Glaucophane and lawsonite substitute for the hornblende and plagioclase of common hornblende schist, with the accessory minerals forming where necessary. Some of these, notably pumpellyite, may develop at a later stage. As Figures 23 and 25 show, the mineral packing indices and rock index are considerably higher than for other foliated rocks. There is a greater possibility than for eclogite that the high degree of packing here is fortuitous and not primarily attributable to high pressure, especially as glaucophane itself is unquestionably a secondary mineral and has a normal amphibole backing index. As these rocks are foliated, stress may play a more important role than in development of eclogite. Eskola (1939, p. 367) discusses the glaucophane schist mineral assemblage but is aware that their equilibrium relations are inadequately known. The problem is left for the present, as more data are necessary than mere computation of packing indices.

CORRELATION OF PACKING INDEX WITH THERMAL AND STRESS ENVIRONMENT OF METAMORPHIC SILICATES

Although precise information about the temperature range of metamorphic silicates is not available, general agreement prevails regarding their relative positions in the thermal scale. The evidence for this need not be elaborated here. Figure 26 shows the packing index-thermal relations of a representative group, the low- and medium-temperature minerals being arbitrarily combined, and each column arranged in order of increasing packing index. No marked contrast in packing indices distinguishes the right and left sides of the figure, and a wide range of indices is present. It may be significant, however, that no silicate of the low-intermediate group has an index equivalent to cordierite (upper right) and that no silicate of the high group has indices equivalent to those of staurolite and kyanite (lower left). That is, high temperature seems to develop minerals of slightly lower packing index than could exist at lower temperature, this despite a tendency toward higher concentration of iron in the Fe-Mg-rich members of the low-intermediate group compared with the high group. As Fe $>$ Mg (ion volumes), Fe-rich silicates would have lower packing indices than Mg-rich types (assuming similar structural types) and so tend to neutralize the relation suggested above. It is significant, however, that, of the four aluminum silicates in Figure 26, mullite, sillimanite, and andalusite (packing indices 5.6 to 6.2) are higher-temperature phases than kyanite (7.0).

These relations are seemingly at variance with those already presented in the discussion of Correlation of Ion Packing with Temperature of

Formation of Minerals. However, when it is noted that three-quarters of the minerals in Figure 26 do not form from solutions in open spaces (the prerequisite for this first group), the anomaly, although unexplained, becomes less serious. A principal difference in the two groups concerns

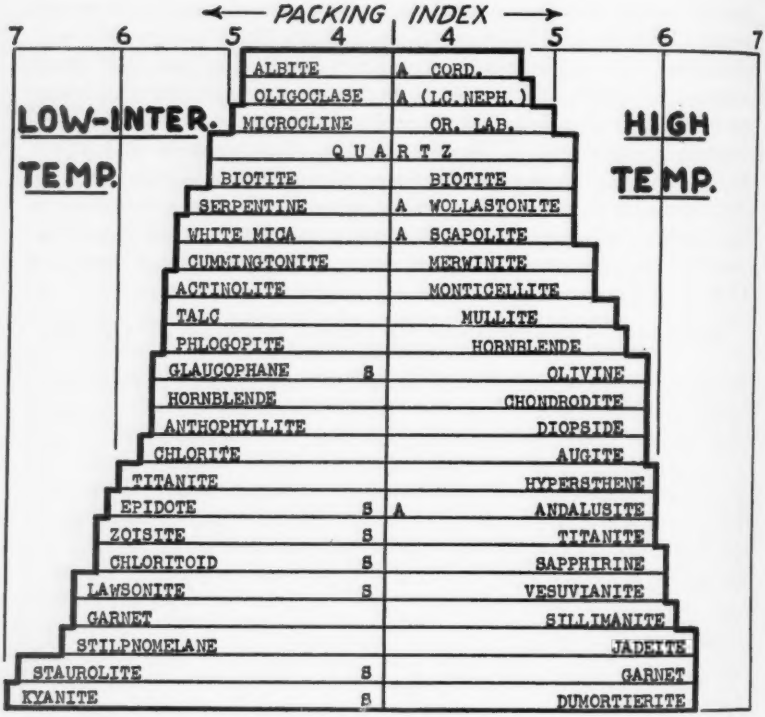

FIGURE 26.—*Packing indices of metamorphic minerals based on thermal characteristics* S—"stress" minerals, A—"anti-stress" minerals. Leucite and nepheline (Lc. Neph.) are included but are not metamorphic minerals.

the role of differential pressure (stress). It is entirely absent in the development of the first group and has variable relations toward metamorphic minerals. Its behavior has been discussed for decades, most recently by Harker (1932, p. 148) and Eskola (1939, p. 331). In contrast with the role ascribed to confining pressure, opinion seems to be that stress operates as a geochemical catalyst, initiating transformations at lower temperatures than would be possible in its absence. Certain min-

erals, notably cordierite, scapolite, and andalusite among the metamorphic silicates, leucite and nepheline among the igneous silicates, are absent in rocks known to have been subjected to stress; others such as glaucophane, chloritoid, kyanite, etc., although found in unstressed rocks, are particularly abundant in schists, gneisses, etc., where stress has played a leading part. Thus has arisen the terminology "stress" and "anti-stress" mineral. A third group, consisting of the commoner rock-forming silicates, seems to be controlled by the thermal environment alone.

It has long been recognized that "stress" minerals have higher density than "anti-stress" types. This relation is also valid for, and is better expressed by, reference to the packing index. It is seen that little overlapping occurs of the packing index value. It is also worthy of note that the stress minerals are all included in the low-intermediate temperature group, whereas the anti-stress silicates are high-temperature. This would seem to lend weight to the opinion that stress acts as a catalyzer and is responsible for development of certain stress-sensitive silicates at subnormal temperatures.

Reference should here be made to the terminology "plus" and "minus" minerals, as anti-stress and stress minerals are sometimes called. This is based on comparison of the sum of the molecular volumes of the "oxides" composing a silicate with the molecular volume of the silicate itself. Becke, Loewinson-Lessing, and others (Doelter, 1906) found that in some cases Σ "oxides" $>$ silicate; in other cases the opposite was true. A refinement of the method was the use of the molecular volumes of the high and low forms of the constituent "oxides" (Holmes, 1930) and the separation of an intermediate group where Σ high "oxides" $>$ silicate $>$ Σ low "oxides." Eskola (1939, p. 334) lists some common minerals classified on this basis—nepheline, leucite, cordierite are "plus" minerals; andalusite, orthoclase, albite are in the intermediate group; olivine, pyroxene, garnet, kyanite, etc., are "minus" minerals. The classification is roughly a packing index subdivision of silicates, the stress minerals as a result being of the minus type.

As most readers probably know, the premises for classification of silicates as plus or minus are invalid. The arbitrary breakdown of a silicate (or any other complex mineral) into a group of oxides has no crystal-structure basis whatsoever. The use of oxide constituents is a habit which derives from the customary statement of rock analyses in this form and from the synthesis of minerals from oxides. Oxides as such are nonexistent in silicates and related substances, and volume relations formulated on this basis are fallacious. Indeed, the oxides of the eight common metals contained in rock silicates represent no less than five structural types, only one of which (SiO_2) is related to the structural

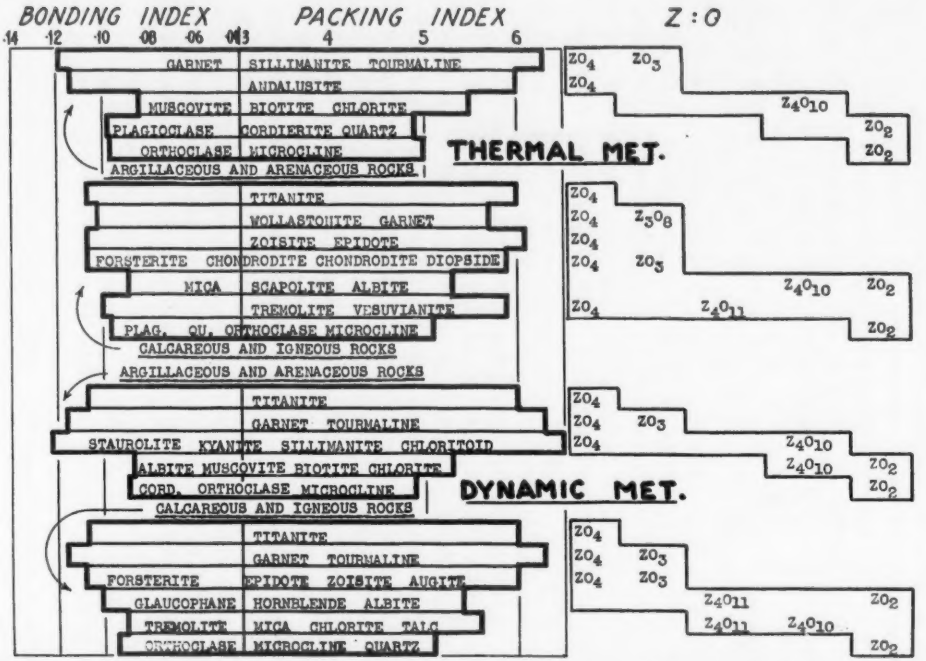

FIGURE 27.—*Relation between bonding-packing indices and position in the "crystalloblastic" series (left)* Common metamorphic minerals. Subdivisions after Harker. Right—correlation of silicate structure type with position in "crystalloblastic" series.

class to which the silicates belong. A "law" similar to that based on "oxides" could be set up with equal justification by using individual elements in the silicates. In consequence, therefore, any geological correlation claimed for the "oxide volume law" must be considered purely coincidental.

CORRELATION OF PACKING INDEX WITH MORPHOLOGICAL DEVELOPMENT OF PORPHYROBLASTS

Students of metamorphic rocks have devoted considerable time and effort to problems concerned with porphyroblasts (metacrysts). The so-called "crystalloblastic series," whereby porphyroblasts are arranged in order of increasing (or decreasing) degree of perfection of face development, is one of the results of such investigations. As the series is based solely on the ability of crystals to exhibit their morphological characters, it is obvious that the appellation "crystalloblastic" (=crystal growth) should be discarded in this connection, as minerals showing no development of crystal faces (*e.g.*, albite) may grow equally as large as others with excellent facial development (*e.g., garnet*).

Harker's classification of such minerals (1932, p. 38, 199) is the most recent and complete known to the writer and is the basis of Figure 27. As no classification of this kind can be precise, the order given is correct only in general terms. Accepting Harker's arrangement, an average packing and bonding index has been computed for each subgroup of silicates (*e.g.*, muscovite, biotite, chlorite near the top of the diagram have an average packing index of 5.6), the values being shown by the lengths of the horizontal columns. Oxides, sulphides, and carbonates are omitted as their packing indices are too dissimilar from those of the silicates to permit valid correlation. As silicates form the core of the series, however, absence of the others does not seriously impair the correlation. From the previous discussion of bonding-packing relations (Figs. 15-20) it would be expected that these two quantities would pursue parallel courses in each section of the figure. Discrepancies can be explained in the manner already described in the section on hardness correlations. It is seen that a general decrease in packing and bonding indices coincides with decrease in ability to develop crystal faces. The agreement is imperfect in detail, but little more could be expected in view of the unavoidable lack of precision in arranging a series of this kind. At the right of the figure is a summary of the (Si, Al)—O ratios (Si, Al expressed as Z) corresponding to the silicate types occurring in each column. The sequence of the Z : O types is similar to the igneous crystallization series of Table 10, although many of the minerals themselves (chloritoid, kyanite, etc.) are not products of magmatic crystallization.

No satisfactory hypothesis explaining the variable degree of development of porphyroblast faces is known. Few if any of the accepted "laws" holding for crystals growing freely in a solution or melt can be directly applied to metamorphic rocks, as the environment of porphyroblast growth is not fluid, and the intergranular space can hold only minor amounts of solution. Porphyroblasts showing facial development exhibit fundamental forms only, such as prism, rhombohedron, etc. Skeletal growths are unknown. Some porphyroblasts have no facial development. All these features contrast sharply with the manner of free crystal growth. The circumstance that growth occurs at all under such apparently unfavorable conditions has always appeared to be one of the minor miracles of geology. Apart from the ever-useful time factor, however, which is permitted to accomplish a great variety of geologic miracles, one of the well-known facts of free crystal growth may have significance here—i.e., small cross section favors rapid growth. Stöber (1931) grew an $NaNO_3$ crystal from a melt saturated with quartz sand and found that a single crystal took 18 minutes to complete its growth. In absence of the sand 12 hours were required. If an analogy is valid, and the intergranular space in a rock can influence new crystal growth in the same way as the pore space in the sand, the occurrence of porphyroblasts (or any metasomatic growth), either with or without facial development, may be conveniently explained. With this basic problem removed the matter of morphological development could then be dealt with independently in terms of packing index, bonding index, and Z : O ratio. Figure 27 does not indicate any possibility of a definite choice between them. From the viewpoint of crystal strength, bonding index might be favored as the decisive quantity. Porphyroblasts, however, seldom show evidence of pressure exerted against their host rock. It is asserted by some authors that porphyroblasts with good cleavage have good facial development; the fallacy of this reasoning is shown by pairs of minerals of the same crystal symmetry such as staurolite (excellent crystal form) and cordierite (no faces), neither of which has well-developed cleavage. The problem is therefore left with the above statement of the pertinent facts and a plea for further investigation by others.

CORRELATION OF PACKING INDEX WITH RATE OF MINERAL ALTERATION

Eskola (1939, p. 329) has recently drawn attention to the contrast in alteration of closely packed silicates such as garnet and olivine compared with relatively open-packed silicates such as feldspars and feldspathoids. The former alter by development of new minerals in fractures or on the outer boundaries (*e.g.*, serpentine in olivine fractures, kelyphitic rims or coronas enclosing garnet); the latter permit alteration products to develop

more or less at random anywhere within the body of the crystal (*e.g.*, epidote and white mica scattered through feldspar grains as a cloud of minute particles). It would be erroneous, however, to assume that the packing index influences the character of alteration. At a given temperature level, the reactions which occur are almost entirely a function of

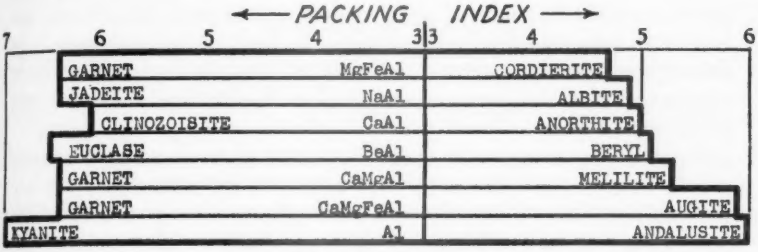

FIGURE 28.—*Comparison of packing indices with rate of mineral alteration*
Pairs of minerals containing the same elements.

composition. It is true that the most stable minerals (oxygen compounds mostly) at the earth's surface are generally those high in Si, Al, Ti, Zr, Fe^{3+}, etc.; in other words, the end-products of rock alteration are those with relatively highly charged cations. Insofar as these are also relatively small ions (*see* Figure 2), structures in which they are prominent will tend to have high packing indices. This, however, is one of the results of the alteration trend, not a cause of it. The principal influence of the packing index is more probably in hastening the rate of alteration. In Figure 28, pairs of silicates containing similar ions have been selected to illustrate this point. Z_4O_{10}-type silicates have been arbitrarily omitted, as the outstanding ease of alteration parallel to their basal planes practically nullifies comparisons based on packing index. The minerals on the left side of the figure show little internal alteration compared with their opposites on the right side. The contrast in this respect between garnet and cordierite is especially striking. (The occurrence of inclusions must not be confused with true alteration products.) The contrast is less marked with the remaining pairs but is nevertheless notable. In all cases the silicates showing alteration confined to grain boundaries or fractures (left side) have higher packing indices than their more easily altered counterparts (right side). The inference is that the degree of packing of the ions influences the rate of alteration by permitting entrance of solutions in varying degree into the structure. The circumstance that garnet is a commoner detrital mineral than cordierite, although each is composed of essentially the same elements, may be attributed to the relatively high

packing index and consequent slow decomposition rate of the former. Figure 28 could be materially expanded for illustrative purposes by inclusion of mineral pairs somewhat less similar in chemical composition.

POSSIBLE INVERSIONS IN STONY METEORITES

In concluding the discussion of geological aspects of ion packing, some mention should be made of stony meteorites, as their constituents are largely silicates and therefore fall under the head of ionic minerals. As the origin of these extra-terrestrial bodies is subject, however, to even more speculation than the genesis of terrestrial rocks, only brief discussion will be attempted here.

In a recent summary by Daly (1943) of facts concerning meteorites, one point emerges which has considerable interest in connection with ion packing problems. This concerns the abundant evidence of brecciation, fracturing, and mylonitization in stony meteorites. They are in consequence remarkably friable as compared with terrestrial rocks of similar composition and show unusual porosity. Daly has presented considerable evidence from density determinations in support of this. The minerals of the enigmatic chondrules, principally olivine and Mg-rich pyroxene, share this textural characteristic. The question may therefore be asked—Is this porosity a result of inversion processes, evidence of which is given, as in terrestrial inversions, by shattering and kindred textures? Fermor (1938) has long believed that the composition of certain enstatite chondrules suggests their genesis from garnet by a pressure inversion (packing index of garnet about 6.5; enstatite 6.0). Until recently this postulated garnet had a composition unknown among terrestrial garnets. Fermor now believes he has evidence of such a garnet in a diamond-bearing pipe in South Africa. If this is so, its association with diamond raises an interesting point, as graphite (packing index 1.7), and not diamond (packing index 3.4), is characteristic of meteorites. Daly (1943) has already independently mentioned the possibility that diamond was the original crystalline form of meteoritic carbon, which has since inverted to graphite by release of pressure.

It is not proposed to follow these speculations further, as sufficient indication has already been given of the quantitative role packing index may play when more concrete evidence of pressure inversion is available.

SUMMARY OF GEOLOGIC APPLICATIONS

The preceding pages show that geologic correlation with packing index is subject to more restrictions than is the case with the mineralogic correlations. Care must be exercised to distinguish cause from effect. Eclogite appears to be the best example of a rock whose packing index is influenced

largely by pressure. Other geologic aspects of packing index having points of interest are summarized in the abstract. Doubtless others have been overlooked. This paper will have served its main purpose, however, if it stimulates some curiosity among geologists concerning packing in rock minerals and succeeds in developing an interest in the geological aspects of such problems.

REFERENCES CITED

Barth, T. F. W. (1937) *Feldspar equilibria and their implication,* Norsk Geol. Tidsschrift, vol. 17, p. 177.

Barth, T. F. W., Correns, C. W., and Eskola, P. (1939) *Die Entstehung der Gesteine,* Springer, Berlin.

Berman, Harry (1937) *Constitution and classification of the natural silicates,* Am. Mineral, vol. 22, p. 342.

Blitz, W. (1934) *Raumchemie der festen Stoffe,* Leopold Voss Verlag, Leipzig.

Bragg, W. L. (1914) *Analysis of crystals by the x-ray spectrometer,* Royal Soc. London, Pr., ser. A, vol. 99, p. 468.

——, (1937) *Atomic structure of minerals,* Cornell Univ. Press.

Bridgman, P. W. (1939) *High pressure behavior of miscellaneous minerals,* Am. Jour. Sci., 5th ser., vol. 37, p. 7.

Buddington, A. F. (1943) *Some petrological concepts and the interior of the earth,* Am. Mineral., vol. 28, p. 119.

Buerger, M. J. (1935) *The silica framework crystals* etc., Zeitschs Kristal. vol. 90, p. 186.

—— (1936) *The kinetic basis of crystal polymorphism,* Nat. Acad. Sci., Pr., vol. 22, p. 682.

Daly, R. A. (1943) *Meteorites and an earth-model,* Geol. Soc. Am., Bull., vol. 54, p, 401.

Doelter, C. (1906) *Petrogenesis,* Fr. Vieweg und Sohn, Braunschweig, p. 196.

Evans, R. C. (1939) *Introduction to crystal chemistry,* Cambridge Univ. Press.

Ewald, Hermann *et al.* (1931) *Strukturbericht,* Zeitschs Kristal, 5 vols.

Fermor, L. L. (1938) *On khoharite a new garnet, and on the nomenclature of garnets,* Geol. Survey India, Records, vol. 73, p. 145.

Fersman, A. E. (1937) *Geochemistry* (Russian), Leningrad, vol. 3.

Folinsbee, R. E. (1941) *Optic properties of cordierite in relation to alkalies in the cordierite-beryl structure,* Am. Mineral., vol. 26, p. 485.

Foster, W. R. (1942) *System* $NaAlSi_2O_6 - CaSiO_3 - NaAlSiO_4$, Jour. Geol., vol. 50, p. 113.

Goldschmidt, V. M. (1926) *Geochemische Verteilungsgesetze der Elemente* VIII, Skr. Norske Videns.-Akad., Oslo, Math.-Natur. Kl.

Harker, A. (1932) *Metamorphism,* Methuen, London.

Heesch and Laves (1933) *Ueber dünne Kugelpackungen,* Zeit Kristal, vol. 85, p. 443.

Hodge, H. C., and McKay, J. H. (1934) *The "microhardness" of minerals comprising the Mohs scale,* Am. Mineral., vol. 19, p. 161.

Holmes, A. (1930) *Petrographic methods and calculations,* Thos. Murby and Co., London.

Jakob, J. (1940) *Ueber den Chemismus des Andalusits,* Schw. min. pet, Mitt., vol. 20, p. 8.

Jakob, J. (1941) *Chemische und strukturelle Untersuchungen am Disthen,* Schw. min. pet. Mitt., vol. 21, p. 131.

Johannsen, A. (1931-1938) *Descriptive petrography,* Univ. Chicago Press, 4 vols.

Kordes, E. (1939a) *Ionenradien und das periodisches System,* Zeitschs. phys. Chemie, ser. B, vol. 43, p. 213.

——— (1939b) *Die Ermittlung von Atomabständen aus der Lichtbrechung,* Zeit. phys. Chem., ser. B, vol. 44, p. 249, 327.

Larsen, E. S., and Bridgman, P. W. (1938) *Shearing experiments on some selected minerals and mineral combinations,* Am. Jour Sci., 5th ser., 36, p. 81.

Lindgren, W. (1912) *The nature of replacement,* Econ. Geol., vol. 7, p. 521.

Lukesh, J. (1942) *The tridymite problem,* Science, vol. 95, p. 20.

Melmore, S. (1942) *Open packing of spheres,* Nature, vol. 149, p. 412.

Mellor, J. W. (1922) *Inorganic and theoretical chemistry,* Longman's, Green and Co., London, p. 228.

Sollas, W. J. (1898) *On the intimate structure of crystals,* Royal Soc. London, Pr., vol. 63, p. 270.

Stillwell, C. W. (1938) *Crystal chemistry,* McGraw-Hill, New York, p. 37, 417.

Stöber, F. (1931) *Der "Kristallisierte Sandstein",* Chemie der Erde, vol. 6, p. 357.

Tilley, C. E. (1936) *Paragenesis of kyanite-eclogites,* Mineral. Mag., vol. 24, p. 423.

Winchell, A. N. (1931) *Microscopic characters of the artificial minerals,* John Wiley, New York.

Massachusetts Institute of Technology, Cambridge, Mass.

Manuscript received by the Secretary of the Society, May 12, 1943.

BULLETIN OF THE GEOLOGICAL SOCIETY OF AMERICA
VOL. 54, PP. 1375-1398, 3 PLS., 15 FIGS. SEPTEMBER 1, 1943

REVERSE FAULTING NORTH OF HARRISBURG, PENNSYLVANIA

BY ERNST CLOOS AND CARL H. BROEDEL

CONTENTS

	Page
Abstract	1375
Introduction	1376
Method of investigation	1377
Terminology used	1380
General geology of the area	1380
Reverse faults	1382
Description	1382
Statistical analysis	1383
Displacements	1384
Mechanical analysis	1386
Conclusions	1388
References cited	1396

ILLUSTRATIONS

Figure	Page
1. Geologic map of the area	1378
2. Diagram showing mutual relation of structure elements	1381
3. Statistical orientation diagrams	1389
4. Statistical orientation diagrams	1389
5. Statistical orientation diagrams	1390
6. Statistical orientation diagrams	1390
7. Statistical orientation diagrams	1391
8. Statistical orientation diagrams	1391
9. Statistical orientation diagrams	1392
10. Statistical orientation diagrams	1392
11. Statistical orientation diagrams	1393
12. Statistical orientation diagrams	1393
13. Statistical orientation diagrams	1394
14. Statistical orientation diagrams	1394
15. Schematic diagrams showing reverse fault positions	1395

Plate	Facing page
1. Drawing of west wall of road cut south of Marysville	1382
2. Thrust planes	1384
3. Thrust planes in thin-bedded Devonian strata	1385

ABSTRACT

Eight hundred and forty-three reverse faults were observed, measured, and analyzed statistically in the section of Susquehanna Gap and Cove Mountain syncline, Pennsylvania. Displacements are from several inches to 12 feet. The

grooves and striae on fault surfaces strike perpendicular to fold axes independently of the fault strikes. The predominant dip is southeast and northwest including an angle which increases gradually from 45° on the south limb to 90° in the center of the Cove Mountain syncline. The faults tend to thicken the rock column vertically and to shorten it horizontally in the same manner as folding. Total accumulated thickening and lateral shortening is several hundred feet. The forces necessary to produce such faults are ample to explain brecciation and slickensiding even with very slight displacements and with dip angles of more than 55° but the forces must exceed the weight of the overlying rock column because of friction. Greater dip variation of northwest-dipping fault planes apparently indicates rotation of shear planes during folding. Steep average dip of northwest-dipping planes south of Marysville may be due to rotation after faulting since work done on steep planes would exceed that done on gentle ones.

The authors believe that reverse faulting of the described kind is an important type of Appalachian deformation. Reverse faults are probably much more numerous and may be observed elsewhere.

INTRODUCTION

The area, along the Susquehanna and Juniata rivers in Perry and Dauphin counties, Pennsylvania, comprises approximately the same section as that described by Willard and Cleaves (1938, Pl. 1).

The first comprehensive study of this area was made by Claypole (1885) who considered that the top of the Silurian, Lower Devonian, and lower Middle Devonian were not deposited at Susquehanna Gap. The section at Susquehanna Gap was investigated by Stose (1930, p. 638-641). Willard (1931) recognized Oriskany on top of Little Mountain at Susquehanna Gap. Cleaves (1935) studied the structure of the New Bloomfield quadrangle. A more detailed study of the stratigraphy of the section was made by Willard and Cleaves (1938, Pl. 10). They interpret the absence of uppermost Silurian and the lower portion of the Devonian at Susquehanna Gap as due to a thrust fault.

Thus, reverse faults have been assumed in this section by Claypole (1885, p. 81-91), Willard (1931), Billings (1933), Cleaves (1935), and by Willard and Cleaves (1938, p. 20-21, Pl. 9), but a systematic or statistical analysis of the innumerable reverse faults of the region has never been undertaken so far as the authors know.

To show the various formations and principal members of the section in their mutual relation, competency, thickness, and importance, the reader is referred to Table 1. Symbols used in Figure 1 are listed in Table 1 opposite formation names.

A new highway along the west side of the Susquehanna River offers two exceptionally large well-exposed cuts, ¾ and 1¾ miles southeast of Marysville. In the northern cut two sets of gently dipping fault planes repeatedly offset these faults. The senior author observed and investigated other well-exposed localities in the area. Thousands of minor reverse faults occur in the Paleozoic section. The fault displace-

ment is generally less than 5 feet, and direction of movement can be determined from slickensides.

The junior author systematically measured slickensided fault planes and plotted them in orientation diagrams. The statistical treatment should show the general relationship between the reverse faults, the bedding, and the fold axes. The direction of movement as shown by the slickensides indicates whether the faulting was local or related to the deformation of the major syncline. Moreover, a systematic study of the reverse faults should provide quantitative data on the deformation of this portion of the Appalachians.

METHOD OF INVESTIGATION

Field work began in the first highway cut southeast of Marysville (localities 4-6) and in the adjacent quarry where well-exposed thrust faults are numerous and then continued northward to Half Falls Mountain. All measurable striae on slickensided thrust planes were recorded. Measurements included strike and dip of the thrust planes, the strike (horizontal projection) and pitch of the striae upon these planes, the relative direction of movement and the approximate displacement, and the attitude of bedding. Fourteen localities were studied in detail including quarries, highway, and railroad cuts which range from 100 yards up to ¾ mile in cross section (Pl. 1).

The orientations of structural elements were plotted into equal area nets (lower half) and counted as on fabric diagrams. The diagrams are not fabric diagrams and are not based on microscopic investigation but show only field data. The statistical treatment is the same as that used in fabric analysis. Striations, axes, and all linear elements are shown as intercepts of the line with the reference sphere; bedding planes, thrust planes, and all planes in general are represented by their poles. The distribution of points was then counted and contoured. All the orientation diagrams show north at the top and are projections into a horizontal plane (map). A full explanation of the method can be found in Haff (1938) or Ingerson (1938).

Two diagrams represent each locality for which a sufficient number of measurements were obtained, one for planar and another for linear elements. There are no diagrams for locations 11 and 12 since available readings were too meager. Plate 1 is a vertical plane table sheet and shows the southwest wall of the first large highway cut southeast of Marysville. Bedding, thrust planes, stratigraphic thicknesses and displacements were measured and plotted into a plane table sheet in the field.

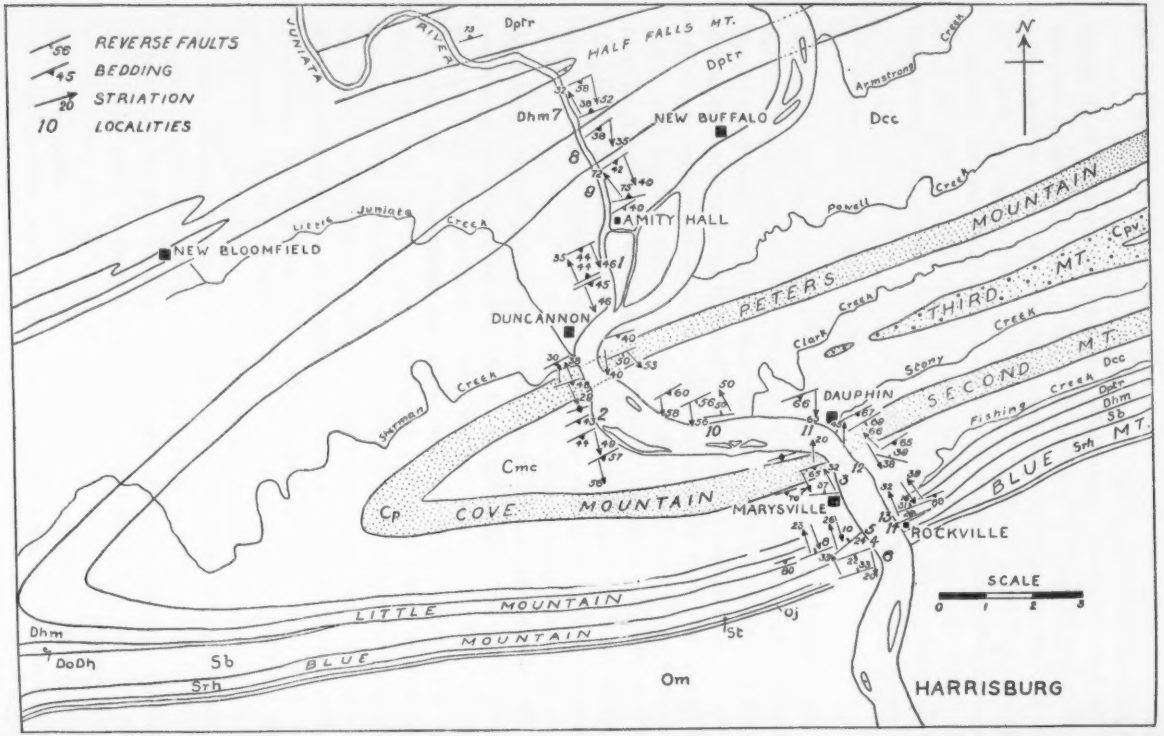

FIGURE 1.—*Geologic map of the area*

TABLE 1.—*Stratigraphic succession in the area*

System	Group	Symbol Fig. 1	Formation or Principal Member	Character and thickness
Pennsylvanian		Cpv	Pottsville conglomerate	Coarse quartz-pebble conglomerate and sandstone
Mississippian		Cmc	Mauch Chunk red beds	Red sandstones and shale, 2000–3000 ft.
		Cp	Pocono formation	Thick- to medium-bedded, resistant sandstone with shale beds, 1600 ft. conglomerate beds
Devonian		Dcc	Catskill red beds including Chemung formation	Red sandstones and shales, 5000 ft.
	Portage	Dptr	Trimmers Rock sandstone, Losh Run, Braillier, Harrell, Burkett and Tully shales	Thin- to medium-bedded sandstone with shale beds, 2160 ft.
	Hamilton	Dhm	Montebello sandstone including Moscow shale and Rockville sandstone	Thin- to medium-bedded sandstone, 800–1000 ft. Shale interbeds
			Marcellus shale and Onondaga limestone	100 ft.
	Oriskany	Do	Oriskany sandstone	Coarse sandstone and chert, 25–70 ft.
	Helderberg	Dh	Helderberg limestone	Shaly limestone with sandstone bed at top, 15 ft.
Silurian		Sb	Bloomsburg red beds	Red sandstones and shales, thin-bedded, 500 ft.
		Srh	Rose Hill formation including Keefer sandstone	Medium-bedded red sandstones, 700–750 ft.
		St	Tuscarora sandstone	Thin- to medium-bedded, resistant sandstone and conglomerate, 275 ft.
Ordovician		Oj	Juniata red beds including Oswego sandstone	Soft red conglomerate, sandstone and shale, 110 ft.
		Om	Martinsburg shale	Shale with sandstone, and limestone beds, 3000 ft. (?)

TERMINOLOGY USED

The term reverse fault is used for those planes along which older rocks were placed above younger ones.

Bedding-plane thrusts are parallel to, or at very low angles to, bedding planes.

Slippage on bedding planes is common, can be normal or reversed, and in many instances direction is hard to determine.

In the analyses of rock fabrics, directions are generally referred to a co-ordinate system: *a* is the direction of transport, flowage, or displacement; *b* is an axis perpendicular to *a* which may be an axis of rotation; and *c* is perpendicular to *a* and *b*, or the *ab*-plane. In this study the fold axes are called *b*, the plane perpendicular to *b* is the *ac*-plane. Inasmuch as the fold axes are predominantly horizontal, the *ac*-plane is mostly vertical. Striations on reverse faults are in the intersection of the *ac*-plane and the fault planes, and since they indicate the direction of transport they represent *a*.

In the diagrams (Figs. 3-14) S is the bedding plane trace and constructed with the average measured direction for bedding as pole; *b* is the horizontal projection or the "strike" of the fold axis; *ac* is the trace of the plane normal to the fold axis *b*.

GENERAL GEOLOGY OF THE AREA

The writers refer to the syncline between Blue Mountain and Half Falls Mountain as the Cove Mountain syncline and the anticline at Half Falls Mountain as the Half Falls Mountain anticline (Fig. 1). The Cove Mountain syncline is a close asymmetrical fold overturned toward the north. This syncline and the adjacent Half Falls Mountain anticline are in a marginal area of close folding within a region of open folding (Willis, 1893, p. 225, Pl. 46). Massive limestones such as those described by Hayes (1891) in the southern Appalachians are almost entirely absent and arenites and argillites predominate.

The assumed large reverse faults parallel the general strike and are considered to have a steep southward dip. Judging from the dip of numerous small reverse faults observed in the northern half of the Cove Mountain syncline, it seems likely that the large thrust faults interpreted along the Half Falls Mountain anticline dip moderately instead of steeply southward. According to Claypole (1885, p. 88) the dip of the Perry County fault is probably less than 45°. The large fault planes probably dip southward at an angle only slightly higher or lower than the south limb of the Half Falls Mountain anticline. This suggestion is based on the fact that minor reverse faults tend to parallel the bedding planes in the northern half of the area.

Willard (1931, p. 703-706) suggests a major strike reverse fault in the valley between Blue Mountain and Little Mountain at Susquehanna Gap which may be referred to as the valley fault. According to him

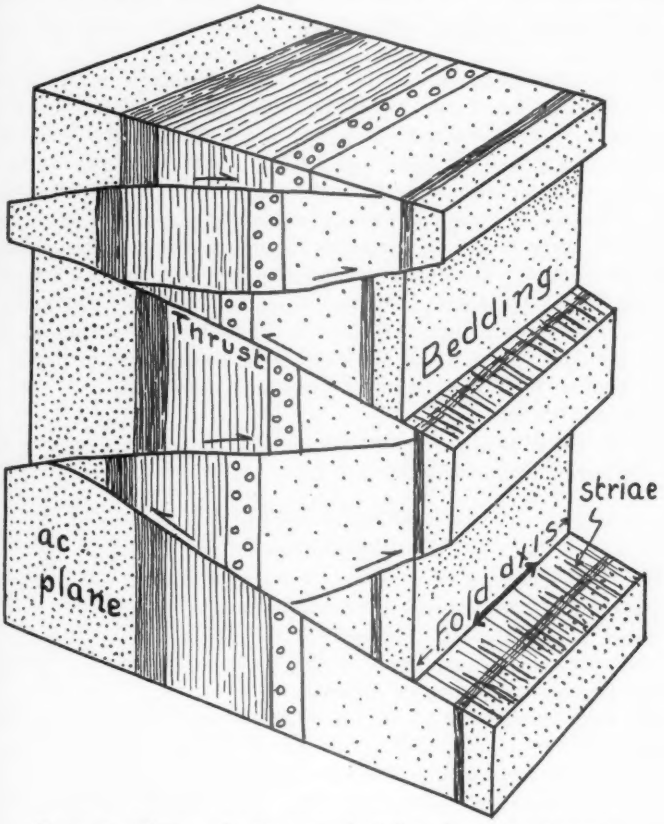

FIGURE 2.—*Diagram showing mutual relation of structure elements*

The inward movement of wedges has heightened the block. If the diagram is turned 90° counter-clockwise the close relationship between thrusts and normal faults in block faulting becomes evident. In "Horst and Graben" regions the angle between faults is larger.

(p. 705) this fault is partly based on the gap in the stratigraphic sequence and partly on the presence of so-called Oriskany on top of Little Mountain at locality 4 (Fig. 1).

To account for the supposed Oriskany, Willard (1931, Fig. 4) postulates a normal fault dipping gently northward along which the Oriskany

has been moved from the valley fault upon the top of Little Mountain. Another gently dipping normal fault is shown by Willard and Cleaves (1938, Pl. 4B) between the Juniata red beds and the Tuscarora sandstone at Rockville. Two intersecting thrust faults have been observed at this location. Billings (1933, p. 153) refers to reverse faults at the same locality.

The present writers, however, believe that the missing sequence between Blue Mountain and Little Mountain is due to lack of deposition and that the supposed Oriskany on top of Little Mountain is Montebello sandstone. Cleaves (Willard and Cleaves, 1931, footnote, p. 1) has thrown considerable doubt on the presence of Oriskany at Susquehanna Gap. The coarse sandstone or conglomerate in the center of the cross section in Plate 1 may be the same horizon as the so-called Oriskany above the section. The divergence in strike mentioned by Willard (1931, p. 703) may be accounted for by the intraformational disconformity shown at the base of this sandstone in Plate 1. The normal fault at Little Mountain suggested by Willard (1931) is considered by the writers as a reverse fault because of direction of movement shown on the slickensided surface.

The thrust plane pictured by Willard (1931) is one of the many small reverse faults described in this paper.

REVERSE FAULTS

DESCRIPTION

The steeply dipping beds within the southern limb of Cove Mountain syncline are transected by innumerable gently dipping reverse faults of small but measurable displacement. On Plate 1, the southwest face of the new road cut southeast of Marysville is shown, and the many gently diping fault planes are striking.

The fault planes may dip in almost any direction. The large surface shown in Figure 1 of Plate 2 dips to the southwest. However, as shown in Plate 1, the average dip is to the southeast and northwest. All fault planes are striated and deeply grooved, indicating the direction of displacement. Without exception the movement was in a reverse sense and perpendicular to the fold axes (in the *ac*-plane). Figure 2 of Plate 2 clearly shows the displacement of a thick sandstone bed and intersection of other gently dipping fault planes. Where two planes intersect both are reverse faults, and there is no definite indication as to relative age. Scaling and chipping of slickensided patches permit determination of relative movements in the absence of offset beds.

In the central and northern portion of Cove Mountain syncline, reverse faults of the same kind are also numerous. Striae show constant

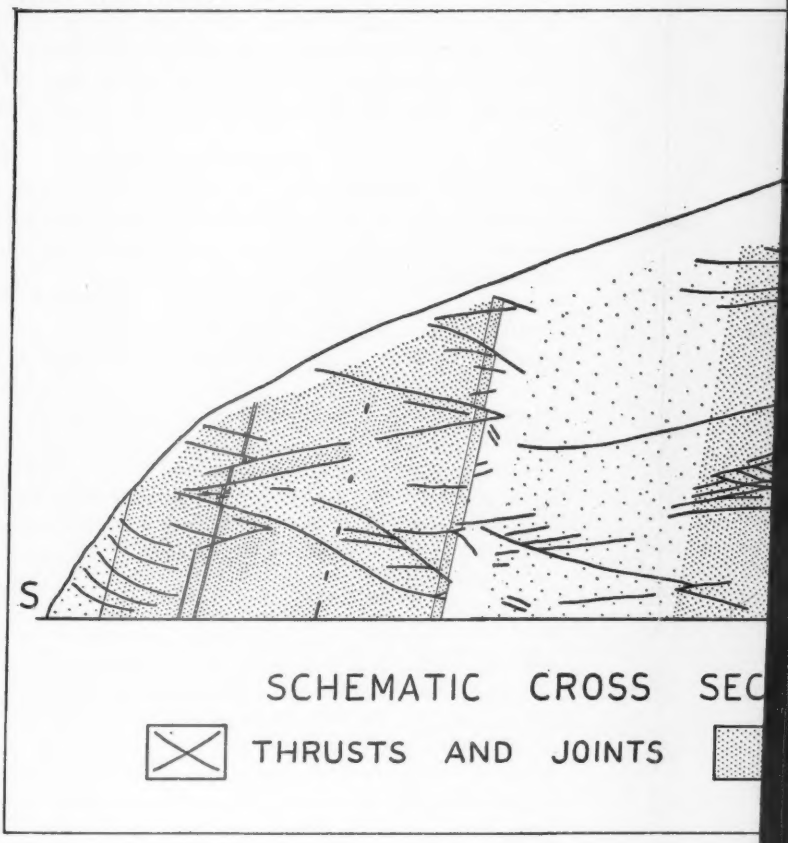
S
SCHEMATIC CROSS SEC
THRUSTS AND JOINTS

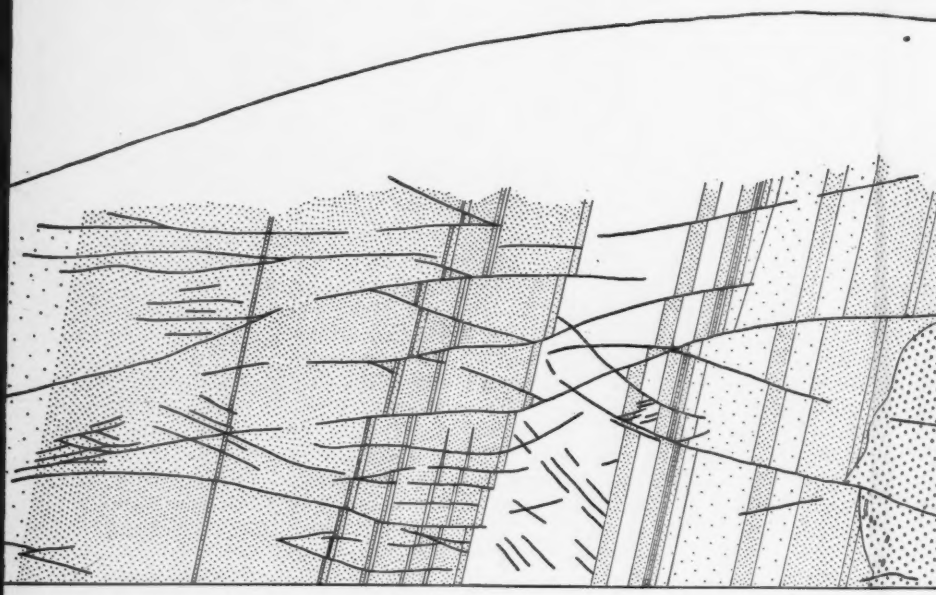

SECTION OF MONTEBELLO SANDSTONE –

SANDSTONE SHALY SANDSTONE

DRAWING OF WEST WALL OF

Shown in Figure 1 of Plate 2.

Measured and dra

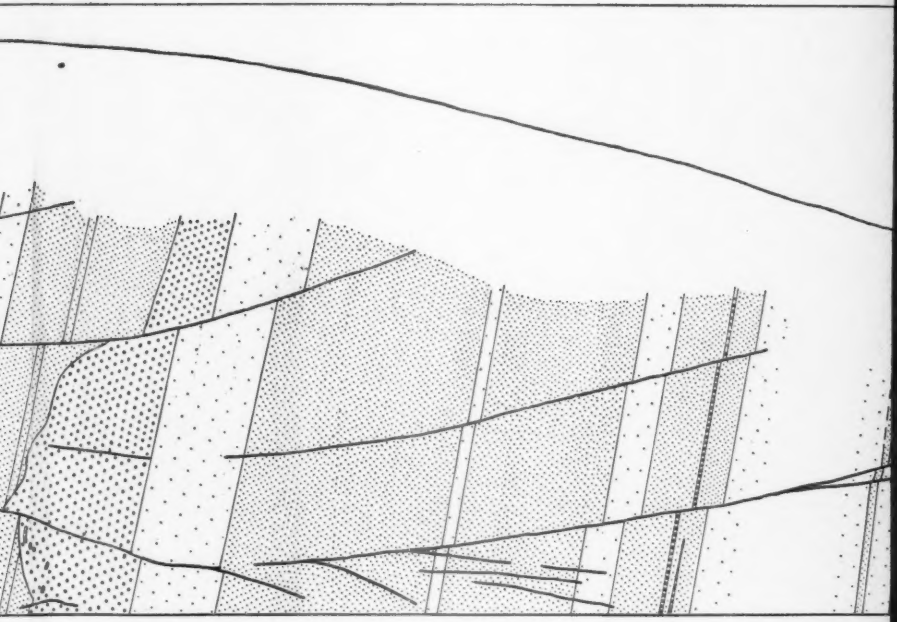

WALL OF ROAD CUT SOUTH OF MARYSVILLE

l of Plate 2. Reverse faults are heavy black lines.
sured and drawn by C. H. Broedel.

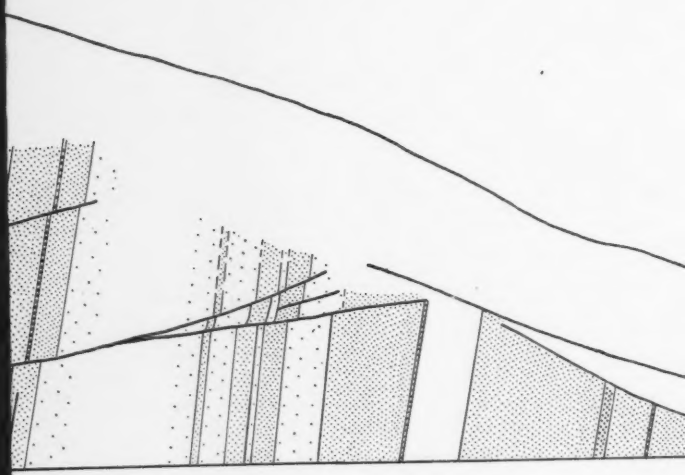

.75 MILE SOUTHEAST OF MA

SCALE

0 10 25 50 FE

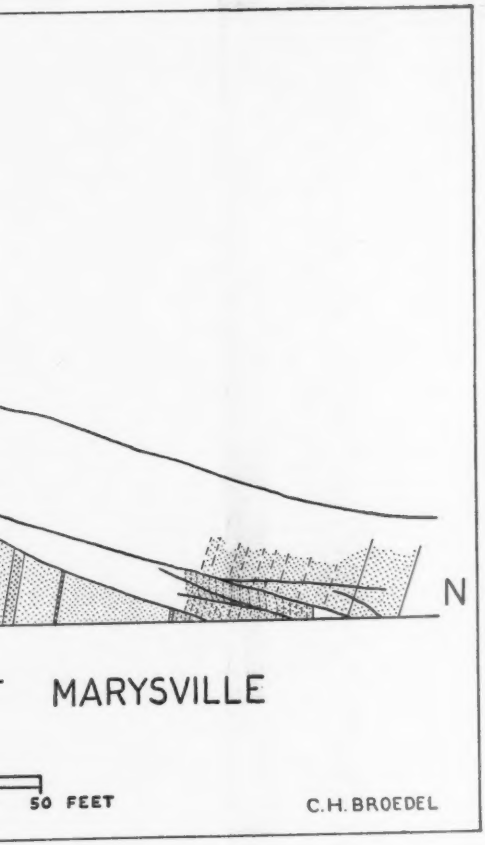
N
MARYSVILLE
50 FEET
C.H. BROEDEL

strike but varying dip. Displacements are also small, but the cumulative effect is considerable. Where bedding is steep the dip of the fault planes is gentle and the angle of intersection large. If bedding planes dip gently and the angle between the fault plane and bedding plane is small, the latter becomes a thrust plane and is covered with grooves and striae. Under such conditions, displacements are difficult to determine. Direction of movement is constant in this area and perpendicular to the direction of the fold axes. The effect of movements along these reverse faults is the same as in the southern area and a general crustal shortening perpendicular to the direction of the fold axes has been accomplished.

STATISTICAL ANALYSIS

The orientation of 843 reverse faults has been measured at 12 localities. The number of observations increases with the size of the exposure, which seems to indicate that there may be more faults at those smaller exposures where the number of observations is rather low, as for instance at localities 2 and 13 (Fig. 1).

The orientation of faults and striation was plotted into equal-area nets and are shown separately in Figures 3 to 14. Locality numbers are indicated in Figure 1.

Figures 6, 7, 8, and 14 show the localities in the southern limb of Cove Mountain syncline. Here the maxima of fault-plane poles are northwest and southeast of the fold axis (*b*) near the center. Each diagram shows a small angle of intersection for the thrusts and a large one for fault and bedding planes. Maxima for fault-plane poles and striation are in the *ac*-plane without much deviation. Figure 7a shows some planes whose strike parallels *ac*—their poles are near the axis, the corresponding striation, however, is perpendicular to *b*, consequently parallels the strike of the plane.

Northward the faults dip more steeply, and their orientations become more scattered. The angle of intersection increases, but at the same time maxima to the northwest of the center of the diagrams show predominantly southeastward dip of fault planes and striation. Near locality 10 (Fig. 12a, b) west of Dauphin, the center of Cove Mountain syncline is reached. Fault planes and striations dip steeply. From here on northward, southeasterly dips predominate as shown in Figures 4a, b; 3a, b; 9, 10, and 11. In this region, bedding dips generally southeastward but is quite variable because of smaller folds in the less competent Mauch Chunk and Catskill red beds.

Figures 10a and b are the most symmetrical diagrams from locality 8 and show orientation in the sandstones and shales. Here the dips of fault planes and bedding are southeast, but the maximum for stria-

tion is not in the trace of the bedding plane (10b) thus indicating an angle of 10° to 20° between bedding and reverse faults. In spite of the suitable dips of bedding, new planes have been formed.

All data were assembled in two generalized diagrams (Figs. 15a, b). The *ac*-plane was used, and the plane of the diagrams is a cross section approximately perpendicular to the average position of the fold axes which emerge in the center. Figure 15a shows the strict orientation of reverse faults in the southern limb of Cove Mountain syncline. The bedding dips steeply southeast and is slightly overturned. Reverse faults are symmetrical with respect to line x which, however, is not horizontal but perpendicular to the bedding. Consequently, southeast-dipping fault planes are gentler than the northwest-dipping ones.

Figure 15b shows two maximum positions for bedding (ruled areas) dipping steeply southeast and northwest. Reverse-fault maxima include an angle of 90° and do not coincide with bedding. The spread of the fault planes as indicated by brackets along the periphery of the circle is four times that in the south limb of Cove Mountain syncline. Some faults parallel bedding, but may be perpendicular to bedding in the other limb. Line x is almost horizontal.

In the northern portion of the region, the orientation of reverse faults is much more scattered and corresponds closely to the many smaller folds in this area, due largely to the incompetency of the formations like the Mauch Chunk and Catskill red beds.

DISPLACEMENTS

Assuming a 1-foot average, the cumulative displacement would be 843 feet. Many faults exceed 2 and 3 feet, and total displacement of over 1000 feet seems conservative. There is no reason to assume that such faults are restricted to the 14 localities examined, but are probably evenly distributed throughout a much larger area. They may also continue at depth and must have existed above the present level of observation before erosion. The accumulated displacement amounts probably to thousands of feet, and in spite of the small individual displacement reverse faulting of this type is an important factor in Appalachian deformation.

Here, the displacement along the fault planes is of less interest than the horizontal and vertical components of this movement and their effect on the deformation of the area. The horizontal component is called h, the vertical component v, and the displacement along the fault plane d. If α is the dip angle then

$$v = d \times \sin \alpha, \quad \text{and} \quad h = d \times \cos \alpha.$$

FIGURE 1. REVERSE FAULT IN FOREGROUND DIPPING SOUTHWEST
New highway cut southeast of Marysville (in background). Locality 5.

FIGURE 2. INTERSECTING REVERSE FAULTS
At first quarry north of Rockville. The heavy sandstone bed has been thrust southward (to the right)
Locality 14.

THRUST PLANES

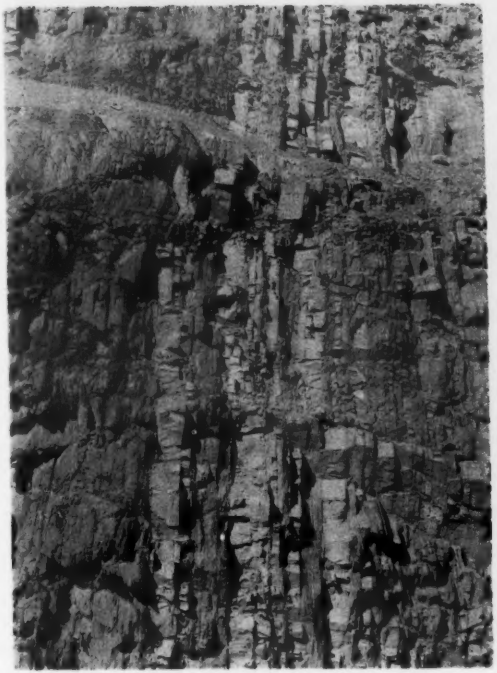

FIGURE 1. CENTRAL PORTION OF ROAD CUT
Shown in Plate 1. Bedding dips steeply south (left). Angle between reverse faults is 35°. Locality 5.

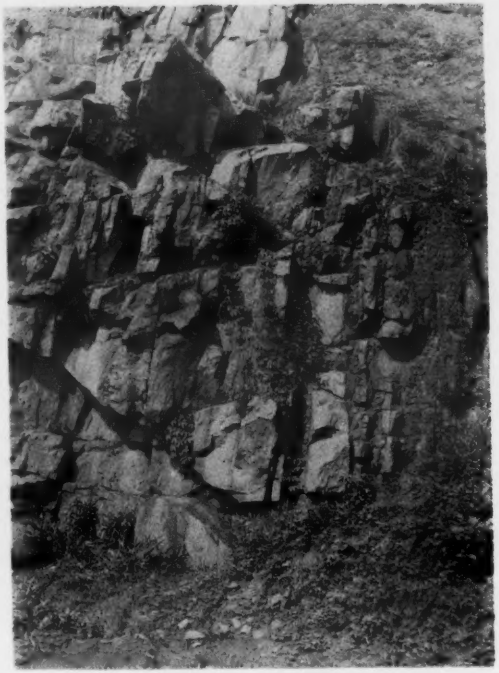

FIGURE 2. WEDGE-SHAPED THRUST BLOCKS
Bedding dips steeply south (left.) Intersection angle is 45° to 50°. Locality 3.

In the southern limb of Cove Mountain syncline, the average dip of the fault planes is 22°, as measured in reference to line x in Figure 15a. Five hundred and twelve faults were measured in that area and if a minimum average displacement of 1 foot is assumed:

$$v = 512 \times 0.374 = 192 \text{ feet and}$$
$$h = 512 \times 0.927 = 475 \text{ feet.}$$

In the central and northern part of the area the average dip of the 331 observed faults is 45°. If 1 foot is the average minimum displacement, then

$$h = v = 331 \times 0.707 = 234 \text{ feet.}$$

These figures show very clearly that the area was shortened laterally and thickened vertically. The above values seem much too small because only very few exposures are available and if one ventures an estimate of 5 per cent exposure versus 95 per cent unexposed terrane the above figures should be multiplied by 20. If a third dimension is added, for instance the thickness of the geologic column above and below, the figures would grow enormously, probably into many thousand feet for each component.

However, this latter conclusion does not consider that the faults die out up and down the dip and are then replaced by roughly parallel ones. In addition, some adjustment may take the form of folding or flowage in less competent beds. In order to arrive at a more reliable figure, one would need vertical exposures of thousands of feet. The west side of the large road cut south of Marysville shows 10 reverse faults per 100 feet vertical elevation—an average displacement of 1 foot per 10 feet vertical exposure. If the height of the south limb of Cove Mountain syncline were 5000 feet there should be 500 feet of accumulated displacement. Using the above formula:

$$v = 187 \text{ feet, and } h = 463 \text{ feet.}$$

In the center of the syncline the displacement is 354 feet.

Possibly such computations, based on many assumptions, are futile. The authors feel, however, that the figures at least show the order of the magnitude of the adjustments.

Furthermore, the steeper average dip of reverse faults in the central portion of the area provides a larger vertical component, possibly due to the crowding of material between the two limbs of the syncline. The more the limbs are pressed together, the smaller the space between them. The material escapes upward as may be seen in crinkling and

minor folding of incompetent beds, flowage and formation of flow cleavage in the axial plane, and in a small way in the reverse faulting.

A gradual increase of the angle between fault-plane maxima is shown in the individual diagrams, Figures 3 to 14. From southeast to northwest the angle increases from 35° to 45° at localities 3, 4, 5, 6, and 14; to 70° at locality 10; and 80° to 90° at locality 2. From here northward, the angle remains large which may be due to the intense minor folding in the incompetent beds of the Juniata River section.

MECHANICAL ANALYSIS

Undoubtedly, the described faults are two intersecting shear planes which dip predominantly southeast and northwest and intersect in the direction of the fold axes. Their attitude is influenced locally by competency of formations, presence or absence of bedding planes which may serve as planes of movement, homogeneity of the faulted complex, presence of small and large folds, and their position within the Cove Mountain syncline.

Attitude of bedding had a strong influence. In the southern limb bedding is almost vertical, and the dips of the faults with reference to the bedding are symmetrical on both sides of line x in Figure 15a but not with reference to the horizontal. Bedding dips 80° SE., and line x dips 10° NW.

The angle between the shear planes is 45° (Fig. 15a) and not 90° as frequently shown experimentally or theoretically.

The orientation of faults in the central and northern portion of Cove Mountain syncline is much more variable because of small-scale folding. Two maxima appear; bedding and shear planes may correspond to either one. Furthermore, the bedding tends to dip gently southeastward, and, where this direction approaches one of the shear planes, movement takes place along the bedding planes. All faults, however, have a uniform direction of slickensides and movement. Seemingly local slips are elevated to regional importance because they all participate in a uniform regional adjustment.

The variation in dip of the fault planes is indicated by brackets along the periphery of the circle in Figure 15. It is less for southeast-dipping faults than for northwest-dipping ones. The difference is 4° in Figure 15a and 23° in Figure 15b. The individual diagrams, for instance Figures 9a, 11b, 12a, and 14b, show the same variation.

All displacements along the reverse faults are "uphill," and thus in defiance of the weight of the overlying rock column. Where the dip angle of the fault surface is small, the vertical component or "lift" is also small but increases with increasing dip. The overlying forma-

tions within the south limb of Cove Mountain syncline must have included the Devonian and Carboniferous; at the center, the Carboniferous was above the faults, and in the northern limb large portions of Devonian and the Carboniferous were above it.

Assuming a density of 2.5 a 15,000-foot column of rock would exert a pressure of 17,000 pounds per square inch on a horizontal plane. This pressure is reduced with increasing dip of the fault planes and changes with the cosine of the dip angle.

The force necessary to move a mass up an incline depends on the coefficient of friction (f), the weight of the body (W), and the degree of incline (α). The force necessary to move the body is:

$$P = W \times \sin \alpha + F,$$
$$F = f \times N \quad \text{and} \quad N = W \times \cos \alpha,$$
$$\text{thus} \quad P = W \times \sin \alpha + f \times (W \times \cos \alpha).$$

N is the component normal to the fault plane, and $W \times \sin \alpha$ the component parallel to and down the incline. The least known factor is the coefficient of friction f. If f is assumed to be 0.5 (wood on wood) and the column to be considered as 17,000 pounds, the force necessary to overcome friction on a plane dipping 30° would be:

$$P = 17{,}000 \times \sin 30 + 0.5 \times 17{,}000 \times \cos 30 = 15{,}861 \text{ pounds}$$

for every column. With a dip of 60°, P equals 18,972 pounds. Due to friction, P exceeds the weight of that column.

Despite uncertainties in such calculations, two facts are clear: (1) The pressure available is ample to produce the most elaborate striation, brecciation, and grooving even if movements do not exceed 1 millimeter. Thus intensity of striation and grooving on a fault plane is no indication for the amount of displacement. (2) The steeper northwest-dipping planes in the south limb of the syncline require a greater force than do the gentler southeast-dipping ones. The work done along the steeper planes is also considerably greater.

This conclusion seems absurd for it can hardly be assumed that greater forces operated from the northwest than in the opposite direction. All evidence points to movements from the southeast which must mean that these forces overcame the resisting and opposing ones.

Figure 15b shows that line x is horizontal in respect to the average dip of the fault planes. If the above deduction is applied for this area, the work done in both directions is equal. In the south limb, line x is inclined northward. This inclination seems to point toward a rotation of this limb into a slightly overturned position after formation of the fault planes.

CONCLUSIONS

Appalachian folding is the reduction of a broad belt of sediments into a narrower space, with simultaneous thickening of the affected sequence. The senior author has previously tried to evaluate the shortening factor (E. Cloos, 1940). Inasmuch as there is little evidence of intervening strong erosion, the sequence must have thickened as it was folded. If the lateral shortening is 50 per cent, the complex has been thickened by 50 per cent of its original thickness. This factor may be reduced by 10 per cent due to elongation parallel to the fold axes due to arcuation. Shortening and thickening can be accomplished by folding, flowage, and reverse faulting. The authors believe that all three were effective. Folding produced large and small folds, flowage resulted in a flow cleavage and may have been as effective as folding. In the authors' opinion, flowage has received much too little attention. (*See* E. Cloos, 1942.) Folding and flowage grade into each other imperceptibly. Reverse faulting is probably the third process and is most likely a manifestation of the end phase of the total deformation. It tends also to reduce the horizontal distance, h (shortening), in favor of the vertical, v (thickening). Reverse faults are numerous in the Devonian and Carboniferous of the area and probably occur everywhere. Uniform orientation of slickensides shows that the faults are not local but are a part of the large process of Appalachian folding; the authors believe that they were formed when folding and flowage were no longer major factors and the mass began to rupture.

Careful and systematic observation elsewhere may well establish this type of deformation as widespread and as the typical reaction of folded areas to continuing stress.

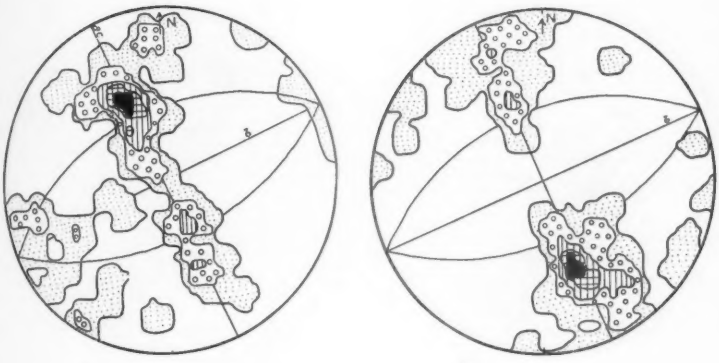

a b

FIGURE 3.—*Statistical orientation diagrams*

Locality 1 (Fig. 1) Railroad section 1½ to 2½ miles NE. of Duncannon.

(a) 94 thrust plane poles, contours 1-3-6-9-12 per cent.

(b) 90 striation measurements, contours 1-3-6-9-12 per cent. Reverse faults dip mostly southeast.

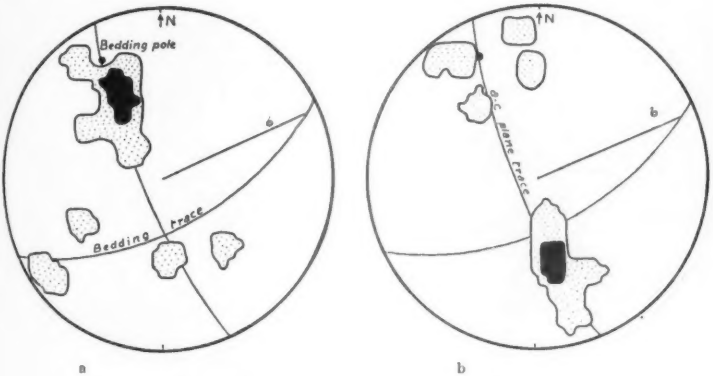

a b

FIGURE 4.—*Statistical orientation diagrams*

Locality 2 (Fig. 1) Highway section 1¼ to 2 miles S. of Duncannon.

(a) 17 thrust plane poles, contours (7-20)-(20-35) per cent.

(b) 15 striation measurements, contours (7-20)-(20-33) per cent. The few measurements show the predominant southern dip of the fault planes.

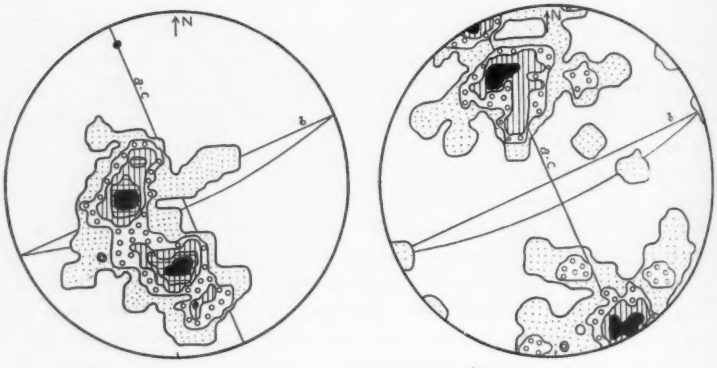

a b

FIGURE 5.—*Statistical orientation diagrams*

Locality 3 (Fig. 1) Railroad section at Marysville along new highway.

(a) 96 thrust plane poles, contours 1-3-6-9-(12-17) per cent.

(b) 105 striation measurements, contours 1-3-6-9-(12-14) per cent.

Note: The gradual decrease in dip from north to south. The angle of intersection decreases correspondingly.

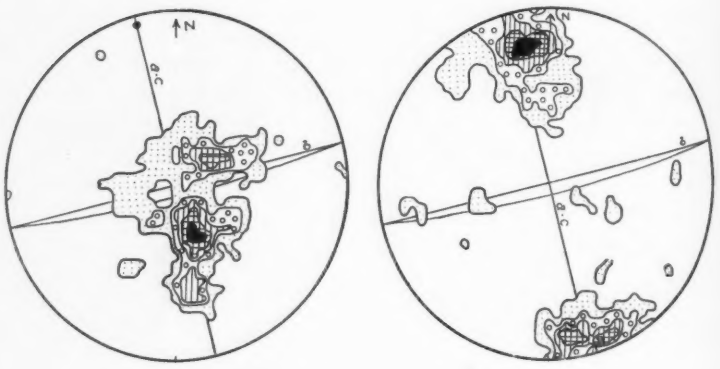

a b

FIGURE 6.—*Statistical orientation diagrams*

Locality 4 (Fig. 1) Quarry 1 mile SE. of Marysville.

(a) 197 thrust plane poles, contours 2-3-5-6-(8-10) per cent.

(b) 205 striation measurements, contours 2-3-5-6-(8-10) per cent.

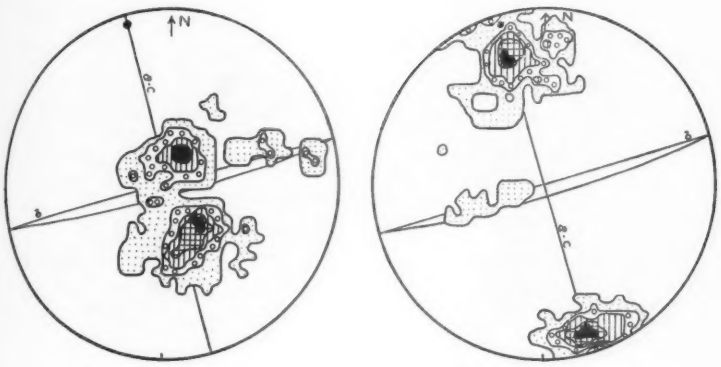

FIGURE 7.—*Statistical orientation diagrams*

Locality 5 (Fig. 1) New highway cut ¾ to 1 mile SE. Marysville.

(a) 174 thrust plane poles contours 2-4-6-7-(9-10) per cent.

(b) 184 striation measurements, contours 2-4-6-7-(9-10) per cent.

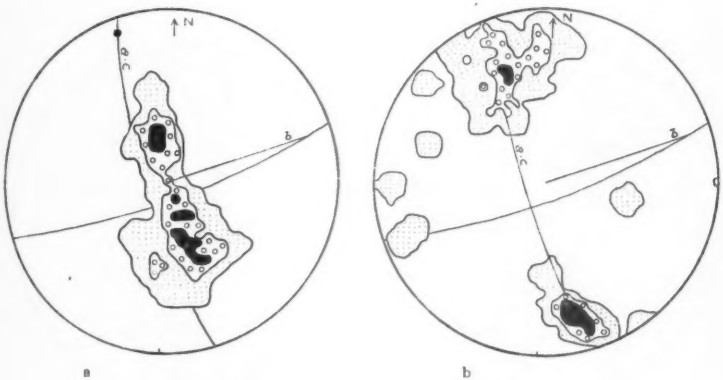

FIGURE 8.—*Statistical orientation diagrams*

Locality 6 (Fig. 1) New highway cut 1¾ miles SE. of Marysville.

(a) 45 thrust plane poles, contours 2-7-(13-20) per cent.

(b) 47 striation measurements, contours 2-7-(13-20) per cent.

Note: Figures 6, 7 and 8 show three localities in the southern limb of Cove Mountain syncline. Reverse faults dip gently and the intersection angle is small.

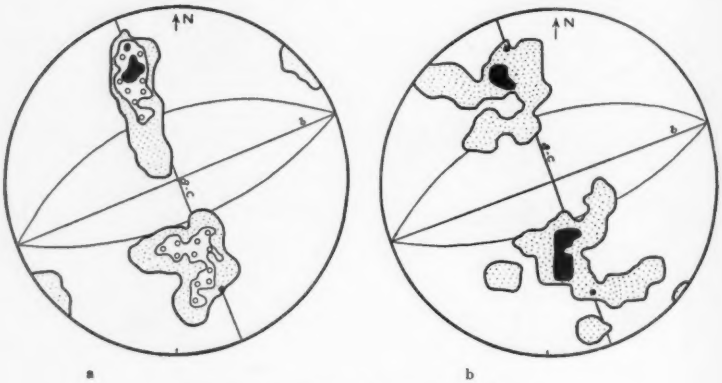

a b

FIGURE 9.—*Statistical orientation diagrams*

Locality 7 (Pl. 1) Highway section 2½ miles NW. of Amity Hall on Juniata River.

(a) 29 thrust plane poles, contours 4-11-(21-24) per cent.

(b) 28 striation measurements, contours 4-(11-18) per cent.

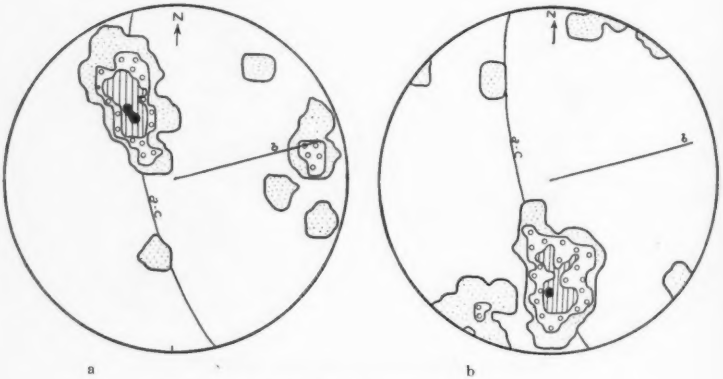

a b

FIGURE 10.—*Statistical orientation diagrams*

Locality 8 (Fig. 1) Highway section 1½ miles NW. of Amity Hall on Juniata River.

(a) 42 thrust plane poles, contours 2-7-14-(21-26) per cent.

(b) 42 striation measurements, contours 2-7-14-(21-26 per cent.

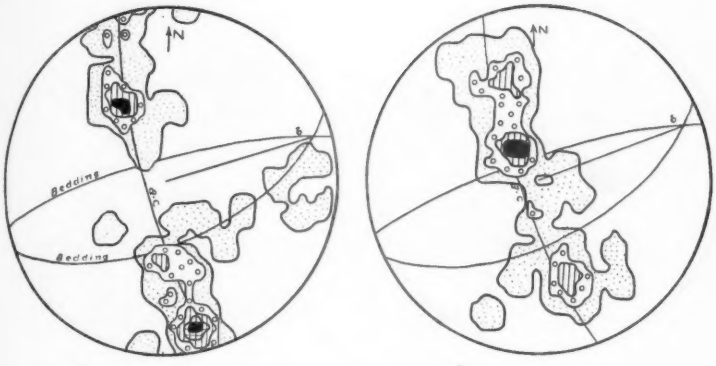

a b

FIGURE 11.—*Statistical orientation diagrams*

Locality 9 (Pl. 1) Highway section ½ mile N. of Amity Hall.

(a) 62 thrust plane poles, contours 2-5-10-15-20 per cent.

(b) 63 striation measurements, contours 2-5-10-15-20 per cent.

Note: Localities shown in Figures 9, 10, and 11 are north of the center of Cove Mountain syncline. The intersecting angle is large but south dip, roughly parallel to the north limb of of the syncline is prevalent.

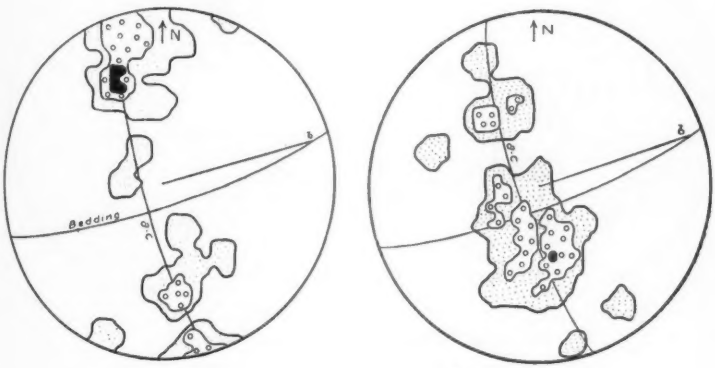

a b

FIGURE 12.—*Statistical orientation diagrams*

Locality 10 (Fig. 1) Railroad section along Susquehanna River west of Clark Creek and Dauphin.

(a) 37 thrust plane poles, contours 3-8-(16-22) per cent.

(b) 35 striation measurements, contours 3-8-(17-20) per cent.

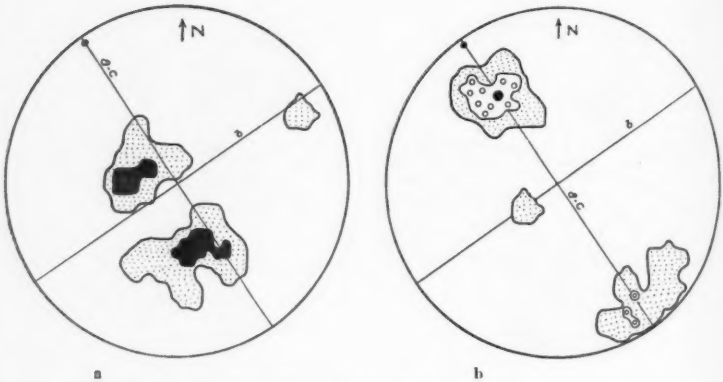

FIGURE 13.—*Statistical orientation diagrams*

Locality 13 Third quarry north of Rockville at Little Mountain.

(a) 24 thrust plane poles, contours 4-(12-25) per cent.

(b) 24 striation measurements, contours 4-12-25 per cent.

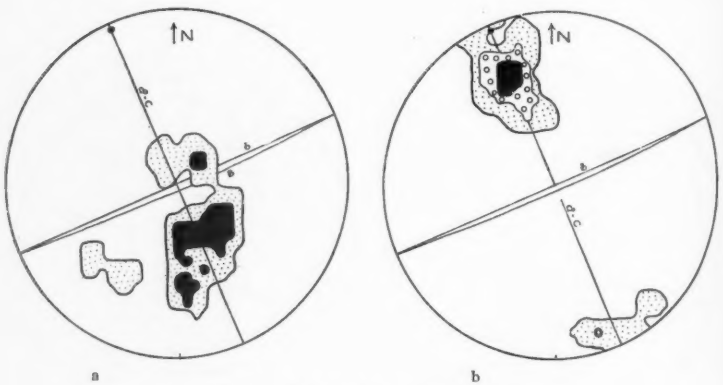

FIGURE 14.—*Statistical orientation diagrams*

Locality 14 Second quarry north of Rockville at Little Mountain.

(a) 26 thrust plane poles, contours 4-(12-23) per cent.

(b) 26 slickenside measurements, contours 4-12-23 per cent.

Note: Locality 10 is almost in the center of Cove Mountain syncline and shows a large angle between thrust planes; localities 13 and 14 are in south limb of Cove Mountain syncline. There are no diagrams for localities 11 and 12.

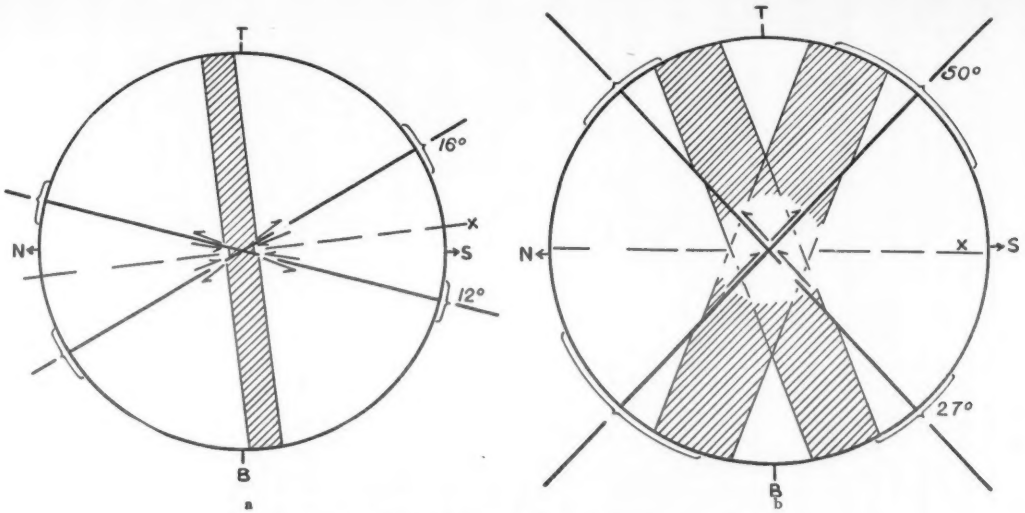

FIGURE 15.—*Schematic diagrams showing reverse fault positions*

(a) in south limb of Cove Mountain syncline.
(b) in central and northern portion of section.
Ruled area average position of bedding. Fold axes emerge in center of diagram. Brackets along periphery indicate spread of measurements. N: north, S: south, T: top, B: bottom, x: line bisecting angle of intersection of fault planes. Arrows indicate relative displacement.

REFERENCES CITED

Ambrose, J. W. (1933) *A discussion of the movement of fault blocks,* Am. Jour. Sci., 5th ser., vol. 26, p. 552-563.

Becker, G. F. (1893) *Finite homogeneous strain, flow and rupture of rocks,* Geol. Soc. Am., Bull., vol. 4, p. 13-90.

Billings, M. P. (1933) *Thrusting younger rocks over older,* Am. Jour. Sci., 5th ser., vol. 25, p. 140-165.

Cadell, H. M. (1888) *Experimental researches in mountain building,* Royal Soc. Edinburgh, Tr., vol. 35, pt. 7, p. 337-357.

Chamberlin, R. T. (1910) *The Appalachian folds of central Pennsylvania,* Jour. Geol., vol. 18, p. 228-251.

——— (1928) *The strain ellipsoid and Appalachian structures,* Jour. Geol., vol. 36, p. 85-90.

———, and Miller. W. T. (1918) *Low angle faulting,* Jour. Geol., vol. 26, p. 1-44.

Claypole, E. W. (1885) *A preliminary report on the paleontology of Perry County, Pennsylvania,* Pa. 2d Geol. Survey, vol. F2, p. 1-437.

Cleaves, A. B. (1935) *Structural geology of the New Bloomfield quadrangle, Pennsylvania,* Pa. Acad. Sci., Pr., vol. 9, p. 141-146.

Cloos, Ernst (1940) *Crustal shortening and axial divergence in the Appalachians of southeastern Pennsylvania and Maryland,* Geol. Soc. Am., Bull., vol. 51, p. 845-872.

——— (1942) *Distortion of stratigraphic thickness due to folding,* Nat. Acad. Sci., vol. 28, no. 10, p. 401-407.

Gill, J. E. (1935) *Normal and reverse faults,* Jour. Geol., vol. 43, p. 1071-1079.

Griggs, D. T. (1936) *Deformation of rocks under high confining pressures,* Jour. Geol., vol. 44, p. 541-577.

Haff, J. C. (1938) *Preparation of petrofabric diagrams,* Am. Mineral., vol. 23, p. 543-574.

Haskell, N. A. (1938) *On shallow-seated folding in massive rocks,* Jour. Geol., vol. 46, p. 166-176.

Hayes, C. W. (1891) *The overthrust faults of the southern Appalachians,* Geol. Soc. Am., Bull., vol. 2, p. 141-154.

Ingerson, Earl (1938) *Laboratory technique of petrofabric analysis,* Geol. Soc. Am., Mem. 6, p. 211-263.

Keith, Arthur (1923) *Outlines of Appalachian structure,* Geol. Soc. Am., Bull., vol. 34, p. 309-380.

Leith, Andrew (1937) *The strain ellipsoid,* Am. Jour. Sci., 5th ser., vol. 33, p. 360-368.

Price, P. H. (1931) *The Appalachian structural front,* Jour. Geol., vol. 39, p. 24-44.

Sander, Bruno (1930) *Gefügekunde der Gesteine,* Gebr. Borntträger, Berlin.

Stark, J. T. (1934) *Reverse faulting in the Sawatch,* Geol. Soc. Am., Bull., vol. 45, p. 1001-1016.

Stose, G. W. (1930) *Unconformity at the base of the Silurian in southeastern Pennsylvania,* Geol. Soc. Am., Bull., vol. 41, p. 629-658.

Willard, Bradford (1931) *Oriskany at Susquehanna Gap, Pennsylvania,* Geol. Soc. Am., Bull., vol. 42, p. 697-706.

———, and Cleaves, A. B. (1938) *A Paleozoic section in south-central Pennsylvania,* Pa. Geol. Survey, Bull. G8, 4th ser., p. 1-28.

Willis, Bailey (1893) *Mechanics of Appalachian structure,* U. S. Geol. Survey, 13th Ann. Rept., pt. 2, p. 217-281.

Willis, Robin (1935) *Development of thrust faults*, Geol. Soc. Am., Bull., vol. 46, p. 409-424.

MAPS

Revision of the geological map of Perry County, Pennsylvania (1885), Pa. 2d Geol. Survey, vol. F2.

Geologic map of Pennsylvania (1931), Pa. Topog. Geol. Survey.

THE JOHNS HOPKINS UNIVERSITY, BALTIMORE, MARYLAND.
MOUAT MINE, NYE, MONTANA.
MANUSCRIPT RECEIVED BY THE SECRETARY OF THE SOCIETY, AUGUST 20, 1942.

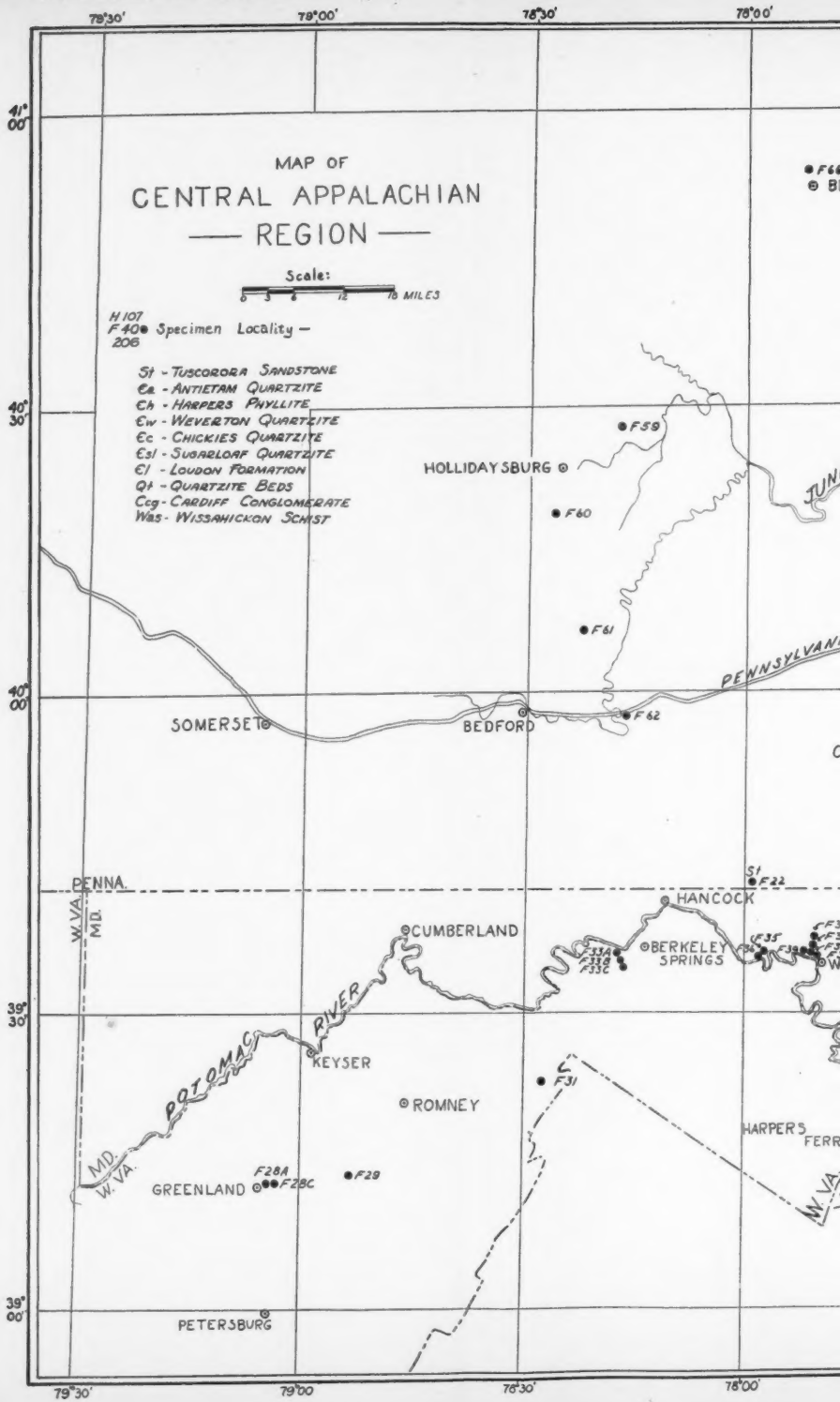
78°30'
79°00'
78°30'
78°00'
41° 00'
40° 30'
40° 00'
39° 30'
39° 00'
MAP OF
CENTRAL APPALACHIAN
— REGION —
Scale:
0 3 6 12 18 MILES
H 107
F 40 Specimen Locality —
206
St - Tuscorora Sandstone
Ca - Antietam Quartzite
Ch - Harpers Phyllite
Cw - Weverton Quartzite
Cc - Chickies Quartzite
Csl - Sugarloaf Quartzite
Cl - Loudon Formation
Qt - Quartzite Beds
Ccg - Cardiff Conglomerate
Was - Wissahickon Schist
F59
HOLLIDAYSBURG
F60
F61
PENNSYLVAN
SOMERSET
BEDFORD
F62
PENNA.
W.VA.
MD.
S1
F22
HANCOCK
CUMBERLAND
F35
BERKELEY SPRINGS
F33A
F33B
F33C
POTOMAC RIVER
KEYSER
F31
ROMNEY
HARPERS FERR
MD.
W.VA.
F28A
F28C
F29
GREENLAND
PETERSBURG
W.VA.

MAP OF SPECIMEN LOCALITIES

76°30'
F53
F54
F51A
F51B
LEBANON
HARRISBURG
Cc
F50A
F50B
Cc
Creek
LANCASTER
Conestoga
YORK
SUSQUEHANNA RIVER
Ccp
H 107
BALTIMORE
CHESAPEAKE BAY
76°30'

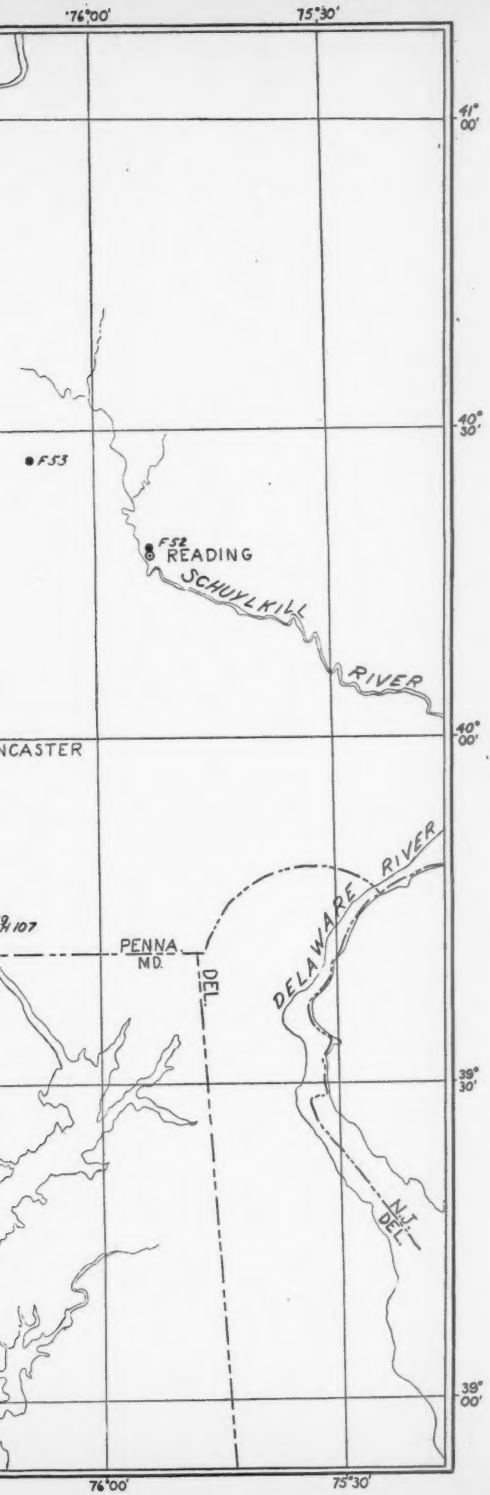
76°00'
75°30'
41° 00'
40° 30'
40° 00'
39° 30'
39° 00'
FS3
FS2
READING
SCHUYLKILL
RIVER
NCASTER
PENNA
MD.
DEL.
DELAWARE
RIVER
N.J.
DEL.

RE

Abstr
Introd
Locali
Ackno
Struct
Petrof
M

Termi
Regio
Local
Nonte
Tecto
M
M
T

F

Deform
E
D
N
L
F
A
Petrof
D
F
I
E
D
D
I

BULLETIN OF THE GEOLOGICAL SOCIETY OF AMERICA
VOL. 54, PP. 1399-1432, 12 PLS., 5 FIGS. SEPTEMBER 1, 1943

RECRYSTALLIZATION AND FLOWAGE IN APPALACHIAN QUARTZITE

BY ROBERT E. FELLOWS

CONTENTS

	Page
Abstract	1400
Introduction and scope	1401
Localities and specimens	1401
Acknowledgments	1403
Structures and field methods	1403
Petrofabric analysis	1404
Method and technique	1404
General considerations	1404
Counting and contouring diagrams	1405
Planimeter measurements	1405
Preparation of cumulative diagrams	1406
Terminology	1406
Regional structure	1409
Local environments	1409
Nontectonites	1409
Tectonites	1411
Megascopic identification	1411
Microscopic identification	1412
Textural features	1412
Microscopic characteristics	1412
Fabric diagrams	1414
Quartz diagrams	1414
Mica diagrams	1415
Cumulative diagrams	1415
Deformation and recrystallization	1415
Early evidence of deformation	1415
Development of crush quartz	1416
Neocrystallization	1417
Linear stretching	1418
Fracturing	1418
Annealing recrystallization	1419
Petrofabrics	1420
Development of maxima during deformation	1420
Fracturing versus granulation	1421
Importance of selective measurements	1422
Effect of rock composition on fabric patterns	1422
Development of a preferred orientation	1423
Dimensional and lattice-controlled fabrics	1424
Interpretation of diagrams	1425

Page

Discussion of special features 1425
Cumulative diagrams 1427
Nontectonite diagrams 1428
Distribution of tectonites 1429
Transition zone 1429
Distance from source of pressure 1429
Age of tectonite horizons 1429
Summary and conclusions 1430
Complicating factors which influence the value of petrofabric analyses of quartzites 1430
References cited 1431

ILLUSTRATIONS

Figure Page

1. Index map 1402
2. Diagram showing bedding, cleavage, and lineation in relation to reference axes *a*, *b*, and *c* 1406
3. Stages in development of recrystallized fabric 1413
4. Frequency-distribution histogram showing relative importance of standard maxima positions 1420
5. Relation between percentage of recrystallizing quartz and ratios of elongation. 1423

Plate Facing page

1. Map of specimen localities 1399
2. Structure and fabric at specimen localities 1408
3. Small flexure folds in nontectonite area 1412
4. Chickies Rock, Pennsylvania 1413
5. Textures of nontectonites 1414
6. Textures of growth quartz and crushed quartz 1415
7. "Tailing" and stretching in tectonites 1418
8. Fracturing in tectonite fabrics 1419
9. Fracturing, straining, and recrystallization of quartz grains 1422
10. Fabric diagrams of nontectonites 1428
11. Fabric diagrams of tectonites 1430
12. Fabric diagrams of tectonites 1432

ABSTRACT

The lower limit of visible traces of penetrative movement in quartz-rich rocks can be defined by studies of orientations and mutual relations of grains. Intensity of deformation in the central Appalachians decreases gradually from the crystalline Piedmont toward the north, northwest, and west perpendicular to the regional trend. The author has attempted to determine the limits of visible deformation geographically and stratigraphically.

Five types of quartz have been distinguished on the basis of texture: original grains, peripheral growth quartz, crush quartz, needle quartz, and recrystallized quartz. Each type indicates a particular degree of deformation grading from original grains showing little or no deformation to completely reoriented and recrystallized SiO_2.

If granulation affects 22 per cent of the quartz present a lineation may become visible megascopically. It is then perpendicular to the fold axis *b*, contained within the flow cleavage plane, and parallel to *a*. Arrangement of grains into physical parallelism precedes the development of preferred optical orientations. Lattice

parallelism develops either through fracturing or through coalescence of reorganized crushed quartz particles.

A study of the regional distribution of recrystallization and flowage on a quantitative basis permits the definition of a transitional zone in which the nontectonites on the northwest merge with the tectonites on the southeast. Fabrics of rocks in the tectonite area are readily deciphered, while those northwest of the demarcation belt are increasingly indistinct.

INTRODUCTION AND SCOPE

The present investigation has a dual purpose: (1) To trace the development of recrystallization and flowage in deformed arenaceous rocks of the central Appalachians; (2) to evaluate preferred orientations developed through such processes. The problem resolves itself into an attempt to discriminate that zone within a folded parametamorphic series in which quartz-rich rocks become tectonites.

The major thesis is the recognized need for a quantitative measure of rock deformation.

> "The pressure-temperature-time factors under which quartz can be deformed with or without losing space-continuity, would help one to understand the metamorphic history of a given quartzite or quartz schist." (Knopf and Ingerson, 1938, p. 33.)

An attempt is made to trace the development of deformation from the earliest indications of stress-induced activity to the extremely deformed quartz schists.

LOCALITIES AND SPECIMENS

The central Appalachian area offers excellent material for such a study. On Figure 1 are plotted the specimen localities. It is believed that the localities are sufficiently widespread to be representative.

Locality or specimen numbers are plotted on Plate 1 along with formation names for tectonite horizons. Localities were chosen with extreme care in an attempt to collect rocks which would show a maximum vertical and horizontal distribution, a variation in composition and texture, and as many structural features as possible.

A formation chart (Table 1) permits a correlation of specimen horizons. Five specimens were collected from the pre-Cambrian (?), 19 from the Cambrian, 5 from the Ordovician, 7 from the Silurian, 5 from the Devonian, and 1 from the Mississippian. The Silurian yielded one tectonite specimen; all others are restricted to pre-Cambrian (?) or lower Cambrian horizons. Localities are spread over approximately 300 square miles across the folded portion of the central Appalachians. The area extends from the little-disturbed Appalachian Plateau region in West Virginia and Pennsylvania to the intensely deformed eastern Piedmont of Maryland and Pennsylvania.

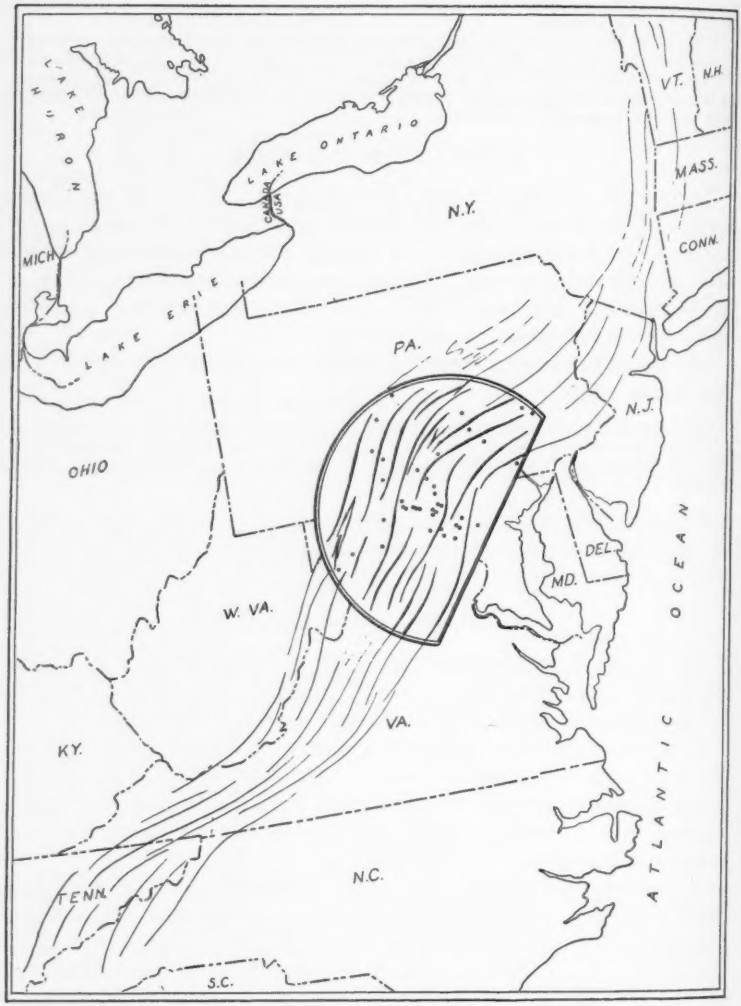

Index Map Showing: area studied ○ specimen localities ⋱ generalized trend of Appalachian Mountains

FIGURE 1.—*Index map*

Rock types include "pure" quartz sandstones, a transitional series of argillaceous sandstones which grade into sandy shales, ferruginous sandstones, and calcareous sandstones which are transitional into arenaceous limestones. These rocks also grade into their metamorphosed equivalents.

Seventy-four oriented specimens were collected during the summer of 1942. Seventy-six quartz and 16 mica diagrams were prepared from 54 oriented thin sections. Four of the rock specimens with oriented sections were contributed for the study by Ernst Cloos. Observation and measurement of 25,000 quartz grains has provided the basis for a somewhat different concept of recrystallization and flowage from that currently held.

ACKNOWLEDGMENTS

It was through the suggestion of Ernst Cloos that this problem was first recognized and undertaken. He contributed especially valuable suggestions and advice through the progress of the work. The author is also indebted to him for editorial comments and advice in preparation of the manuscript. J. L. Anderson offered pertinent suggestions regarding petrographic descriptions and photographic technique which are gratefully acknowledged. The companionship and competent assistance of Glenn Fellows during the field work were distinct contributions as was his diligence during part of the statistical laboratory analyses. Walter C. Boyer and W. Worthington Ewell kindly drafted some of the illustrations. The Pennsylvania Geological Survey granted permission to reproduce two photographs of Chickies Rock.

STRUCTURES AND FIELD METHODS

Attitudes of bedding, flow cleavage, lineation, and fold axes are plotted in the structure map (Pl. 2). Quartz axes concentrations are shown in miniature fabric diagrams at those tectonite localities where maxima exceed 3 per cent.

Bedding and flow cleavage were measured in the field except for a few microscopic determinations (F 31, F 64, F 65, F 77, F 78). The majority of lineations shown on the structure map were determined or verified microscopically. Fold axes were measured in the field only where intersections of cleavage and bedding or dependable *ac* joint faces were available. Few outcrops provide dependable readings, and determination of *b* (fold axis) was usually possible only by plotting microscopic data into an equal-area net.

An arcuate belt indicates the zone where subtectonites grade into tectonites.

Small folds were special objects of search since it was suspected that deformation by solid flow in such environments would reveal an interpretable series of fabric diagrams. Plate 3 shows four folds of the type studied. All folds similar to those shown in the field photographs proved to be simply flexures and not tectonitic.

Results here presented are not intended to apply to all quartz tectonites. They may, however, be considered applicable to any arenaceous series whose structural character closely parallels that of the central portion of the folded Appalachians.

PETROFABRIC ANALYSIS

METHOD AND TECHNIQUE

General considerations.—In conformity with standard practice the author has used the lower half of the equal-area net into which quartz axes and mica cleavage poles have been plotted. Quartz grains measured averaged 330 per slide with a minimum of 100 and a maximum of 500. One hundred mica cleavage poles were sufficient in most instances, although 200 measurements were made for those with less obvious orientations.

The arrow and bar at the center of each diagram represent the strike and dip of the oriented section from which the diagram was prepared. Interpretation of strike and dip values is given on diagram F 98 (Pl. 11).

Each diagram represents approximate *ac* plane projections whereby the fold axis *b* appears at or near the center. This holds except for those specimens for which two or more analyses have been made from mutually perpendicular cuts.

The fabric co-ordinates *a*, *b*, and *c* appear on the diagrams where the information was available; *a* could not be determined in nontectonite specimens since a direction of movement was not apparent. The nontectonite fold axes are determined from field measurements which in a few cases are necessarily inferential.

S-planes are labeled according to custom in order of their origin: S_1 refers to bedding, S_2 to flow cleavage, and S_3 to fracture cleavage.

Diagrams are segregated for ease of comparison into two groups. Plate 10 includes 31 nontectonite diagrams; Plates 11 and 12 include 61 tectonite diagrams and 5 cumulative or interpretative analyses. Legends accompany both sets. A summary of general fabric data appears on Tables 8 and 9. The information includes specimen numbers, orientations of cuts, number and types of grains measured, planimeter measurements of areas covered by 4, 5, and 6 per cent axes concentrations, plotted maxima in relation to known maxima, and general remarks.

Counting and contouring diagrams.—The technique involved in counting and contouring is a variation from the standard practice outlined by Knopf and Ingerson (1939, Pt. 2). The method used obviates the need of a grid for guiding and permits the count to be placed directly on the point sheet rather than through a tracing. Equipment includes a T-square calibrated to half a centimeter divisions, a stationary vertical guide inked onto the base sheet with the same intervals, carbon paper, and a composite circle counter which allows both peripheral and center counting and is easily fashioned from a celluloid triangle.

Counts are made in the usual fashion except that half-centimeter intervals are used for greater accuracy. As the circle strip slides along the graduated T-square numbers are placed at the center of the window according to the number of points appearing at each interval. When a traverse is completed the T-square and counter are moved half a centimeter to a new position controlled by the vertical scale, and a new traverse is begun. In order that the original point sheet may be kept for reference a hard pencil or stylus is used which not only produces a sharp and easily legible carbon but also allows the original point diagram to remain unobscured by figures. The contouring can then be made on the carbon reproduction, and the completed diagram transferred to a final tracing.

The chief advantages are: (1) It alleviates eyestrain developed by counting through a tracing sheet; (2) it requires fewer pieces of equipment; (3) it allows more freedom in the measurement of interspace maxima since the rigid grid is not used to control the location of the counts.

Planimeter measurements.—Fairbairn (1942, p. 129) describes great accuracy in contouring as "time . . . largely wasted." He lists reasons for avoiding detail based on "the origin of data . . . and the method of projection." His point is well taken for diagrams where obvious symmetries or well-defined maxima are developed. Such is not the case in the present investigation. A study of the transition from undeformed rocks into tectonites requires more rather than less detail.

The author has been able to differentiate random from significant maxima by measuring the percentage of area included within any given contour. A planimeter is well adapted to this purpose since the contouring is controlled by points plotted into an equal-area net. Thus the planimeter figures can be converted easily into true percentages of the surface area of the sphere covered by a particular maximum.

The significance of this technique becomes apparent where evaluation of concentrations is concerned. It is a method by which concentrations

of axes can be evaluated quantitatively. Thus the restricted or general distribution of maxima can be indicated in absolute terms. Its application to the interpretation of diagrams will be apparent to anyone familiar with the problem.

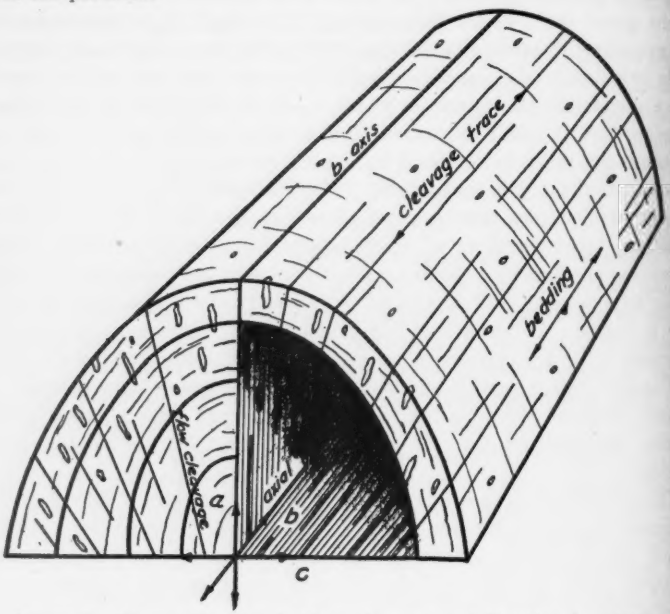

FIGURE 2.—*Diagram showing bedding, cleavage, and lineation in relation to reference axes* a, b, *and* c

Preparation of cumulative diagrams.—Diagrams F 93 and F 95 (Pl. 12) represent plotted and contoured maxima from all diagrams which showed concentrations of more than 3 per cent. After plotting, each maximum was broken up into a number of points equivalent to its relative percentage weight. Thus 20 points would replace four 5-per cent maxima, and 12 points would appear in place of three 4-per cent concentrations. The resulting count was made from 277 points representing 62 maxima.

TERMINOLOGY

Any study dealing with fabric analysis requires the use of an unstable terminology. The author's interpretations of numerous confusing terms are presented in an effort to minimize any misinterpretations of the data here presented.

TABLE 1.—*Correlation of specimen horizons in*

	Northern West Virginia	West of Frederick Valley, Md.	East of Frederick Valley, Md.
Miss.			
Devonian	Catskill Series Chemung Series Portage Series 29 Genesee Series Hamilton Series Marcellus Series Oriskany Sandstone 31 Helderberg Limestone	Catskill Formation Jennings Formation Romney Shale 36 Oriskany Sandstone Helderberg Limestone	
Silurian	Bossardville Limestone Rondout Waterline Bloomsburg Niagara 33 Clinton White Medina 28 Red Medina Gray Medina	 Tonoloway Limestone Wills Creek Shale McKenzie Formation Clinton Shale Tuscarora Sandstone-Sc 22*	
Ordovician		Juniata Formation Martinsburg Shale 37, 38, 39 Chambersburg Limestone Stones River Limestone Beekmantown Limestone	
Cambrian		Upper Cambrian:- Conococheague Limestone 35 Middle Cambrian:- Elbrook Limestone Lower Cambrian:- Waynesboro Formation Tomstown Dolomite Antietam Quartzite, ϵ_a 20* Harpers Phyllite, ϵ_h 46* Weverton quartzite ϵ_w 10,11,12,13,23,24,75* Loudoun Formation, ϵ_l 74,76*, Md 37*	 Antietam Quartzite Harpers Phyllite ·Sugarloaf Mountain Quartzite (Cambrian ?) ϵ_{sl} 71*
Pre-Cambrian			Pre-Cambrian (?) Glenarm Series:- Quartzite Beds, Qc Md 35*, 77, 78* Ijamsville phyllite Urbanna phyllite, Marburg Schist (formerly Harpers) Wissahickon, W_{gs}; Albite Chlorite Schist 206* Metarhyolite and meta-andesite, Metabasalt Silver Run Limestone Wakefield Marble

Sources of information for stratigraphic sections:

Those horizons which have contributed specimens are underlined, and specimen numbers indicated. Each tectonite horizon is marked with an asterisk.

(1) West Virginia Geological Survey reports for:
Jefferson, Berkeley, Morgan counties 1916
Hampshire, Hardy counties 1926
Grant, Mineral counties 1923

(2) *Geologic map of Frederick County* by Jonas and Stose, Maryland Geological Survey..... 1938
Geologic map of Washington County, compiled by E. Cloos, Maryland Geological Survey.... 1941

(3) *Geologic map of Frederick County* by Jonas and Stose, Maryland Geological Survey..... 1939
Geologic map of Howard County by E. Cloos and C. Broedel, Maryland Geological Survey.. 1940

erick Valley, Md.	Central & South Central Pa.	Susquehanna River below Harrisburg, Pa.	
	Mauch Chunk Series Loyalhanna sandy Limestone Pocono Sandstone		
	Catskill Facies 62 Chemung Facies Portage Facies Hamilton Sandstone & Shales Onondaga Shales & Limestone Oriskany (including Ridgeley and Shriver) Sandstone and limestone Helderberg Limestone		
	Keyser Limestone Tonoloway Limestone Wills Creek Shale Bloomsburg Shale & Sandstone McKenzie Limestone & Shale Keefer Sandstone Rosehill (Clinton) Shale & Sandstone Tuscarora Sandstone 51, 60, 61, 66		
	Juniata Sandstone Bald Eagle Sandstone Martinsburg Shale Chambersburg Limestone 63 Stones River Limestone Beekmantown Limestone		Martinsburg formation 53 Leesport Limestone Beekmantown Limestone
rtzite yllite ountain mbrian ?) Esl 71*	Conococheague Limestone Elbrook Limestone Waynesboro formation Tomstown Dolomite Antietam Sandstone Harpers Schist with Montalto Quartzite Member Weverton Sandstone Ew 21, 64, 65* Loudoun Formation	Upper Cambrian:- Conococheague Limestone Lower Cambrian:- Ledger Dolomite Linzers formation Vintage Dolomite Antietam Quartzite Harpers phyllite Chickies Quartzite Ec 50* and Chickies Shale	Conococheague Limestone Elbrook Limestone Tomstown Limestone Hardyston Quartzite 52*
(?) eries:- dg Qc 78* yllite te Marburg Harpers), Albite 206* nd meta- basalt imestone arble		Glenarm Series:- Peach Bottom Slate Cardiff Conglomerate Cy H-107* Peters Creek Formation Wissahickon formation Cockeysville Marble Baltimore Gneiss	

(4) *Blair Atlas* by F. Platt, Second Geological Survey of Pennsylvania..... 1881
Geology of Centre County by E. V. d'Invilliers, Second Geological Survey of Pennsylvania.. 1884
Geologic map of Pennsylvania by Stose and Ljungstedt..... 1931
A Paleozoic section in south central Pennsylvania by B. Willard and Cleaves, Pennsylvania Geologic Survey, 4th series, Bulletin G-8..... 1938
A Guidebook to geology of the Pennsylvania Turnpike by Cleaves and Ashley, Topographic and Geologic Survey of Pennsylvania, Bulletin G-20..... 1942
Mercersburg-Chambersburg Folio by G. W. Stose, U. S. Geologic Survey, Folio no. 170..... 1909
(5) *Geology and mineral resources of the Middletown quadrangle, Pennsylvania* by Stose and Jonas, U. S. Geological Survey, Bulletin 840..... 1933
Geology of the McCalls Ferry-Quarryville district by Knopf and Jonas, U. S. Geological Survey, Bulletin 799..... 1929
(6) *Highway geology—Philadelphia to Pittsburgh* by B. Willard, Pennsylvania Geologic Survey, 4th series, Bulletin G-12..... 1939

licated.

. 1916
. 1926
. 1923
. 1938
. 1941
. 1939
. 1940

Figure 2 shows schematically the structural elements of a fold in relation to the co-ordinate reference axes. The fold axis is horizontal, therefore the strike of the bedding is parallel to *b*. Cleavage (or "flow cleavage") has a genetic as well as descriptive connotation and is synonymous with "axial plane foliation" (Fairbairn, 1942, p. 98-100). The cleavage

TABLE 2.—*Definition of reference axes according to Albert Heim*

Reference axes		Definitions of axes
Sander	Heim	
b	a	"The axis of least deformation or of constant dimension. It lies approximately parallel to the fold axis in the cleavage plane and transverse to the lineation. It is the axis of intermediate stress and of least deformation."
c	b	"The axis of strongest deformation lies perpendicular to the cleavage plane."
a	c	"The axis of most intense stretching is in the direction of movement. It lies precisely in the direction of stretched elements in the cleavage plane and approximately in the direction of dip of axial planes in steep isoclinal folds." (Heim, 1921, p. 83–84.)

traces on the *ac* plane show a characteristic fanning outward from the axial plane and parallelism on the bedding plane. Two lineations are shown in the schematic fold: (1) as stretched particles lying in the cleavage plane parallel to *a*; (2) as the intersection of cleavage and bedding. Measurement of the elongation of grains or other fabric elements is another quantitative method by which flowage and recrystallization can be analyzed. In the present discussion "elongation ratios" refer to micrometer measurements of the longest to the shortest dimensions of the grain or grains under observation. It does not refer to maximum elongation since the cuts expose an appreciable but seldom a maximum elongation.

Most workers agree on the restrictions of the terms "tectonite" and "nontectonite." The author interprets "tectonite" as any rock in which a rearrangement of constituents has been controlled by a traceable scheme of deformation. Such rearrangements may result in a preferred dimensional or a preferred lattice orientation of rock elements.

Albert Heim in his monumental work, *Geologie der Schweiz* (Heim, 1921, p. 81) has included a comprehensive discussion of linear stretching ("Linearsteckung"). His reference axes are labeled differently from Sander's, but the elements on which the terminology is built are identical. Table 2 defines the references axes *a*, *b*, and *c* with a free translation

from Heim's work. Sander's axes are included in the table for comparison.

Heim (1921, p. 82) further defines linear stretching as follows:

"In many rock masses all cleavage or lamination surfaces reveal extension in a uniform direction giving rise to linear stretching ('faser') of components parallel to the dip of the cleavage plane. Each mineral grain, each petrifact, and each tiny irregularity is then stretched in the direction of c." (Heim, 1921, p. 82.)

Deformation of belemnites, fish, oölites, augen, and mineral grains all confirm Heim's contentions. Block diagrams, photographs, and sketches strikingly display lineation in *c* (*a* of Sander's system) and leave no room for doubt of the validity of Heim's contribution.

Gefügekunde der Gesteine (Sander, 1930) appeared 9 years later, and petrofabrics was immediately grasped by European geologists as a new tool in interpreting rock deformations. A revised nomenclature was developed largely from fabric data. Heim's conclusions were apparently masked by the new approach, and reference axes were redefined. Lineation was now defined as parallel to the tectonic axes of the regions studied. The present author does not intend to belittle the importance or character of Sander's work, nor to disregard the possibility of elongation (lineation) in *b*. The important fact is that Sander's recognition of lineation parallel to the fold axis has been widely accepted as a principle to be applied to any rock type in all regions. Diagrams prepared from fabric analyses are often interpreted on the assumption that such a generality is a principle. A statement by Billings (1942, p. 347) reflects the attitude of many investigators:

"That the lineation is perpendicular to the direction of movement is one of the fundamental tenets of structural petrology."

Lineation in *a* is a fact, yet it is seldom recognized as an important element. Sander describes lineation in *a* in conjunction with *bc* tension fractures which develop in shear zones:

"where deformation is relatively rapid, severe, and rotation is unimportant." (Fairbairn, 1942, p. 97.)

Lineation in *b* involves the fold axis as:

"an axis of bodily rotation around which the elements of the fabric have been rolled during the forward transport of material, the rolling movement involves a compression similar to the compression of dough in rolling a noodle. Therefore, this is an *elongation* of material in a direction normal to the movement of slip of material." (Knopf, 1939.)

Without close inspection, Appalachian structures seem to suggest a situation similar to that found in the Alps from which Sander has described persistent lineation in *b*. Stretching in *a* is common in the folded Appalachians. Lineations are produced through extension of oölites and

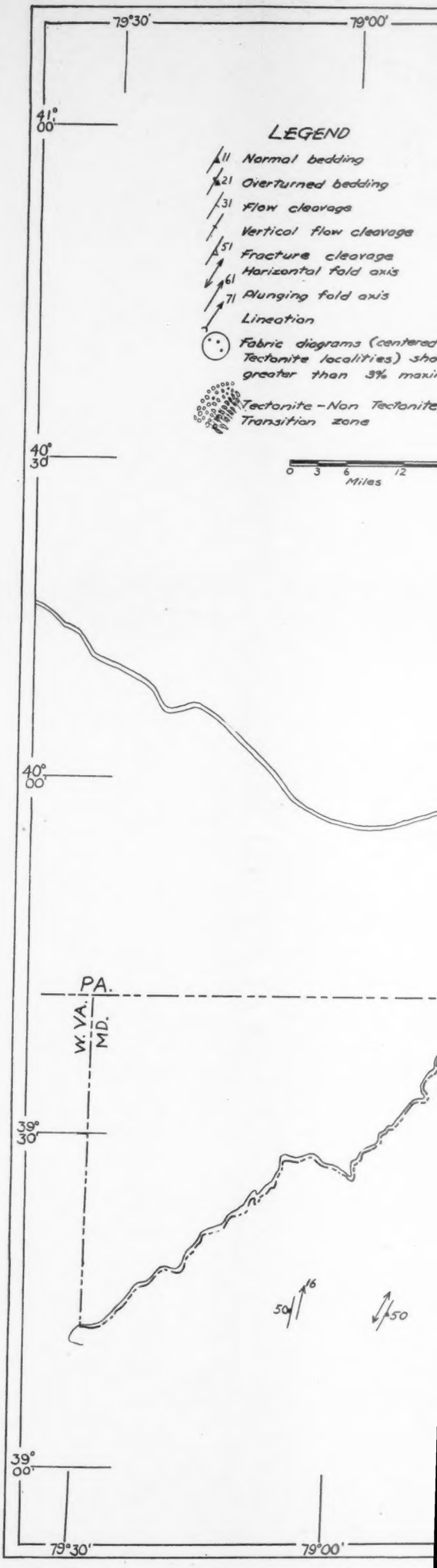
79°30'
79°00'
41° 00'
LEGEND
11 Normal bedding
21 Overturned bedding
31 Flow cleavage
Vertical flow cleavage
51 Fracture cleavage
61 Horizontal fold axis
71 Plunging fold axis
Lineation
Fabric diagrams (centered
Tectonite localities) sho
greater than 3% maxi
Tectonite - Non Tectonite
Transition zone
40° 30'
0 3 6 12
Miles
40° 00'
PA.
W. VA.
MD.
39° 30'
50
16
50
39° 00'
79°30'
79°00'

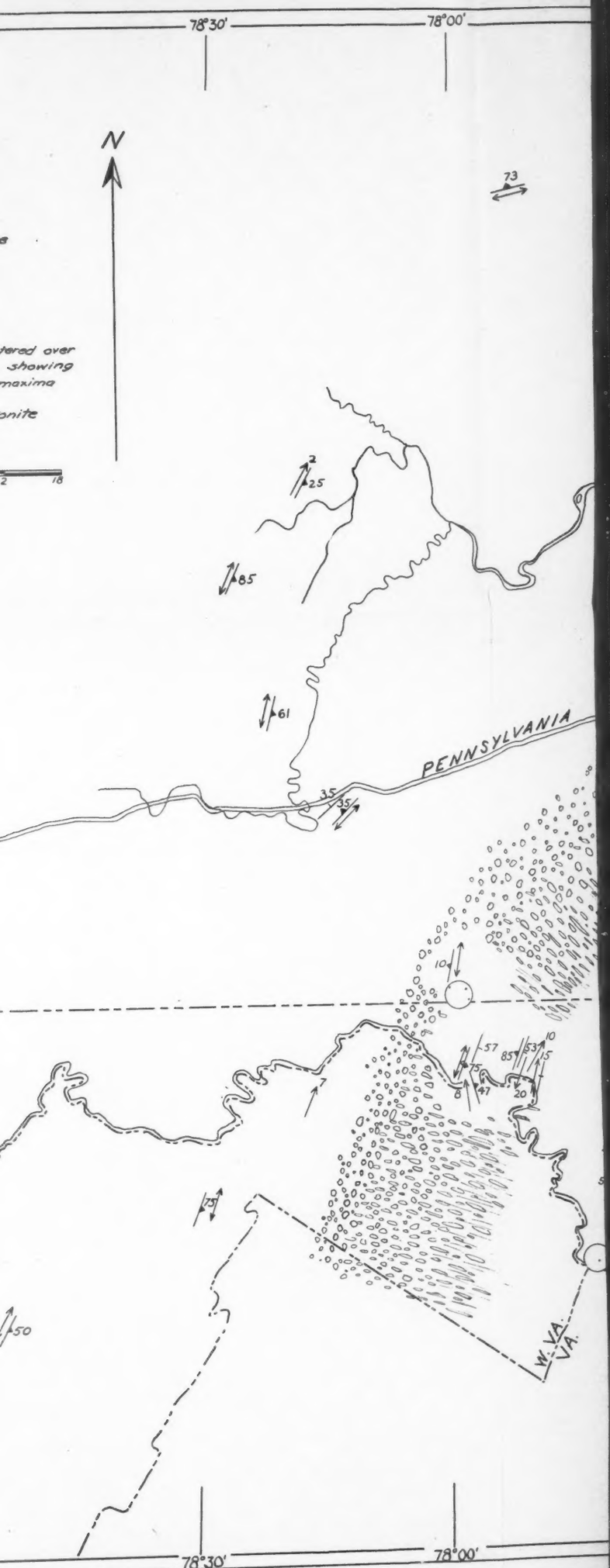
78°30'
78°00'
N
73
tered over
showing
maxima
onite
2
18
25
85
61
PENNSYLVANIA
35
35
10
57
85
53
10
75
15
47
20
25
50
W. VA.
VA.
78°30'
78°00'

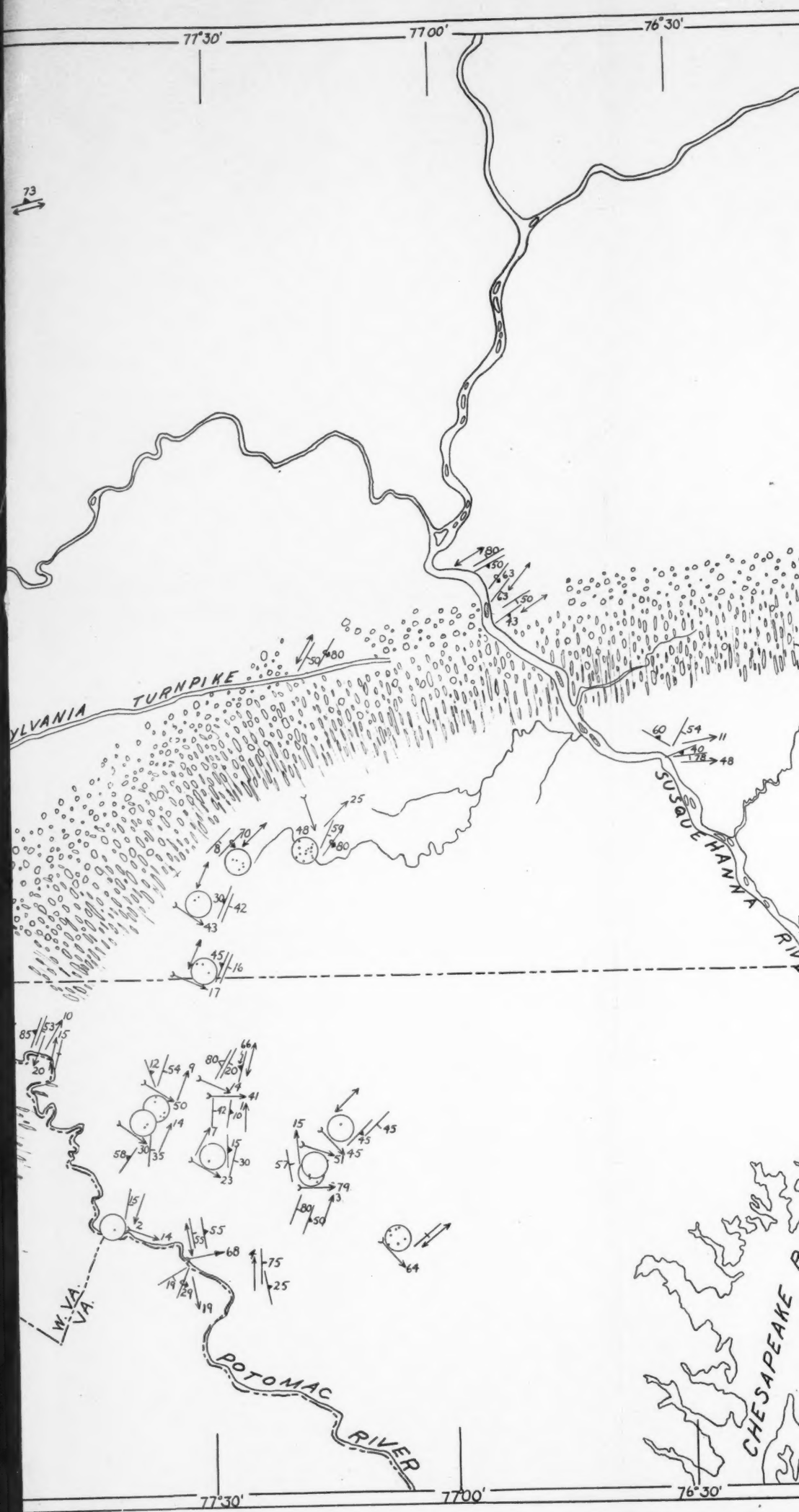

STRUCTURE AND FABRIC AT SPECIMEN LOCALITIES

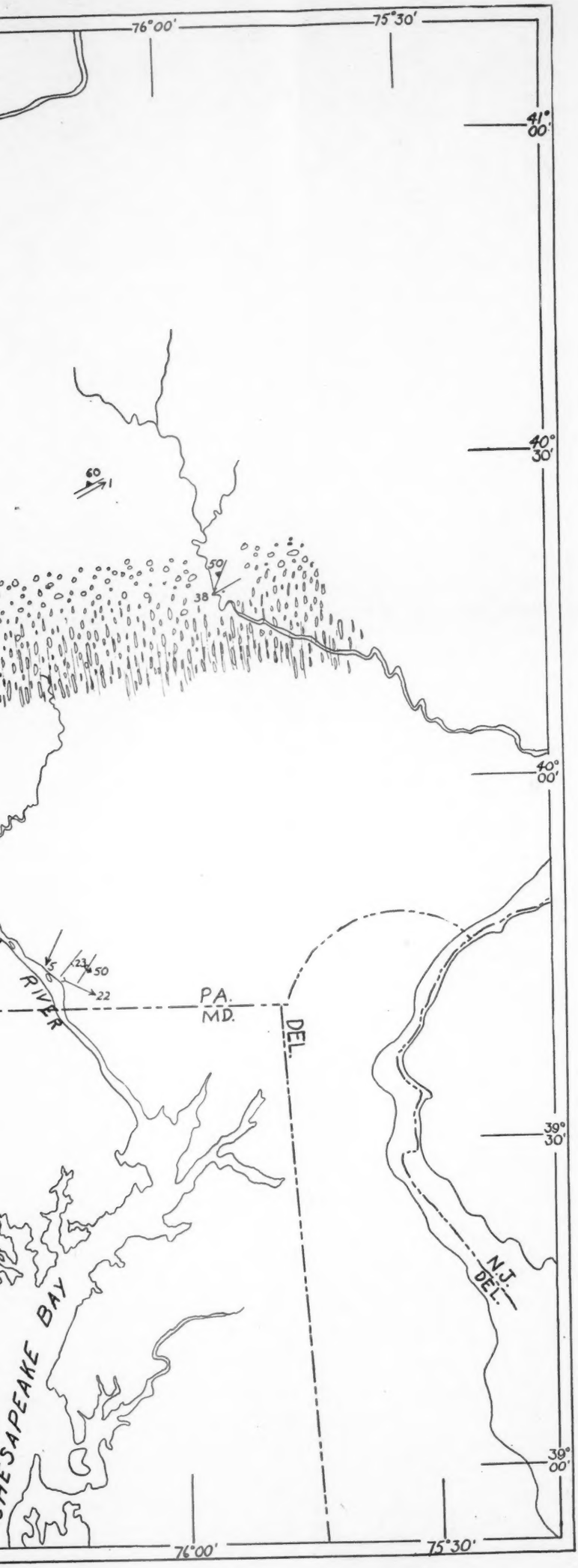
76°00'
75°30'
41° 00'
40° 30'
40° 00'
39° 30'
39° 00'
60
50
38
23
50
22
PA.
MD.
DEL.
N.J.
DEL.
RIVER
CHESAPEAKE BAY

fossils (Cloos, 1941; 1942) as well as quartz grains within the cleavage plane and perpendicular to *b*. Such lineations are sometimes described as "flow lines." Balk (1937, p. 10) makes the distinction and proposes the term:

"'flow lines' for all linear structures that are believed to have resulted from more or less viscous flow of magmas. The term, 'linear stretching', may be used wherever more or less plastic flow and deformation are referred to, such as in crystalline schists, slates, marbles, cataclastic gneisses, mylonites."

A detailed description of the development and texture of stretched quartz grains will be found in the section on Deformation and Recrystallization of Quartz.

REGIONAL STRUCTURE

The area occupies a major salient in the Appalachian system. The trend of the mountain axes swings from north-south in the western portion to nearly east-west in the northeastern portion of the area studied. This is shown schematically on the index map (Fig. 1) and is more accurately indicated by the attitude of fold axes on the structure map (Pl. 2).

LOCAL ENVIRONMENTS

Locality F 10-13 near Harpers Ferry, West Virginia, shows an overturned fold in Elk Ridge. A vertical section through the thickest portion of the doubled beds is estimated at 200 feet. Inaccessibility prevented accurate measurement of possible thickening in the crest of the fold, and the strata are too massive to estimate any variation.

Thickness measurements were made in all folds, but no variation from crest to limb was evident, and none should be expected from flexure folds.

Chickies Rock on the Susquehanna River south of Harrisburg is a large tectonitic fold. The familiar but misleading photograph (Pl. 4, fig. 1) commonly shown in geologic reports of the area indicates a beautifully symmetrical anticline; however, the fold plunges steeply eastward, and a series of prominent undulations on the northern limb disturbs the symmetry and disrupts the bedding planes (Pl. 4, fig. 2). Any attempt to measure variations in thickness therefore is useless. As at Harpers Ferry the horizons are massive and inaccessible.

A large majority of tectonite localities consist of restricted outcrops showing portions of limbs or crests of folds of larger but indeterminable size.

NONTECTONITES

Table 3 lists the critical data pertaining to those specimens which fail to qualify as tectonites. The percentages listed under "composition"

and "per cent of quartz recrystallizing" were determined with the Wentworth integrating stage. On Plate 5, Figure 1 shows angular quartz in Romney sandstone. Figure 2 shows a calcite lens interlaminated with bands of subrounded quartz grains from the Conococheague limestone,

TABLE 3.—*Microscopic data pertaining to nontectonites*

Specimen number	Composition*					Per cent of quartz recrystallizing	Largest maximum per cent	Per cent area covered by maxima over 3%
	Qtz.	Mica	Calc.	Feld. et al	FeO			
F28A	93.7	.....	.....	6.3	.....	11.3	4	0.12
28C	98.0	2.0	.....	.....	.....	16.2	3	.....
29	76.0	4.3	19.7	.....	.....	10.4	4	0.08
31	98.4	1.6	.....	.....	.....	12.8	4	0.08
33	89.2	10.8	.....	.....	.....	14.0	4	0.19
35	58.5	1.5	40.0	.....	24.6	3.8	3	.....
36	74.0	1.4	.....	.....	.....	8.5	4	0.14
37	49.6	50.4	.....	.....	.....	29.3	4	0.45
38	35.0	65.0	.....	.....	.....	23.5	4	0.19
39	20.9	72.0	.....	6.5	.....	13.8	3	.....
51A	69.0	31.0	.....	.....	.....	26.2	3	.....
51B	100.0	.....	.....	.....	.....	21.7	3	.....
52	94.6	5.4	.....	.....	.....	17.2	3	.....
53	40.4	.....	58.3	1.3	.....	5.6	3	.....
54	55.7	39.1	.....	5.2	.....	16.6	3	.....
59	55.4	.....	44.6	.....	.....	2.2	3	.....
60	81.6	.....	.....	3.4	15.0	21.9	3	.....
61	47.6	46.8	.....	5.8	.....	9.2	3	.....
62	29.9	65.5	.....	4.6	.....	4.3	3	.....
63	36.8	58.4	.....	4.8	.....	1.7	3	.....
66	34.3	17.0	.....	2.7	.....	10.7	4	0.06

* General headings to include: "qtz." (arenaceous), "mica" (argillaceous), "Calc." (calcareous), "Feld. et al." (feldspar and detritals), "FeO" (iron oxide cement).

Nontectonites include "pure" quartz rocks (specimens F 51B, F 28A, F 28C, F 31, F 52), argillaceous sandstones and quartzites (F 33, F 37, F 38, F 39, F 51A, F 54, F 61, F 62, F 66), and calcareous sandstones (F 36, F 60). Many of the rock types listed are somewhat arkosic.

and Figure 3 represents calcite comb structure and the development of included fine-grained quartz as a lens in the Portage sandstone.

Some evidence of recrystallization is seen in the quartz of every specimen. The lowest percentage of affected quartz is 1.7; the highest is 29.3. The average, however, is less than 14. Maxima of 3 and 4 per cent appear consistently on the nontectonite diagrams. A planimeter measurement shows that an average of 0.16 per cent of the area of each diagram is covered by 4-per cent concentrations.

An analysis of the significant maxima has made it possible to set a somewhat arbitrary limit of 0.5 per cent by planimeter measure below which a maximum can be considered truly random.

TECTONITES

MEGASCOPIC IDENTIFICATION

It is not easy to identify quartz tectonites in the field. Where elongation ratios reach 3:1, however, the specimens reveal a distinct lineation parallel to *a* within the flow cleavage plane. In equigranular or fine-grained rocks lineation can be inferred only by recognition of strong flow cleavage in adjacent micaceous horizons or through association with struc-

TABLE 4.—*Microscopic data pertaining to tectonites*

Spec. No.	Composition in per cent					Per cent qtz. recrystallizing	Common max. ratio of elongation	cut	Largest max. per cent	Per cent of area covered by maxima of more than 1%
	Qtz.	Mica	Calc.	Feld. et al.	Magt.					
HF 10	93.0	4.4	.....	2.6	.....	23.8	1.4:1	*ac*	3	.....
HF 11b	67.0	25.0	.....	8.0	.....	35.5	2.6:1	*ac*	3	.....
HF 11c	.....	.....	.....	.....	.....	.....	2.7:1	*ab*	3	.....
HF 12a	91.7	7.2	.....	1.1	.....	29.7	3.7:1	*ac*	3	.....
HF 12b	.....	.....	.....	.....	.....	.....	3.3:1	*bc*	4	0.08
HF 13a	85.4	13.6	.....	1.0	.....	22.2	2.8:1	*ac*	3	.....
HF 13b	.....	.....	.....	.....	.....	.....	I.E.	*bc*	3	.....
F 20a	33.8	64.6	1.6	.....	.....	9.5	I.E.	*bc*	4	0.12
F 20c	.....	.....	.....	.....	.....	.....	I.E.	*ac*	4	0.54
F 21a	84.6	9.5	.....	5.9	.....	22.5	3.5:1	*ac*	4	0.41
F 21b	.....	.....	.....	.....	.....	.....	2.7:1	*bc*	4	0.29
F 22a	89.5	10.5	.....	.....	.....	22.5	I.E.	*ac*	5	0.29
F 22b	.....	.....	.....	.....	.....	.....	I.E.	*ab*	5	0.72
F 23b	80.5	19.5	.....	.....	.....	23.5	2.3:1	*ac*	3	.....
F 23c	.....	.....	.....	.....	.....	.....	2.3:1	*ab*	6	4.14
F 24a	95.0	5.0	.....	.....	.....	93.5	3.5:1	*bc*	5	0.68
F 24b	.....	.....	.....	.....	.....	.....	5:1	*ac*	3	.....
Md.35	93.0	7.0	.....	.....	.....	57.5	S.C.	*ac*	4	0.45
Md.37	17.9	68.3	.....	.....	13.8	73.5	4:1	*ac*	3	.....
F 40	90.3	9.7	.....	.....	.....	39.2	S.C.	*ac*	4	0.27
F 50A	100.0	.....	.....	.....	.....	62.0	S.C.	*ab*	5	0.41
F 50B	.....	.....	.....	.....	.....	.....	2.2:1	*ac*	3	.....
F 64	57.4	41.6	.....	.....	1.0	24.4	3.5:1	*ac*	6 needle quartz	1.4
F 65	100.0	.....	.....	.....	.....	47.6	3.2:1	*ac*	6 needle quartz	1.4
F 71	98.7	1.3	.....	.....	.....	50.4	S.C.	*ac*	2	.....
F 74	86.9	13.1	.....	.....	.....	74.2	S.C.	*ac*	3	.....
F 75	94.0	6.0	.....	.....	.....	60.0	2.6:1	*ac*	3	.....
F 76	60.8	39.2	.....	.....	.....	31.0	2.8:1	*ac*	3	.....
F 77	90.5	9.5	.....	.....	.....	47.1	S.C.	*ac*	4	0.17
F 78	95.6	4.4	.....	.....	.....	48.2	2.8:1	*ac*	4	0.14
H 107	34.0	48.2	.....	17.8	.....	100.0	S.C.	*ac*	3	.....
206a	.....	.....	.....	.....	.....	.....	S.C.	*ab*	4	0.52
206b	97.0	2.2	.....	0.8	.....	98.1	S.C.	*bc*	6	3.74
206c	.....	.....	.....	.....	.....	.....	S.C.	*ac*	6	4.67

I.E. = insignificant elongation.
S.C. = stretched clusters not measurable.

tures which may favor the development of a lineation through recrystallization.

MICROSCOPIC IDENTIFICATION

The specimens have been separated into two groups on the basis of microscopic evidence. The nontectonite group includes those relatively undeformed rocks which show no evidence of a secondary lineation. Tectonite specimens reveal a preferred linear direction of both the lattice and dimensional types.

Those specimens whose texture reveals a dimensional parallelism of grains in the process of recrystallization are here classified as tectonites. The pertinent rock and fabric data are listed in Table 4. A Wentworth analysis of the 34 thin sections listed in the table reveals "pure" quartzites (F 10, F 12, F 24, Md 35, F 40, F 50, F 65, F 71, F 75, F 77, F 78, 206), argillaceous and micaceous quartzites (F 11, F 13, F 20, F 21, F 22, F 23, F 64, F 74, F 76), magnetitic arenaceous phyllites (Md 37), and a mica-rich arkose (H-107).

A single analysis (F 20) shows granulation of less than 22 per cent of the available quartz.

Evidence of stretching is seen in all tectonite specimens although the intensity differs. In some sections an elongation is apparent, but not sufficiently developed to permit measurement (F 13B, F 20A, F 20C, F 22A, F 22B). The feature becomes gradually more clearly defined and reaches a maximum in F 24B where the ratio of elongation commonly reaches 5:1. Sections containing *a* invariably show a more pronounced stretching than that seen in *bc* cuts.

Analyses of four tectonite specimens expose 6-per cent maxima (F 23, F 24, F 50), and only one shows a 4-per cent maximum of sufficient size to be considered significant (F 20). A planimeter measurement was made of all areas enclosed by 4-per cent contours. The average per cent of area covered by these concentrations of 4 per cent is 1.8, although the measurements reach a minimum of 0.08 per cent (F 12B) and an exceptional maximum of 4.67 per cent (206C).

TEXTURAL FEATURES

Microscopic characteristics.—Quartz-rich tectonites (over 60 per cent quartz) reveal such a consistent and characteristic microscopic texture that a generalized description is a fairly accurate guide to their recognition.

Tectonite quartz can be divided into five descriptive types: original grains, peripheral growth quartz, crush quartz, needle quartz, and recrystallized quartz.

FIGURE 1. SANDSTONE ANTICLINE IN SILURIAN NIAGARA SERIES

From east bank of river ¼ mile south of Great Cacapon, W. Va. Specimen locality F 33 A, B, C.

FIGURE 2. SYNCLINE IN ORDOVICIAN MARTINSBURG SANDY SHALE

From north bank of Conococheague Creek 3 miles northeast of Upton, Pa. (Note hammer near trough of fold.)

FIGURE 3. SMALL OVERTURNED ANTICLINE

In Ordovician Martinsburg sandy shale from 1.5 miles due south of Stone Bridge, (Mercersburg Quadrangle) Pennsylvania.

FIGURE 4. FOLD COMPLEX IN SILURIAN UPPER CLINTON FLAGGY SHALES

On railroad cut near Pinto, Maryland. (Hammer and notebook show scale.)

SMALL FLEXURE FOLDS IN NONTECTONITE AREA

FIGURE 1. ANTICLINE OF CHICKIES QUARTZITE
As seen from Hellam Point on the Susquehanna River. From Stose and Jonas (1939) by permission of State Geologist.

FIGURE 2. STRUCTURAL DETAILS AT CHICKIES ROCK
Source same as Figure 1.

CHICKIES ROCK, PENNSYLVANIA

Original grains are those discrete particles which have resisted deformation by fracturing and granulation. They commonly display strong strain shadows and dusty inclusions. Their borders are usually delineated by a rim of dust which suggests the etched and dirt-filled surface

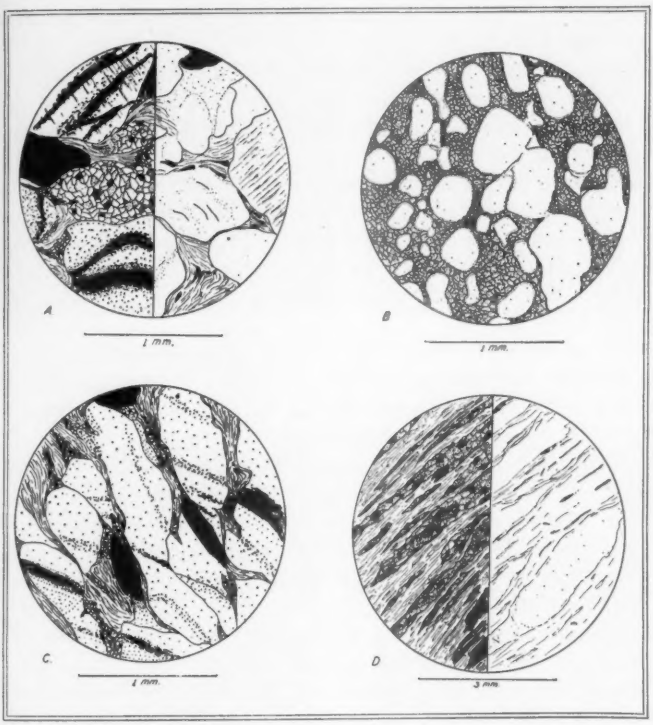

FIGURE 3.—*Stages in development of recrystallized fabric*

A. Mylonitized grains with crushed particles still strikingly optically uniform. The right half of the field portrays the effect in plane light; the left with crossed nicols. Flowage of material has progressed to the point where irregularities in adjacent grain boundaries and interstices between grains are filled with crush quartz. Specimen F 21.

B. Peripheral growth quartz developed around well-rounded quartz grains set in a calcite matrix. No straining is apparent. Specimen F 59.

C. Strained and stretched quartz grains with interstitial muscovite and crush quartz. "Tailed" grains are apparent as are partially annealed slivers of quartz. Specimen HF 12.

D. Maximum stretching of granulated clusters. Crush quartz in lenslike attenuated stringers sometimes transgressing the entire slide. A metacryst of annealed quartz shows at the right (plane light). A gypsum plate reveals uniformity of color, signifying well-developed preferred lattice orientation in the grains of each stringer as well as in the metacryst. Specimen 206.

of the original detrital fragment. Grains show all gradations of roundness and angularity. The texture is generally inequigranular since fine-grained crush quartz is a common associate of larger original grains or larger annealed metacrysts. Original grains are shown in various combinations with other textural types of quartz in Figure 4 of Plate 5 and in Plates 6, 7, 8, and 9. Camera lucida drawings (Figs. 3a, b) also illustrate this feature.

Peripheral growth quartz, a distinct and discernible textural type, constitutes a large proportion of the interstitial binding in the fabric. Absence of contamination and its restricted peripheral distribution are characteristic (Pl. 5, fig. 4).

Crush quartz is a descriptive and genetic term used in this discussion to define granulated original grains. The shattering or crushing of quartz grains during movement produces an even-granular mat of equant and polygonal particles averaging 0.05 mm. in diameter. Such clusters retain for a time their original collective grain boundary (Fig. 3A, D; Pl. 6, fig. 1; Pl. 7).

Needle quartz, early recognized and named by Sander, is bounded by plane surfaces and displays optical parallelism of those needles which have not suffered appreciable rotation since fracturing. The slivers constitute the major portion of the fabric in many cases with interstitial crush quartz usually a common associate. Lineation developed from slivering of the original grains is generally well defined. "Elongation" ratios of 3:1 are common but vary with the number of glide planes which take part in fracturing. The more glide planes per grain the thinner are the slivers and, therefore, the greater is the ratio of "elongation" (Pl. 8; Pl. 9, figs. 1, 2).

Recrystallized quartz is the ultimate development of crush quartz. When the component parts of stretched clusters reach optical homogeneity, the counterparts coalesce, and the individual crushed particles form a large elongated and annealed grain (Fig. 3C). Figure 2 of Plate 9 shows recrystallized fabric in which a granoblastic texture is developed.

FABRIC DIAGRAMS

Quartz diagrams.—Partial diagrams were made for thin sections which showed an abundance of more than one quartz type. The majority of these represent textures in which original grains and crush quartz are common associates. Needle quartz, crush quartz, and original grains are associated in specimens F 64 and F 65. A special study was made of these sections, and 7 diagrams were prepared by measurement of 2000 quartz grains. Composite diagrams were prepared for the majority of thin sections either from random or selective measurements.

FIGURE 1. UNDEFORMED FERRUGINOUS SANDSTONE WITH ANGULAR QUARTZ GRAINS
F 36 A, plane light (×14).

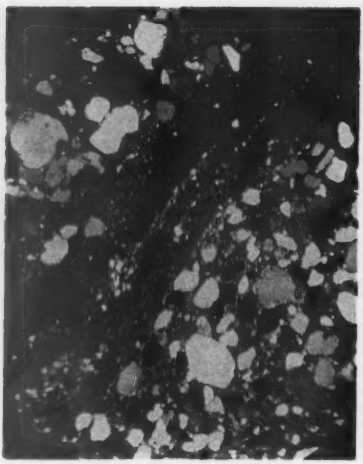

FIGURE 2. CALCITE LENS INTERLAMINATED WITH QUARTZ-RICH BANDS
F 35 A. ×-nicols (×15).

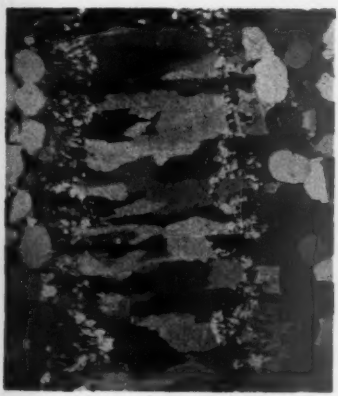

FIGURE 3. COMB STRUCTURE DEVELOPED IN CALCITE WITH INCLUDED FINE-GRAIN QUARTZ
F 29, ×-nicols, (×17).

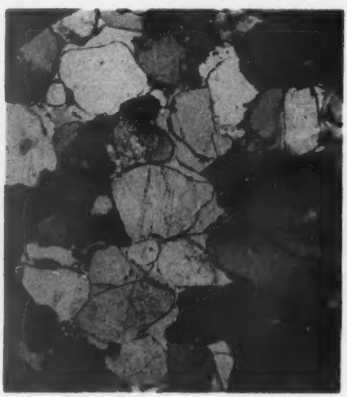

FIGURE 4. UNSTRAINED PERIPHERAL GROWTH QUARTZ
F 60. ×-nicols (×43).

FIGURE 1. STRAIN SHADOWS PASSING INTO PERIPHERAL GROWTH QUARTZ
HF 10. X-nicols (×43).

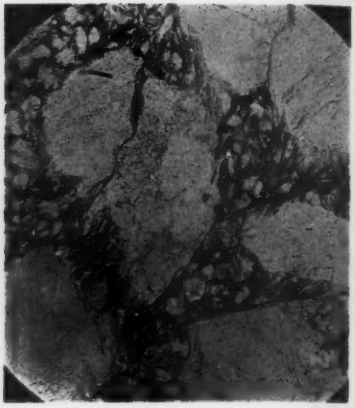

FIGURE 2. CRUSH QUARTZ CLUSTER, PLANE LIGHT
F 20 C. (×47).

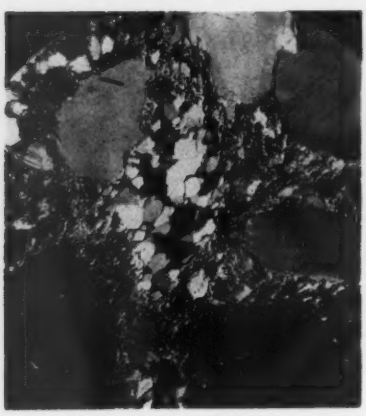

FIGURE 3. SAME AS FIGURE 2, UNDER X-NICOLS

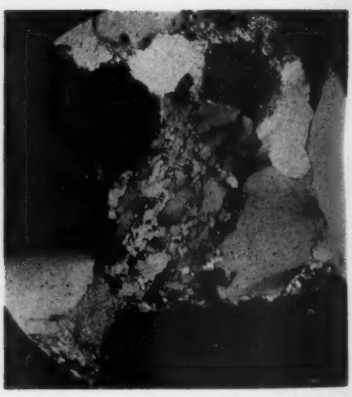

FIGURE 4. READJUSTMENT WITHIN CRUSH QUARTZ CLUSTER
Showing internal sutured boundaries. HF 10. X-nicols. (×44).

TEXTURES OF GROWTH QUARTZ
AND CRUSHED QUARTZ

Mica diagrams.—Three of the 16 mica diagrams represent orientation of sericitic muscovite which makes up the bulk of the groundmass of highly argillaceous sandstones. No neocrystallized micas are present. Maxima peaks for these sections are 12, 14, and 15 per cent. An average maximum of 19 per cent is revealed in the mica diagrams of tectonite specimens. The highest maximum concentration of mica cleavage poles was 29 per cent and resulted from the measurement of 100 partially chloritized biotite flakes (H 107, Pl. 12). Two hundred muscovite flakes were measured from the same specimen. The positions of the maxima on the two diagrams are identical (Pl. 12).

Cumulative diagrams.—Diagram F 93 (Pl. 12) represents a plot of all maxima over 3 per cent related to fabric co-ordinates with the north end of *b* at the center of the net and the west end of *a* at the left. The collection of data is repeated in diagram F 94 (Pl. 12) for tectonite analyses only. The general picture from both analyses is similar. The effect produced by accumulated data seems to emphasize fabric characteristics that are scarcely noticeable in individual diagrams. An incomplete but clearly defined *ac* girdle appears with individual maxima generally congregated in the vicinity of the II-IV standard maxima positions.

Diagram F 95 (Pl. 12) shows an accumulation of all maxima over 3 per cent plotted into a plan view with north at the top of the net. Diagram F 96 (Pl. 12) restricts this cumulative information to tectonite specimens. The two diagrams show general similarities. A concentration of maxima is shown in the southeast quadrant of the diagram.

DEFORMATION AND RECRYSTALLIZATION

EARLY EVIDENCE OF DEFORMATION

The five types of quartz are found in all proportions depending on the degree of recrystallization. The order of recrystallization does not lend itself to sharp boundaries. Evidence of stress is apparent in rocks from nearly every locality. The first indication of deformation is seen in the development of peripheral growth quartz which fuses original grains. Figure 3B shows rounded quartz grains cemented by peripheral growth quartz. Quartz known to develop through precipitation from ground water cannot be considered evidence of deformation unless it is reasoned that stress on a rock mass will aid the percolation of ground water with the resulting precipitation of silica. Strain shadows are not apparent at this earliest stage (Pl. 5, fig. 4). As stress continues, strain shadows appear which pass uninterruptedly into the newly developed border zones of the original grains.

DEVELOPMENT OF CRUSH QUARTZ

Undeformed quartz fabrics generally show random orientation of components. The vector properties vary with the crystallographic orientation of the quartz. Thus selective shattering develops in those grains which are unfavorably oriented with respect to the stress. Plate 6 shows selective shattering with the production of crush quartz. Crushing then predominates through the fabric and leaves a minority of original grains as islands in a matrix of fine crush quartz. As the few grains which are least favorably oriented are crushed they relieve the stress somewhat by more efficient packing, thereby allowing the crushing to increase at a decreasing rate as more and more crush quartz is formed. In this way, the crush quartz has an effect similar to the shock-absorbing qualities of a calcite or mica matrix. Figure 3A shows a grain after granulation. The grain boundaries as seen at the right of the sketch (in plane light) are smooth and regular. At the left (under crossed nicols) "tailing" and straining is apparent.

Moderately deformed rocks show clusters of crush quartz which tend toward optical homogeneity. However, the superindividuals act independently and give no suggestion of a common lattice orientation. To this point preferred lattice and dimensional orientations are sharply differentiated as factors which control the development of a tectonite. The distinction is lost, however, as deformation proceeds. A transitional stage is marked by an interdependence of the two factors in which case both contribute to the development of the tectonite. Preferred lattice orientation finally gains control as clusters merge and the texture becomes granoblastic (Pl. 9, fig. 2). Cluster boundaries melt into the fabric, the grains become equant, and a general preferred lattice parallelism develops which is accentuated by the use of a gypsum plate. Figure 3D shows the texture in a lattice-controlled tectonite. Optical parallelism exists not only within clusters but also between clusters.

An appreciation of this relationship between lattice and dimensional control in tectonites is fundamental to the interpretation of statistical data. The relative importance of the two factors can be determined only by a regional quantitative study of recrystallization and flowage.

Redistribution of crush quartz which accompanies continued or increased pressure appears to be controlled by two factors: (1) a tendency toward granoblastic texture both within the superindividual, and also with respect to the remaining uncrushed original grains; (2) a stretching in *a* in which the crushed particles within each stretched cluster tend toward an optical unity.

Ernst Cloos (Chapman, 1942) investigated the relationship between preferred lattice orientation and grain shape in a highly deformed

"pseudomigmatite." A comparison of these results with the results of this investigation shows how clearly a lattice-controlled tectonite can be differentiated from tectonites which depend only on parallelism of inequant fabric elements. Cloos found that the height of the maxima was influenced by the extent of elongation of the grains measured. Both elements were plotted into a maxima diagram, and concentration of the greatest ratios of elongation were superimposed on the quartz axes maxima. Such a correspondence is not found in the rocks here described. It is predicted, however, that such an index may be found useful in tracing the development of fabric from a preferred dimensional to a preferred lattice type.

The terms "recrystallized" and "recrystallization" often lead to confusion. Both words are applied loosely in discussion dealing with deformation and metamorphism. Crush quartz is not recrystallized quartz; it is merely a stage in the development of recrystallization. Only thoroughly reorganized and annealed quartz should be referred to as "recrystallized." Restriction in the use of these terms will allow more discrimination in textural studies and descriptions.

NEOCRYSTALLIZATION

The production of crush quartz in granulation allows migrating solutions to percolate through the rock. Thus recrystallization is aided by the presence of water, and neocrystallization is made possible by the introduction of mineral solutions. Neocrystallized muscovite, magnetite, and quartz are commonly scattered through crushed fabrics. The muscovite develops in cleavage planes of least resistance. Mica shreds encircle quartz metacrysts and are intimately mingled with quartz strands to form the tails of stretched grains. Magnetite is visible even megascopically as undistorted tetrahedra. Local growth textures develop where crystal faces of magnetite serve as basal planes for newly introduced quartz. Veinlets of quartz are found to transect all textures.

Orientation of crushed particles is controlled largely by a reallotment of space to accommodate the pressure. As neocrystallization proceeds, the crush quartz begins a process of local coalescence, but there is no reason to assume physical rotation of crush quartz particles to produce optical homogeneity. The individual clusters will contain particles which still retain in large measure their optical unity even though some solid flow has occurred in the redistribution of components. The lower threshold at which solid flow first succeeds in developing a recognizable preferred orientation is largely determined by the extent and degree of recrystallization.

LINEAR STRETCHING

Numerous instances (Pl. 7) show clearly the actual linear expansion to which stressed grains have been subjected. Often the result is a granulation of the original grain and the production of crush quartz. In some instances, however, the optically parallel portions of the original grain are stretched apart and held intact by strands of quartz and

TABLE 5.—*Relation of elongation ratios to orientation of cut*

Specimen	Ratios of elongation in:		
	ab	bc	ac
HF 11	2.7	.....	2.6
HF 12	.....	3.3	3.7
HF 13	.....	I.E.*	2.8
F 21	.....	2.7	3.5
F 23	2.3	.....	2.3
F 24	.....	2.3	5.0

* Insignificant elongation (not measurable).

neocrystallized muscovite (Pl. 7, fig. 3). A characteristic feature of stretching is seen in "tailed" grains in which both ends of the affected grain are drawn out in both directions parallel to *a* to form tapering tails of quartz streamers and neocrystallized muscovite which join to form a stylolitelike intergrowth with the original grain (Pl. 7, figs. 1, 2, 4).

Table 5 shows the variations in ratios of elongation in different cuts from one specimen. Those measured in *ac* or *ab* cuts (in which the full value of *a* is measurable) invariably show more pronounced lineation than *bc* or random cuts.

Elongation figures as listed in Table 4 are commonly exceeded in measurements of local extremes. Specimen 206 (Fig. 3D) shows single clusters which extend in narrow lensing streaks across the entire slide. Elongation ratios lose their meaning when individual crush quartz clusters become inseparable. More highly deformed tectonites of this type show a preferred lattice orientation.

FRACTURING

Development of fracturing is shown by incipient breaks suggested by offsets in strain shadows, partially separated couples, and isolated needles in Plate 8.

The glide plane controlling a fracture can be determined by universal stage measurements. Reference elements are strain shadows which

FIGURE 1. "TAILED" CLUSTERS OF CRUSH QUARTZ
F 12 A. X-nicols (×45).

FIGURE 2. "TAILED" CLUSTERS OF CRUSH QUARTZ
F 64. X-nicols (×45).

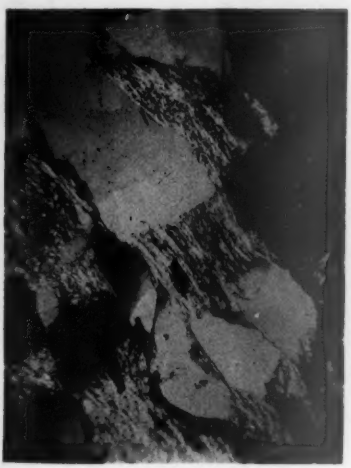

FIGURE 3. TEXTURE OF INTERGRANULAR SPACE AFTER STRETCHING
F 64. X-nicols (×31).

FIGURE 4. BOEHM'S LAMELLAE ASSOCIATED WITH "TAILED" GRAINS
F 21 A. X-nicols (×40).

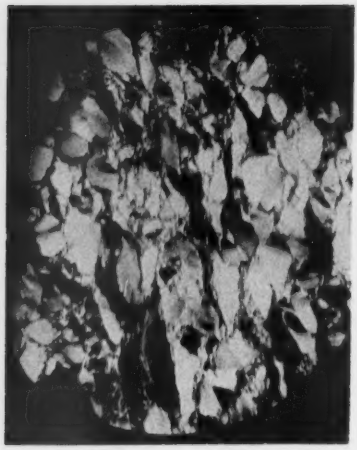

FIGURE 1. ELONGATION OF QUARTZ PRODUCED BY FRACTURING
F 12 A. X-nicols (×16).

FIGURE 2. INCIPIENT FORMATION OF NEEDLE QUARTZ IN LARGE ORIGINAL GRAIN
F 52. X-nicols (×13).

FIGURE 3. QUARTZ SLIVERS PARALLEL TO MICA SHREDS IN MUSCOVITE SCHIST
Md. 37. X-nicols (×15).

FIGURE 4. INCIPIENT FRACTURING PARALLEL TO STRAIN SHADOWS
F 12 B. X-nicols (×49).

develop parallel to the optic axis of the grains and Boehm's lamellae which form parallel to the base (0001) (Hietanen, 1938). Figure 1 of Plate 9 shows the relations between fracturing, strain shadows, and lamellae.

Eleven grains were measured on the universal stage and produced an average angle of 36 degrees between the *c* axes and the fractures. This corresponds closely with the angle of 38°13′ given by Dana for *mr* ($10\bar{1}0$-$10\bar{1}1$) (Ford, 1932). Therefore, needle quartz developed in the rocks has been produced by gliding along rhombohedron planes.

Grains may rotate until a crystal glide plane parallels the direction of shear, although evidence for such rotation is largely inferential. Thin-section study suggests that such fracturing could occur without rotation. The fracture hypothesis recognizes a number of glide planes in a crystal along which movement may take place in response to a nonrotational stress. A crystal oriented so that one of the possible glide planes parallels or nearly parallels the direction of maximum stress theoretically can fracture along that plane, whereas grains with no favorably oriented glide plane will be granulated.

Crush quartz may form under almost any condition where stress exceeds strength. Original grains which fracture into needles seem to require either preferred crystallographic properties or preferred dimensional arrangement in a fabric and probably both. Quartz needle tectonites are not common in the area. Specimens F 64 and F 65 are from localities along the northwest slope of South Mountain. Intense stretching and thrusting toward the northwest is in evidence, but at these localities the maximum movement may be localized in thrust planes. The evidence is inconclusive but suggests that local structural environments may influence the mode of deformation of quartz.

ANNEALING RECRYSTALLIZATION

Annealing of crush quartz clusters into truly elongated entities represents a late stage of recrystallization. "Annealing recrystallization" has been suggested by Fairbairn (1942, p. 54-55) to describe metal fabrics. The above discussion concerning rock fabrics should be considered supplementary and not contradictory to those qualifications listed by Fairbairn for metals.

Coalescing and annealing of needle quartz produces elongation in which the needle axis is often 12 times the length of the short axis. The amount of extension depends on how many end-to-end attachments are made. Figure 3C shows an end-to-end attachment of two needles with the joint between them partially annealed.

Newly formed muscovites may be trapped within a recrystallizing quartz grain especially near the tapered ends where quartz strands and micas are most easily coalesced.

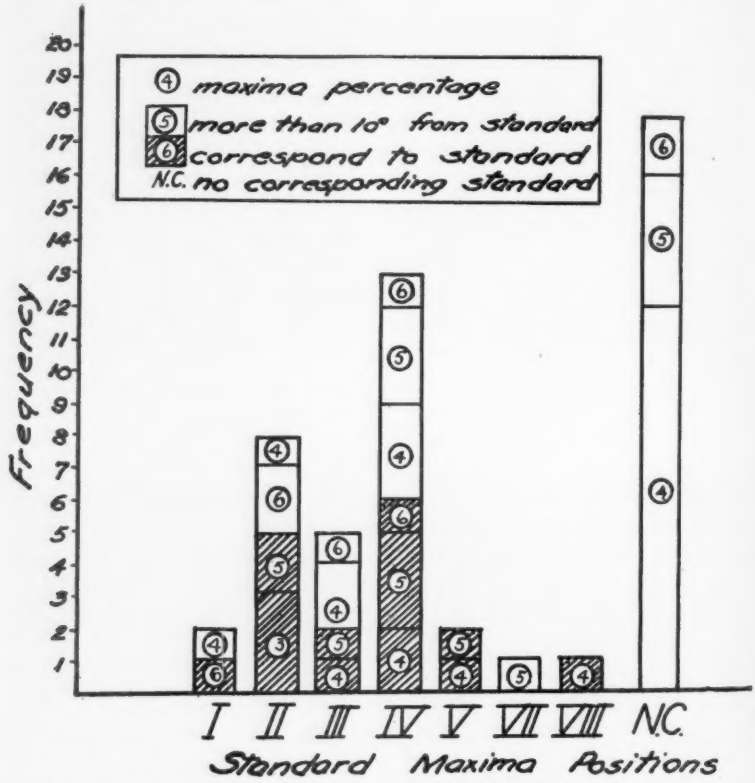
④ maxima percentage
⑤ more than 10° from standard
⑥ correspond to standard
N.C. no corresponding standard
Frequency
I II III IV V VII VIII N.C.
Standard Maxima Positions

FIGURE 4.—*Frequency-distribution histogram showing relative importance of standard maxima positions*

PETROFABRICS

DEVELOPMENT OF MAXIMA DURING DEFORMATION

The fracture hypothesis developed by Griggs and Bell (1938) has received wide recognition. Fairbairn (1939, p. 1490) suggests that "All the known quartz maxima in tectonites may be correlated with the fracture hypothesis."

Inasmuch as the tectonites under discussion are metamorphosed less than those usually discussed in studies of this kind the results are not

strictly applicable. However, there appears to be scattered evidence to support fracturing. Fairbairn (1939, p. 1485) has proceeded beyond Sander's conclusion concerning formation of needle quartz and has developed by experiment a probability series based on lattice-structure studies. He lists the possible directions of fracture within the crystal in the order of decreasing probability on the basis of the possible

TABLE 6.—*Expected frequency of occurrence of known quartz maxima*

most probable—maxima positions I, IV, VI
less probable—maxima position III
still less probable—maxima position II
least probable—maxima position V

glide planes and the differential ease of movement along them. In addition Fairbairn has outlined a series for the probable occurrence of standard maxima positions which correspond to the controlling glide planes. Table 6 is fashioned from Fairbairn's article and indicates the sequence in decreasing order of probable maxima positions based on the fracture hypothesis. These maxima positions are nearly the same as those in Fairbairn's revised set (1942, p. 67) (Pl. 12, F 97) except that Fairbairn has abandoned position VI by combining it with IV.

FRACTURING VERSUS GRANULATION

Little confidence can be placed on the correspondence of quartzite maxima to those of the standard set. The majority of tectonites studied were granulated rather than fractured and no consistent position of maxima is revealed. Figure 4 is a frequency-distribution histogram. The frequency of occurrence of 3-, 4-, 5-, and 6-per-cent maxima is plotted above the standard maxima position to which each is related. The circled numbers refer to percentage of axes concentration. The hachured blocks represent close correspondence of maxima with standard positions; the white blocks refer to maxima that diverge from 10 to 20 degrees from a standard position. A separate column labeled "N.C." illustrates those maxima positions for which there are no corresponding standard positions.

The apparent dominance of positions II and IV reflects the rhombohedral glide planes in the needle quartz specimens F 64 and F 65. These two sections have contributed four number II maxima and five number IV maxima.

Maxima which cannot be correlated with any standard position outnumber those which correspond closely. This plus the possibility of correspondence by chance precludes the interpretation of crush quartz maxima according to the fracture hypothesis.

IMPORTANCE OF SELECTIVE MEASUREMENTS

Not all rock flowage leaves traces that are legible in a fabric diagram. Selectivity in measurement is the most important single factor in determining what fabric pattern will result. Any of three general pattern types can result from an analysis of a recrystallizing rock: (1) Random measurement of any and all grain types will result in a completely random distribution of points even though lineation is apparent (*note* partial diagrams for F 64 on Pl. 12); (2) a random selection of crush quartz particles from the entire section may result in a few minor maxima (4 or 5 per cent), the height of maxima increasing with more measurements made on grains of any one superindividual; (3) a series of selective measurements of crush quartz comprising only a few clusters will result in higher yet unrelated maxima. As crush quartz begins to coalesce, the number of grains available for selective measurement in any one cluster is reduced with a corresponding decrease in the height of maxima obtained. This fusion of crush quartz particles within a cluster is shown on Figure 1 of Plate 9. Therefore up to this point in the development of a tectonite the maxima percentages will increase with granulation and decrease with annealing recrystallization. Figure 1 of Plate 9 shows a recrystallized fabric in which granoblastic texture is developed. Thus the validity of the interpretations of such diagrams is a function of the degree of selectivity in measurement. Diagrams prepared by independent investigators are hardly comparable unless they are accompanied by detailed quantitative data and strict definitions of grain types measured.

EFFECT OF ROCK COMPOSITION ON FABRIC PATTERNS

Evidence of rock flowage is often obscured or distorted by compositional changes. A high clay content may alter the mode of accommodation of quartz grains to stress and thereby prevent the development of lineation. Specimens F 37, F 38, and F 51 A (Table 3) show the effect of an argillaceous matrix on stressed quartz grains. Granulation exceeds 22 per cent of the total quartz in each case, but no linear stretching is apparent, and the rocks are therefore classed as nontectonites. Texture is conditioned by composition, but not always in similar fashion. Specimen F 20 (Table 4) contains 34 per cent large quartz grains scattered through a fine-grained matrix of chlorite, magnetite, feldspar, and calcite, with a small amount of cryptocrystalline quartz as a binder. This matrix rigidly controls the granulation of original quartz grains. Only 9 per cent of the quartz shows effect of granulation, although lineation is sufficiently prominent to class the specimen as a tectonite.

FIGURE 1. FRACTURED GRAIN
With strain shadows, Boehm's lamellae, and fracturing developed along a rhombohedral plane. F 65. X-nicols (×35).

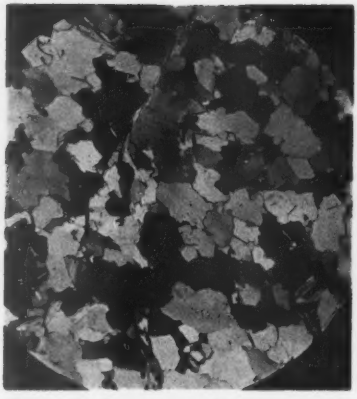

FIGURE 2. GRANOBLASTIC TEXTURE CHARACTERISTIC OF COMPLETELY RECRYSTALLIZED QUARTZ
F 74. X-nicols (×45).

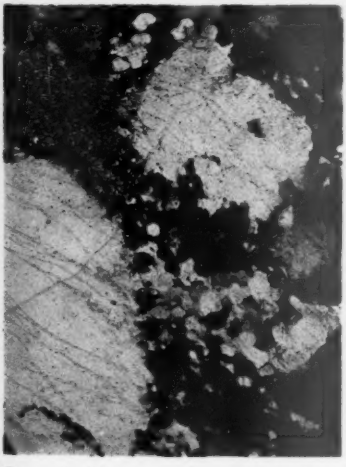

FIGURE 3. "ANNEALING RECRYSTALLIZATION" BETWEEN ORIGINAL GRAINS AND CRUSH QUARTZ CLUSTERS
F 40 A. X-nicols (×17).

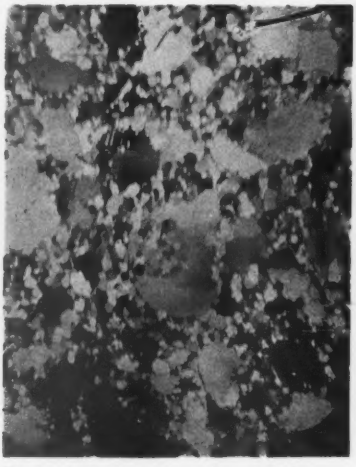

FIGURE 4. CRUSH QUARTZ CLUSTERS SHOWING LOCAL FUSION OF PARTICLES
F 50 A. X-nicols (×17).

FRACTURING, STRAINING, AND RECRYSTALLIZATION OF QUARTZ GRAINS

DEVELOPMENT OF A PREFERRED ORIENTATION

The development of a preferred orientation parallels the progress of recrystallization. As seen in Tables 3 and 4 all quartz-rich rocks which reveal a dimensional parallelism have undergone sufficient deformation to cause partial or complete recrystallization of at least 22 per cent

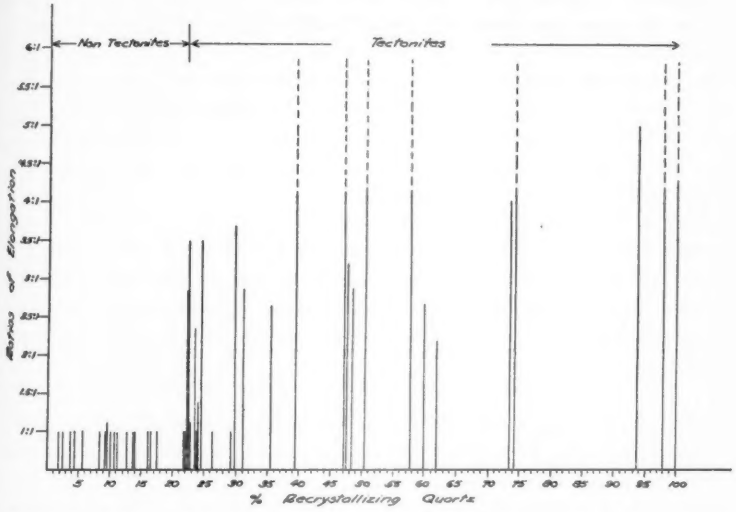

FIGURE 5.—*Relation between percentage of recrystallizing quartz and ratios of elongation*

of the quartz. However, the per cent of recrystallizing quartz bears no relation to the percentage of quartz axes concentration. Extreme cases might be cited: 50.4 per cent of the quartz in specimen F 71 has become partially recrystallized, yet no more than 2 per cent maxima are developed (Pl. 12, F 71 a and b). Conversely, in F 23 where only 23.5 per cent of quartz is in the process of recrystallization there is a 6-per-cent maximum developed (Pl. 11, F 23 Ca).

The relationship between percentage of granulated quartz and the appearance of a preferred dimensional arrangement of clusters is measurable, and it is possible to set a fairly well-defined boundary below which lineation is not apparent and above which it becomes measurable.

The tectonite-nontectonite boundary can be drawn clearly (Fig. 5). The graph shows per cent of granulated quartz plotted against elongation ratios. Measurement of parallel elongated grains provides a means

of expressing lineation quantitatively. The graph shows 22 per cent as the limit above which lineation becomes apparent.

Fairbairn (1942, p. 22-23) presents diagrams to illustrate an instance where "recrystallized quartz" (crush quartz?) of the groundmass showed a lattice orientation identical to the larger "undulatory grains" (original grains?). Selective measurements were made of different grain types in numerous slides of the collection under discussion (F 20 C, F 23, Md 35, F 40, F 50, F 53, F 64, F 65, F 71, F 77, F 78). Only one set (F 40) from this series of partial diagrams shows a similar location of maxima. Though similar, the maxima are unrelated to any rotation axis or standard maxima position. Thus the need for careful discrimination of textures becomes apparent in relation to the validity or significance of fabric interpretations.

Figure 3 of Plate 9 shows clearly the interrelation between crush quartz and original grains. The uniform birefringence of the original grain and a large number of crush quartz particles indicates the former optical homogeneity of the two quartz types. Thus partial diagrams prepared from each quartz type should and do reflect this significant texture.

DIMENSIONAL AND LATTICE-CONTROLLED FABRICS

The relative importance of dimensional and lattice-controlled fabrics can be determined by a quantitative measurement of recrystallization and flowage. A tectonite is first dominated by a preferred dimensional orientation which involves mechanical crushing and stretching. Preferred lattice orientations overlap and supersede the dimensionally controlled tectonites. The height of maxima, which represent lattice parallelism, increases with the development of recrystallization and flowage when measurements are selective. Thus the transition from a quartzite to a quartz schist shows a parallel transition from dimensional to lattice control of preferred orientations. Evidence is abundant from closely controlled and detailed studies of texture in relation to fabric patterns.

Weak maxima as well as unrelated fabric patterns prepared from two cuts of the same specimen (*e.g.*, F 24A,B) indicate a general lack of optical parallelism. On the other hand, marked similarity exists in the fabric patterns of three mutually perpendicular cuts from a quartz schist (206A, B, and C) and thus clearly indicates the dominance of lattice-controlled orientations in more strongly deformed rocks.

A study of recrystallization observed in the Appalachian quartzites seems to confirm Fairbairn's prediction (1942, p. 81) that "annealed rock fabrics should show inequant grain shape and possible dimensional orientation."

INTERPRETATION OF DIAGRAMS

Discussion of special features.—Diagram F 11 B (Pl. 11) represents a depositional fabric of fine-grained muscovite. Its presence in the bedding plane of a tectonite indicates that quartz reacts to deformation earlier than mica.

TABLE 7.—*Fabric data pertaining to needle quartz tectonites*

	Grain type	Number measured	Highest max. %	% area covered by max. of			% concentrations occurring in standard maxima positions							
				4%	5%	6%	I	II	III	IV	V	VII	VIII	NC*
F 64	slivers parallel to 'a'	100	6	1.4	0.48	0.12		5 4		5? 4?				4, 6
	Original	100	5	0.72	0.35			4		5		5		4, 4 4, 4
	crush quartz**	300	3											
	undifferentiated	500	2											
F 65	slivers parallel to 'a'	300	6	1.4	0.39	0.04		6?		5				
	random oriented slivers	200	5	0.39	0.06					5?	4			4.
	undifferentiated	500	3											

* No corresponding position for quartzite maxima.
** Measurement of a majority of grains in any one superindividual carefully avoided.

Diagram F 22 A and B (Pl. 11) show maxima reaching 5 per cent. The analysis of these specimens (Table 4) shows 22.5 per cent of the quartz in the process of recrystallization. A study of the texture suggests a tendency toward inequant but random orientation of grains. It is a border-line case and included with the tectonite group only because of the advanced stage of recrystallization and the preferred lattice orientation indicated by the 5 per cent maxima. These concentrations should be discounted, however, on the basis of insufficient evidence because 200 grains (F 22 A and 250 (F 22 B) cannot be considered representative from a texture of crush quartz and original grains where measurement was not selective.

Diagram F 23 B (Pl. 11) represents the random (3 per cent) distribution of quartz axes in the *ac* plane. F 23 C is parallel to the *ab* plane and shows a 6-per cent maximum. Granulation and stretching are more in evidence in the *ab* cut to explain the increased maximum

TABLE 8.—*Summary of fabric data pertaining to nontectonites*

NONTECTONITE ANALYSES

Spec. and diagram number	"cut"	Number of grains measured	Type of grains measured	Per cent of net surface covered by maxima of:			Position of maxima (above 3% concentration)								Largest mica maxima
				4%	5%	6%	I	II	III	IV	V	VII	VIII	N.C.*	
F 28A	ac	300	quartz—large	0.12					4						
F 28C	ac	300	quartz—large												
F 29	ab	300	quartz—large	0.08							4				
F 31A	ab	225	quartz—large	0.08										4	
F 33A–1	ac	300	quartz—large	0.19						4?					
F 33B–1	ac	300	quartz—large												
F 33B–2	ab	300	quartz—large												
F 33C–1	ac	300	quartz—large												
F 35A	ac	300	quartz—large												
F 35B	ab	300	quartz—large												
F 36A	ac	300	quartz—large	0.14			4								
F 37	ac	300	quartz—large	0.45										444	
F 38A–1	ac	300	quartz—large												
F 38B–2	ac	300	quartz—large												
F 38C–1	ab	330	quartz—large	0.19					4						
F 38C–1	ab	100	muscovite												15
F 39	ac	300	quartz—large												
F 39	ac	100	muscovite												12
F 51A	ac	400	quartz—large												
F 51B	ac	400	quartz—large												
F 52	ac	400	large and small qz												
F 53	ac	400	quartz—large												
F 53	ac	350	quartz—small												
F 54	ac	420	quartz—large												
F 54	ac	100	muscovite												14
F 59	ac	400	quartz—large												
F 60	ac	420	quartz—large												
F 61	ac	400	quartz—large												
F 62	ac	400	quartz—large												
F 63	ac	400	quartz—large												
F 66	ac	400	quartz—large	0.06										4	

* No correspondence between quartzite and known maxima.

TABLE 9.—*Summary of fabric data pertaining to tectonites*

TECTONITE ANALYSES

Spec. and diagram number	"cut"	Number of grains measured	Type of grains measured	Per cent of net surface covered by maxima of:			Position of maxima (above 3% concentration)								Largest mica maxima
				4%	5%	6%	I	II	III	IV	V	VII	VIII	N.C.*	
HF 10	ac	400	quartz—large												
HF 11B	ac	300	quartz—large												
HF 11B	ac	200	muscovite												11
HF 11C	ab	300	quartz—large												
HF 12A	ac	400	quartz—large												
HF 12B	bc	350	quartz—large	0.08										4	
HF 13A	ac	340	quartz—large												
HF 13B	bc	200	quartz—large												
F 20A	bc	320	quartz—large	0.12					4						
F 20C	ac	225	quartz—large												
F 20C	ac	300	quartz—small	0.54				4							
F 21A	ac	300	quartz—large	0.41										4	
F 21B	bc	225	quartz—large	0.29					4?						
F 22A	ac	200	quartz—large	0.29	0.08									45	
F 22B	ab	250	quartz—large	0.72	0.21						5				
F 23B	ac	300	quartz—large												
F 23C	ab	300	quartz—large												
F 23C	ab	150	quartz—small	4.14	0.81	0.25		6?	6?				4		
F 24A	bc	500	quartz—large	0.68	0.21				5						
F 24A	bc	100	muscovite												28
F 24B	ac	500	quartz—large												
F 24B	ac	100	muscovite												23
Md 35	ac	300	quartz—large												
Md 35	ac	300	quartz—small	0.45			4?							4	
Md 37	ac	400	quartz—large							4					
F 40A	ac	300	quartz—large	0.27						4?4					
F 40A	ac	300	quartz—small	0.33	0.10			5	4?						
F 50A	ab	300	quartz—large	0.41											
F 50A	ab	400	quartz—small												
F 50B	ac	300	quartz—large												
F 50B	ac	400	quartz—small												
F 64	ac	100	quartz—large	0.72	0.35			4		5		5?		4444	
F 64	ac	300	quartz—small												
F 64	ac	100	quartz slivers	1.40	0.48	0.12		54		5?4?				46	
F 64	ac	500	undifferentiated qtz												
F 64	ac	125	muscovite												19
F 65	ac	300	parallel elong. qtz	1.40	0.39	0.04		6?		5					
F 65	ac	200	random elongate qtz	0.39	0.06					5?	4			4	
F 65	ac	500	undifferentiate qtz												
F 71	ac	350	quartz—large												
F 71	ac	400	quartz—small												
F 71	ac	150	muscovite												10
F 74	ac	400	quartz—large												
F 74	ac	200	muscovite												14
F 75	ac	400	quartz—small												
F 75	ac	100	muscovite												23
F 76	ac	300	quartz—large												
F 76	ac	125	muscovite												16
F 77	ac	350	quartz—large												
F 77	ac	400	quartz—small	0.17				4?							
F 77	ac	100	muscovite												14
F 78	ac	200	quartz—large	0.14					4?						
F 78	ac	400	quartz—small												
F 78	ac	100	muscovite												16
H–107	ac	400	quartz—large												
H–107	ac	200	muscovite												15
H–107	ac	100	chloritic biotite												28
206 A	ab	300	quartz—small	0.52										4	
206 A	ab	100	muscovite												25
206 B	bc	300	quartz—small	3.74	1.10	0.10	6			5?5				56	
206 C	ac	300	quartz—small	4.67	1.20	0.21				6?6				455	

* No correspondence between quartzite and known maxima.

percentage of concentration of axes. Growth of quartz around magnetite metacrysts also confuses the picture since the quartz axes are controlled by the position of the magnetite crystal faces on which they grow.

Specimen F 24 Ab (Pl. 11) shows a 5-per cent maximum attributable to the nearly complete breakdown of the original grains into a mosaic of crush quartz. Poor selectivity resulted in an overabundance of measurements of grains from a single crush cluster with the resulting development of misleading and meaningless maxima.

Specimens F 64 and F 65 (Pl. 12) were reserved for a selective study since numerous quartz types were present in the textures. Needle quartz is prominently developed in these specimens. Table 7 shows the decreasing series of maxima percentages which closely conforms to what should be expected with the corresponding quartz types. The close parallelism in fabric between needle quartz in both rock specimens is striking not only in the comparable planimeter measurements of areas covered by maxima but also in their common correspondence to the standard maxima position IV. Fairbairn's list of expected frequencies of maxima occurrence (Table 6, p. 29) includes Maximum IV as one of the most likely to occur and relates the deformation to slip along rhombohedral planes.

Diagram F 71 (Pl. 12) is included with the tectonites, yet the analysis shows the least lattice parallelism of any rock in the entire collection. Two-per cent maxima were obtained for measurements of 350 original grains as well as 400 crush quartz grains, indicative that superindividuals react to stress as independent clusters rather than in the uniform manner suggested by more highly deformed types. Selection of grains for measurement was on an apportioned basis in order to obviate any tendency to dwell on any one cluster of crush quartz.

Diagrams 206 A, B, and C (Pl. 12) are prepared from analyses of the most highly deformed rock in the series. It is a quartz schist and thus is not directly comparable to the quartzite fabric patterns. The preferred orientation is due to lattice parallelism and represents a deformation stage far beyond that of the quartzites in which dimensional parallelism controls the pattern. All three diagrams from the schist show restricted *ac* girdles with maxima in the vicinity of *a*. Two 6-per cent and one 4-per cent maxima represent the peaks of concentration.

Cumulative diagrams.—Cumulative diagrams emphasize general tendencies which are often obscure in any single diagram. *F 93 and F 94* (Pl. 12) reveal an *ac* girdle with a concentration of maxima near the known positions II and IV. The author attaches a special significance to the girdle. Similar girdles are commonly known from analyses of highly deformed schists and gneisses and are usually associated with

preferred lattice orientations. The Appalachian quartzites show a general absence of lattice parallelism in their fabrics; therefore the appearance of an *ac* girdle in a cumulative diagram strongly suggests the transitional nature of fabric development. The transition from dimensionally controlled tectonites to those with lattice parallelism is a result of increasing deformation.

Diagrams F 95 and F 96 (Pl. 12) show a general accumulation of maxima in the southeast quadrant of the net. Such a concentration seems to conflict with the evidence, since no concentration of maxima should result where preferred dimensional orientation dominates. On closer examination this discrepancy dissolves since 9 out of the 20 maxima in the southeast quadrant are traceable to fracture-controlled tectonites where needle quartz is abundant. Fracturing has produced a lineation in which the elongated grains are bounded by rhombohedral glide planes. Therefore the lineation (*a*) can be interpreted from the diagram as lying on a circle 38 degrees from the greatest concentration of maxima. Lineation cannot be determined accurately since it is not known which rhombohedron plane is responsible for the glide. The attitude of lineation, however, will be represented by a point on a circle 38° 13′ away from the center of the concentrated maxima. Nearly any point on such a circle would still fall in the southeast quadrant, thereby supporting the fact that field measurements of lineation indicate a southeast strike for this structure.

Nontectonite diagrams.—Maxima of 2, 3, and 4 per cent characterize the remaining diagrams. Their significance lies in their general lack of "character." The transitional development of fabric types becomes apparent only when both extremes of deformation are analyzed along with the intermediate stages. Three-per cent concentration of axes is generally considered worthless in an analysis; however, it may be significant if detailed textural features are noted and if the investigator makes accurate and selective measurements. Under these conditions numerous small maxima may indicate a granulation in the fabric long before extension of clusters has produced a tectonite.

Special attention is drawn to nontectonite diagrams, F 28 A-2, F 29, F 31 A, F 33A-1, F 37-A, F 38C-1 and F 66 (Pl. 10), which show average granulation of over 16 per cent of the available quartz. Four-per cent maxima are developed in each case. Random measurements and poor selectivity could easily account for these maxima which, although random, take on a possible new significance in the light of the present discussion.

Diagram number	Number and type of grains measured	Contours in percent	Rock type	Locality
F28A-2	300 large quartz	1-2-3	Sm	Greenland Gap, W. Va.
F28C-1	300 large quartz	1-2-3	Sm	
F29A	300 large quartz	1-2-3-4	Dp	South of Junction, W. Va.
F31A	225 large quartz	1-2-3-4	Do	Gaudy's Castle, W. Va.
F33A-1	300 large quartz	1-2-3-4	Sn	Great Cacapon, W. Va.
F33B-1	300 large quartz	1-2-3	Sn	
F33B-2	300 large quartz	1-2-3	Sn	
F33C-1	300 large quartz	1-2-3	Sn	
F35A	300 large quartz	1-2-3	Cc	North of McCoy's Ferry, Md.
F35B	300 large quartz	1-2-3	Cc	
F36A	300 large quartz	1-2-3-4	Dr	McCoy's Ferry, Md.
F37A	300 large quartz	1-2-3-4	Om	West of Williamsport, Md.
F38A-1	300 large quartz	1-2-3	Om	
F38B-2	300 large quartz	1-2-3	Om	
F38C-1a	100 muscovite	1-3-5-10-15	Om	
F38C-1b	330 large quartz	1-2-3-4	Om	
F39Aa	300 large quartz	1-2-3	Om	
F39Ab	100 muscovite	1-3-5-10-12	Om	
F51A	400 large quartz	1-2-3	St	Rockville, Pa.
F51B	400 large quartz	1-2-3	St	
F52	400 undifferentiated quartz	1-2-3	Ch	Reading, Pa.
F53a	400 large quartz	1-2-3	Om	Straustown, Pa.
F53b	350 small quartz	1-2-3	Om	
F54a	420 large quartz	1-2-3	Mmc	North of Dauphin, Pa.
F54b	100 muscovite	1-3-5-10-14	Mmc	
F59	400 large quartz	1-2-3	Cm	Fox Run School (Tyrone Quad.) Pa.
F60	420 large quartz	1-2-3	St	McKee's Gap, Pa.
F61	400 large quartz	1-2-3	St	East of Loysburg, Pa.
F62	400 large quartz	1-2-3	Dp	Pa.- Turnpike-Sideling Hill.
F63	400 large quartz	1-2-3	Oc	Pa. Turnpike near Carlisle, Pa.
F66	400 large quartz	1-2-3-4	St	North of Bellefonte, Pa.
F98	Scheme to show orientation of arrows in diagrams.			
F99	Equal area net.			

Sm—Medina ss.; Dp—Portage ss.; Do—Oriskany ss.; Sn—Niagara Series; Cc—Conococheague limestone; Dr—Romney shale; Om—Martinsburg shale; St—Tuscarora ss; Ch—Hardystone quartz; Mmc—Mauch Chunk series; Cm—Mines dolomite; Oc—Chambersburg shale.

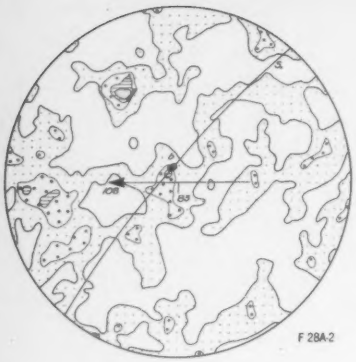

F 28A-2

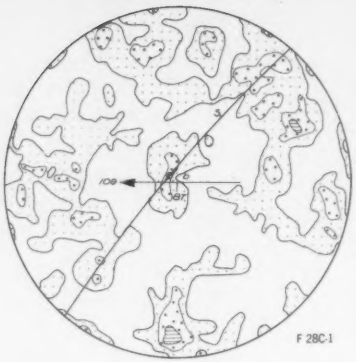

F 28C-1

F 37A

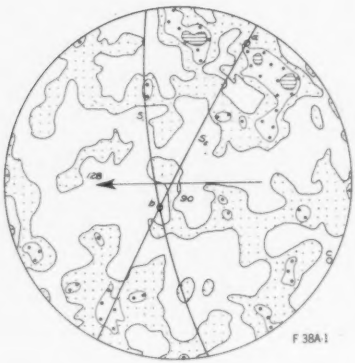

F 38A-1

F 53b

F 54a

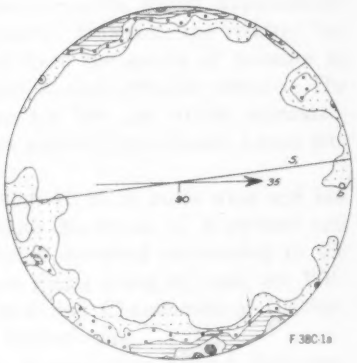

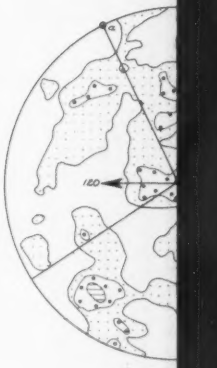

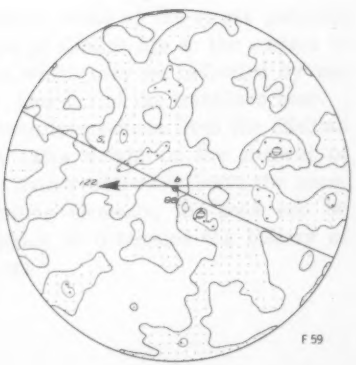

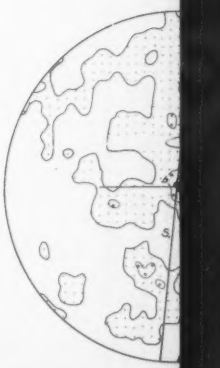

FABRIC DIAGRAM

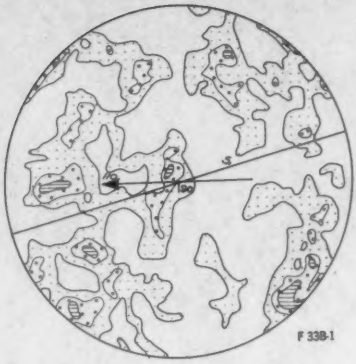

BRIC DIAGRAMS OF NONTECTONITES

F 33B-2

F 33C-1

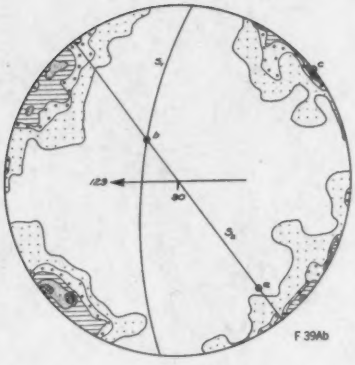
F 39Ab

F 51A

F62

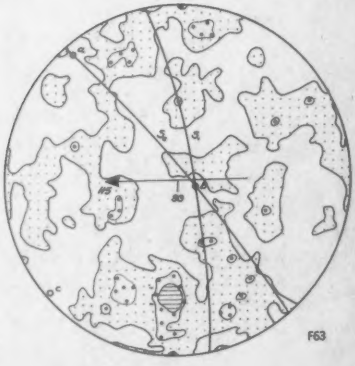
F63

F 35A

F 35B

F 51B

F 52

F 66

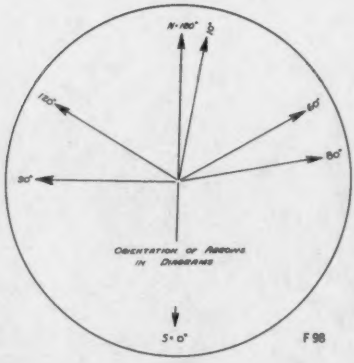

F 98

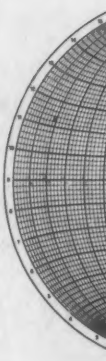

F 36A

F 53a

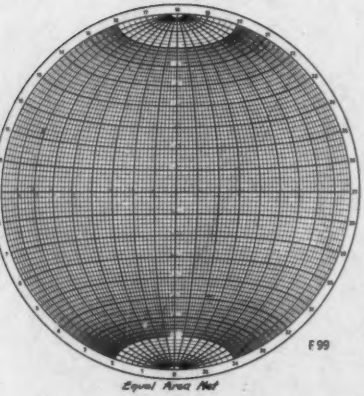
F 99
Equal Area Net

The reader should realize that no attempt is made here to interpret 3- and 4-per cent maxima in relation to the mechanics of deformation. Such an attempt would be hazardous in the light of present knowledge. The significance lies in exposing early stages of deformation by recognizing the relict optical parallelism of granulated and clustered particles.

Rocks in which the development of peripheral growth quartz is the only indication of dynamic activity produce a fabric that reveals nothing that can be used in the interpretation of texture. Specimens F 35, F 39, F 51, F 52, F 53, F 54, and F 59 (Pl. 10) fall in this category and show an average of 11 per cent of the quartz developed as peripheral-growth material.

DISTRIBUTION OF TECTONITES

TRANSITION ZONE

Distance from source of pressure.—The boundary zone between subtectonites and tectonites can be delineated in the folded Appalachians from a study of the data here presented. However, the relative importance of age (depth) and distance from the source of pressure as factors controlling the location of such a zone remains obscure. The critical localities which limit the zone are few and widely separated. The result is a schematic rather than an accurate plot of such a zone into a map (Pl. 2).

As shown on Plate 2, the zone is about 10 to 20 miles wide and lies west and north of Elk Ridge and South Mountain in Maryland and south-central Pennsylvania. It continues eastward conforming to the trend of the mountain axis. Reference points along its path are Williamsport and Hagerstown in Maryland and Chambersburg, Carlisle, Harrisburg, Lebanon, and Reading in Pennsylvania.

The arcuate character of the zone is concentric around Baltimore which is approximately the pivot of the salient arc. As such the distance from the origin of pressure could be considered the controlling element in locating the zone.

Age of tectonite horizons.—The general strike of the strata parallels the arcuation and therefore brings beds of similar age to the surface at all points. Thus depth of deformation which may be indicated by age is a possible controlling element in the location of the transition zone.

The presence of one questionable tectonite specimen from the Silurian Tuscarora horizon (F 22) may place extra weight on the element of distance from source of pressure. The author prefers to leave the question open. Regardless of the controlling elements, the zone can be traced and therefore is useful as a guide to determine the history of deformation in the central Appalachians.

SUMMARY AND CONCLUSIONS

Numerous exhaustive reports have appeared in English since Knopf's *Petrotectonics* (1933) was published. Most of these studies deal with the interpretation of quartz fabrics developed from highly deformed schists and gneisses, whereas this investigation deals with quartz-rich rocks which are loosely referred to as "unmetamorphosed."

The results here obtained have made it possible to place a transitional boundary through the deformed central Appalachian area which divides nontectonitic rocks from those in which a deformation pattern can be deciphered. The meaning of fabric analyses of quartz-rich sedimentary rocks becomes clearer gradually from west to east in the central Appalachians. Those specimens collected from localities west of the transitional zone show no preferred orientations and are therefore of interest only for the light they shed on the early stages of the recrystallization process. Preferred orientations are first developed within the transition zone which might be called a tectonite frontier. Eastward from this zone dimensional orientation is superseded by lattice parallelism which reaches an extreme in the highly deformed and most ancient quartz schists of the eastern Piedmont.

The amount of quartz which is granulated during deformation may be used as an index to the development of a tectonite. If 22 per cent of the quartz in a quartz-rich fabric is granulated, a preferred dimensional orientation may develop; however, such a generality cannot be applied to "impure" quartzites since the strength of the fabric will be altered, and a different mode of accommodation to stress will result.

COMPLICATING FACTORS WHICH INFLUENCE THE VALUE OF PETROFABRIC ANALYSES OF QUARTZITES

(1) The fabric pattern varies with the ability of the individual to make selective measurements and to interpret textures correctly.

(2) Predepositional history of the individual grains produces a differential strength to resist deformation.

(3) A more complicated postdepositional history is shown by beds of increasing age in a rock series, the oldest showing the most extreme tectonitic characteristics.

(4) Localized and widespread development of late introduced quartz, which occurs as growths around metacryst nuclei, leads to confusion in the interpretation of a diagram.

(5) The fabric pattern varies with the type of effective metamorphism (load or dynamic).

Diagram number	Number and type of grains measured	Contours in percent	Rock type	Locality
HF10	400 large quartz	1-2-3	Cw	Harpers Ferry (Md. side)
HF11Ba	200 muscovite	1-3-5-8-11	Cw	
HF11Bb	300 large quartz	1-2-3	Cw	
HF11C	300 large quartz	1-2-3	Cw	
HF12A	400 large quartz	1-2-3	Cw	
HF12B	350 large quartz	1-2-3-4	Cw	
HF13A	340 large quartz	1-2-3	Cw	
HF13B	200 large quartz	1-2-3	Cw	
F20A	320 large quartz	1-2-3-4	Ca	North of Rouzerville, Pa.
F20Ca	225 large quartz	1-2-3	Ca	
F20Cb	300 small quartz	1-2-3-4	Ca	
F21A	300 large quartz	1-2-3-4	Cw	West of Montalto, Pa. (The Narrows).
F21B	225 large quartz	1-2-3-4	Cw	
F22A	200 large quartz	1-2-3-4-5	St	Cross Mountain, Pa. (at fire tower).
F22B	250 large quartz	1-2-3-4-5	St	
F23B	300 large quartz	1-2-3	Cw	Mt. Summit, Hwy U. S. 40.
F23Ca	150 small quartz	1-2-3-4-5-6	Cw	
F23Cb	300 large quartz	1-2-3	Cw	
F24Aa	100 muscovite	1-5-10-15-20-25-28	Cw	High Knob, Md.
F24Ab	500 large quartz	1-2-3-4-5	Cw	
F24Ba	100 muscovite	1-3-5-10-15-20-23	Cw	
F24Bb	500 large quartz	1-2-3	Cw	
Md35a	300 small quartz	1-2-3-4	Qtz	Linganore Creek, Md.
Md35b	300 small quartz	1-2-3	Qtz	
Md37	400 large quartz	1-2-3	Cl	Catoctin Mt. near Salamander Rk., Md.
F40Aa	300 large quartz	1-2-3-4	Ch	East of Boonsboro, Md.
F40Ab	300 small quartz	1-2-3-4	Ch	
F50Aa	400 small quartz	1-2-3	Cc	Chickies Rock, Pa.
F50Ab	300 large quartz	1-2-3-4-5	Cc	
F50Ba	300 large quartz	1-2-3-4-5	Cc	
F50Bb	400 small quartz	1-2-3	Cc	
F64a	300 small quartz	1-2-3	Cw	West of Arendtsville, Pa.
F64b	100 large quartz	1-2-3-4-5	Cw	

Cw—Weverton qzt.; Ca—Antietam qzt.; St—Tuscarora ss.; Qtz—Quartzite lentils in volcanics; Cl—Loudon qzt.; Ch—Harpers phyllite; Cc—Chickies qzt.; Csl—Sugarloaf qzt.; Ccgl—Cardiff congl.; Was—Wissahickon schist

HF 10

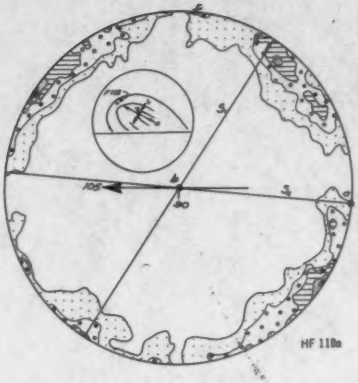

HF 11Ba

F 21A

F 21B

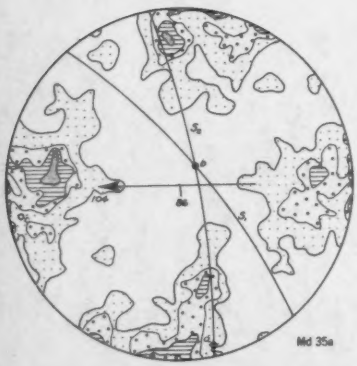

Md 35a

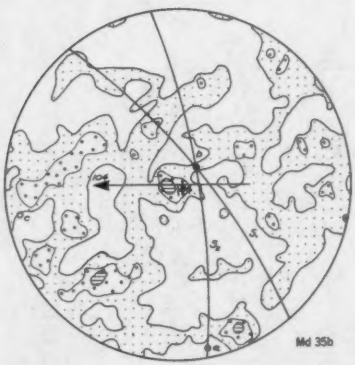

Md 35b

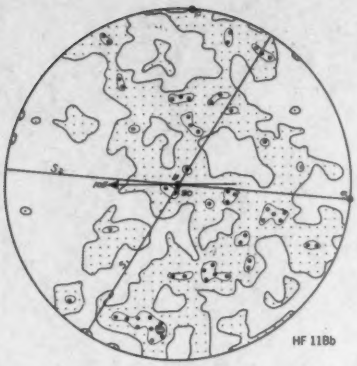

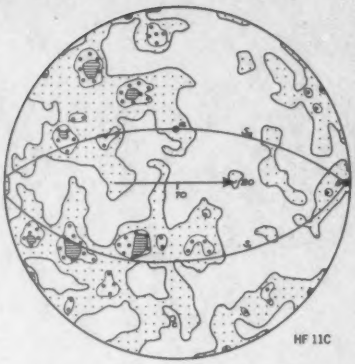

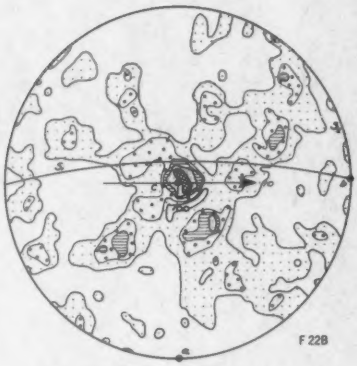

FABRIC DIAGR

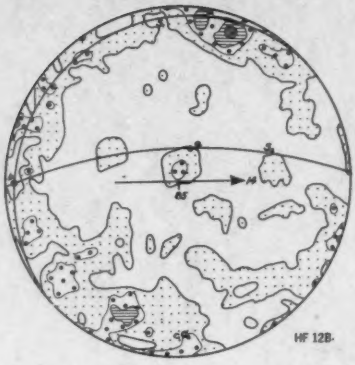

BRIC DIAGRAMS OF TECTONITES

HF 13A

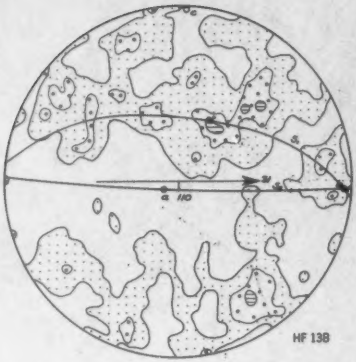
HF 13B

F 23Cb

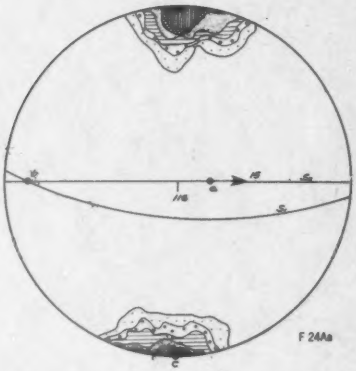
F 24Aa

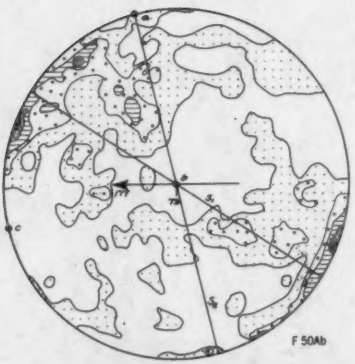
F 50Ab

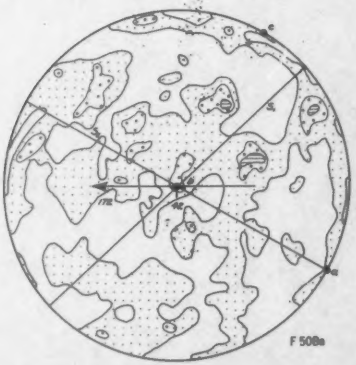
F 508a

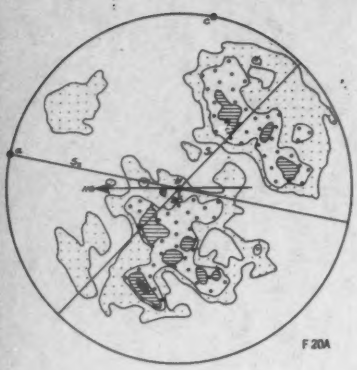
F 20A

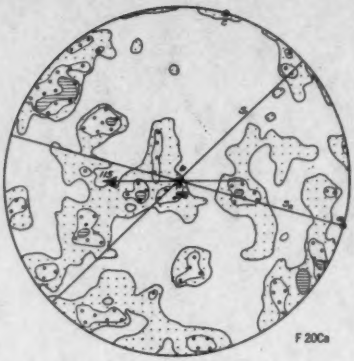
F 20Ca

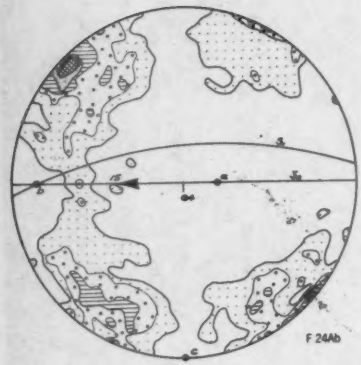
F 24Ab

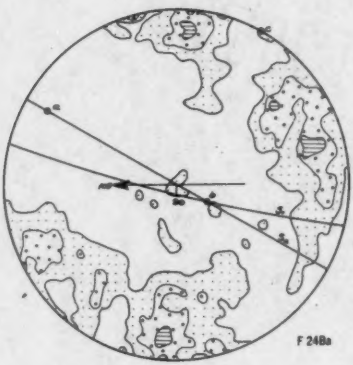
F 24Ba

F 50 Bb

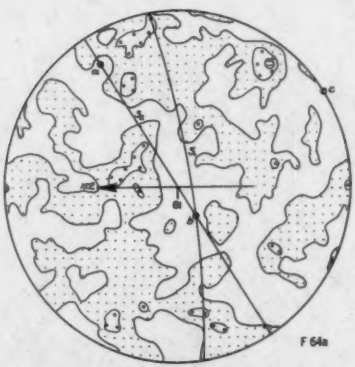
F 64a

F 20Cb

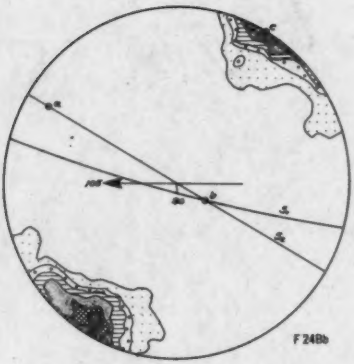
F 24Bb

F 64b

(6) Development of recrystallization from crush quartz to annealed grains reduces the maxima percentages obtainable from random measurements.

(7) Thin sections of crush quartz derived from one or two original grains will produce much larger maxima than those of crush quartz from numerous originals.

(8) Thin sections including the *a* fabric axis will make available for measurement a maximum number of crush particles from one individual and thereby give a different fabric pattern from a *bc* section.

(9) Compositional variations, even within the area of a thin section, will increase or reduce the development of preferred dimensional orientation.

(10) Structural environment will control the type of applied stress affecting the rock. Correspondingly different fabric patterns result.

REFERENCES CITED

Balk, Robert (1937) *Structural behavior of igneous rocks,* Geol. Soc. Am., Mem. 5.

Billings, M. P. (1942) *Structural geology,* Prentice-Hall, Inc.

Chapman, R. W. (1942) *"Pseudomigmatite" in the Piedmont of Maryland,* Geol. Soc. Am., Bull., vol. 53, p. 1299-1330.

Cloos, Ernst (1941) *Flowage and cleavage in Appalachian folding,* N. Y. Acad. Sci., Tr., ser. II, vol. 3, no. 7, p. 185-190.

—— (1942) *Distortion of stratigraphic thicknesses due to folding,* Nat. Acad. Sci., Pr., vol. 28, no. 10, p. 401-407.

——, and Hietanen, A. (1941) *Geology of the "Martic Overthrust" and the Glenarm series in Pennsylvania and Maryland,* Geol. Soc. Am., Spec. Paper, no. 35, 207 pages.

Fairbairn, H. W. (1939) *Hypothesis of quartz orientation in tectonites,* Geol. Soc. Am., Bull., vol. 50, p. 1475-1492.

—— (1942) *Structural petrology of deformed rocks,* Addison Wesley Press, Inc.

Ford, W. E. (1932) *Dana's textbook of mineralogy,* John Wiley & Sons, Inc., 4th ed.

Griggs, D., and Bell, J. F. (1928) *Experiments bearing on the orientation of quartz in deformed rocks,* Geol. Soc. Am., Bull., vol. 49, p. 1723-1746.

Heim, Albert (1921) *Geologie der Schweiz,* Bd. II, Leipzig.

Hietanen, Anna (1938) *On the petrology of the Finnish quartzites,* Bull. de la Comm. Geol. de Finlande no. 122.

Knopf, E. B. (1933) *Petrotectonics,* Am. Jour. Sci., 5th ser., vol. 25, p. 433-470.

—— (1938) *Report of Committee on Structural Petrology* (discussion by E. B. Knopf), Nat. Res. Council, p. 61.

——, and Ingerson, E. (1939) *Structural petrology,* Geol. Soc. Am., Mem. 6.

Sander, Bruno (1930) *Gefügekunde der Gesteine,* Julius Springer, Vienna.

Stose, George, and Jonas, Anna (1939) *Geology and mineral resources of York County, Pennsylvania,* Pa. Geol. Survey, Rept. C-67.

U. S. Geological Survey, Washington, D. C.

Manuscript Received by the Secretary of the Society, May 11, 1943.

Diagram number	Number and type of grains measured	Contours in percent	Rock type	Locality
F64c	125 muscovite	1-3-5-10-15-19	Cw	West of Arendtsville, Pa.
F64d	100 quartz slivers	1-2-3-4-5-6	Cw	
F64e	500 undifferentiated qtz.	1-2	Cw	
F65a	200 random elongated qtz.	1-2-3-4-5	Cw	West of Gettysburg, Pa.
F65b	300 parallel elongated qtz.	1-2-3-4-5-6	Cw	
F65c	500 undifferentiated qtz.	1-2-3	Cw	
F71a	350 large quartz	1-2	Csl	Sugarloaf Mt., Md.
F71b	400 small quartz	1-2	Csl	
F71c	150 muscovite	1-3-5-8-10	Csl	
F74a	200 muscovite	1-3-5-10-14	Cl	Point of Rocks, Va.
F74b	400 large quartz	1-2-3	Cl	
F75a	100 muscovite	1-3-5-10-15-20-23	Cw	West of Pt of Rocks, Md.
F75b	400 small quartz	1-2-3	Cw	
F76a	125 muscovite	1-2-5-4-8-12-16	Cw	Catoctin Mt. (Step Crk. Reservoir, Md.)
F76b	300 large quartz	1-2-3	Cw	
F77a	100 muscovite	1-3-5-10-14	Qtz	Libertytown, Md.
F77b	400 small quartz	1-2-3-4	Qtz	
F77c	350 large quartz	1-2-3	Qtz	
F78a	100 muscovite	1-3-5-10-16	Qtz	Linganore Creek, Md.
F78b	200 large quartz	1-2-3-4	Qtz	
F78c	400 small quartz	1-2-3	Qtz	
H107a	400 large quartz	1-2-3	Ccgl	Peach Bottom, Pa.
H107b	200 muscovite	1-3-5-7-8-10-12	Ccgl	
H107c	100 chloritic biotite	1-5-10-15-20-25-28	Ccgl	
206Aa	100 muscovite	1-5-10-15-20-25	Was	North of Florence, Md., (Howard County).
206Ab	300 small quartz	1-2-3-4	Was	
206B	300 small quartz	1-2-3-4-5-6	Was	
206C	300 small quartz	1-2-3-4-5-6	Was	

F93 All maxima above 3% plotted into net with north end of 'b' in the center and the west end of 'a' at the left.

F94 Same as F 93 but restricted to tectonite analyses.

F95 All maxima above 3% plotted into net with compass coordinates at the periphery (north at the top)

F96 Same as F95 but restricted to tectonite analyses

F97 Standard maxima positions (adapted from Fairbairn 1942 p. 67).

Cw—Weverton qzt.; Ca—Antietam qzt.; St—Tuscarora ss.; Qzt—Quartzite lentils in volcanics; Cl—Loudon qzt.; Ch—Harpers phyllite; Cc—Chickies qzt.; Csl—Sugarloaf qzt.; Ccgl—Cardiff congl.; Was—Wissahickon schist

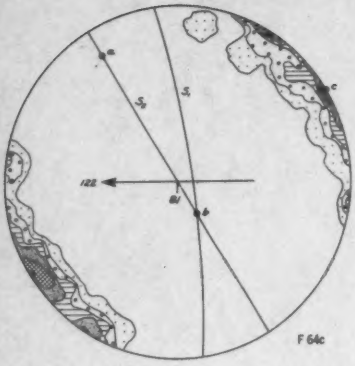

F 64c

F 64d

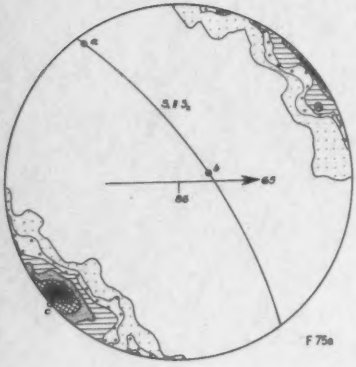

F 75a

F 75b

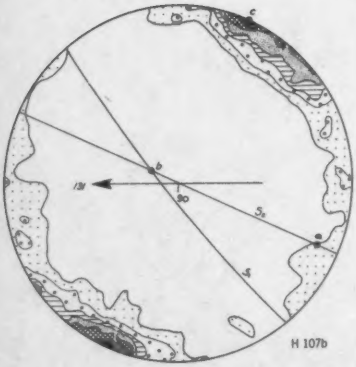

H 107b

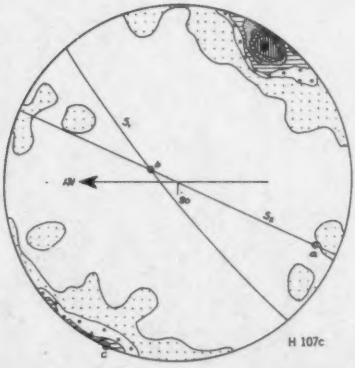

H 107c

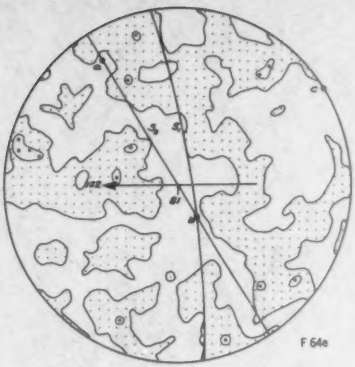

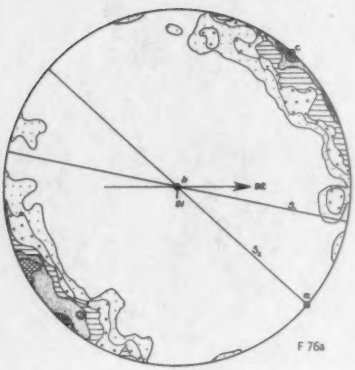

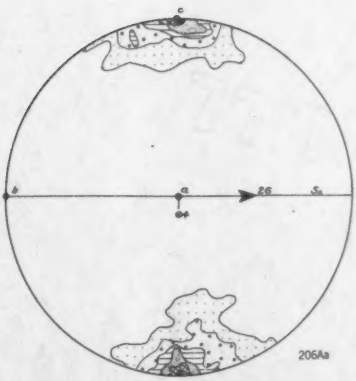

FABRIC DIAGR

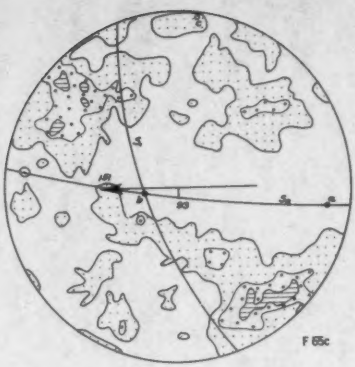

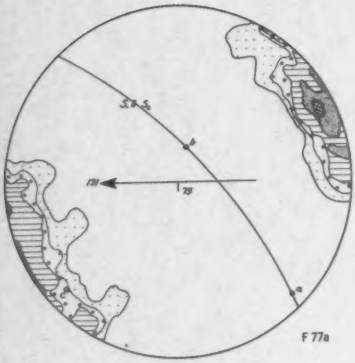

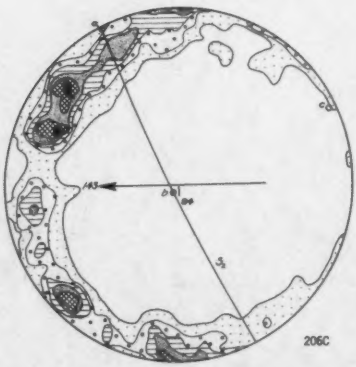

RIC DIAGRAMS OF NONTECTONITES

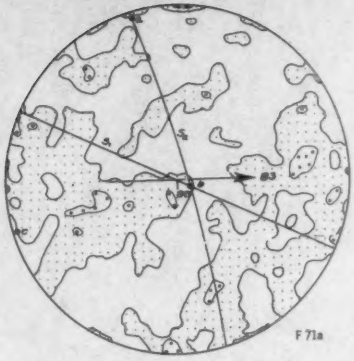

F 71a

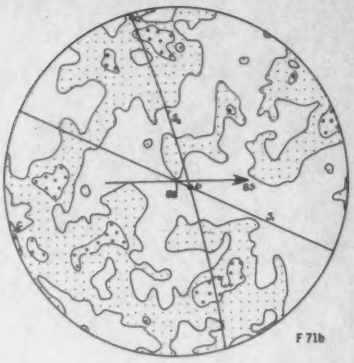

F 71b

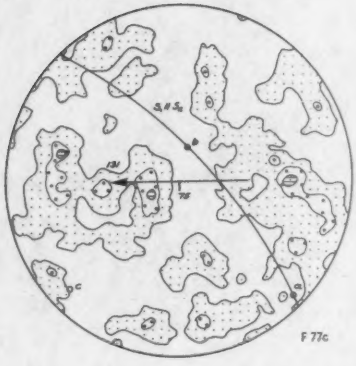

F 77c

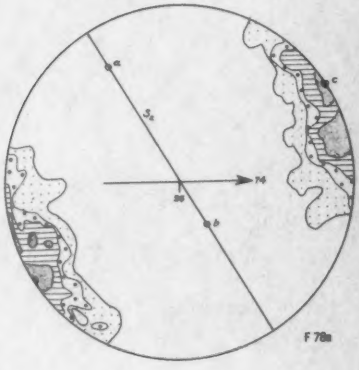

F 78m

F 93

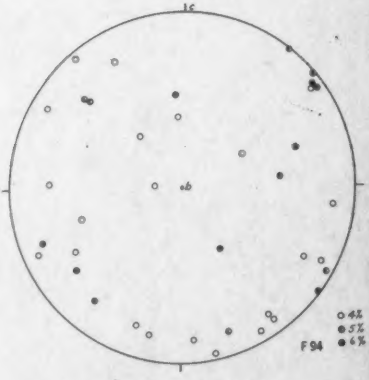

F 94

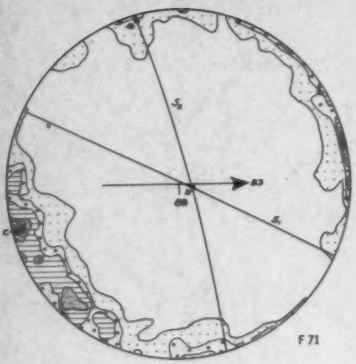
S_0
S_1
c
F 71

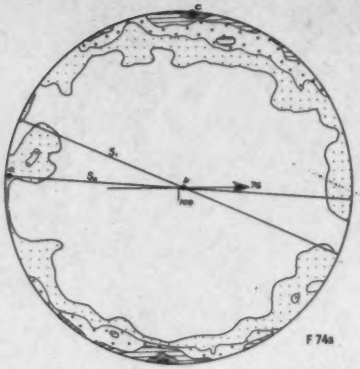
c
S_0
S_1
F 74a

c
S_0
S_1
F 78b

c
S_0
S_1
F 78c

N
W
E
S
F 95

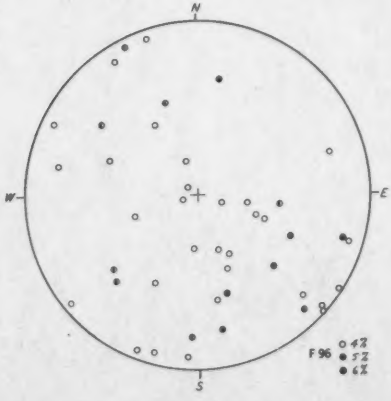
N
W
E
S
F 96
4%
5%
6%

F 74b

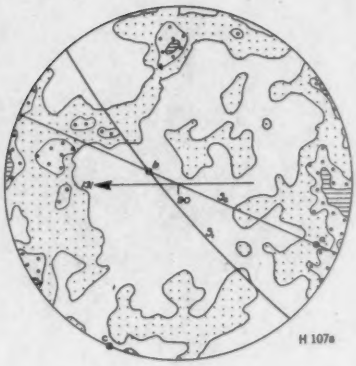
H 107a

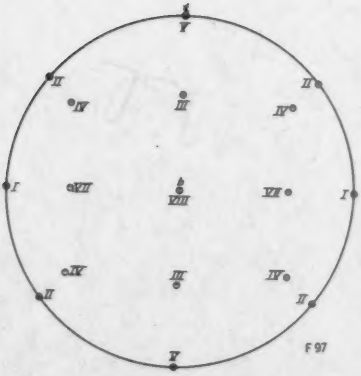
F 97